

The role of *B4galnt2* in shaping the outcome of antibiotic treatment and susceptibility to enteric pathogens

Dissertation
in fulfilment of the requirements for the degree
Doctor rerum naturalium (Dr. rer. nat)
of the Faculty of Mathematics and Natural Sciences
at the Christian Albrechts University of Kiel

Submitted by
Aleksa Čepić

Max Planck Institute for Evolutionary Biology
Plön, June 2024

First examiner: Prof. Dr. John F. Baines

Second examiner: Prof. Dr. Hinrich Schulenburg

Date of Oral Examination: 18.07.2024

Table of Contents

Abstract.....	5
Zusammenfassung.....	7
General introduction	9
Microbiota composition and biogeography.....	9
Within-host microbiota evolution	11
Colonization resistance	12
Antibiotics and gut microbiota	15
Glycans and gut microbiota.....	15
The <i>B4galnt2</i> gene.....	16
Aims of the study	16
References	17
Chapter 1: The role of the blood group-related glycosyltransferases <i>FUT2</i> and <i>B4GALNT2</i> in susceptibility to infectious disease	29
Chapter 2: Role of <i>B4galnt2</i> and Microbial Diversity in Colonization Resistance against <i>Salmonella Typhimurium</i>	43
Introduction	45
Materials and methods	49
Results.....	52
Discussion	66
Supplementary information	69
References	81
Chapter 3: The role of <i>B4galnt2</i> in shaping the outcome of antibiotic treatment.	89
Introduction	91
Materials and methods	94
Results.....	99
Discussion	112
Supplementary information	116
References	143

Chapter 4: The <i>B4galnt2</i>-Associated Microbiota Plays a Protective Role in Susceptibility to Intestinal Infections in Wild Mice	155
Introduction	157
Materials and methods.....	159
Results.....	161
Discussion	166
Supplementary information	168
References	175
General conclusion.....	181
Declaration	183
Author contributions.....	184
Acknowledgements.....	185

Abstract

The gut microbiota, comprising of a diverse group of bacteria and other microorganisms, plays important roles in nutrient metabolism, immune system development, and protection against pathogens. The *B4galnt2* gene, which exhibits a tissue-specific expression pattern, influences the composition and function of these microbial communities, which in turn affects the host's susceptibility to infections like *Salmonella Typhimurium*. This thesis examines the influence of *B4galnt2* expression on the dynamics of the gut microbiota, with a particular focus on the effects of antibiotic treatment and infection by intestinal pathogens. The study employs a shotgun metagenomic sequencing approach to analyze taxonomic and functional profiles of gut associated microbial communities.

Our findings reveal that intestinal *B4galnt2* expression patterns shape microbial diversity and functions, affecting the recovery process following antibiotic treatment and the ability of the microbiota to resist colonization by pathogens. In all mice, microbial diversity was reduced following streptomycin treatment. However, *B4galnt2*-deficient mice associated microbiota exhibited accelerated recovery post-streptomycin treatment, and reduced colonization success by *Salmonella Typhimurium*. The results of the second chapter identified *Blautia* as a biomarker associated with decreased inflammation in *B4galnt2*-deficient mice post-infection, suggesting its role in colonization resistance.

Additionally, our experiments described in the third chapter revealed differential responses in microbiota recovery post-antibiotic treatment, with notable enrichment of beneficial species like *Akkermansia muciniphila*, *Enterocloster clostridioformis*, and the *Blautia* genus in *B4galnt2*-deficient mice.

Moreover, the results of the fourth chapter have confirmed the association of pathogenic taxa, such as *Morganella morganii*, and mice homozygous for the C57BL6/J allele class at *B4galnt2*. In contrast, potentially beneficial bacteria including the butyrate producers *Intestinimonas butyriciproducens* and *Anaerostipes caccae* are linked to mice homozygous for the RIII/J allele class at *B4galnt2*, highlighting their role in colonization resistance, mitigating inflammation, and maintaining intestinal homeostasis.

In conclusion, this thesis emphasizes the important role of *B4galnt2* expression patterns on gut microbial diversity, recovery mechanisms of microbiota following antibiotic treatment, and colonization resistance against invading pathogens.

Zusammenfassung

Darmmikrobiota sind eine vielfältige Gruppe aus Bakterien und anderen Mikroorganismen. Sie spielen eine wichtige Rolle beim Stoffwechsel, bei der Entwicklung des Immunsystems und beim Schutz vor Krankheitserregern. Das gewebespezifisch exprimierte Gen *B4galnt2* beeinflusst die Zusammensetzung und Funktion dieser mikrobiellen Gemeinschaften insofern, dass wiederum die Anfälligkeit des Wirts für Infektionen mit beispielsweise *Salmonella Typhimurium* verändert ist. In dieser Dissertation wird der Einfluss der *B4galnt2*-Expression auf die Dynamik der Darmmikrobiota untersucht, wobei die Auswirkungen von Antibiotikabehandlungen und von Infektionen mit Darmpathogenen im Fokus liegen. Für die Analyse wird ein Shotgun-Metagenom-Sequenzierungsansatz verwendet, um taxonomische und funktionelle Profile von darmassoziierten mikrobiellen Gemeinschaften zu untersuchen.

Die Ergebnisse dieser Arbeit zeigen, dass die *B4galnt2*-Expressionsmuster im Darm die mikrobielle Vielfalt und ihre Funktionen prägen und dadurch zum einen den Genesungsprozess nach einer Antibiotikabehandlung und zum anderen die Besiedlung durch Krankheitserreger beeinflussen können. Die mikrobielle Diversität war bei allen Versuchsmäusen nach einer Streptomycin-Behandlung reduziert. Allerdings erholten sich jene Mikrobiota, welche mit *B4galnt2*-defizienten Mäusen assoziiert sind, schneller nach einer solchen Behandlung und bedingten zeitgleich einen geringeren Besiedlungserfolg durch *Salmonella Typhimurium*. Die Ergebnisse des zweiten Kapitels identifizierten *Blautia* als einen Biomarker, der postinfektiös mit verringelter Entzündung in *B4galnt2*-defizienten Mäusen assoziiert ist, was auf einen Einfluss von *Blautia* auf die Kolonisationsresistenz hindeutet.

Die dem dritten Kapitel zugrundeliegenden Experimente deckten unterschiedliche Erholungsreaktionen der Mikrobiota nach einer Antibiotikabehandlung auf, wobei es zu einer beachtlichen Anreicherung von nützlichen Arten wie *Akkermansia muciniphila*, *Enterocloster clostridioformis* und der Gattung *Blautia* in *B4galnt2*-defizienten Mäusen kommt.

Abschließend bestätigten die Ergebnisse des vierten Kapitels die Assoziation von pathogenen Taxa wie *Morganella morganii* mit Mäusen, die homozygot für die C57BL6/J-Allelkasse von *B4galnt2* sind. Für Mäuse, die homozygot für die RIII/J-Allelkasse von

B4galnt2 sind, besteht im Gegensatz dazu ein Zusammenhang mit potentiell nützlichen Bakterien wie den Butyratproduzenten *Intestinimonas butyriciproducens* und *Anaerostipes caccae*, womit deren Rolle bei der Kolonisationsresistenz in Form von Abschwächung von Entzündungen und Aufrechterhaltung der intestinalen Homöostase hervorgehoben wird.

Zusammenfassend stellt diese Arbeit die zentrale Rolle der verschiedenen *B4galnt2*-Expressionsmuster für die mikrobielle Vielfalt im Darm heraus und beleuchtet darüber hinaus zum einen die Erholungsmechanismen der Mikrobiota infolge einer Antibiotikabehandlung und zum anderen die Kolonisationsresistenz gegen eindringende Krankheitserreger.

General introduction

The mammalian body is inhabited by a diverse array of microorganisms, including bacteria, viruses, fungi, and archaea, collectively known as the microbiota. These microorganisms have a strong and long-lasting relationship with their hosts. The composition of the microbiota varies over time and is influenced by both the host genotype and environmental factors (Blekhman et al., 2015; Rothschild et al., 2018; Zoetendal et al., 2001). The stability and resilience of the microbiota is dependent on the body site, with the oral and intestinal microbiota exhibiting greater stability than the skin or nasal microbiota (Zhou et al., 2024).

Microbiota composition and biogeography

The gut microbiota is the most densely populated and diverse microbial community in body (Sender et al., 2016). Its composition and function are influenced by variety factors such as host genetics, age, diet, medication, and lifestyle. (Antinozzi et al., 2022; Cahana and Iraqi, 2020; García-Peña et al., 2017; Lopera-Maya et al., 2022; Patangia et al., 2022; Qin et al., 2024; Singh et al., 2017). The microbial composition and load vary significantly along the gastrointestinal tract (Sender et al., 2016). The oral cavity is estimated to contain approximately 10^9 bacteria per milliliter of saliva. The stomach harbors a relatively smaller number of species and a less complex microbiota, with bacterial concentrations ranging from 10^3 to 10^4 bacteria per milliliter. The density of bacteria gradually increases in the small intestine, with the duodenum and jejunum contain between 10^3 and 10^4 bacteria per milliliter, and the ileum exhibiting a higher microbial concentration of approximately 10^8 bacteria per milliliter. The large intestine hosts the most diverse and complex ecosystem, with bacterial concentrations reaching up to 10^{11} bacteria per milliliter of content (Sender et al., 2016). The majority of bacterial species in the gut belong to the Bacteroidetes, Firmicutes, and Proteobacteria phyla, with other notable phyla including Actinobacteria, Fusobacteria, and Verrucomicrobia (Eckburg et al., 2005). In addition to the longitudinal variations, microbial composition differs between the gut mucosa and gut lumen. Limited information exists on mucosa-

associated microbiota compared to those found in feces, due to the complexity of isolating mucosa-associated microorganisms (Juge, 2022; Paone and Cani, 2020). These mucosa-associated microbial communities represent a distinct microbial ecosystem separate from luminal microbiota, differing significantly in microbial diversity and composition (Juge, 2022; Ringel et al., 2015). Dysbiosis, characterized by a persistent perturbation of the gut microbiota, has been implicated in the development and progression of numerous health conditions, including metabolic and autoimmune disorders, inflammatory bowel diseases, and certain types of cancer (Brennan and Garrett, 2016; Caruso et al., 2020; De Luca and Shoenfeld, 2018; Fan and Pedersen, 2021).

The upper and lower respiratory tract have distinct microbiota and microbial loads (Natalini et al., 2023). The upper respiratory tract, which includes the nasal cavity, paranasal sinuses, pharynx, and supraglottic larynx, is densely colonized with bacteria, exhibiting spatial differences (Natalini et al., 2023). The nasal cavity and nasopharynx are dominated by *Moraxella*, *Staphylococcus*, *Corynebacterium*, *Haemophilus*, and *Streptococcus* species, while the oropharynx is rich in *Prevotella*, *Veillonella*, *Streptococcus*, *Leptotrichia*, *Rothia*, *Neisseria*, and *Haemophilus* species (De Steenhuijsen Piters et al., 2020; Natalini et al., 2023). In contrast, the lower respiratory tract, which consists of the trachea and lungs, has a relatively low microbial biomass. Once believed to be a sterile environment, it is now recognized that the lungs are regularly exposed to a variety of microorganisms (Natalini et al., 2023). The most common phyla in the lungs are Firmicutes and Bacteroidetes, with *Prevotella*, *Streptococcus*, and *Veillonella* being the most dominant genera (Dickson et al., 2017; Natalini et al., 2023). Similar to the gut microbiota, dysbiosis in the respiratory tract microbiota has been associated to various lung diseases such as cystic fibrosis, asthma, and chronic obstructive pulmonary disease (Huang et al., 2011; LiPuma, 2010; Natalini et al., 2023; Sze et al., 2012; Teo et al., 2015).

The skin is primary barrier against external threats and harbors a diverse population of microbes. Most of these microbes are either commensals, harmless permanent residents, or transient, temporary members of the skin microbiota (Pistone et al., 2021). The skin surface conditions vary due to anatomical differences, which results in different microbial communities. In addition to skin topography, other factors, such as age, sex, or environmental conditions also influence the skin microbiota composition (Dimitriu et al., 2019; Fierer et al., 2008; Luna, 2020; Ross et al., 2017; Zhai et al., 2018).

Common skin commensals belong to four main phyla: Actinobacteria, Firmicutes, Proteobacteria, and Bacteroidetes (Pistone et al., 2021). The skin topography can be divided into three main microenvironment types based on moisture and oil levels: oily/sebaceous areas (forehead, upper back, external auditory canal, and nose), dry areas (forearm, palm of the hand, and lower back), and moist areas (armpits, backs of knees, inner elbow, nostrils, and groin) (Grice et al., 2009; Pistone et al., 2021). Specific microbes prefer different skin microenvironments, with *Propionibacterium* in sebaceous areas, *Corynebacterium* and *Staphylococcus* in moist zones, and β -Proteobacteria and Flavobacteriales in dry sites (Grice et al., 2009; Pistone et al., 2021). Dysbiosis of skin microbiota is linked to various skin diseases, such as rosacea (Jarmuda et al., 2012; Whitfeld et al., 2011; Yang, 2018), atopic dermatitis (Geoghegan et al., 2018; Ong and Leung, 2016), and psoriasis (Pistone et al., 2021; Thio, 2018; Yan et al., 2017).

The vaginal microbiome is unique, exhibiting lower diversity compared to microbial communities found elsewhere in the body. It is often dominated by only one or few species of *Lactobacillus* (France et al., 2022; Witkin and Linhares, 2017). *Lactobacillus* members produce lactic acid, lowering pH to inhibit growth of potential pathogens and benefit the host epithelium through immune modulation (Aldunate et al., 2015; Boskey et al., 1999; France et al., 2022; O'Hanlon et al., 2013). Changes in vaginal microbiota composition have been associated with increased risks of acquiring HIV and other sexually transmitted infections like gonorrhea, chlamydia, and herpes simplex virus 2 (Brotman et al., 2010; Chernes et al., 2003; France et al., 2022; Gosmann et al., 2017; Van Houdt et al., 2018).

Within-host microbiota evolution

Microbial communities have evolved over millions of years with their mammalian hosts, resulting in well-adapted commensal strains to the specific ecological niches within their host species' environment (Dapa et al., 2023; Moeller et al., 2016). Recent research in mouse and human microbiomes using time-resolved sequencing, has shown that genetic changes can occur rapidly within gut microbial populations, with changes occurring within months or even days (Barroso-Batista et al., 2020, 2014; Dapa et al.,

2023, 2022; Garud et al., 2019; Lescat et al., 2017; Vasquez et al., 2021; Zhao et al., 2019). The evolutionary selection pressures on gut microbiota are shaped by interactions with the host and other microbial community members (Dapa et al., 2023). Experimental evolution experiments in murine models have shown that *E. coli* evolution is predictable across hosts with similar diets and genetic backgrounds, although the specific patterns of mutations can vary under different host conditions (Barroso-Batista et al., 2020; Dapa et al., 2023; Vasquez et al., 2021). External host factors, such as diet, can also influence the evolution of gut microbiota. In a murine model, *Bacteroides thetaiotaomicron* acquires different mutations depending on whether the diet is high in plant polysaccharides and fiber or high in fat and simple sugars, with the latter selecting for mutants that have an ability to degrade mucin-derived glycans (Dapa et al., 2023, 2022). Additionally, interactions with other microbiota members affect evolutionary pressures. For example, co-colonization with *Blautia coccoides* alters *E. coli* evolution, shifting from mutations that increase *E. coli*'s ability to compete for amino acids to those favoring anaerobic respiration (Barroso-Batista et al., 2020; Dapa et al., 2023).

Evolution within the gut microbiota can significantly impact various functions including metabolic phenotypes, drug breakdown, antibiotic resistance, and resistance against pathogens (Barroso-Batista et al., 2020; Dapa et al., 2023, 2022).

Colonization resistance

Intestinal microbiota plays an important role in the development of the host immune system, maintenance of tissue integrity, production of vitamins, and establishment of colonization resistance (Lawley and Walker, 2013). Colonization resistance refers to the capacity of the host's indigenous microbiota to protect the host against the invasion of pathogens, or against the overgrowth of resident bacterial populations typically present within the microbiome (Lawley and Walker, 2013). The initial colonization of the gastrointestinal tract commences immediately postpartum and is characterized by the establishment of simple microbial communities that are shaped by the local environment (Lawley and Walker, 2013; Palmer et al., 2007). During vaginal delivery, the infant's initial microbiome exposure is to the maternal birth canal and

intestinal microbiota, while during caesarean section delivery, the infant is more exposed to the maternal skin and the hospital environment microbes (Dominguez-Bello et al., 2010; Jangi and Lamont, 2010; Koenig et al., 2011; Lawley and Walker, 2013; Wampach et al., 2017). The composition of the infant's gut microbiota is significantly influenced by the infant's diet in the postpartum period (Lawley and Walker, 2013). Breast-fed infants exhibit a gut microbiota dominated by *Bifidobacterium* and *Bacteroides* species due to the growth-promoting oligosaccharides present in human milk. In contrast, formula-fed infants exhibit a microbiota that is temporarily more diverse with less dominant *Bifidobacterium* members (Harmsen et al., 2000; Lawley and Walker, 2013; Ma et al., 2020; Zivkovic et al., 2011). Weaning period introduces complex dietary carbohydrates that induce significant changes in microbiota composition, leading to the development of a dense and diverse adult-like microbiota (Lawley and Walker, 2013; Palmer et al., 2007). Although the adult intestinal microbiota is relatively stable, its composition fluctuates with dietary changes, antibiotic treatments, and intestinal diseases (Lawley and Walker, 2013; Li et al., 2021; Patangia et al., 2022; Zmora et al., 2019). In healthy hosts, despite exposure to intestinal pathogens, disease is rare due to the failure of pathogens to establish successful colonization. Dysbiosis of intestinal microbiota increases the risk of pathogen infection. The protective mechanisms conferred by the microbiota are complex and may be direct or indirect (Lawley and Walker, 2013).

Direct mechanisms of colonization resistance take place between bacteria, and can include production of inhibitory compounds, competition for resources and contact-dependent inhibition (Caballero-Flores et al., 2022). Diverse and healthy microbiota fills a wide range of available niches, competing with pathogens for available nutrients, such as carbohydrates, amino acids, and micronutrients like iron and zinc (Behnsen et al., 2021; Caballero-Flores et al., 2022; Deriu et al., 2013; Fuchs, 2023). Another direct mechanism is production of various antimicrobial compounds, including bacteriocins, short-chain fatty acids, and secondary metabolites. Short-chain fatty acids (SCFAs), produced by microbial fermentation of polysaccharides, inhibit the growth of pathogenic *Escherichia coli*, *Citrobacter rodentium*, and *Salmonella enterica* (Caballero-Flores et al., 2022; Gantois et al., 2006; Immerseel et al., 2004; Osbelt et al., 2020; Shin et al., 2002). Primary bile acids are synthesized by the host are modified by gut microbiota into secondary bile acids which inhibit many Gram-positive bacteria including *Clostridium difficile* (Buffie et al., 2015; Caballero-Flores et al., 2022). Some direct mechanisms

require direct cell-cell contact (Caballero-Flores et al., 2022). Contact-dependent inhibition was first discovered in *E. coli*, and mediated by type V secretion system (Aoki et al., 2005; Caballero-Flores et al., 2022). The discovery of contact-dependent inhibition in *E. coli* has since led to the identification of similar systems in other bacterial species, highlighting the importance of contact-dependent mechanisms in microbial competition (Caballero-Flores et al., 2022; Ikryannikova et al., 2020).

Intestinal bacteria and their metabolites can stimulate the intestinal immune system, impacting epithelial cell health, and provide colonization resistance against pathogens through indirect means (Caballero-Flores et al., 2022). For instance, the microbiota stimulates the production of various antimicrobial peptides and proteins by host epithelial cells, such as lipocalin 2, which sequesters bacterial iron-scavenging siderophores, limiting iron acquisition (Caballero-Flores et al., 2022; Singh et al., 2016). Moreover, the gut microbiota influences induction of intestinal Th17 cells cytokine production, which leads to increased resistance to *Citrobacter rodentium* infection (Caballero-Flores et al., 2022; Ivanov et al., 2009).

Pathogens evolved various strategies to overcome colonization resistance. These strategies include altering gut environment and outcompeting resident microbiota (Caballero-Flores et al., 2022). For instance, *S. Typhimurium* uses the type III secretion system (T3SS) to induce host metabolic changes and trigger inflammation, creating favorable conditions for its growth (Caballero-Flores et al., 2022; Fattinger et al., 2021). Furthermore, pathogens can engage in direct inhibition against resident microbiota through systems like the Type VI secretion system (T6SS). *Vibrio cholerae* utilizes its T6SS to kill competing *E. coli*, allowing successful colonization (Caballero-Flores et al., 2022; Zhao et al., 2018). Another intestinal pathogen, *Shigella sonnei* uses its T6SS that can target *E. coli*, and a relative *Shigella flexneri*, enhancing its ability to outcompete resident microbiota and establish colonization (Anderson et al., 2017; Caballero-Flores et al., 2022).

Antibiotics and gut microbiota

Antibiotic exposure can impact gut microbiota by reducing overall diversity, causing the loss of important taxa, metabolic shifts, reduced colonization resistance, and the development of antibiotic resistance (Lange et al., 2016). Shortly after treatment, increase in antibiotic resistance genes has been noted, even against drug classes not directly administered (Lange et al., 2016; Looft et al., 2014, 2012). Different classes of antibiotics have varying effects on the gut microbiota, ranging from transient changes in microbiota composition, to longer lasting changes in the microbiome, including the emergence of increased prevalence of antibiotic resistance genes (Lange et al., 2016). These changes in microbial composition have been linked to a number of diseases, including inflammatory bowel disease, type 1 diabetes, rheumatoid arthritis, atopy, and asthma (Keeney et al., 2014). Additionally, antibiotic-induced alterations are also known to compromise microbiota's ability to protect against invading pathogens, including *Clostridium difficile* and *Salmonella Typhimurium* (Barthel et al., 2003; Lange et al., 2016; Schubert et al., 2015).

Glycans and gut microbiota

Glycans are polymers composed of multiple simple sugars linked together by covalent bonds. Glycans may be attached to other molecules, such as lipids, forming glycolipids, or proteins, forming glycoproteins (Koropatkin et al., 2012). Dietary and host-derived glycans play important role in shaping the gut microbiota function and composition. The biochemistry of host and dietary glycans of mammalian gut is highly diverse, with many different glycosidic linkages requiring specific degradative enzymes (Koropatkin et al., 2012). The diversity of gut microorganisms is reflected in their glycan-degrading capabilities. For instance, *Bacteroides thetaiotaomicron*, the human gut symbiont, is able to degrade over a dozen different glycans, while others are limited to targeting only one or a few (Koropatkin et al., 2012; Salyers et al., 1977a, 1977b). No single gut microbe can degrade all host and dietary glycans, rather, different strains are specialized in breaking down specific glycans (Koropatkin et al., 2012).

The *B4galnt2* gene

The *B4galnt2* gene encodes the enzyme beta-1,4-N-acetyl-galactosaminyltransferase 2, responsible for the transfer of N-acetylgalactosamine (GalNAc) to the sub-terminal galactose of α-2,3-linked sialic acid-containing glycans. This enzyme was first identified in the kidneys of guinea pigs (Duca et al., 2022; Serafini-Cessi et al., 1986; Serafini-Cessi and Dall'Olio, 1983). Subsequently, the *B4galnt2* gene was cloned from both mice and humans (Lo Presti, 2003; Montiel et al., 2003; Smith and Lowe, 1994). *B4galnt2* plays important role in the modification of glycan structures on the surface of epithelial cells, particularly in the gastrointestinal tract. The expression of the *B4galnt2* gene varies among different tissues and organisms, and it has been linked to various physiological and pathological processes (Duca et al., 2022). Alterations in *B4galnt2* expression patterns have been shown to impact immune responses, regulate physiological mechanisms, and affect microbial colonization (Dall'Olio et al., 2014; Duca et al., 2022). Notably, *B4galnt2* intestinal expression has been implicated in the modulation of host-microbe interactions by affecting the composition and functions of the gut microbiota (Duca et al., 2022; Rausch et al., 2015; Vallier et al., 2023).

Aims of the study

The aim of this thesis is to investigate the intricate interplay between differential expression of the *B4galnt2* gene, microbial diversity, and their combined impact on colonization resistance against intestinal infections. Through comprehensive analysis and experimental investigation, this research seeks to illuminate the multifaceted roles of *B4galnt2* expression and its associated microbiota in modulating host-pathogen interactions and shaping the dynamics of intestinal health.

References

- Aldunate, M., Srbinovski, D., Hearps, A.C., Latham, C.F., Ramsland, P.A., Gugasyan, R., Cone, R.A., Tachedjian, G., 2015. Antimicrobial and immune modulatory effects of lactic acid and short chain fatty acids produced by vaginal microbiota associated with eubiosis and bacterial vaginosis. *Front. Physiol.* 6. <https://doi.org/10.3389/fphys.2015.00164>
- Anderson, M.C., Vonaesch, P., Saffarian, A., Marteyn, B.S., Sansonetti, P.J., 2017. *Shigella sonnei* Encodes a Functional T6SS Used for Interbacterial Competition and Niche Occupancy. *Cell Host & Microbe* 21, 769-776.e3. <https://doi.org/10.1016/j.chom.2017.05.004>
- Antinozzi, M., Giffi, M., Sini, N., Gallè, F., Valeriani, F., De Vito, C., Liguori, G., Romano Spica, V., Cattaruzza, M.S., 2022. Cigarette Smoking and Human Gut Microbiota in Healthy Adults: A Systematic Review. *Biomedicines* 10, 510. <https://doi.org/10.3390/biomedicines10020510>
- Aoki, S.K., Pamma, R., Hernday, A.D., Bickham, J.E., Braaten, B.A., Low, D.A., 2005. Contact-Dependent Inhibition of Growth in *Escherichia coli*. *Science* 309, 1245–1248. <https://doi.org/10.1126/science.1115109>
- Barroso-Batista, J., Pedro, M.F., Sales-Dias, J., Pinto, C.J.G., Thompson, J.A., Pereira, H., Demengeot, J., Gordo, I., Xavier, K.B., 2020. Specific Eco-evolutionary Contexts in the Mouse Gut Reveal *Escherichia coli* Metabolic Versatility. *Current Biology* 30, 1049-1062.e7. <https://doi.org/10.1016/j.cub.2020.01.050>
- Barroso-Batista, J., Sousa, A., Lourenço, M., Bergman, M.-L., Sobral, D., Demengeot, J., Xavier, K.B., Gordo, I., 2014. The First Steps of Adaptation of *Escherichia coli* to the Gut Are Dominated by Soft Sweeps. *PLoS Genet* 10, e1004182. <https://doi.org/10.1371/journal.pgen.1004182>
- Barthel, M., Hapfelmeier, S., Quintanilla-Martínez, L., Kremer, M., Rohde, M., Hogardt, M., Pfeffer, K., Rüssmann, H., Hardt, W.-D., 2003. Pretreatment of Mice with Streptomycin Provides a *Salmonella enterica* Serovar Typhimurium Colitis Model That Allows Analysis of Both Pathogen and Host. *Infect Immun* 71, 2839–2858. <https://doi.org/10.1128/IAI.71.5.2839-2858.2003>
- Behnsen, J., Zhi, H., Aron, A.T., Subramanian, V., Santus, W., Lee, M.H., Gerner, R.R., Petras, D., Liu, J.Z., Green, K.D., Price, S.L., Camacho, J., Hillman, H., Tjokrosurjo, J., Montaldo, N.P., Hoover, E.M., Treacy-Abarca, S., Gilston, B.A., Skaar, E.P., Chazin, W.J., Garneau-Tsodikova, S., Lawrenz, M.B., Perry, R.D., Nuccio, S.-P., Dorrestein,

P.C., Raffatellu, M., 2021. Siderophore-mediated zinc acquisition enhances enterobacterial colonization of the inflamed gut. *Nat Commun* 12, 7016. <https://doi.org/10.1038/s41467-021-27297-2>

Blekhman, R., Goodrich, J.K., Huang, K., Sun, Q., Bukowski, R., Bell, J.T., Spector, T.D., Keinan, A., Ley, R.E., Gevers, D., Clark, A.G., 2015. Host genetic variation impacts microbiome composition across human body sites. *Genome Biol* 16, 191. <https://doi.org/10.1186/s13059-015-0759-1>

Boskey, E.R., Telsch, K.M., Whaley, K.J., Moench, T.R., Cone, R.A., 1999. Acid Production by Vaginal Flora In Vitro Is Consistent with the Rate and Extent of Vaginal Acidification. *Infect Immun* 67, 5170–5175. <https://doi.org/10.1128/IAI.67.10.5170-5175.1999>

Brennan, C.A., Garrett, W.S., 2016. Gut Microbiota, Inflammation, and Colorectal Cancer. *Annu. Rev. Microbiol.* 70, 395–411. <https://doi.org/10.1146/annurev-micro-102215-095513>

Brotman, R.M., Klebanoff, M.A., Nansel, T.R., Yu, K.F., Andrews, W.W., Zhang, J., Schwebke, J.R., 2010. Bacterial Vaginosis Assessed by Gram Stain and Diminished Colonization Resistance to Incident Gonococcal, Chlamydial, and Trichomonal Genital Infection. *J INFECT DIS* 202, 1907–1915. <https://doi.org/10.1086/657320>

Buffie, C.G., Bucci, V., Stein, R.R., McKenney, P.T., Ling, L., Gobourne, A., No, D., Liu, H., Kinnebrew, M., Viale, A., Littmann, E., Van Den Brink, M.R.M., Jenq, R.R., Taur, Y., Sander, C., Cross, J.R., Toussaint, N.C., Xavier, J.B., Pamer, E.G., 2015. Precision microbiome reconstitution restores bile acid mediated resistance to *Clostridium difficile*. *Nature* 517, 205–208. <https://doi.org/10.1038/nature13828>

Caballero-Flores, G., Pickard, J.M., Núñez, G., 2022. Microbiota-mediated colonization resistance: mechanisms and regulation. *Nat Rev Microbiol.* <https://doi.org/10.1038/s41579-022-00833-7>

Cahana, I., Iraqi, F.A., 2020. Impact of host genetics on gut microbiome: Take-home lessons from human and mouse studies. *Anim Models and Exp Med* 3, 229–236. <https://doi.org/10.1002/ame.212134>

Caruso, R., Lo, B.C., Núñez, G., 2020. Host–microbiota interactions in inflammatory bowel disease. *Nat Rev Immunol* 20, 411–426. <https://doi.org/10.1038/s41577-019-0268-7>

Chernes, T.L., Meyn, L.A., Krohn, M.A., Lurie, J.G., Hillier, S.L., 2003. Association between Acquisition of Herpes Simplex Virus Type 2 in Women and Bacterial Vaginosis. *Clinical Infectious Diseases* 37, 319–325. <https://doi.org/10.1086/375819>

- Dall'Olio, F., Malagolini, N., Chiricolo, M., Trinchera, M., Harduin-Lepers, A., 2014. The expanding roles of the Sda/Cad carbohydrate antigen and its cognate glycosyltransferase *B4GALNT2*. *Biochimica et Biophysica Acta (BBA) - General Subjects* 1840, 443–453. <https://doi.org/10.1016/j.bbagen.2013.09.036>
- Dapa, T., Ramiro, R.S., Pedro, M.F., Gordo, I., Xavier, K.B., 2022. Diet leaves a genetic signature in a keystone member of the gut microbiota. *Cell Host & Microbe* 30, 183-199.e10. <https://doi.org/10.1016/j.chom.2022.01.002>
- Dapa, T., Wong, D.P., Vasquez, K.S., Xavier, K.B., Huang, K.C., Good, B.H., 2023. Within-host evolution of the gut microbiome. *Current Opinion in Microbiology* 71, 102258. <https://doi.org/10.1016/j.mib.2022.102258>
- De Luca, F., Shoenfeld, Y., 2018. The microbiome in autoimmune diseases. *Clinical and Experimental Immunology* 195, 74–85. <https://doi.org/10.1111/cei.13158>
- De Steenhuijsen Piters, W.A.A., Binkowska, J., Bogaert, D., 2020. Early Life Microbiota and Respiratory Tract Infections. *Cell Host & Microbe* 28, 223–232. <https://doi.org/10.1016/j.chom.2020.07.004>
- Deriu, E., Liu, J.Z., Pezeshki, M., Edwards, R.A., Ochoa, R.J., Contreras, H., Libby, S.J., Fang, F.C., Raffatellu, M., 2013. Probiotic Bacteria Reduce *Salmonella Typhimurium* Intestinal Colonization by Competing for Iron. *Cell Host & Microbe* 14, 26–37. <https://doi.org/10.1016/j.chom.2013.06.007>
- Dickson, R.P., Erb-Downward, J.R., Freeman, C.M., McCloskey, L., Falkowski, N.R., Huffnagle, G.B., Curtis, J.L., 2017. Bacterial Topography of the Healthy Human Lower Respiratory Tract. *mBio* 8, e02287-16. <https://doi.org/10.1128/mBio.02287-16>
- Dimitriu, P.A., Iker, B., Malik, K., Leung, H., Mohn, W.W., Hillebrand, G.G., 2019. New Insights into the Intrinsic and Extrinsic Factors That Shape the Human Skin Microbiome. *mBio* 10, e00839-19. <https://doi.org/10.1128/mBio.00839-19>
- Dominguez-Bello, M.G., Costello, E.K., Contreras, M., Magris, M., Hidalgo, G., Fierer, N., Knight, R., 2010. Delivery mode shapes the acquisition and structure of the initial microbiota across multiple body habitats in newborns. *Proc. Natl. Acad. Sci. U.S.A.* 107, 11971–11975. <https://doi.org/10.1073/pnas.1002601107>
- Duca, M., Malagolini, N., Dall'Olio, F., 2022. The story of the Sda antigen and of its cognate enzyme B4GALNT2: What is new? *Glycoconj J.* <https://doi.org/10.1007/s10719-022-10089-1>

- Eckburg, P.B., Bik, E.M., Bernstein, C.N., Purdom, E., Dethlefsen, L., Sargent, M., Gill, S.R., Nelson, K.E., Relman, D.A., 2005. Diversity of the Human Intestinal Microbial Flora. *Science* 308, 1635–1638. <https://doi.org/10.1126/science.1110591>
- Fan, Y., Pedersen, O., 2021. Gut microbiota in human metabolic health and disease. *Nat Rev Microbiol* 19, 55–71. <https://doi.org/10.1038/s41579-020-0433-9>
- Fattinger, S.A., Sellin, M.E., Hardt, W.-D., 2021. *Salmonella* effector driven invasion of the gut epithelium: breaking in and setting the house on fire. *Current Opinion in Microbiology* 64, 9–18. <https://doi.org/10.1016/j.mib.2021.08.007>
- Fierer, N., Hamady, M., Lauber, C.L., Knight, R., 2008. The influence of sex, handedness, and washing on the diversity of hand surface bacteria. *Proc. Natl. Acad. Sci. U.S.A.* 105, 17994–17999. <https://doi.org/10.1073/pnas.0807920105>
- France, M., Alizadeh, M., Brown, S., Ma, B., Ravel, J., 2022. Towards a deeper understanding of the vaginal microbiota. *Nat Microbiol* 7, 367–378. <https://doi.org/10.1038/s41564-022-01083-2>
- Fuchs, L.M., 2023. Identification of carbon and nitrogen sources promoting *Salmonella* Typhimurium gut colonization. ETH Zurich. <https://doi.org/10.3929/ETHZ-B-000642973>
- Gantois, I., Ducatelle, R., Pasmans, F., Haesebrouck, F., Hautefort, I., Thompson, A., Hinton, J.C., Van Immerseel, F., 2006. Butyrate Specifically Down-Regulates *Salmonella* Pathogenicity Island 1 Gene Expression. *Appl Environ Microbiol* 72, 946–949. <https://doi.org/10.1128/AEM.72.1.946-949.2006>
- García-Peña, C., Álvarez-Cisneros, T., Quiroz-Baez, R., Friedland, R.P., 2017. Microbiota and Aging. A Review and Commentary. *Archives of Medical Research* 48, 681–689. <https://doi.org/10.1016/j.arcmed.2017.11.005>
- Garud, N.R., Good, B.H., Hallatschek, O., Pollard, K.S., 2019. Evolutionary dynamics of bacteria in the gut microbiome within and across hosts. *PLoS Biol* 17, e3000102. <https://doi.org/10.1371/journal.pbio.3000102>
- Geoghegan, J.A., Irvine, A.D., Foster, T.J., 2018. *Staphylococcus aureus* and Atopic Dermatitis: A Complex and Evolving Relationship. *Trends in Microbiology* 26, 484–497. <https://doi.org/10.1016/j.tim.2017.11.008>
- Gosmann, C., Anahtar, M.N., Handley, S.A., Farcasanu, M., Abu-Ali, G., Bowman, B.A., Padavattan, N., Desai, C., Droit, L., Moodley, A., Dong, M., Chen, Y., Ismail, N., Ndung'u, T., Ghebremichael, M.S., Wesemann, D.R., Mitchell, C., Dong, K.L., Huttenhower, C., Walker, B.D., Virgin, H.W., Kwon, D.S., 2017. Lactobacillus-Deficient Cervicovaginal Bacterial Communities Are Associated with Increased

HIV Acquisition in Young South African Women. *Immunity* 46, 29–37.
<https://doi.org/10.1016/j.immuni.2016.12.013>

Grice, E.A., Kong, H.H., Conlan, S., Deming, C.B., Davis, J., Young, A.C., NISC Comparative Sequencing Program, Bouffard, G.G., Blakesley, R.W., Murray, P.R., Green, E.D., Turner, M.L., Segre, J.A., 2009. Topographical and Temporal Diversity of the Human Skin Microbiome. *Science* 324, 1190–1192.
<https://doi.org/10.1126/science.1171700>

Harmsen, H.J.M., Wildeboer-Veloo, A.C.M., Raangs, G.C., Wagendorp, A.A., Klijn, N., Bindels, J.G., Welling, G.W., 2000. Analysis of Intestinal Flora Development in Breast-Fed and Formula-Fed Infants by Using Molecular Identification and Detection Methods: *Journal of Pediatric Gastroenterology and Nutrition* 30, 61–67. <https://doi.org/10.1097/00005176-200001000-00019>

Huang, Y.J., Nelson, C.E., Brodie, E.L., DeSantis, T.Z., Baek, M.S., Liu, J., Woyke, T., Allgaier, M., Bristow, J., Wiener-Kronish, J.P., Sutherland, E.R., King, T.S., Icitovic, N., Martin, R.J., Calhoun, W.J., Castro, M., Denlinger, L.C., DiMango, E., Kraft, M., Peters, S.P., Wasserman, S.I., Wechsler, M.E., Boushey, H.A., Lynch, S.V., 2011. Airway microbiota and bronchial hyperresponsiveness in patients with suboptimally controlled asthma. *Journal of Allergy and Clinical Immunology* 127, 372–381.e3. <https://doi.org/10.1016/j.jaci.2010.10.048>

Ikryannikova, L.N., Kurbatov, L.K., Gorokhovets, N.V., Zamyatnin, A.A., 2020. Contact-Dependent Growth Inhibition in Bacteria: Do Not Get Too Close! *IJMS* 21, 7990. <https://doi.org/10.3390/ijms21217990>

Immerseel, F.V., Buck, J.D., Smet, I.D., Pasmans, F., Haesebrouck, F., Ducatelle, R., 2004. Interactions of Butyric Acid- and Acetic Acid-Treated *Salmonella* with Chicken Primary Cecal Epithelial Cells In Vitro. *Avian Diseases* 48, 384–391. <https://doi.org/10.1637/7094>

Ivanov, I.I., Atarashi, K., Manel, N., Brodie, E.L., Shima, T., Karaoz, U., Wei, D., Goldfarb, K.C., Santee, C.A., Lynch, S.V., Tanoue, T., Imaoka, A., Itoh, K., Takeda, K., Umesaki, Y., Honda, K., Littman, D.R., 2009. Induction of Intestinal Th17 Cells by Segmented Filamentous Bacteria. *Cell* 139, 485–498. <https://doi.org/10.1016/j.cell.2009.09.033>

Jangi, S., Lamont, J.T., 2010. Asymptomatic Colonization by *Clostridium difficile* in Infants: Implications for Disease in Later Life. *J. pediatr. gastroenterol. nutr.* 51, 2–7. <https://doi.org/10.1097/MPG.0b013e3181d29767>

- Jarmuda, S., O'Reilly, N., Źaba, R., Jakubowicz, O., Szkaradkiewicz, A., Kavanagh, K., 2012. Potential role of Demodex mites and bacteria in the induction of rosacea. *Journal of Medical Microbiology* 61, 1504–1510. <https://doi.org/10.1099/jmm.0.048090-0>
- Juge, N., 2022. Relationship between mucosa-associated gut microbiota and human diseases. *Biochemical Society Transactions* 50, 1225–1236. <https://doi.org/10.1042/BST20201201>
- Keeney, K.M., Yurist-Doutsch, S., Arrieta, M.-C., Finlay, B.B., 2014. Effects of Antibiotics on Human Microbiota and Subsequent Disease. *Annu. Rev. Microbiol.* 68, 217–235. <https://doi.org/10.1146/annurev-micro-091313-103456>
- Koenig, J.E., Spor, A., Scalfone, N., Fricker, A.D., Stombaugh, J., Knight, R., Angenent, L.T., Ley, R.E., 2011. Succession of microbial consortia in the developing infant gut microbiome. *Proc. Natl. Acad. Sci. U.S.A.* 108, 4578–4585. <https://doi.org/10.1073/pnas.1000081107>
- Koropatkin, N.M., Cameron, E.A., Martens, E.C., 2012. How glycan metabolism shapes the human gut microbiota. *Nat Rev Microbiol* 10, 323–335. <https://doi.org/10.1038/nrmicro2746>
- Lange, K., Buerger, M., Stallmach, A., Bruns, T., 2016. Effects of Antibiotics on Gut Microbiota. *Dig Dis* 34, 260–268. <https://doi.org/10.1159/000443360>
- Lawley, T.D., Walker, A.W., 2013. Intestinal colonization resistance. *Immunology* 138, 1–11. <https://doi.org/10.1111/j.1365-2567.2012.03616.x>
- Lescat, M., Launay, A., Ghalayini, M., Magnan, M., Glodt, J., Pintard, C., Dion, S., Denamur, E., Tenaillon, O., 2017. Using long-term experimental evolution to uncover the patterns and determinants of molecular evolution of an *Escherichia coli* natural isolate in the streptomycin-treated mouse gut. *Molecular Ecology* 26, 1802–1817. <https://doi.org/10.1111/mec.13851>
- Li, Y., Xia, S., Jiang, X., Feng, C., Gong, S., Ma, J., Fang, Z., Yin, J., Yin, Y., 2021. Gut Microbiota and Diarrhea: An Updated Review. *Front. Cell. Infect. Microbiol.* 11, 625210. <https://doi.org/10.3389/fcimb.2021.625210>
- LiPuma, J.J., 2010. The Changing Microbial Epidemiology in Cystic Fibrosis. *Clin Microbiol Rev* 23, 299–323. <https://doi.org/10.1128/CMR.00068-09>
- Lo Presti, L., 2003. Molecular Cloning of the Human 1,4-N-Acetylgalactosaminyltransferase Responsible for the Biosynthesis of the Sda Histo-Blood Group Antigen: The Sequence Predicts a Very Long Cytoplasmic

Domain. Journal of Biochemistry 134, 675–682.
<https://doi.org/10.1093/jb/mvg192>

Looft, T., Allen, H.K., Cantarel, B.L., Levine, U.Y., Bayles, D.O., Alt, D.P., Henrissat, B., Stanton, T.B., 2014. Bacteria, phages and pigs: the effects of in-feed antibiotics on the microbiome at different gut locations. *The ISME Journal* 8, 1566–1576.
<https://doi.org/10.1038/ismej.2014.12>

Looft, T., Johnson, T.A., Allen, H.K., Bayles, D.O., Alt, D.P., Stedtfeld, R.D., Sul, W.J., Stedtfeld, T.M., Chai, B., Cole, J.R., Hashsham, S.A., Tiedje, J.M., Stanton, T.B., 2012. In-feed antibiotic effects on the swine intestinal microbiome. *Proceedings of the National Academy of Sciences* 109, 1691–1696.
<https://doi.org/10.1073/pnas.1120238109>

Lopera-Maya, E.A., Kurilshikov, A., Van Der Graaf, A., Hu, S., Andreu-Sánchez, S., Chen, L., Vila, A.V., Gacesa, R., Sinha, T., Collij, V., Klaassen, M.A.Y., Bolte, L.A., Gois, M.F.B., Neerincx, P.B.T., Swertz, M.A., LifeLines Cohort Study, Aguirre-Gamboa, R., Deelen, P., Franke, L., Kuivenhoven, J.A., Lopera-Maya, E.A., Nolte, I.M., Sanna, S., Snieder, H., Swertz, M.A., Vonk, J.M., Wijmenga, C., Harmsen, H.J.M., Wijmenga, C., Fu, J., Weersma, R.K., Zhernakova, A., Sanna, S., 2022. Effect of host genetics on the gut microbiome in 7,738 participants of the Dutch Microbiome Project. *Nat Genet* 54, 143–151. <https://doi.org/10.1038/s41588-021-00992-y>

Luna, P.C., 2020. Skin Microbiome as Years Go By. *Am J Clin Dermatol* 21, 12–17.
<https://doi.org/10.1007/s40257-020-00549-5>

Ma, J., Li, Z., Zhang, W., Zhang, C., Zhang, Y., Mei, H., Zhuo, N., Wang, H., Wang, L., Wu, D., 2020. Comparison of gut microbiota in exclusively breast-fed and formula-fed babies: a study of 91 term infants. *Sci Rep* 10, 15792.
<https://doi.org/10.1038/s41598-020-72635-x>

Moeller, A.H., Caro-Quintero, A., Mjungu, D., Georgiev, A.V., Lonsdorf, E.V., Muller, M.N., Pusey, A.E., Peeters, M., Hahn, B.H., Ochman, H., 2016. Cospeciation of gut microbiota with hominids. *Science* 353, 380–382.
<https://doi.org/10.1126/science.aaf3951>

Montiel, M.-D., Krzewinski-Recchi, M.-A., Delannoy, P., Harduin-Lepers, A., 2003. Molecular cloning, gene organization and expression of the human UDP-GalNAc:Neu5Ac α 2-3Gal β -R beta1,4-N-acetylgalactosaminyltransferase responsible for the biosynthesis of the blood group Sda/Cad antigen: evidence for an unusual extended cytoplasmic domain. *Biochemical Journal* 373, 369–379.
<https://doi.org/10.1042/bj20021892>

- Natalini, J.G., Singh, S., Segal, L.N., 2023. The dynamic lung microbiome in health and disease. *Nat Rev Microbiol* 21, 222–235. <https://doi.org/10.1038/s41579-022-00821-x>
- O'Hanlon, D.E., Moench, T.R., Cone, R.A., 2013. Vaginal pH and Microbicidal Lactic Acid When Lactobacilli Dominate the Microbiota. *PLoS ONE* 8, e80074. <https://doi.org/10.1371/journal.pone.0080074>
- Ong, P.Y., Leung, D.Y.M., 2016. Bacterial and Viral Infections in Atopic Dermatitis: a Comprehensive Review. *Clinic Rev Allerg Immunol* 51, 329–337. <https://doi.org/10.1007/s12016-016-8548-5>
- Osbelt, L., Thiemann, S., Smit, N., Lesker, T.R., Schröter, M., Gálvez, E.J.C., Schmidt-Hohagen, K., Pils, M.C., Mühlen, S., Dersch, P., Hiller, K., Schlüter, D., Neumann-Schaal, M., Strowig, T., 2020. Variations in microbiota composition of laboratory mice influence *Citrobacter rodentium* infection via variable short-chain fatty acid production. *PLoS Pathog* 16, e1008448. <https://doi.org/10.1371/journal.ppat.1008448>
- Palmer, C., Bik, E.M., DiGiulio, D.B., Relman, D.A., Brown, P.O., 2007. Development of the Human Infant Intestinal Microbiota. *PLoS Biol* 5, e177. <https://doi.org/10.1371/journal.pbio.0050177>
- Paone, P., Cani, P.D., 2020. Mucus barrier, mucins and gut microbiota: the expected slimy partners? *Gut* 69, 2232–2243. <https://doi.org/10.1136/gutjnl-2020-322260>
- Patangia, D.V., Anthony Ryan, C., Dempsey, E., Paul Ross, R., Stanton, C., 2022. Impact of antibiotics on the human microbiome and consequences for host health. *MicrobiologyOpen* 11, e1260. <https://doi.org/10.1002/mbo3.1260>
- Pistone, D., Meroni, G., Panelli, S., D'Auria, E., Acunzo, M., Pasala, A.R., Zuccotti, G.V., Bandi, C., Drago, L., 2021. A Journey on the Skin Microbiome: Pitfalls and Opportunities. *IJMS* 22, 9846. <https://doi.org/10.3390/ijms22189846>
- Qin, Y., Havulinna, A.S., Liu, Y., Jousilahti, P., Ritchie, S.C., Tokolyi, A., Sanders, J.G., Valsta, L., Brożyńska, M., Zhu, Q., Tripathi, A., Vázquez-Baeza, Y., Loomba, R., Cheng, S., Jain, M., Niiranen, T., Lahti, L., Knight, R., Salomaa, V., Inouye, M., Méric, G., 2024. Author Correction: Combined effects of host genetics and diet on human gut microbiota and incident disease in a single population cohort. *Nat Genet* 56, 554–554. <https://doi.org/10.1038/s41588-024-01693-y>
- Rausch, P., Steck, N., Suwandi, A., Seidel, J.A., Künzel, S., Bhullar, K., Basic, M., Bleich, A., Johnsen, J.M., Vallance, B.A., Baines, J.F., Grassl, G.A., 2015. Expression of the Blood-

Group-Related Gene *B4galnt2* Alters Susceptibility to *Salmonella* Infection. PLoS Pathog 11, e1005008. <https://doi.org/10.1371/journal.ppat.1005008>

Ringel, Y., Maharshak, N., Ringel-Kulka, T., Wolber, E.A., Sartor, R.B., Carroll, I.M., 2015. High throughput sequencing reveals distinct microbial populations within the mucosal and luminal niches in healthy individuals. Gut Microbes 6, 173–181. <https://doi.org/10.1080/19490976.2015.1044711>

Ross, A.A., Doxey, A.C., Neufeld, J.D., 2017. The Skin Microbiome of Cohabiting Couples. mSystems 2, e00043-17. <https://doi.org/10.1128/mSystems.00043-17>

Rothschild, D., Weissbrod, O., Barkan, E., Kurilshikov, A., Korem, T., Zeevi, D., Costea, P.I., Godneva, A., Kalka, I.N., Bar, N., Shilo, S., Lador, D., Vila, A.V., Zmora, N., Pevsner-Fischer, M., Israeli, D., Kosower, N., Malka, G., Wolf, B.C., Avnit-Sagi, T., Lotan-Pompan, M., Weinberger, A., Halpern, Z., Carmi, S., Fu, J., Wijmenga, C., Zhernakova, A., Elinav, E., Segal, E., 2018. Environment dominates over host genetics in shaping human gut microbiota. Nature 555, 210–215. <https://doi.org/10.1038/nature25973>

Salyers, A.A., Vercellotti, J.R., West, S.E., Wilkins, T.D., 1977a. Fermentation of mucin and plant polysaccharides by strains of *Bacteroides* from the human colon. Appl Environ Microbiol 33, 319–322. <https://doi.org/10.1128/aem.33.2.319-322.1977>

Salyers, A.A., West, S.E., Vercellotti, J.R., Wilkins, T.D., 1977b. Fermentation of mucins and plant polysaccharides by anaerobic bacteria from the human colon. Appl Environ Microbiol 34, 529–533. <https://doi.org/10.1128/aem.34.5.529-533.1977>

Schubert, A.M., Sinani, H., Schloss, P.D., 2015. Antibiotic-Induced Alterations of the Murine Gut Microbiota and Subsequent Effects on Colonization Resistance against *Clostridium difficile*. mBio 6, e00974-15. <https://doi.org/10.1128/mBio.00974-15>

Sender, R., Fuchs, S., Milo, R., 2016. Revised Estimates for the Number of Human and Bacteria Cells in the Body. PLoS Biol 14, e1002533. <https://doi.org/10.1371/journal.pbio.1002533>

Serafini-Cessi, F., Dall'Olio, F., 1983. Guinea-pig kidney β -N-acetylgalactosaminyltransferase towards Tamm-Horsfall glycoprotein. Requirement of sialic acid in the acceptor for transferase activity. Biochemical Journal 215, 483–489. <https://doi.org/10.1042/bj2150483>

Serafini-Cessi, F., Dall'Olio, F., Malagolini, N., 1986. Characterization of N-acetyl- β -d-galactosaminyl-transferase from guinea-pig kidney involved in the biosynthesis of

Sda antigen associated with tamm-horsfall glycoprotein. Carbohydrate Research 151, 65–76. [https://doi.org/10.1016/S0008-6215\(00\)90330-6](https://doi.org/10.1016/S0008-6215(00)90330-6)

Shin, R., Suzuki, M., Morishita, Y., 2002. Influence of intestinal anaerobes and organic acids on the growth of enterohaemorrhagic *Escherichia coli* O157:H7. Journal of Medical Microbiology 51, 201–206. <https://doi.org/10.1099/0022-1317-51-3-201>

Singh, R.K., Chang, H.-W., Yan, D., Lee, K.M., Ucmak, D., Wong, K., Abrouk, M., Farahnik, B., Nakamura, M., Zhu, T.H., Bhutani, T., Liao, W., 2017. Influence of diet on the gut microbiome and implications for human health. J Transl Med 15, 73. <https://doi.org/10.1186/s12967-017-1175-y>

Singh, V., Yeoh, B.S., Chassaing, B., Zhang, B., Saha, P., Xiao, X., Awasthi, D., Shashidharamurthy, R., Dikshit, M., Gewirtz, A., Vijay-Kumar, M., 2016. Microbiota-Inducible Innate Immune Siderophore Binding Protein Lipocalin 2 Is Critical for Intestinal Homeostasis. Cellular and Molecular Gastroenterology and Hepatology 2, 482-498.e6. <https://doi.org/10.1016/j.jcmgh.2016.03.007>

Smith, P.L., Lowe, J.B., 1994. Molecular cloning of a murine N-acetylgalactosamine transferase cDNA that determines expression of the T lymphocyte-specific CT oligosaccharide differentiation antigen. Journal of Biological Chemistry 269, 15162–15171. [https://doi.org/10.1016/S0021-9258\(17\)36587-0](https://doi.org/10.1016/S0021-9258(17)36587-0)

Sze, M.A., Dimitriu, P.A., Hayashi, S., Elliott, W.M., McDonough, J.E., Gosselink, J.V., Cooper, J., Sin, D.D., Mohn, W.W., Hogg, J.C., 2012. The Lung Tissue Microbiome in Chronic Obstructive Pulmonary Disease. Am J Respir Crit Care Med 185, 1073–1080. <https://doi.org/10.1164/rccm.201111-2075OC>

Teo, S.M., Mok, D., Pham, K., Kusel, M., Serralha, M., Troy, N., Holt, B.J., Hales, B.J., Walker, M.L., Hollams, E., Bochkov, Y.A., Grindle, K., Johnston, S.L., Gern, J.E., Sly, P.D., Holt, P.G., Holt, K.E., Inouye, M., 2015. The Infant Nasopharyngeal Microbiome Impacts Severity of Lower Respiratory Infection and Risk of Asthma Development. Cell Host & Microbe 17, 704–715. <https://doi.org/10.1016/j.chom.2015.03.008>

Thio, H.B., 2018. The Microbiome in Psoriasis and Psoriatic Arthritis: The Skin Perspective. J Rheumatol 94, 30–31. <https://doi.org/10.3899/jrheum.180133>

Vallier, M., Suwandi, A., Ehrhardt, K., Belheouane, M., Berry, D., Čepić, A., Galeev, A., Johnsen, J.M., Grassl, G.A., Baines, J.F., 2023. Pathometagenomics reveals susceptibility to intestinal infection by *Morganella* to be mediated by the blood group-related *B4galnt2* gene in wild mice. Gut Microbes 15, 2164448. <https://doi.org/10.1080/19490976.2022.2164448>

- Van Houdt, R., Ma, B., Bruisten, S.M., Speksnijder, A.G.C.L., Ravel, J., De Vries, H.J.C., 2018. *Lactobacillus iners* -dominated vaginal microbiota is associated with increased susceptibility to *Chlamydia trachomatis* infection in Dutch women: a case-control study. *Sex Transm Infect* 94, 117–123. <https://doi.org/10.1136/sextrans-2017-053133>
- Vasquez, K.S., Willis, L., Cira, N.J., Ng, K.M., Pedro, M.F., Aranda-Díaz, A., Rajendram, M., Yu, F.B., Higginbottom, S.K., Neff, N., Sherlock, G., Xavier, K.B., Quake, S.R., Sonnenburg, J.L., Good, B.H., Huang, K.C., 2021. Quantifying rapid bacterial evolution and transmission within the mouse intestine. *Cell Host & Microbe* 29, 1454-1468.e4. <https://doi.org/10.1016/j.chom.2021.08.003>
- Wampach, L., Heintz-Buschart, A., Hogan, A., Muller, E.E.L., Narayanasamy, S., Laczny, C.C., Hugerth, L.W., Bindl, L., Bottu, J., Andersson, A.F., De Beaufort, C., Wilmes, P., 2017. Colonization and Succession within the Human Gut Microbiome by Archaea, Bacteria, and Microeukaryotes during the First Year of Life. *Front. Microbiol.* 8, 738. <https://doi.org/10.3389/fmicb.2017.00738>
- Whitfeld, M., Gunasingam, N., Leow, L.J., Shirato, K., Preda, V., 2011. *Staphylococcus epidermidis*: A possible role in the pustules of rosacea. *Journal of the American Academy of Dermatology* 64, 49–52. <https://doi.org/10.1016/j.jaad.2009.12.036>
- Witkin, S., Linhares, I., 2017. Why do lactobacilli dominate the human vaginal microbiota? *BJOG* 124, 606–611. <https://doi.org/10.1111/1471-0528.14390>
- Yan, D., Issa, N., Afifi, L., Jeon, C., Chang, H.-W., Liao, W., 2017. The Role of the Skin and Gut Microbiome in Psoriatic Disease. *Curr Derm Rep* 6, 94–103. <https://doi.org/10.1007/s13671-017-0178-5>
- Yang, X., 2018. Relationship between *Helicobacter pylori* and Rosacea: review and discussion. *BMC Infect Dis* 18, 318. <https://doi.org/10.1186/s12879-018-3232-4>
- Zhai, W., Huang, Y., Zhang, Xuelei, Fei, W., Chang, Y., Cheng, S., Zhou, Y., Gao, J., Tang, X., Zhang, Xuejun, Yang, S., 2018. Profile of the skin microbiota in a healthy Chinese population. *The Journal of Dermatology* 45, 1289–1300. <https://doi.org/10.1111/1346-8138.14594>
- Zhao, S., Lieberman, T.D., Poyet, M., Kauffman, K.M., Gibbons, S.M., Groussin, M., Xavier, R.J., Alm, E.J., 2019. Adaptive Evolution within Gut Microbiomes of Healthy People. *Cell Host & Microbe* 25, 656-667.e8. <https://doi.org/10.1016/j.chom.2019.03.007>
- Zhao, W., Caro, F., Robins, W., Mekalanos, J.J., 2018. Antagonism toward the intestinal microbiota and its effect on *Vibrio cholerae* virulence. *Science* 359, 210–213. <https://doi.org/10.1126/science.aap8775>

- Zhou, X., Shen, X., Johnson, J.S., Spakowicz, D.J., Agnello, M., Zhou, W., Avina, M., Honkala, A., Chleilat, F., Chen, S.J., Cha, K., Leopold, S., Zhu, C., Chen, L., Lyu, L., Hornburg, D., Wu, S., Zhang, X., Jiang, C., Jiang, Liuyiqi, Jiang, Lihua, Jian, R., Brooks, A.W., Wang, M., Contrepois, K., Gao, P., Rose, S.M.S.-F., Tran, T.D.B., Nguyen, H., Celli, A., Hong, B.-Y., Bautista, E.J., Dorsett, Y., Kavathas, P.B., Zhou, Y., Sodergren, E., Weinstock, G.M., Snyder, M.P., 2024. Longitudinal profiling of the microbiome at four body sites reveals core stability and individualized dynamics during health and disease. *Cell Host & Microbe* 32, 506-526.e9. <https://doi.org/10.1016/j.chom.2024.02.012>
- Zivkovic, A.M., German, J.B., Lebrilla, C.B., Mills, D.A., 2011. Human milk glycobiome and its impact on the infant gastrointestinal microbiota. *Proc. Natl. Acad. Sci. U.S.A.* 108, 4653–4658. <https://doi.org/10.1073/pnas.1000083107>
- Zmora, N., Suez, J., Elinav, E., 2019. You are what you eat: diet, health and the gut microbiota. *Nat Rev Gastroenterol Hepatol* 16, 35–56. <https://doi.org/10.1038/s41575-018-0061-2>
- Zoetendal, E.G., Akkermans, A.D.L., Akkermans-van Vliet, W.M., de Visser, J.A.G.M., de Vos, W.M., 2001. The Host Genotype Affects the Bacterial Community in the Human Gastronintestinal Tract. *Microbial Ecology in Health and Disease* 13, 129–134. <https://doi.org/10.1080/089106001750462669>

Chapter 1: The role of the blood group-related glycosyltransferases *FUT2* and *B4GALNT2* in susceptibility to infectious disease



The role of the blood group-related glycosyltransferases *FUT2* and *B4GALNT2* in susceptibility to infectious disease

Alibek Galeev ^{a,1}, Abdulhadi Suwandi ^{b,1}, Aleksa Cepic ^a, Meghna Basu ^a, John F. Baines ^{a,*},
Guntram A. Grassl ^{b,*}

^a Max Planck Institute for Evolutionary Biology, Plön, Germany and Institute for Experimental Medicine, Kiel University, Kiel, Germany

^b Institute of Medical Microbiology and Hospital Epidemiology, Hannover Medical School and German Center for Infection Research (DZIF), Hannover, Germany

ARTICLE INFO

ABSTRACT

Keywords:
Glycosyltransferases
Histo-blood group antigens
Pathogens
Adhesion
Nutrients
Microbiota

The glycosylation profile of the gastrointestinal tract is an important factor mediating host-microbe interactions. Variation in these glycan structures is often mediated by blood group-related glycosyltransferases, and can lead to wide-ranging differences in susceptibility to both infectious- as well as chronic disease. In this review, we focus on the interplay between host glycosylation, the intestinal microbiota and susceptibility to gastrointestinal pathogens based on studies of two exemplary blood group-related glycosyltransferases that are conserved between mice and humans, namely *FUT2* and *B4GALNT2*. We highlight that differences in susceptibility can arise due to both changes in direct interactions, such as bacterial adhesion, as well as indirect effects mediated by the intestinal microbiota. Although a large body of experimental work exists for direct interactions between host and pathogen, determining the more complex and variable mechanisms underlying three-way interactions involving the intestinal microbiota will be the subject of much-needed future research.

1. Introduction

The vast majority of proteins and lipids in the human body are glycosylated, *i.e.* possess covalently attached sugars, and referred to as glycoproteins and glycolipids. Glycosylation is a co- or post-translational, enzyme-directed modification of glycan structures, and it is involved in a plethora of physiological and pathological processes including aging (Dall'Olio et al., 2013), cancer (Pinho and Reis, 2015), inflammatory diseases (Larsson et al., 2011) and infectious diseases (Moran et al., 2011). In the gastrointestinal tract (GIT), transmembrane glycoproteins (mucins) constitute the glycocalyx protecting the mucosal surfaces, while secreted mucins form mucus layers (Corfield et al., 2001). Notably, most of the 346 histo-blood group antigens described to date are carbohydrates, glycoproteins, or glycolipids (Storry et al., 2016). Originally discovered on the surface of erythrocytes (Landsteiner, 1900), blood group antigens are also expressed in most epithelial tissues and were found in bodily secretions, such as saliva, urine, feces, and milk (Ravn and Dabelsteen, 2000).

The histo-blood group system ABO (H) and the structurally related Lewis histo-blood group are the major human alloantigen systems. ABH

and Lewis antigens decorate the terminal structures of various glycans, including O- or N-glycoproteins, mucins, as well as the glycolipids of the lacto, globo and ganglio series and lactosylceramide (Marionneau et al., 2001). ABH and Lewis antigens are synthesized by a number of different glycosyltransferases acting in a successive manner. For example, addition of an α 1,2-linked fucose to disaccharide precursors creates the Lewis^b and H antigens. Subsequent attachment of N-acetylgalactosamine (GalNAc) or galactose (Gal) residues to H antigen structures creates A or B antigens, respectively (Table 1). These antigens are present in GIT epithelia, in nasal epithelium and in trachea, as well as in the lower genito-urinary tract, and in bodily secretions.

Due to their location in tissues that serve important barrier functions, histo-blood group antigens can mediate important first interactions with microbes (Koropatkin et al., 2012). Accordingly, these structures are frequently involved in the evolutionary arms race between host and pathogen, as evidenced by striking signatures of natural selection at the DNA sequence level (Saitou and Yamamoto, 1997; Fumagalli et al., 2009; Linnenbrink et al., 2011). Variation at histo-blood group genes can influence host-pathogen interactions in at least three ways: either directly by affecting bacterial adhesion and invasion, indirectly via

* Corresponding authors.

E-mail addresses: baines@evolbio.mpg.de (J.F. Baines), grassl.guntram@mh-hannover.de (G.A. Grassl).

¹ Contributed equally.

<https://doi.org/10.1016/j.ijmm.2021.151487>

Received 15 September 2020; Received in revised form 1 February 2021; Accepted 23 February 2021

Available online 25 February 2021

1438-4221/© 2021 The Authors. Published by Elsevier GmbH. This is an open access article under the CC BY-NC-ND license (<http://creativecommons.org/licenses/by-nc-nd/4.0/>).

Table 1
Structures of histo-blood antigens.

Histo-blood antigens	Structure
Blood group H (O)	Fuc α 1-2Gal β 1-3GlcNAc β -
H-1 antigen	Fuc α 1-2Gal β 1-4GlcNAc β -
H-2 antigen	Fuc α 1-2Gal β 1-3GalNAc β -
H-3 antigen	Fuc α 1-2-(GalNAc α 1-3)Gal β -
Blood group A	Fuc α 1-2-(Gal α 1-3)Gal β -
Blood group B	Gal β 1-3-(Fuc α 1-4)GlcNAc β -
Lewis ^a	Fuc α 1-2Gal β 1-3-(Fuc α 1-4)GlcNAc β -
Lewis ^b	Neu5Ac α 2-3Gal β 1-3(Fuc α 1-4)GlcNAc β -
Sialyl-Lewis ^a	Gal β 1-4-(Fuc α 1-3)GlcNAc β -
Lewis ^x	Fuc α 1-2Gal β 1-4(Fuc α 1-3)GlcNAc β -
Lewis ^y	Neu5Ac α 2-3Gal β 1-4(Fuc α 1-3)GlcNAc β -
Sialyl-Lewis ^x	GalNAc β 1-4(Neu5Ac α 2-3)Gal β -R
Core structure Sd ^a /Cad	GalNAc β 1-4(Neu5Ac α 2-3)Gal β -R
Sd ^a antigen	GalNAc β 1-4(Neu5Ac α 2-3)Gal β -R
Cad antigen (glycophorin A)	GalNAc β 1-4(Neu5Ac α 2-3)Gal β 1-3(Neu5Ac α 2-6)GalNAc-Ser/Thr
Cad antigen (glycolipid sialylparagloboside)	GalNAc β 1-4(Neu5Ac α 2-3)Gal β 1-4GlcNAc β 1-3Gal β 1-4Glc-ceramide

modification of gut microbiota composition or as a nutrient source. Excellent recent reviews emphasize an importance of mucosal glycans in bacterial adhesion and bacteria-mucus interactions (Formosa-Dague et al., 2018; Josenhans et al., 2020; Juge, 2019). In this review, we discuss the roles of mucosal *Fut2* and *B4galnt2* histo-blood group-related glycans in susceptibility to microbial infections. We focus on two general modes of action: (i) direct interactions with glycan structures and (ii) indirect effects that may be mediated by the endogenous microbiota.

2. FUT2

In humans, the *FUT2* gene (Chr19q13.33, termed the “secretor gene”) encoding the α -2-fucosyltransferase enzyme is expressed in mucosal tissues by several epithelial cell types (Fig. 1). This enzyme facilitates the transfer of L-fucose (Fuc) residues from the GDP-Fuc precursor to Gal in an α (1,2)-linkage, and thus generates the terminal glycan epitope Fuc α 1-2-Gal β -R (Kelly et al., 1995, p. 2). In individuals with a functional *FUT2* (so-called “secretors”), α (1,2)-fucosylated and poly-fucosylated proteins and lipids are secreted into the gut lumen and also found in abundance on the apical side of the mucosal epithelium (Björk et al., 1987). In mucosal tissues, *FUT2*-dependent, α (1,2)-fucosylated glycans are required to form the ABH and most of the Lewis histo-blood group antigens (Table 1).

The *FUT2* gene displays a high degree of polymorphism in functional- versus non-functional alleles, which varies according to geography (Ferrer-Admetlla et al., 2009). Along with two commonly found functional *FUT2* alleles (Se and Se³⁵⁷), more than 20 different single nucleotide polymorphisms (SNPs) within the *FUT2* gene have been discovered in different populations (Soejima et al., 2012). It is estimated that around 20 % of humans are homozygous for *FUT2*-inactivating nonsense mutations, and are thus “non-secretors” (Koda et al., 2001). In non-secretor individuals, α (1,2)-fucosylated Lewis^b and Lewis^y antigens, as well as all ABH antigens are not produced in mucosal tissues or in bodily secretions (Henry et al., 1995). The frequencies of secretor and non-secretor phenotypes appear to be similar in different human populations (Ferrer-Admetlla et al., 2009). Multiple studies highlighted important roles of the secretor status in various diseases: e.g., secretors were shown to be more susceptible to graft-versus-host disease (Rayes

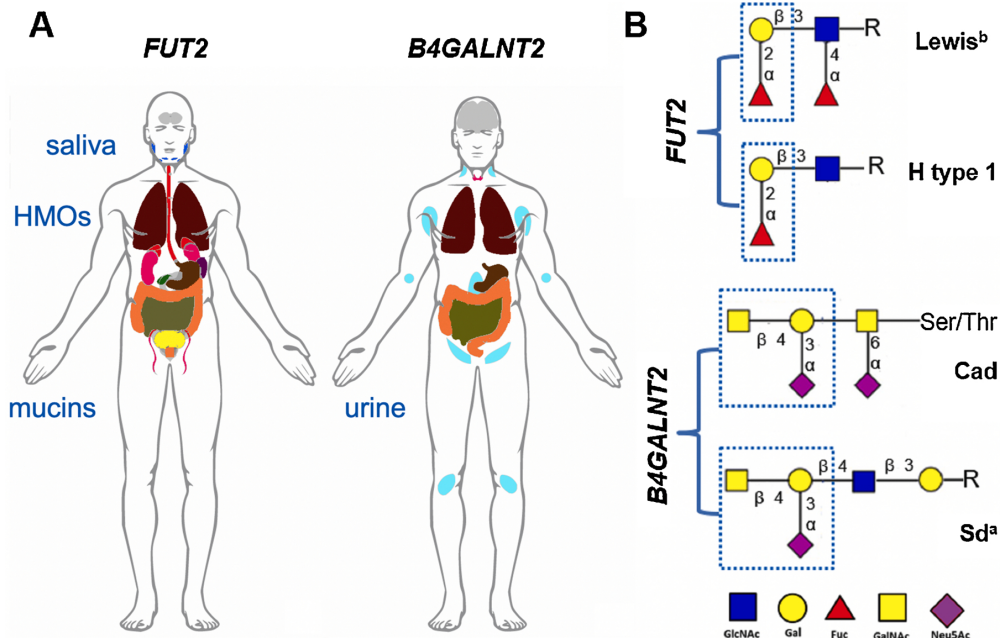


Fig. 1. Tissue distribution and the representative structures of *B4GALNT2*- and *FUT2*-dependent antigens. A, Tissues with high levels of either *B4GALNT2* or *FUT2* gene expression are depicted. Additionally, bodily secretions containing aforementioned antigens are indicated. HMOs – human milk oligosaccharides. Anatomograms are adopted from the EMBL Expression Atlas (Papatheodorou et al., 2020). B, Examples of *B4GALNT2*- and *FUT2*-dependent antigen structures. The *FUT2* enzyme governs the transfer of fucose (red triangle) residues to galactose (yellow circle) in an α (1,2)-linkage, thus producing the terminal epitope Fuc α 1-2-Gal β -R (Kelly et al., 1995). Subsequent activity of the *FUT3* enzyme creates Lewis^b antigen. Different glycosyltransferases can further decorate H-antigen with GalNAc- or Gal-residues which creates A or B blood group antigens. The *B4GALNT2* enzyme catalyzes the transfer of GalNAc (yellow square) to the sialylated glycans containing Neu5Ac α 2-3Gal β motif which facilitates the synthesis of Sda and Cad antigens (Piller et al., 1986) (For interpretation of the references to colour in this figure legend, the reader is referred to the web version of this article.).

et al., 2016), asthma exacerbation (Innes et al., 2011), and non-CF bronchiectasis (Taylor et al., 2017). In contrast, non-secretors have higher risks to develop primary sclerosing cholangitis (Folseraas et al., 2012), intestinal-type gastric cancer (Duell et al., 2015), Crohn's disease (McGovern et al., 2010), and type 1 diabetes (Smyth et al., 2011). Importantly, infectious disease also differs according to secretor status. For example, an increased incidence of infections with *Neisseria meningitidis*, *Streptococcus pneumoniae* (Blackwell et al., 1986a), and *Haemophilus influenzae* (Blackwell et al., 1986b) is reported in non-secretors, whereas non-secretors are protected from norovirus (Lindesmith et al., 2003). In addition, it was shown that *Fut2*-deficient mice are more resistant to vaginal *Candida albicans* infection (Hurd and Domino, 2004).

3. B4GALNT2

In 1967, a new antigen termed Sd^a (or Sid) was discovered on the membrane of erythrocytes by two independent groups (Macvie et al., 1967; Renton et al., 1967). Subsequent studies demonstrated that approximately 90 % of humans express the Sd^a antigen not only on red blood cells, but also in bodily secretions – with the highest concentration detected in urine (Morton et al., 1970) (see also Fig. 1). While expression levels of Sd^a antigen vary considerably between individuals, genetic polymorphisms are not described (Zhao et al., 2018). It was shown that GalNAc-binding lectins agglutinate the Sd^a antigen and its more reactive form, the Cad antigen (Tollefson and Kornfeld, 1983). While the Sd^a/Cad antigens and the blood group A antigen both contain GalNAc and Gal, they are, in fact, structurally different (Table 1).

Serafini-Cessi and colleagues described the Sd^a synthase isolated from guinea pig kidneys: β 1,4-N-acetylgalactosaminyl transferase 2 enzyme, which catalyzes the transfer of GalNAc from UDP-GalNAc to the sialylated N-linked chains of Tamm-Horsfall-like glycoprotein (Serafini-Cessi et al., 1986). Accordingly, a human analogue recognizing (Neu5Ac₂3)Gal β groups as acceptors and facilitating the synthesis of Sd^a/Cad antigens was identified (Piller et al., 1986). It was shown that the human *B4GALNT2* gene (Chr17q21.33), initially discovered in the colon carcinoma Caco-2 cell line, has two different isoforms: a short and a long isoform with an extended cytoplasmic domain (Lo Presti et al., 2003; Montiel et al., 2003). The major short *B4GALNT2* transcript variant and the corresponding protein were found to be mostly expressed in normal, but not in cancerous, epithelial colonic cells and also in healthy colon and stomach (Groux-Degroote et al., 2014). *B4GALNT2* is down-regulated in colo-rectal cancers and associated with increased metastasis (Dall'Olio et al., 2013). Introduction of Sd^a antigen in gastrointestinal cancer cells inhibited their metastatic potential and resulted in a total loss of cell-surface sialyl-Lewis^x and sialyl-Lewis^a antigens (Kawamura et al., 2005). Indeed, because the Sd^a and sialyl-Lewis antigens share a common α 2,3-sialylated type 2 structure (Table 1), it was suggested that their biosynthesis is mutually exclusive (Pucci et al., 2020).

The gene encoding murine Sd^a synthase *B4galnt2* was cloned and characterized; cDNA predicted a type 2 transmembrane protein of a topology similar to other Golgi-glycosyltransferases (Smith and Lowe, 1994). Mohlke and colleagues discovered a novel *Mwfl* ("Modifier of von Willebrand Factor-1") allele in the RIIS/J inbred mouse strain which has reduced levels of von Willebrand factor (VWF) antigen in plasma and a prolonged bleeding time (Mohlke et al., 1996). Subsequent studies identified RIIS/J-like *B4galnt2* alleles, conferring a unique tissue-specific switch in *B4galnt2* expression from intestinal epithelium to vascular endothelium, in multiple wild-derived mouse strains (Johnsen et al., 2008), as well as in wild mice (Johnsen et al., 2009). The expression of *B4galnt2* in murine blood vessels causes aberrant VWF glycosylation and enhances VWF clearance from the circulation, which results in a phenotype that closely resembles von Willebrand disease, a human bleeding disorder (Mohlke et al., 1999). Nevertheless, it appears that *B4galnt2* allelic polymorphisms have been maintained for at least 2.8 million years in the mouse lineage, suggesting that a loss of *B4galnt2*

expression in the gut- and/or gain in blood vessels might be important for host-pathogen interactions (Linnenbrink et al., 2011; Vallier et al., 2017).

4. Direct interaction (glycan-mediated pathogen adhesion)

Carbohydrate-containing structures (glycans) have many important roles for the interaction between bacterial pathogens and their hosts. These interactions mediate bacterial adhesion, invasion, and immune evasion. Furthermore, glycans can serve as a source of nutrients or as ligands for bacterial toxins. Secretory and membrane-bound glycans also protect the host from pathogenic and opportunistic microorganisms. As previously mentioned, the blood group-related glycosyltransferases FUT2/Fut2 and B4GALNT2/B4galnt2 can influence susceptibility to various pathogens. Interestingly, while some pathogens can clearly benefit from the host expression of these genes, FUT2- and B4GALNT2-dependent glycosylation can also be detrimental to other pathogens. In this section we will discuss the role of *Fut2* and *B4galnt2*-dependent glycans for the direct interaction with individual bacterial and viral pathogens.

4.1. *Salmonella enterica*

S. enterica is a common human pathogen and constitutes a major disease burden worldwide. It can have several primary clinical manifestations from gastroenteritis to typhoid fever depending on the infecting serovar (Gal-Mor et al., 2014), and uses host glycans in the mucus and on the cell surface to adhere to and invade host cells (Taylor et al., 2018). This facultative anaerobic, Gram-negative bacterium is an intracellular pathogen that uses its virulence factors including fimbriae/pili, flagella and type 3 secretion systems (T3SS), encoded by *Salmonella* pathogenicity island (SPI)-1 and SPI-2, to infect host cells (Ibarra and Steele-Mortimer, 2009). Fimbriae as one of the adhesive structures present on the bacterial surface are important for the initial attachment to host cell surfaces. Depending on the serotype, *Salmonella* has up to 20 fimbrial adhesins (Wagner and Hensel, 2011; Yue et al., 2012). The *std* fimbrial operon encodes the π -class Std fimbriae, which bind terminal α (1,2)-fucose residues (Chessa et al., 2009). *Fut2*-deficient mice were shown to be more susceptible to *Salmonella* infection at an early time point post infection (Goto et al., 2014; Suwandi et al., 2019). In contrast, *Fut2*-deficient mice displayed a substantial reduction in bacterial colonization and inflammation after long-term *Salmonella* infection (Suwandi et al., 2019; Weening et al., 2005). It is hypothesized that at day one after infection, α (1,2)-fucose-containing glycans in epithelial cells and secreted mucus may prevent *Salmonella* infection, although the exact mechanism is not clear (Goto et al., 2016). At later time points of infection, the presence of α (1,2)-fucose-containing glycans present in the intestine of *Fut2*-proficient mice can be exploited by *Salmonella*. Furthermore, we and others also demonstrated that bacteria expressing *std* fimbriae exhibited increased adhesion to human cell lines and murine intestinal organoids when terminal α (1,2)-fucose was present (Chessa et al., 2009; Suwandi et al., 2019). Taken together, both *in vivo* and *in vitro* results demonstrate that *Salmonella* can exploit host fucosylation in the intestine using its Std fimbriae.

Less is known how *B4galnt2* expression influences the direct interaction of *Salmonella* with intestinal epithelial cells. Invasion assays showed that knockdown of *B4galnt2* expression significantly decreased *Salmonella* invasion compared to *B4galnt2*-expressing cells (Rausch et al., 2015). Although *Salmonella* does not seem to directly bind to *B4galnt2*-dependent GalNAc residues *in vitro* (Giannasca et al., 1996), the overall glycan profile might also change in the cells not expressing *B4galnt2* in addition to the lack of Sd^a antigen (Dall'Olio et al., 2014; Groux-Degroote et al., 2014), and thus impair *Salmonella* invasion. Overexpression of the *B4galnt2* gene in MDCK cells convert α 2,3-sialic acid receptors into Sd^a-like epitopes, which might influence the susceptibility of *Salmonella* infection (Wong et al., 2019). However, a direct

link between *B4galnt2* expression and *Salmonella* susceptibility still remains elusive and needs further study.

4.2. *Escherichia coli*

E. coli is a Gram-negative, facultative anaerobic and rod-shaped bacterium. It is a commensal bacterium of the gastrointestinal tract, but there are also pathogenic *E. coli* strains that cause a variety of diseases. At least six different pathogenic *E. coli* strains cause enteric disease, whereas others cause extra-intestinal infections such as urinary tract infection and meningitis (Kaper et al., 2004). Enterotoxigenic *E. coli* (ETEC) is a leading cause of infectious diarrhea in the developing world, particularly in young children. These pathogens are also a major cause of traveller's diarrhea in endemic areas (Black, 1990). In a clinical study, it was demonstrated that children with a *FUT2* non-secretor status are more likely to have symptomatic ETEC infection in comparison to those with secretor status (Mottram et al., 2018).

ETEC, like commensal and other pathogenic *E. coli*, has adherence factors including fimbrial and non-fimbrial adhesins that are important for attachment to the host surface. This bacterium encodes at least 23 distinct fimbriae (named colonization factors, CFs) (Torres et al., 2005). Interestingly, it was reported that children with a *FUT2* non-secretor status are more likely to be infected by ETEC expressing the colonization factor antigen I (CFA/I) and other ETEC CF family fimbriae (Ahmed et al., 2009). Mottram and colleagues demonstrated that CfaB, the major subunit of ETEC CFA/I fimbriae and of another four related ETEC fimbriae, increases binding to Chinese Hamster Ovary (CHO)-K1 cell line expressing Lewis^a (mimicking *FUT2* non-secretor status) compared to cells carrying Lewis^b antigens (*FUT2* secretor status) or wild-type CHO-K1 cells. Furthermore, the authors performed an *in-silico* analysis, which predicted the potential structural binding region between Lewis^a and CfaB of CFA/I and related fimbriae (Mottram et al., 2018). In addition to ETEC, a clinical study showed that in women, Lewis blood-group non-secretor status is associated with an increased frequency of recurrent urinary tract infections caused by uropathogenic *E. coli* (UPEC) (Sheinfeld et al., 1989). In another study, UPEC strain R45 expressing both P and F adhesins was shown to bind to glycosphingolipids extracted from vaginal epithelial cells from non-secretors, but not from secretors (Stapleton et al., 1992). Taken together, these studies indicate that the expression of *Fut2* plays an important role in protecting the host against pathogenic *E. coli* infection.

Less is known about a possible role of *B4galnt2* glycans on *E. coli* interaction with the host. There is no evidence for direct binding of *E. coli* to *B4galnt2* glycans. In contrast, *B4galnt2* mediated modification of Tamm-Horsfall glycoprotein may even protect against *E. coli* infections by masking its receptor by blocking its binding sites in the large intestine and kidney (Serafini-Cessi et al., 2005).

4.3. *Helicobacter pylori*

H. pylori is one of the most common human infectious agents and causes chronic infection of the human stomach. This Gram-negative and flagellated bacterium is considered as the main cause of ulcers and gastric cancer (Marshall and Warren, 1984; Warren and Marshall, 1983). This microaerophilic bacterium is often found within the mucus that covers the gastric epithelium. *H. pylori* attaches to gastric epithelial cells which is important in establishing persistent colonization and induction of gastric inflammation (Celli et al., 2009; Hessey et al., 1990; Schreiber et al., 2004). The best-characterized *H. pylori* adhesin is the blood group antigen-binding adhesin (BabA) that binds to ABO(H)/Lewis^b blood group antigens located on the surface of gastric epithelial cells and mucins (Borén et al., 1993; Ilver et al., 1998; Nell et al., 2014). In the Lewis^b blood group, the *FUT2* gene adds a fucose molecule in α(1,2)-linkage onto a galactose residue. *FUT2*-deficient individuals are unable to synthesize ABO(H)/Lewis^b antigens, but can express Lewis^a antigens due to the action of *FUT3* (Bergstrom and Xia, 2013).

Fut2-deficient mice are characterized by a significantly decreased degree of α1,2-fucosylation, and hence Lewis^b antigen expression in the stomach. Interestingly, this change impairs gastric mucosal binding of *H. pylori* BabA adhesion in epithelial cells and mucus (Magalhães et al., 2016, 2009). Thus, *H. pylori* is able to exploit *Fut2*-dependent host glycans using its BabA adhesin.

Similar to the situation in *E. coli*, there is no evidence for direct binding of *H. pylori* to *B4galnt2* glycans. However, *H. pylori* binds to sialic acid via its adhesin Saba (Mahdavi et al., 2002). It would be interesting to clarify whether *B4GALNT2* expression in the stomach could reduce *H. pylori* attachment through the masking of sialylated residues.

4.4. Viruses

Glycans also contribute to viral infection, serving as entry receptors for virions. Clinical studies revealed an association between secretor status and multiple respiratory viral diseases, e.g., those caused by influenza virus A and B, rhinoviruses, respiratory syncytial virus and echoviruses (Raza et al., 1991). In addition, several studies also showed an association between non-secretor status and a reduced risk for HIV-1 infection (Ali et al., 2000; Chanzu et al., 2015; Kindberg et al., 2006).

Recently, a CRISPR activation screen identified that *B4galnt2* overexpression can inhibit influenza A virus infection (Heaton et al., 2017). *B4galnt2* overexpression modifies sialic acid-containing glycans, which can be used by influenza A viruses as a receptor, recognized by the viral glycoprotein hemagglutinin. The same study also showed that *B4galnt2* overexpression prevented infection with several avian influenza virus strains tested, including H5, H9, and H7 subtypes. Another study also demonstrated that overexpression of *B4galnt2* in MDCK cells modified surface α2,3-sialyllectose receptors, which lead to a decreased binding and invasion capability of influenza viruses with α2,3-receptor (Wong et al., 2019). Thus, expression of *B4galnt2* can inhibit influenza A virus infection through the modification of sialic-acid containing glycans, which are important for viral attachment.

Human noroviruses, previously known as Norwalk virus, are one of the common causes of gastroenteritis in children and adults worldwide (Lopman et al., 2016). These single stranded RNA viruses belong to the Caliciviridae family and are transmitted via the fecal-oral route, including consumption of contaminated food or water and direct person to person contact (Robilotti et al., 2015). Human norovirus is classified into at least five genogroups (GI-GV), which are further subdivided into genotypes. GI.4 is the predominant human norovirus that causes the majority of gastroenteritis outbreaks (Robilotti et al., 2015). Several studies showed that the susceptibility to norovirus infection is mediated by *FUT2*, whereby non-secretors are resistant to several norovirus genotypes, including GI.4 (Currier et al., 2015; Lindesmith et al., 2003; Lopman et al., 2015; Nordgren et al., 2013). Histo-blood group antigens (HBGAs), influenced by *FUT2* gene, are cell attachment factors for norovirus and important for a productive norovirus infection. Crystallography studies revealed that α(1,2)-fucose-containing H- and A-type HBGAs and Lewis antigens are important binding sites for a majority of human noroviruses. (Bu et al., 2008; Cao et al., 2007; Choi et al., 2008).

Rotavirus infections are the leading cause of severe gastroenteritis and diarrhea in children below 5 years of age. Infection with these non-enveloped double-stranded RNA viruses leads to vomiting, malaise and fever. The mode of transmission is mainly through the faecal-oral route by direct contact to an infected person or consumption of contaminated food or water (Crawford et al., 2017). Rotaviruses use the outer capsid protein viral protein (VP)4 (through its VP8* domain) for adhesion to sialoglycans (such as gangliosides GM1 and GD1a) and to HBGAs (Hu et al., 2012; Huang et al., 2012) on the host cell surface. Interestingly, Ramani and co-authors reported that the infectivity of rotavirus strain G10 P was significantly enhanced by the expression of H type II precursor in CHO cells (Ramani et al., 2013), and proposed that the glycan-binding specificity of certain rotaviruses may explain the tropism for neonates. Importantly, non-secretor individuals were shown to not

be recognized by most human rotavirus A strains (Imbert-Marcille et al., 2014), indicating that secretor status also plays a role in susceptibility to this viral pathogen.

Importantly, ABO blood group antigens were recently shown to influence the risk for infection with the pandemic coronavirus strain SARS-CoV2. Several studies showed that individuals with blood group A bear a greater risk of SARS-CoV2 infection, COVID-19 severity and mortality, in contrast to a protective effect for blood group O (Amoroso et al., 2021; Muñiz-Díaz et al., 2020; Severe Covid-19 GWAS Group et al., 2020; Zhao et al., 2020). However, a recent retrospective case-control study challenges this view and found no significant association between ABO blood groups and susceptibility to SARS-CoV2 infection (Khalil et al., 2020). Future analyses of larger patient cohorts may be needed to define the effect of ABO on SARS-CoV2 susceptibility.

5. Indirect interactions (influencing endogenous microbiota)

The intestinal microbiota is known to have a strong effect on the health and physiology of their hosts. The commensal bacteria contribute to the development and response of the immune system, defense against pathogens and colonization resistance (Ducarmon et al., 2019; Round and Mazmanian, 2009). Moreover, abnormal changes in these communities, termed dysbiosis, are linked to the development and progression of various diseases, such as chronic inflammatory bowel disease (Lane et al., 2017), irritable bowel syndrome (Rajilić-Stojanović et al., 2011) as well as susceptibility to infections (Ubeda et al., 2017).

The gastrointestinal tract of humans and other mammals is covered by a glycosylated mucus layer. The mucus layer acts as a physical barrier between a host and microbial communities, and as a site of host-microbe interactions. Importantly, glycans represent a first interaction point between the host and intestinal microbes, and can thus modulate commensal microbiota composition (Koropatkin et al., 2012).

5.1. B4GALNT2

Two independent studies demonstrated changes in composition of the gut microbiota in mice lacking intestinal *B4galnt2* expression (Rausch et al., 2015; Staubach et al., 2012). The study by Rausch et al. (2015) further carried out a murine model of *Salmonella*-induced colitis. Under normal circumstances *S. Typhimurium* is unable to successfully colonize the mouse gut and cause inflammation. Thus, Rausch et al. (2015) administered a pretreatment with streptomycin to break the colonization resistance of the resident microbiota (Barthel et al., 2003), revealing a lack of intestinal *B4galnt2* expression to be associated with reduced gut inflammation. Moreover, the severity of inflammation in the experiment positively correlated with the extent of change in microbiota composition before and after infection with *S. Typhimurium*. Accordingly, mice lacking intestinal *B4galnt2* expression displayed less microbiota turnover and less inflammation, suggesting a role of the gut microbiota. Intriguingly, fecal microbiota transfer experiments demonstrated that the greater inflammation in *B4galnt2* expressing mice is largely dependent on the *B4galnt2* genotype-specific microbiota, rather than *B4galnt2* expression itself. The mechanism(s) surrounding this effect remain unclear and are a subject of future study, but likely involve differences in resistance and/or resilience of the gut microbiota.

5.2. FUT2

Similar to *B4galnt2*, metagenomic studies in humans and mice have revealed differences in the intestinal microbiota according to *FUT2* genotype (Folseraas et al., 2012; Rausch et al., 2017, 2011; Tong et al., 2014; Wacklin et al., 2011). These studies were based on material from colonic biopsies, bile fluid, endoscopic lavage samples of the cecum and colon, or fecal material from a controlled laboratory mouse setting. In contrast, other large-scale studies analyzing fecal samples failed to observe an association with *FUT2* genotype (Davenport et al., 2016;

Turpin et al., 2018). These discrepancies indicate that the overall genotype effect on inter-individual differences may be subtle, and/or that the material/site of the GIT is important. It should be pointed out, however, that even the *FUT2* genotype/secretor status of the maternal lineage was found to be important in some studies (Rausch et al., 2017; Smith-Brown et al., 2016).

Despite inconsistencies between metagenomic studies, there are many biological reasons to consider the *FUT2* gene's influence on intestinal microbes in the context of infection. As mentioned earlier, the functional *FUT2* gene present in secretors facilitates the addition of α -2-fucose residues at the terminal end of glycan chains abundant in the human gut epithelia. In contrast, the gut epithelia of non-secretors lack these fucosylated carbohydrate moieties (Bry et al., 1996; Moran et al., 2011). As a result, the resources available for utilization by the gut microbes in the two distinct phenotypes tend to vary depending on the diet of the host (Kashyap et al., 2013). However, when fucose is unavailable through dietary sources, the gut bacteria resort to utilizing the host derived fucose in secretors (Becker and Lowe, 2003).

It is known that only certain bacteria are capable of cleaving host-derived fucose, thereby releasing fucose into the gut environment and making it freely available to be utilized by other non-cleaving microbes (Pacheco et al., 2012). For example, *Bacteroides thetaiotaomicron* can cleave and release host fucose in the intestinal environment, making it readily available for utilization by *Lactobacillus rhamnosus* GG, which lacks the cleaving activity (Becerra et al., 2015; Hooper et al., 1999). Thus, gut commensals like *B. thetaiotaomicron*, *Akkermansia muciniphila*, segmented filamentous bacteria, etc. promote the ecological succession of fucose utilizing bacteria like *E. coli* Nissle 1917, *L. rhamnosus* GG, *Ruminococcus gnavus*, among others, most of which are known for their beneficial effects in the human gut (Becerra et al., 2015; Hooper et al., 1999; Shin et al., 2019; Tailford et al., 2015; Wu et al., 2020). Similarly, (e.g. after the presence of free fucose (e.g. after antibiotic treatment) can lead to an environment conducive to a number of fucose utilizing pathogens (Ikehara et al., 2001; Stahl et al., 2011; Suwandi et al., 2019). For example, *Campylobacter jejuni*, a common pathogen responsible for pediatric diarrhea, can metabolize free fucose and induce intestinal disease (Stahl et al., 2011; van der Hooft et al., 2018). Other similar examples include *H. pylori*, *Salmonella* spp., enterotoxigenic *E. coli*, and *Brucella abortus* (Budnick et al., 2018; Coddens et al., 2009; Ikehara et al., 2001; Suwandi et al., 2019).

Another important point to consider with regard to susceptibility to infection is that host fucosylation plays a role in the microbiota-mediated immunity of the host. Fucose-cleaving commensals can directly influence host fucosylation by inducing type 3 innate lymphoid cells (ILC3) to produce interleukin-22 (IL-22), which in turn signals the intestinal epithelial cells (IEC) to produce fucose (Goto et al., 2014). Up-regulation of fucosylation was shown to strengthen barrier function and enhance colonization resistance to invading pathogens (Pham et al., 2014). In this study, *Il22* and *Fut2* were up-regulated during *S. Typhimurium* and *Citrobacter rodentium* infection, and *Il22*^{-/-} mice showed an increased bacterial burden compared to wild-type mice. Additionally, proliferation of the opportunistic pathogen *Enterococcus faecalis* was observed. Interestingly, administration of 2'-fucosyllactose (2'FL), an α 1,2-fucosylated oligosaccharide, resulted in significant mitigation of the symptoms in *Il22*-deficient mice (Pham et al., 2014). Another study by Pickard et al., further demonstrated how host fucosylation is used as a defense mechanism in response to pathogen-induced stress, and the role gut microbiota plays in enabling this process (Pickard et al., 2014; Pickard and Chervonsky, 2015). Thus, in sum, many commensal bacteria can take advantage of host fucosylation not only as a source of nutrition and site of adhesion, but also to modify host gene expression and strengthen its colonization resistance towards pathogenic bacteria.

5.3. Viruses

Although it is well-established that host secretor status affects

susceptibility to norovirus and rotavirus infections by modulating viral adherence, recent studies indicate that the gut microbiota can also facilitate the infectivity of these viruses. Accordingly, depletion of the intestinal microbiota with antibiotics significantly reduced the replication of norovirus and rotavirus in the murine gut (Jones et al., 2014; Uchiyama et al., 2014). While the exact mechanism of this suppression is not clear, it was proposed that the gut microbiota may assist viral entry by regulating the expression of host receptors and/or bacterial ligands (Uchiyama et al., 2014). Indeed, it was demonstrated *in vitro* that HBGA-expressing enteric bacteria promoted norovirus infection of human B cells (Jones et al., 2014). Moreover, Rodriguez-Díaz and colleagues reported a negative correlation between the relative abundances of the gut commensals *Faecalibacterium* and Ruminococcaceae and IgA titers against norovirus and rotavirus (Rodríguez-Díaz et al., 2017). *Faecalibacterium* benefits from acetate metabolism and Ruminococcaceae can utilize fucose, and both of these metabolites are supplied by *Bacteroides* spp. (Wrzosek et al., 2013). Interestingly, a higher relative abundance of a *Bacteroides* operational taxonomic unit (OTU) was detected in secretors compared to non-secretors (Rodríguez-Díaz et al., 2017). Taken together, these findings suggest that variation in gut microbiota communities determined by *FUT2* genotype can also affect susceptibility to viral pathogens.

6. Therapeutic applications of blood group-related glycans

As discussed in the previous chapters, *FUT2*- and *B4GALNT2*-dependent mucosal glycans can act as receptors to promote microbial adhesion or as nutrients for commensal or pathogenic bacteria. Hence, it is appealing to utilize histo-blood group-related glycans in therapeutic interventions, either as decoy targets to selectively bind pathogens or to support glycan-metabolizing commensals *in situ*. In this case, human milk oligosaccharides (HMOs) serve as inspiration, due to their prebiotic and anti-infective properties (see Walsh et al., 2020 for an excellent review). Structurally, they represent a diverse family (>150 HMOs) of linear or branched oligosaccharides comprised of a lactose core, N-acetylglucosamine (GlcNAc), D-glucose and D-galactose (German et al., 2008). Additionally, the majority of HMOs are terminally sialylated and fucosylated; notably, $\alpha(1\text{-}2)$ fucosylation of HMOs is governed by the *FUT2* enzyme in secretors (Fig. 1).

HMOs are not digested and reach the large intestine of breast-fed infants, where they provide selective substrates for specific gut commensals such as bifidobacteria and *B. thetaiotaomicron* (Salli et al., 2021). Indeed, it was shown that three major fucosylated components of HMOs, 2'-O-fucosyllactose (2'FL), lactodifucotetraose and 3-fucosyllactose, sustained *in vitro* growth of *Bifidobacterium* spp. isolated from infant fecal samples, while *E. coli* K12 or *Clostridium perfringens* were not able to metabolize fucosylated oligosaccharides (Yu et al., 2013). In a double-blind, placebo-controlled study, oral supplementation with HMOs (2'FL and lacto-N-neotetraose, LNnT) was well-tolerated by healthy adults and resulted in a significant increase in relative abundances of Actinobacteria and *Bifidobacterium* (Elison et al., 2016). As of Jan 2021, ClinicalTrials.gov lists six trials (four at the recruiting stage) aiming to investigate the potential benefits of a prebiotic 2'FL therapy in various diseases and conditions, such as hematopoietic stem cell transplant, IBD, bowel dysfunction, and anemia. Several studies explored the effect of 2'FL treatment on Fuc $\alpha(1\text{-}2)$ -binding pathogens. For example, Weichert et al. demonstrated that 2'-fucosyllactose and 3-fucosyllactose inhibited adhesion of EPEC, *Pseudomonas aeruginosa*, and *S. enterica* serovar Typhimurium to human intestinal and respiratory cell lines (Weichert et al., 2013). It was also shown that 2'FL blocked 80 % of *C. jejuni* invasion into human colon carcinoma cells and substantially reduced *C. jejuni* colonization and intestinal inflammation in mice (Yu et al., 2016). Accordingly, high concentrations of $\alpha(1\text{-}2)$ fucosylated HMOs (2'FL, specifically) in maternal milk had been previously associated with lower susceptibility to *C. jejuni*-caused infant diarrhea (Morrow et al., 2004). An inhibitory effect of fucosylated HMOs on norovirus (Morrow et al.,

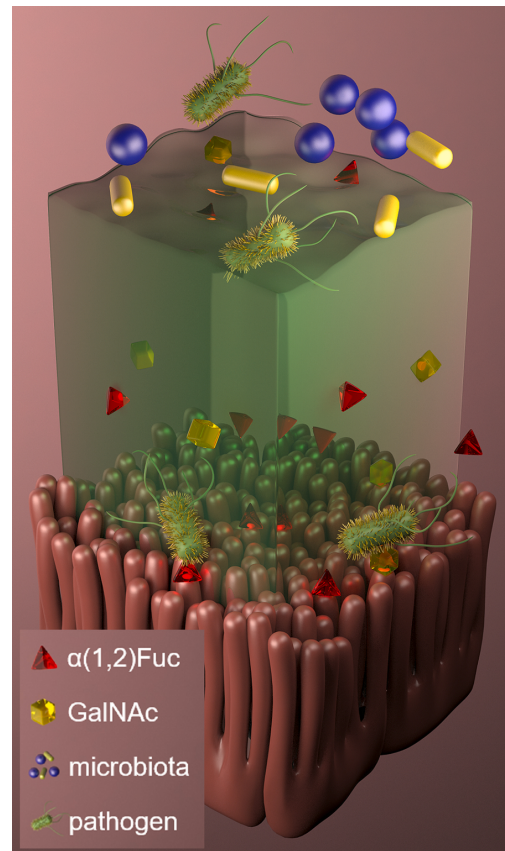


Fig. 2. Host microbiota and pathogens utilize *B4GALNT2*- and *FUT2*-dependent glycans as nutrients and/or adhesion sites. Commensal microbes can cleave $\alpha(1\text{-}2)$ -Fuc of histo-blood group antigens (HBGAs) which are expressed in abundance on mucins. Many pathogens (including *S. Typhimurium*) are able to metabolize free fucose (red pyramids) present in the mucus (green). Furthermore, pathogens can penetrate the mucus inner layer and adhere to the mucosa by employing multiple adhesins. Many of these adhesins can attach to host HBGAs: for example, to bind terminal $\alpha(1\text{-}2)$ -Fuc residues, *S. Typhimurium* employs Std fimbriae while *H. pylori* utilizes BabA adhesin (Borén et al., 1993). The *B4GALNT2*-dependent GalNAc-containing glycans (yellow cubes) may act as nutrients and enhance colonization resistance (For interpretation of the references to colour in this figure legend, the reader is referred to the web version of this article.).

2005; Shang et al., 2013) and rotavirus (Lau Cirica et al., 2017; Walsh et al., 2020) adhesion to host cells was also demonstrated.

The therapeutic potential of free monosaccharides (fucose (Ke et al., 2020), galactose (Pfeiffer, 2020)), of porcine mucin glycans (Pruss et al., 2020), and of synthetic glycoconjugates, including so-called “glycomimetics” (Imberty et al., 2008; Kalas et al., 2018; Meiers et al., 2019), is also very promising. For instance, an inhalation of fucose and galactose significantly reduced *P. aeruginosa* burdens in the sputum of patients with cystic fibrosis, presumably by binding bacterial lectins LecA and LecB and thus competing with the epitopes expressed on lung epithelia (Hauber et al., 2008). Once a glycan-binding affinity of a given pathogen is characterized (see Chapter 4), it is possible to enhance decoy properties by rational design. Boukerb et al. synthesized calix[4]arene-based glycoclusters functionalized with galactosides/fucosides, which induced *P. aeruginosa* clumping in a LecA-dependent manner and reduced biofilm formation, adhesion to epithelial cells, and alveolar injury (Boukerb

et al., 2014). Another interesting strategy was recently proposed by Meiers et al. (2020): conjugation of glycomimetics targeting *P. aeruginosa* LecA and LecB to ciprofloxacin resulted in accumulation of the antibiotic/carbohydrate in *P. aeruginosa* biofilms, as well as in reduced host cytotoxicity. However, the authors noted that an attachment of glycomimetics also decreased the antibiotic activity of ciprofloxacin (Meiers et al., 2020).

In summary, recent technological advances combined with a deeper understanding of host-microbial glycobiology offer an opportunity to employ fucosylated HMOs naturally occurring in human milk or synthetic glycomimetics as novel therapeutic approaches.

7. Conclusions

The expression pattern of histo-blood group glycans in blood, epithelia, mucus and bodily secretions exposes them to intimate contact with commensal and pathogenic bacteria, viruses and fungi. FUT2 and B4GALNT2 glycans modulate the intestinal microbiota and influence susceptibility to gastrointestinal infections by several mechanisms (Fig. 2). A more detailed understanding of the complex mechanisms of interaction between pathogens and host glycans is needed in order to develop novel therapeutic treatments by targeted modification of these glycans or inhibition of the interaction of pathogens with these glycans. This may ultimately lead to new treatments to prevent or cure infections and possibly other glycan-related diseases.

Funding information

This work was supported by the German Research Foundation (DFG) priority program SPP1656/1 and SPP1656/2 "Intestinal Microbiota – a Microbial Ecosystem at the Edge between Immune Homeostasis and Inflammation" to GAG (GR 2666/5-1 and 5-2) and JFB (BA 2863/5-1 and 5-2).

Declaration of Competing Interest

The authors report no declarations of interest.

Acknowledgment

Authors would like to thank Alexander Permyakov for the help with 3D artwork.

References

- Ahmed, T., Lundgren, A., Arifuzzaman, M., Qadri, F., Teneberg, S., Svennerholm, A.-M., 2009. Children with the Le(a-b-) blood group have increased susceptibility to diarrhea caused by enterotoxigenic Escherichia coli Expressing colonization factor I group fimbriae. *Infect. Immun.* 77, 2059–2064. <https://doi.org/10.1128/IAI.01571-08>.
- Ali, S., Niang, M.A.F., N'doye, I., Critchlow, C.W., Hawes, S.E., Hill, A.V.S., Kiviat, N.B., 2000. Secretor polymorphism and human immunodeficiency virus infection in senegalese women. *J. Infect. Dis.* 181, 737–739. <https://doi.org/10.1086/315234>.
- Amoroso, A., Magistroni, P., Vespasiano, F., Bella, A., Bellino, S., Puoti, F., Alizzi, S., Vaisitti, T., Boros, S., Grossi, P.A., Trapani, S., Lombardini, L., Pezzotti, P., Deaglio, S., Brusaferro, S., Cardillo, M., Centers, on behalf of the I.N. of R.T.C., 2021. HLA and AB0 polymorphisms may influence SARS-CoV-2 infection and COVID-19 severity. *Transplantation* 105, 193–200. <https://doi.org/10.1097/TP.0000000000003507>.
- Barthel, M., Hapfelmeyer, S., Quintanilla-Martinez, L., Kremer, M., Rohde, M., Hogardt, M., Pfeffer, K., Rüssmann, H., Hardt, W.-D., 2003. Pretreatment of mice with streptomycin provides a *Salmonella enterica* serovar Typhimurium colitis model that allows analysis of both pathogen and host. *Infect. Immun.* 71, 2839–2858. <https://doi.org/10.1128/iai.71.5.2839-2858.2003>.
- Becerra, J.E., Yebra, M.J., Monedero, V., 2015. An L-Fucose operon in the probiotic *Lactobacillus rhamnosus* GG is involved in adaptation to gastrointestinal conditions. *Appl. Environ. Microbiol.* 81, 3880–3888. <https://doi.org/10.1128/AEM.00260-15>.
- Becker, D.J., Lowe, J.B., 2003. Fucose: biosynthesis and biological function in mammals. *Glycobiology* 13, 41R–53R. <https://doi.org/10.1093/glycob/cwg054>.
- Bergstrom, K.S.B., Xia, L., 2013. Mucin-type O-glycans and their roles in intestinal homeostasis. *Glycobiology* 23, 1026–1037. <https://doi.org/10.1093/glycob/cwt045>.
- Björk, S., Breimer, M.E., Hansson, G.C., Karlsson, K.A., Leffler, H., 1987. Structures of blood group glycosphingolipids of human small intestine. A relation between the expression of sialic acids of epithelial cells and the ABO, Le and Se phenotype of the donor. *J. Biol. Chem.* 262, 6758–6765.
- Black, R.E., 1990. Epidemiology of travelers' diarrhea and relative importance of various pathogens. *Rev. Infect. Dis.* 12, S73–S79. https://doi.org/10.1093/clinids/12.Supplement_1.S73.
- Blackwell, C.C., Jónsdóttir, K., Hanson, M., Todd, W.T., Chaudhuri, A.K., Mathew, B., Brettle, R.P., Weir, D.M., 1986a. Non-secretion of ABO antigens predisposing to infection by *Neisseria meningitidis* and *Streptococcus pneumoniae*. *Lancet* 2, 284–285. [https://doi.org/10.1016/S0140-6736\(86\)92103-3](https://doi.org/10.1016/S0140-6736(86)92103-3).
- Blackwell, C.C., Jónsdóttir, K., Hanson, M.F., Weir, D.M., 1986b. Non-secretion of ABO blood group antigens predisposing to infection by *haemophilus influenzae*. *Lancet* 328–687. [https://doi.org/10.1016/S0140-6736\(86\)90193-5](https://doi.org/10.1016/S0140-6736(86)90193-5). Originally published as Volume 2, Issue 8508.
- Borén, T., Falk, P., Roth, K.A., Larson, G., Normark, S., 1993. Attachment of *Helicobacter pylori* to human gastric epithelium mediated by blood group antigens. *Science* 262, 1892–1895. <https://doi.org/10.1126/science.1801846>.
- Bouker, A.M., Roussel, A., Galanos, N., Mear, J.-B., Thépaut, M., Grandjean, T., Gillon, E., Cecioni, S., Abderrahmen, C., Faure, K., Redelberger, D., Kipnis, E., Dessein, R., Havet, S., Darblade, B., Matthews, S.E., de Bentzmann, S., Guéry, B., Cournoyer, B., Imberty, A., Vidal, S., 2014. Antiahesive properties of glycoclusters against *Pseudomonas aeruginosa* lung infection. *J. Med. Chem.* 57, 10275–10289. <https://doi.org/10.1021/jm500038p>.
- Bry, L., Falk, P.G., Midtvedt, T., Gordon, J.I., 1996. A model of host-microbial interactions in an open mammalian ecosystem. *Science* 273, 1380–1383. <https://doi.org/10.1126/science.273.5280.1380>.
- Bu, W., Mamedova, A., Tan, M., Xia, M., Jiang, X., Hegde, R.S., 2008. Structural basis for the receptor binding specificity of the Norwalk virus. *J. Virol.* <https://doi.org/10.1128/JVI.00135-08>.
- Budnick, J.A., Sheehan, L.M., Kang, L., Michalak, P., Caswell, C.C., 2018. Characterization of three small proteins in *Brucella abortus* linked to fucose utilization. *J. Bacteriol.* 200, e00127–18. <https://doi.org/10.1128/JB.00127-18>.
- Cao, S., Lou, Z., Tan, M., Chen, Y., Liu, Y., Zhang, Z., Zhang, X.C., Jiang, X., Li, X., Rao, Z., 2007. Structural basis for the recognition of blood group trisaccharides by norovirus. *J. Virol.* 81, 5949–5957. <https://doi.org/10.1128/JVI.00219-07>.
- Celli, J.P., Turner, B.S., Afshai, N.H., Keates, S., Ghiran, I., Kelly, C.P., Ewoldt, R.H., McKinley, G.H., So, P., Erramilli, S., Bansil, R., 2009. *Helicobacter pylori* moves through mucus by reducing mucin viscoelasticity. *Proc. Natl. Acad. Sci. U. S. A.* 106, 14321–14326. <https://doi.org/10.1073/pnas.0903438106>.
- Chanzu, N.M., Mwanda, W., Oyugi, J., Anzala, O., 2015. Mucosal blood group antigen expression profiles and HIV infections: a study among female sex workers in Kenya. *PLoS One* 10, e0133049. <https://doi.org/10.1371/journal.pone.0133049>.
- Chessa, D., Winter, M.G., Jakomin, M., Baumler, A.J., 2009. *Salmonella enterica* serotype Typhimurium Std fimbriae bind terminal alpha(1,2)fucose residues in the cecal mucosa. *Mol. Microbiol.* 71, 864–875. <https://doi.org/10.1111/j.1365-2958.2008.06566.x>.
- Choi, J.M., Hutson, A.M., Estes, M.K., Prasad, B.V.V., 2008. Atomic resolution structural characterization of recognition of histo-blood group antigens by Norwalk virus. *Proc. Natl. Acad. Sci. U. S. A.* 105, 9175–9180. <https://doi.org/10.1073/pnas.0803275105>.
- Coddens, A., Diswall, M., Angström, J., Breimer, M.E., Goddeeris, B., Cox, E., Teneberg, S., 2009. Recognition of blood group ABH type 1 determinants by the FcdF adhesin of F18-fimbriated *Escherichia coli*. *J. Biol. Chem.* 284, 9713–9726. <https://doi.org/10.1074/jbc.M807866200>.
- Corfield, A.P., Carroll, D., Myerscough, N., Probert, C.S., 2001. Mucins in the gastrointestinal tract in health and disease. *Front. Biosci.* 6, D1321–1357. <https://doi.org/10.2741/corfield>.
- Crawford, S.E., Ramani, S., Tate, J.E., Parashar, U.D., Svensson, L., Hagbom, M., Franco, M.A., Greenberg, H.B., O'Ryan, K., Kang, G., Desselberger, U., Estes, M.K., 2017. Rotavirus infection. *Nat. Rev. Dis. Primers* 3, 1–16. <https://doi.org/10.1038/rdp.2017.83>.
- Currier, R.L., Payne, D.C., Staat, M.A., Selvarangan, R., Shirley, S.H., Halasa, N., Boom, J. A., Englund, J.A., Szilagyi, P.G., Harrison, C.J., Klein, E.J., Weinberg, G.A., Wikswo, M.E., Parashar, U., Vinjé, J., Morrow, A.L., 2015. Innate susceptibility to norovirus infections influenced by FUT2 genotype in a United States pediatric population. *Clin. Infect. Dis.* 60, 1631–1638. <https://doi.org/10.1093/cid/civ165>.
- Dall'Olio, F., Vanhooren, V., Chen, C.C., Slagboom, P.E., Wuhrer, M., Franceschi, C., 2013. N-glycomic biomarkers of biological aging and longevity: a link with inflammaging. *Ageing Res. Rev.* 12, 685–698. <https://doi.org/10.1016/j.arr.2012.02.002>.
- Dall'Olio, F., Malagolini, N., Chiricolo, M., Trinchera, M., Harduin-Lepers, A., 2014. The expanding roles of the Sd(a)/Cad carbohydrate antigen and its cognate glycosyltransferase B4GALNT2. *Biochim. Biophys. Acta* 1840, 443–453. <https://doi.org/10.1016/j.bbagen.2013.09.036>.
- Davenport, E.R., Goodrich, J.K., Bell, J.T., Spector, T.D., Ley, R.E., Clark, A.G., 2016. ABO antigen and secretor statuses are not associated with gut microbiota composition in 1,500 twins. *BMC Genomics* 17. <https://doi.org/10.1186/s12864-016-3290-1>.
- Ducarmon, Q.R., Zwittink, R.D., Hornung, B.V.H., Schaik, Wvan, Young, V.B., Kuijper, E. J., 2019. Gut microbiota and colonization resistance against bacterial enteric infection. *Microbiol. Mol. Biol. Rev.* 83. <https://doi.org/10.1128/MMBR.00007-19>.
- Duell, E.J., Bonet, C., Muñoz, X., Lujan-Barroso, L., Weiderpass, E., Boutron-Ruault, M.-C., Racine, A., Severi, G., Canzian, F., Rizzato, C., Boeing, H., Overvad, K., Tjønneland, A., Argüelles, M., Sánchez-Cantalejo, E., Chamosa, S., Huerta, J.M., Barricarte, A., Khaw, K.-T., Wareham, N., Travis, R.C., Trichopoulou, A.,

- Trichopoulos, D., Yiannakouris, N., Palli, D., Agnoli, C., Tumino, R., Naccarati, A., Panico, S., Bueno-de-Mesquita, H.B., Siersema, P.D., Peeters, P.H.M., Ohlsson, B., Lindkvist, B., Johansson, I., Ye, W., Johansson, M., Fenger, C., Riboli, E., Sala, N., González, C.A., 2015. Variation at ABO histo-blood group and FUT loci and diffuse and intestinal gastric cancer risk in a European population. *Int. J. Cancer* 136, 880–893. <https://doi.org/10.1002/ijc.29034>.
- Elison, E., Vignaes, L.K., Krogsgaard, L.R., Rasmussen, J., Sørensen, N., McConnell, B., Hennet, T., Sommer, M.O.A., Bytzer, P., 2016. Oral supplementation of healthy adults with 2'-O-fucosylactose and lacto-N-neotetraose is well tolerated and shifts the intestinal microbiota. *Br. J. Nutr.* 116, 1356–1368. <https://doi.org/10.1017/S0007114516003354>.
- Ferrer-Admetlla, A., Sikora, M., Laayouni, H., Esteve, A., Roubinet, F., Blancher, A., Calafell, F., Bertranpetti, J., Casals, F., 2009. A natural history of FUT2 polymorphisms in humans. *Mol. Biol. Evol.* 26, 1993–2003. <https://doi.org/10.1093/molbev/msp108>.
- Folseraas, T., Melum, E., Rausch, P., Juran, B.D., Ellinghaus, E., Shiryaev, A., Laerdahl, J. K., Ellinghaus, D., Schramm, C., Weismüller, T.J., Gotthardt, D.N., Hov, J.R., Clausen, O.P., Weersma, R.K., Janse, M., Boberg, K.M., Björnsson, E., Marschall, H. U., Cleynen, I., Rosenstiel, P., Holm, K., Teufel, A., Rust, C., Gieger, C., Wichmann, H.-E., Bergquist, A., Ryu, E., Ponsioen, C.Y., Runz, H., Sterneck, M., Vermeire, S., Beuers, U., Wijnenga, C., Schrumpf, E., Manns, M.P., Lazaridis, K.N., Schreiber, S., Baines, J.F., Franke, A., Karlsén, T.H., 2012. Extended analysis of a genome-wide association study in primary sclerosing cholangitis detects multiple novel risk loci. *J. Hepatol.* 57, 366–375. <https://doi.org/10.1016/j.jhep.2012.03.031>.
- Formosa-Dague, C., Castelain, M., Martin-Yken, H., Dunker, K., Dague, E., Sletmoen, M., 2018. The role of glycans in bacterial adhesion to mucosal surfaces: how can single-molecule techniques advance our understanding? *Microorganisms* 6, 39. <https://doi.org/10.3390/microorganisms600039>.
- Fumagalli, M., Cagliani, R., Pozzoli, U., Riva, S., Comi, G.P., Menozzi, G., Bresolin, N., Sironi, M., 2009. Widespread balancing selection and pathogen-driven selection at blood group antigen genes. *Genome Res.* 19, 199–212. <https://doi.org/10.1101/gr.082768.108>.
- Gal-Mor, O., Boyle, E.C., Grassl, G.A., 2014. Same species, different diseases: how and why typhoidal and non-typhoidal *Salmonella enterica* serovars differ. *Front. Microbiol.* 5. <https://doi.org/10.3389/fmicb.2014.00391>.
- German, J.B., Freeman, S.L., Lebrilla, C.B., Mills, D.A., 2008. Human milk oligosaccharides: evolution, structures and bioselectivity as substrates for intestinal bacteria. *Pers. Nutr. Divers. Infants Children* 62, 205–222. <https://doi.org/10.1159/000146322>.
- Giannasca, K.T., Giannasca, P.J., Neutra, M.R., 1996. Adherence of *Salmonella* typhimurium to Caco-2 cells: identification of a glycoconjugate receptor. *Infect. Immun.* 64, 135–145. <https://doi.org/10.1128/IAI.64.1.135-145.1996>.
- Goto, Y., Obata, T., Kunisawa, J., Sato, S., Ivanov, I.I., Lamichhane, A., Takeyama, N., Kamioka, M., Sakamoto, M., Matsuki, T., Setoyama, H., Imaoka, A., Uematsu, S., Akira, S., Domino, S.E., Kulig, P., Becher, B., Renaud, J.-C., Sasakawa, C., Umesaki, Y., Benno, Y., Kiyono, H., 2014. Innate lymphoid cells regulate intestinal epithelial cell glycosylation. *Science* 345, 1254009. <https://doi.org/10.1126/science.1254009>.
- Goto, Y., Uematsu, S., Kiyono, H., 2016. Epithelial glycosylation in gut homeostasis and inflammation. *Nat. Immunol.* 17, 1244–1251. <https://doi.org/10.1038/ni.3587>.
- Groux-Degroote, S., Wavelet, C., Krzewinski-Reccchi, M.-A., Portier, L., Mortuaille, M., Mihalache, A., Trinchera, M., Delannoy, P., Malagolini, N., Chiricolo, M., Dall'Olio, F., Harduin-Leper, A., 2014. B4GALNT2 gene expression controls the biosynthesis of Sda and sialyl Lewis X antigens in healthy and cancer human gastrointestinal tract. *Int. J. Biochem. Cell Biol.* 53, 442–449. <https://doi.org/10.1016/j.jbiocell.2014.06.009>.
- Hauber, H.-P., Schulz, M., Pforte, A., Mack, D., Zabel, P., Schumacher, U., 2008. Inhalation with fucose and galactose for treatment of *Pseudomonas aeruginosa* in cystic fibrosis patients. *Int. J. Med. Sci.* 5, 371–376.
- Heaton, B.E., Kennedy, E.M., Dumm, R.E., Harding, A.T., Sacco, M.T., Sachs, D., Heaton, N.S., 2017. A CRISPR activation screen identifies a pan-avian influenza virus inhibitory host factor. *Cell Rep.* 20, 1503–1512. <https://doi.org/10.1016/j.celrep.2017.07.060>.
- Henry, S., Oriol, R., Samuelsson, B., 1995. Lewis histo-blood group system and associated secretory phenotypes. *Vox Sang.* 69, 166–182. <https://doi.org/10.1111/j.1423-0410.1995.tb02591.x>.
- Hessey, S.J., Spencer, J., Wyatt, J.I., Sobala, G., Rathbone, B.J., Axon, A.T., Dixon, M.F., 1990. Bacterial adhesion and disease activity in *Helicobacter* associated chronic gastritis. *Gut* 31, 134–138.
- Hooper, L.V., Xu, J., Falk, P.G., Midtfeldt, T., Gordon, J.I., 1999. A molecular sensor that allows a gut commensal to control its nutrient foundation in a competitive ecosystem. *Proc. Natl. Acad. Sci. U. S. A.* 96, 9833–9838. <https://doi.org/10.1073/pnas.96.17.9833>.
- Hu, L., Crawford, S.E., Czako, R., Cortes-Penfield, N.W., Smith, D.F., Pendu, J.L., Estes, M.K., Prasad, B.V.V., 2012. Cell attachment protein VP8* of a human rotavirus specifically interacts with A-type histo-blood group antigen. *Nature* 485, 256–259. <https://doi.org/10.1038/nature10996>.
- Huang, P., Xia, M., Tan, M., Zhong, W., Wei, C., Wang, L., Morrow, A., Jiang, X., 2012. Spike protein VP8* of human rotavirus recognizes histo-blood group antigens in a type-specific manner. *J. Virol.* 86, 4833–4843. <https://doi.org/10.1128/JV.05507-11>.
- Hurd, E.A., Domino, S.E., 2004. Increased susceptibility of secretor factor gene *Fut2*-null mice to experimental vaginal candidiasis. *Infect. Immun.* 72, 4279–4281. <https://doi.org/10.1128/IAI.72.7.4279-4281.2004>.
- Ibarra, J.A., Steele-Mortimer, O., 2009. *Salmonella*—the ultimate insider. *Salmonella* virulence factors that modulate intracellular survival. *Cell. Microbiol.* 11, 1579–1586. <https://doi.org/10.1111/j.1462-5822.2009.01368.x>.
- Ikehara, Y., Nishihara, S., Yasutomi, H., Kitamura, T., Matsuo, K., Shimizu, N., Inada, K., Kodera, Y., Yamamura, Y., Narimatsu, H., Hamajima, N., Tatematsu, M., 2001. Polymorphisms of two fucosyltransferase genes (*Lewis* and *Secretor* genes) involving type I Lewis antigens are associated with the presence of anti-*Helicobacter pylori* IgG antibody. *Cancer Epidemiol. Biomarkers Prev.* 10, 971–977.
- Iver, D., Arqvist, A., Ogren, J., Frick, I.M., Kersulyte, D., Incencik, E.T., Berg, D.E., Covacci, A., Engstrand, L., Borén, T., 1998. *Helicobacter pylori* adhesin binding fucosylated histo-blood group antigens revealed by retagging. *Science* 279, 373–377. <https://doi.org/10.1126/science.279.5439.373>.
- Imbert-Marcellin, B.-M., Barbe, L., Dupé, M., Le Moullac-Vaidye, B., Besse, B., Peltier, C., Ruvoen-Clouet, N., Le Pendu, J., 2014. A *FUT2* gene common polymorphism determines resistance to rotavirus *a* of the P[8] genotype. *J. Infect. Dis.* 209, 1227–1230. <https://doi.org/10.1093/infdis/jit655>.
- Imbert, A., Chabre, Y.M., Roy, R., 2008. Glycomimetics and glycodendrimers as high affinity microbial anti-adhesins. *Chem. Eur. J.* 14, 7490–7499. <https://doi.org/10.1002/chem.200800700>.
- Innes, A.L., McGrath, K.W., Dougherty, R.H., McCulloch, C.E., Woodruff, P.G., Seibold, M.A., Okamoto, K.S., Ingundson, K.J., Solon, M.C., Carrington, S.D., Fahy, J.V., 2011. The H antigen at epithelial surfaces is associated with susceptibility to asthma exacerbation. *Am. J. Respir. Crit. Care Med.* 183, 189–194. <https://doi.org/10.1164/rccm.201003-0488OC>.
- Johnsen, J.M., Levy, G.G., Westrick, R.J., Tucker, P.K., Ginsburg, D., 2008. The endothelial-specific regulatory mutation, *Mwf1*, is a common mouse founder allele. *Mamm. Genome* 19, 32–40. <https://doi.org/10.1007/s00335-007-9079-4>.
- Johnsen, J.M., Teschke, M., Pavlidis, P., McGee, B.M., Tautz, D., Ginsburg, D., Baines, J. F., 2009. Selection on cis-regulatory variation at *B4galnt2* and its influence on von willebrand factor in house mice. *Mol. Biol. Evol.* 26, 567–578. <https://doi.org/10.1093/molbev/msn284>.
- Jones, M.K., Watanabe, M., Zhu, S., Graves, C.L., Keyes, L.R., Grau, K.R., Gonzalez-Hernandez, M.B., Iovine, N.M., Wobus, C.E., Vinjé, J., Tibbetts, S.A., Wallet, S.M., Karst, S.M., 2014. Enteric bacteria promote human and mouse norovirus infection of B cells. *Science* 346, 755–759. <https://doi.org/10.1126/science.1257147>.
- Josenhans, C., Müthing, J., Elling, L., Barföld, S., Schmidt, H., 2020. How bacterial pathogens of the gastrointestinal tract use the mucosal glyco-code to harness mucus and microbiota: new ways to study an ancient bag of tricks. *Int. J. Med. Microbiol.* 310, 151392. <https://doi.org/10.1016/j.ijmm.2020.151392>.
- Juge, N., 2019. Special issue: gut bacteria–mucus interaction. *Microorganisms* 7, 6. <https://doi.org/10.3390/microorganisms7010006>.
- Kalas, N., Hibbing, M.E., Maddirala, A.R., Chugani, R., Pinkner, J.S., Mydock-McGrane, L.K., Conover, M.S., Janetka, J.W., Hultgren, S.J., 2018. Structure-based discovery of glycomimetic FimH ligands as inhibitors of bacterial adhesion during urinary tract infection. *PNAS* 115, E2819–E2828. <https://doi.org/10.1073/pnas.1720140115>.
- Kaper, J.B., Nataro, J.P., Mobley, H.L.T., 2004. Pathogenic *Escherichia coli*. *Nat. Rev. Microbiol.* 2, 123–140. <https://doi.org/10.1038/nrmicro818>.
- Kashyap, P.C., Marcolai, A., Ursell, L.K., Smits, S.A., Sonnenburg, E.D., Costello, E.K., Higginbottom, S.K., Domino, S.E., Holmes, S.P., Relman, D.A., Knight, R., Gordon, J., Sonnenburg, J.L., 2013. Genetically dictated change in host mucus carbohydrate landscape exerts a diet-dependent effect on the gut microbiota. *Proc. Natl. Acad. Sci. U. S. A.* 110, 17059. <https://doi.org/10.1073/pnas.1306070110>.
- Kawamura, Y.I., Kawashima, R., Fukunaga, R., Hirai, K., Toyama-Sorimachi, N., Tokuhara, M., Shimizu, T., Dohi, T., 2005. Introduction of sda carbohydrate antigen in gastrointestinal cancer cells eliminates selectin ligands and inhibits metastasis. *Cancer Res.* 65, 6220–6227. <https://doi.org/10.1158/0008-5472.CAN-05-0639>.
- Ke, J., Li, Y., Han, C., He, R., Lin, R., Qian, W., Hou, X., 2020. Fucose ameliorate intestinal inflammation through modulating the crosstalk between bile acids and gut microbiota in a chronic colitis murine model. *Inflamm. Bowel Dis.* 26, 863–873. <https://doi.org/10.1093/ibd/izaa007>.
- Kelly, R.J., Rouquier, S., Giorgi, D., Lennon, G.G., Lowe, J.B., 1995. Sequence and expression of a candidate for the human Secretor blood group alpha(1,2)-fucosyltransferase gene (*FUT2*). Homozygosity for an enzyme-inactivating nonsense mutation commonly correlates with the non-secretor phenotype. *J. Biol. Chem.* 270, 4640–4649. <https://doi.org/10.1074/jbc.270.9.4640>.
- Khalil, A., Feghali, R., Hassoun, M., 2020. The lebanese COVID-19 cohort; a challenge for the ABO blood group system. *Front. Med.* 7. <https://doi.org/10.3389/fmed.2020.585341>.
- Kindberg, E., Hejdeman, B., Bratt, G., Wahren, B., Lindblom, B., Hinkula, J., Svensson, L., 2006. A nonsense mutation (428G→A) in the fucosyltransferase *FUT2* gene affects the progression of HIV-1 infection. *AIDS* 20, 685–689. <https://doi.org/10.1093/aid/0000216368.23325.be>.
- Koda, Y., Tachida, H., Pang, H., Liu, Y., Soejima, M., Ghaderi, A.A., Takenaka, O., Kimura, H., 2001. Contrasting patterns of polymorphisms at the ABO-Secretor gene (*FUT2*) and plasma α(1,3)Fucosyltransferase gene (*FUT6*) in human populations. *Genetics* 158, 747–756.
- Koropatkin, N.M., Cameron, E.A., Martens, E.C., 2012. How glycan metabolism shapes the human gut microbiota. *Nat. Rev. Microbiol.* 10, 323–335. <https://doi.org/10.1038/nrmicro2746>.
- Landsteiner, K., 1900. Zur Kenntnis der antifерmentativen, lytischen und agglutinierenden Wirkungen des Blutserums und der Lymphe. *Zentralbl. Bakteriol.* 27, 357–362.
- Lane, E.R., Zisman, T.L., Suskind, D.L., 2017. The microbiota in inflammatory bowel disease: current and therapeutic insights. *J. Inflamm. Res.* 10, 63–73. <https://doi.org/10.2147/JIR.S116088>.

- Larsson, J.M.H., Karlsson, H., Crespo, J.G., Johansson, M.E.V., Eklund, L., Sjövall, H., Hansson, G.C., 2011. Altered O-glycosylation profile of MUC2 mucin occurs in active ulcerative colitis and is associated with increased inflammation. *Inflamm. Bowel Dis.* 17, 2299–2307. <https://doi.org/10.1002/ibd.21625>.
- Laucirica, D.R., Triantis, V., Schoemaker, R., Estes, M.K., Ramani, S., 2017. Milk oligosaccharides inhibit human rotavirus infectivity in MA104 cells. *J. Nutr.* 147, 1709–1714. <https://doi.org/10.3945/jn.116.246090>.
- Lindesmith, L., Moe, C., Marionneau, S., Ruvoen, N., Jiang, X., Lindblad, L., Stewart, P., LePendu, J., Baric, R., 2003. Human susceptibility and resistance to Norwalk virus infection. *Nat. Med.* 9, 548–553. <https://doi.org/10.1038/nm860>.
- Linnemann, M., Johnsen, J.M., Montero, I., Brzezinski, C.R., Harr, B., Baines, J.F., 2011. Long-term balancing selection at the blood group-related gene B4galnt2 in the genus Mus (Rodentia; Muridae). *Mol. Biol. Evol.* 28, 2999–3003. <https://doi.org/10.1093/molbev/msr150>.
- Lo Presti, L., Cabuy, E., Chiricolo, M., Dall'Olio, F., 2003. Molecular cloning of the human β1,4 N-Acetylgalactosaminyltransferase responsible for the biosynthesis of the Sda histo-blood group antigen: the sequence predicts a very long cytoplasmic domain. *J. Biochem.* 134, 675–682. <https://doi.org/10.1093/jb/mvg192>.
- Lopman, B.A., Trivedi, T., Vicuna, Y., Costantini, V., Collins, N., Gregorius, N., Parashar, U., Sandoval, C., Broncano, N., Vacca, M., Chico, M.E., Vinjé, J., Cooper, P.J., 2015. Norovirus infection and disease in an ecuadorian birth cohort: association of certain norovirus genotypes with host FUT2 secretor status. *J. Infect. Dis.* 211, 1813–1821. <https://doi.org/10.1093/infdis/jiu672>.
- Lopman, B.A., Steele, D., Kirkwood, C.D., Parashar, U.D., 2016. The vast and varied global burden of norovirus: prospects for prevention and control. *PLoS Med.* 13, e1001999. <https://doi.org/10.1371/journal.pmed.1001999>.
- Macvie, S.I., Morton, J.A., Pickles, M.M., 1967. The reactions and inheritance of a new blood group antigen. *Sda*. *Vox Sang.* 13, 485–492. <https://doi.org/10.1111/j.1423-0410.1967.tb03795.x>.
- Magalhães, A., Gomes, J., Ismail, M.N., Haslam, S.M., Mendes, N., Osório, H., David, L., Le Pendu, J., Haas, R., Dell, A., Borén, T., Reis, C.A., 2009. Fut2-null mice display an altered glycosylation profile and impaired BabA-mediated Helicobacter pylori adhesion to gastric mucosa. *Glycobiology* 19, 1525–1536. <https://doi.org/10.1093/glycob/cwp131>.
- Magalhães, A., Rossez, Y., Robbe-Masselot, C., Maes, E., Gomes, J., Shevtsova, A., Bugaytsova, J., Borén, T., Reis, C.A., 2016. MucSac gastric mucin glycosylation is shaped by FUT2 activity and functionally impacts Helicobacter pylori binding. *Sci. Rep.* 6, 25575. <https://doi.org/10.1038/srep25575>.
- Mahdavi, J., Sondén, B., Hurtig, M., Olfat, F.O., Forsberg, L., Roche, N., Angstrom, J., Larsson, T., Teneberg, S., Karlsson, K.-A., Altraja, S., Wadström, T., Kersulyte, D., Berg, D.E., Dubois, A., Peterson, C., Magnusson, K.-E., Norberg, T., Lindh, F., Lundskog, B.B., Arqvist, A., Hammarström, L., Borén, T., 2002. Helicobacter pylori SabA adhesin in persistent infection and chronic inflammation. *Science* 297, 573–578. <https://doi.org/10.1126/science.1069076>.
- Marionneau, S., Caillau-Thomas, A., Rocher, J., Le Moullac-Vaidye, B., Ruvoen, N., Clément, M., Le Pendu, J., 2001. ABH and Lewis histo-blood group antigens, a model for the meaning of oligosaccharide diversity in the face of a changing world. *Biochimie* 83, 565–573. [https://doi.org/10.1016/S0300-9084\(01\)01321-9](https://doi.org/10.1016/S0300-9084(01)01321-9).
- Marshall, B., Warren, J.R., 1984. Unidentified curved bacilli in the stomach of patients with gastritis and peptic ulceration. *Lancet* 1311–1315. [https://doi.org/10.1016/S0140-6736\(84\)91816-6](https://doi.org/10.1016/S0140-6736(84)91816-6). Originally published as Volume 1, Issue 8390 323.
- McGovern, D.P.B., Jones, M.R., Taylor, K.D., Marciante, K., Yan, X., Dubinsky, M., Ippoliti, A., Vasiliauskas, E., Beresh, D., Derkowsky, C., Dutridge, D., Fleshner, P., Shih, D.Q., Melmed, G., Mengesha, E., King, L., Pressman, S., Haritunians, T., Guo, X., Targan, S.R., Rotter, J.I., 2010. Fucosyltransferase 2 (FUT2) non-secretor status is associated with Crohn's disease. *Hum. Mol. Genet.* 19, 3468–3476. <https://doi.org/10.1093/hmg/ddq248>.
- Meiers, J., Siebs, E., Zahorska, E., Titz, A., 2019. Lectin antagonists in infection, immunity, and inflammation. *Curr. Opin. Chem. Biol.* 53, 51–67. <https://doi.org/10.1016/j.cbpa.2019.07.005>.
- Meiers, J., Zahorska, E., Röhrig, T., Hauck, D., Wagner, S., Titz, A., 2020. Directing drugs to bugs: antibiotic-carbohydrate conjugates targeting biofilm-associated lectins of *Pseudomonas aeruginosa*. *J. Med. Chem.* 63, 11707–11724. <https://doi.org/10.1021/acs.jmedchem.0c00856>.
- Mohilke, K.L., Nichols, W.C., Westrick, R.J., Novak, E.K., Cooney, K.A., Swank, R.T., Ginsburg, D., 1996. A novel modifier gene for plasma von Willebrand factor level maps to distal mouse chromosome 11. *Proc. Natl. Acad. Sci. U. S. A.* 93, 15352–15357. <https://doi.org/10.1073/pnas.93.26.15352>.
- Mohilke, K.L., Purkayastha, A.A., Westrick, R.J., Smith, P.L., Petryniak, B., Lowe, J.B., Ginsburg, D., 1999. Mwf, a dominant modifier of murine von willebrand factor, results from altered lineage-specific expression of a glycosyltransferase. *Cell* 96, 111–120. [https://doi.org/10.1016/S0009-8674\(00\)80964-2](https://doi.org/10.1016/S0009-8674(00)80964-2).
- Montiel, M.-D., Krzewinski-Recchi, M.-A., Delanoy, P., Harduin-Lepers, A., 2003. Molecular cloning, gene organization and expression of the human UDP-GalNAc: Neu5Acα2-3Galβ1-Rα1,4-N-acetylglactosaminyltransferase responsible for the biosynthesis of the blood group Sda/Cad antigen: evidence for an unusual extended cytoplasmic domain. *Biochem. J.* 373, 369–379. <https://doi.org/10.1042/bj20021892>.
- Moran, A.P., Gupta, A., Joshi, L., 2011. Sweet-talk: role of host glycosylation in bacterial pathogenesis of the gastrointestinal tract. *Gut* 60, 1412–1425. <https://doi.org/10.1136/gut.2010.212704>.
- Morrow, A.L., Ruiz-Palacios, G.M., Altaye, M., Jiang, X., Lourdes Guerrero, M., Meinzen-Derr, J.K., Farkas, T., Chaturvedi, P., Pickering, L.K., Newburg, D.S., 2004. Human milk oligosaccharides are associated with protection against diarrhea in breast-fed infants. *J. Pediatr.* 145, 297–303. <https://doi.org/10.1016/j.jpeds.2004.04.054>.
- Morrow, A.L., Ruiz-Palacios, G.M., Jiang, X., Newburg, D.S., 2005. Human-milk glycans that inhibit pathogen binding protect breast-feeding infants against infectious diarrhea. *J. Nutr.* 135, 1304–1307. <https://doi.org/10.1093/jn/135.5.1304>.
- Morton, J.A., Pickles, M.M., Terry, A.M., 1970. The SdaBlood group antigen in tissues and body fluids. *Vox Sang.* 19, 472–482. <https://doi.org/10.1111/j.1423-0410.1970.tb01779.x>.
- Mottram, L., Liu, J., Chavan, S., Tobias, J., Svensson, A.-M., Holgersson, J., 2018. Glyco-engineered cell lines and computational docking studies reveals enterotoxigenic Escherichia coli CFA/I fimbria bind to Lewis a glycans. *Sci. Rep.* 8, 11250. <https://doi.org/10.1038/s41598-018-29258-0>.
- Muñiz-Díaz, E., Llopis, J., Parra, R., Roig, J., Ferrer, G., Grifols, J., Millán, A., Ene, G., Ramiro, L., Maglio, L., García, N., Pinacho, A., Jaramillo, A., Peró, A., Artaza, G., Vallés, R., Sauleda, S., Puig, L., Contreras, E., 2020. Relationship between the ABO blood group and COVID-19 susceptibility, severity and mortality in two cohorts of patients. *Blood Transfusion*. <https://doi.org/10.2450/2020.0256-20>.
- Nell, S., Kenne, L., Schwarz, S., Josenhans, C., Suerbaum, S., 2014. Dynamics of Lewis b binding and sequence variation of the babA adhesin gene during chronic *Helicobacter pylori* infection in humans. *mBio* 5. <https://doi.org/10.1128/mBio.02281-14>.
- Nordgren, J., Niitima, L.W., Ouermi, D., Simpore, J., Svensson, L., 2013. Host genetic factors affect susceptibility to norovirus infections in Burkina Faso. *PLoS One* 8, e69557. <https://doi.org/10.1371/journal.pone.0069557>.
- Pacheco, A.R., Curtis, M.M., Ritchie, J.M., Munera, D., Waldor, M.K., Moreira, C.G., Sperandio, V., 2012. Fucose sensing regulates bacterial intestinal colonization. *Nature* 492, 113–117. <https://doi.org/10.1038/nature11623>.
- Papatheodorou, I., Moreno, P., Manning, J., Fuentes, A.M.-P., George, N., Fexova, S., Fonseca, N.A., Füllgrabe, A., Green, M., Huang, N., Huerta, L., Iqbal, H., Jianu, M., Mohammadi, S., Zhao, L., Jarnuczak, A.F., Jupp, S., Marioni, J., Meyer, K., Petryszak, R., Prada Medina, C.A., Talavera-López, C., Teichmann, S., Vizcaino, J.A., Brazma, A., 2020. Expression Atlas update: from tissues to single cells. *Nucleic Acids Res.* 48, D77–D83. <https://doi.org/10.1093/nar/gkz947>.
- Pfeiffer, P.D. med A.H.F., 2020. Diabetes Nutrition Algorithms - Sugars: Galactose- and Fiber-induced Metabolic Improvement in the Diabetic Treatment of Type 2 Diabetes (Clinical Trial Registration No. NCT01776099). <https://clinicaltrials.gov..>
- Pham, T.A.N., Clare, S., Goulding, D., Arasteh, J.M., Stares, M.D., Browne, H.P., Keane, J.A., Page, A.J., Kumasaki, N., Kane, L., Mottram, L., Harcourt, K., Hale, C., Arends, M.J., Gaffney, D.J., Dougan, G., Lawley, T.D., 2014. Epithelial IL-22RA1-Mediated fucosylation promotes intestinal colonization resistance to an opportunistic pathogen. *Cell Host Microbe* 16, 504–516. <https://doi.org/10.1016/j.chom.2014.08.017>.
- Pickard, J.M., Chervonsky, A.V., 2015. Intestinal fucose as a mediator of host-microbe symbiosis. *J. Immunol.* 194, 5588–5593. <https://doi.org/10.4049/jimmunol.1500395>.
- Pickard, J.M., Maurice, C.F., Kinnebrew, M.A., Abt, M.C., Schenten, D., Golovkina, T.V., Bogatyrev, S.R., Ismagilov, R.F., Palmer, E.G., Turnbaugh, P.J., Chervonsky, A.V., 2014. Rapid fucosylation of intestinal epithelium sustains host-commensal symbiosis in sickness. *Nature* 514, 638–641. <https://doi.org/10.1038/nature13823>.
- Piller, F., Blanchard, D., Huet, M., Cartron, J.-P., 1986. Identification of a α-NeuAc-(2→3)-β-D-galactopyranosyl N-acetyl-β-D-galactosaminyltransferase in human kidney. *Carbohydr. Res.* 149, 171–184. [https://doi.org/10.1016/S0008-6215\(00\)90376-8](https://doi.org/10.1016/S0008-6215(00)90376-8).
- Pinho, S.S., Reis, C.A., 2015. Glycosylation in cancer: mechanisms and clinical implications. *Nat. Rev. Cancer* 15, 540–555. <https://doi.org/10.1038/nrc3982>.
- Pruss, K.M., Marcobal, A., Southwick, A.M., Dahan, D., Smits, S.A., Ferreyra, J.A., Higginbottom, S.K., Sonnenburg, E.D., Kashyap, P.C., Choudhury, B., Bode, L., Sonnenburg, J.L., 2020. Mucin-derived O-glycans supplemented to diet mitigate diverse microbiota perturbations. *ISME J.* 1–15. <https://doi.org/10.1038/s41396-020-00798-6>.
- Pucci, M., Gomes Ferreira, I., Orlandani, M., Malagolini, N., Ferracini, M., Dall'Olio, F., 2020. High expression of the sda synthase B4GALNT2 associates with good prognosis and attenuates stemness in colon cancer. *Cells* 9, 948. <https://doi.org/10.3390/cells9040948>.
- Rajilić-Stojanović, M., Biagi, E., Heilig, H.G.H.J., Kajander, K., Kekkonen, R.A., Tims, S., de Vos, W.M., 2011. Global and deep molecular analysis of microbiota signatures in fecal samples from patients with irritable bowel syndrome. *Gastroenterology* 141, 1792–1801. <https://doi.org/10.1053/j.gastro.2011.07.043>.
- Ramani, S., Cortes-Penfield, N.W., Hu, L., Crawford, S.E., Czako, R., Smith, D.F., Kang, G., Ramig, R.F., Pendu, J.L., Prasad, B.V.V., Estes, M.K., 2013. The VP8* domain of neonatal rotavirus strain G10P[1] binds to type II precursor glycans. *J. Virol.* 87, 7255–7264. <https://doi.org/10.1128/JVI.03518-12>.
- Rausch, P., Rehman, A., Kunzel, S., Hasler, R., Ott, S.J., Schreiber, S., Rosenstiel, P., Franke, A., Baines, J.F., 2011. Colonic mucus-associated microbiota is influenced by an interaction of Crohn disease and FUT2 (Secretor) genotype. *Proc. Natl. Acad. Sci.* 108, 19030–19035. <https://doi.org/10.1073/pnas.1106408108>.
- Rausch, P., Steck, N., Suwandi, A., Seidel, J.A., Kunzel, S., Bhullar, K., Basic, M., Bleich, A., Johnsen, J.M., Vallance, B.A., Baines, J.F., Grassl, G.A., 2015. Expression of the blood-group-Related gene B4galnt2 alters susceptibility to *Salmonella* infection. *PLoS Pathog.* 11, e1005008. <https://doi.org/10.1371/journal.ppat.1005008>.
- Rausch, P., Kunzel, S., Suwandi, A., Grassl, G.A., Rosenstiel, P., Baines, J.F., 2017. Multigenerational influences of the *Fut2* gene on the dynamics of the gut microbiota in mice. *Front. Microbiol.* 8, 991. <https://doi.org/10.3389/fmicb.2017.00991>.
- Ravn, V., Dabelsteen, E., 2000. Tissue distribution of histo-blood group antigens. *APMIS* 108, 1–28. <https://doi.org/10.1034/j.1600-0463.2000.d01-1.x>.
- Rayes, A., Morrow, A.L., Payton, L.R., Lake, K.E., Lane, A., Davies, S.M., 2016. A genetic modifier of the gut microbiome influences the risk of graft-versus-host disease and

- bacteremia after hematopoietic stem cell transplantation. *Biol. Blood Marrow Transplant.* 22, 418–422. <https://doi.org/10.1016/j.bbmt.2015.11.017>.
- Raza, M.W., Blackwell, C.C., Molyneaux, P., James, V.S., Ogilvie, M.M., Inglis, J.M., Weir, D.M., 1991. Association between secretor status and respiratory viral illness. *BMJ* 303, 815–818. <https://doi.org/10.1136/bmj.303.6806.815>.
- Renton, P.H., Howell, P., Ikin, E.W., Giles, C.M., Goldsmith, D.K.L.G., 1967. Anti-sda, a new blood group antibody. *Vox Sang.* 13, 493–501. <https://doi.org/10.1111/j.1423-0410.1967.tb03796.x>.
- Robilotto, E., Deresinski, S., Pinsky, B.A., 2015. Norovirus. *Clin. Microbiol. Rev.* 28, 134–164. <https://doi.org/10.1128/CMR.00075-14>.
- Rodríguez-Díaz, J., García-Mantrana, I., Villa-Vicent, S., Gozalbo-Rovira, R., Buesa, J., Monedero, V., Collado, M.C., 2017. Relevance of secretor status genotype and microbiota composition in susceptibility to rotavirus and norovirus infections in humans. *Sci. Rep.* 7, 45595. <https://doi.org/10.1038/srep45595>.
- Round, J.L., Mazmanian, S.K., 2009. The gut microbiota shapes intestinal immune responses during health and disease. *Nat. Rev. Immunol.* 9, 313–323. <https://doi.org/10.1038/nri2515>.
- Saitou, N., Yamamoto, F., 1997. Evolution of primate ABO blood group genes and their homologous genes. *Mol. Biol. Evol.* 14, 399–411. <https://doi.org/10.1093/oxfordjournals.molbev.a025776>.
- Sallai, K., Hirvonen, J., Siitonen, J., Ahonen, I., Anglenius, H., Maukonen, J., 2021. Selective utilization of the human milk oligosaccharides 2'-Fucosyllactose, 3-Fucosyllactose, and difucosyllactose by various probiotic and pathogenic bacteria. *J. Agric. Food Chem.* 69, 170–182. <https://doi.org/10.1021/acs.jafc.0c06041>.
- Schreiber, S., Konradt, M., Grolli, C., Scheid, P., Hanauer, G., Werling, H.-O., Josenhans, C., Suerbaum, S., 2004. The spatial orientation of Helicobacter pylori in the gastric mucus. *Proc. Natl. Acad. Sci. U. S. A.* 101, 5024–5029. <https://doi.org/10.1073/pnas.030836101>.
- Serafini-Cessi, F., Dall'Olio, F., Malagolini, N., 1986. Characterization of N-acetyl- β -d-galactosaminyl-transferase from guinea-pig kidney involved in the biosynthesis of Sda antigenic substrates with Tamm-Horsfall glycoprotein. *Carbohydr. Res.* 151, 65–76. [https://doi.org/10.1016/S0008-6215\(00\)90330-6](https://doi.org/10.1016/S0008-6215(00)90330-6).
- Serafini-Cessi, F., Monti, A., Cavallone, D., 2005. N-Glycans carried by Tamm-Horsfall glycoprotein have a crucial role in the defense against urinary tract diseases. *Glycoconj. J.* 22, 383–394. <https://doi.org/10.1007/s10719-005-2142-z>.
- Severe Covid-19 GWAS Group, Ellinghaus, D., Degenhardt, F., Bujanda, L., Buti, M., Albillios, A., Invernizzi, P., Fernández, J., Prati, D., Baselli, G., Assetta, R., Grimsrud, M.M., Milani, C., Aziz, F., Kässens, J., May, S., Wendorff, M., Wienbrandt, L., Ullendahl-Werth, F., Zheng, Y., Yi, X., de Pablo, R., Chercos, A.G., Palom, A., García-Fernandez, A.-E., Rodríguez-Frias, F., Zanella, A., Bandera, A., Protti, A., Agheamo, A., Lleo, A., Biondi, A., Caballero-Garralda, A., Gori, A., Tanck, A., Carreras Nolla, A., Latiano, A., Fracanza, A., Peschuck, A., Julià, A., Pesenti, A., Vozza, A., Jiménez, D., Mateos, B., Nazaria Jiménez, B., Quereda, C., Paccapelo, C., Gassner, C., Angelini, C., Cea, C., Solier, A., Pestana, D., Muñiz-Díaz, E., Sandoval, E., Paraboschi, E.M., Navas, E., García Sánchez, F., Cerilli, F., Martinelli-Boneschi, F., Peyvandi, F., Blasi, F., Téllez, L., Blanco-Grau, A., Hemmrich-Stanislak, G., Grasselli, G., Costantino, G., Cardamone, G., Foti, G., Aneli, S., Kurihara, H., ElAbd, H., My, I., Galván-Femenia, I., Martín, J., Erdmann, J., Ferrusquía-Latorre, J., García-Extebarria, K., Izquierdo-Sánchez, L., Bettini, L.R., Sumoy, L., Terranova, L., Moreira, L., Santoro, L., Scudeller, L., Mesonero, F., Roade, L., Rühlemann, M.C., Schaefer, M., Carrabba, M., Riveiro-Barcelo, M., Figuera-Basso, M., Valsecchi, M.G., Hernández-Tejero, M., Acosta-Herrera, M., D'Angio, M., Baldini, M., Cazzaniga, M., Schulzky, M., Cecconi, M., Wittig, M., Ciccarelli, M., Rodríguez-Gandía, M., Bocciolone, M., Miozzo, M., Montano, N., Braun, N., Sacchi, N., Martínez, N., Özér, O., Palmieri, O., Faverio, P., Preanton, P., Bonfanti, P., Omodei, P., Tentorio, P., Castro, P., Rodrigues, P.M., Blandino Ortiz, A., de Cid, R., Ferrer, R., Gualtierotti, R., Nieto, R., Goerg, S., Badalamenti, S., Marsal, S., Matullo, G., Pelusi, S., Juzenas, S., Aliberti, S., Monzani, V., Moreno, V., Wesse, T., Lenz, T.L., Pumarola, T., Rimoldi, V., Bosari, S., Albrecht, W., Peter, W., Romero-Gómez, M., D'Amato, M., Duga, S., Banales, J.M., Hov, J.R., Folseras, T., Valenti, L., Franke, A., Karlsten, T.H., 2020. Genomewide association study of severe covid-19 with respiratory failure. *N. Engl. J. Med.* 383, 1522–1534. <https://doi.org/10.1056/NEJMoa2020283>.
- Shang, J., Piskarev, V.E., Xia, M., Huang, P., Jiang, X., Likhoshsterstov, L.M., Novikova, O.S., Newburg, D.S., Ratner, D.M., 2013. Identifying human milk glycans that inhibit norovirus binding using surface plasmon resonance. *Glycobiology* 23, 1491–1498. <https://doi.org/10.1093/glycob/cwt077>.
- Sheinfeld, J., Schaeffer, A.J., Cordon-Carbo, C., Rogatko, A., Fair, W.R., 1989. Association of the lewis blood-group phenotype with recurrent urinary tract infections in women. *N. Engl. J. Med.* 320, 773–777. <https://doi.org/10.1056/NEJM198903233201205>.
- Shin, J., Noh, J.-R., Chang, D.-H., Kim, Y.-H., Kim, M.H., Lee, E.S., Cho, S., Ku, B.J., Rhee, M.-S., Kim, B.-C., Lee, C.-H., Cho, B.-K., 2019. Elucidation of Akkermansia muciniphila probiotic traits driven by mucin depletion. *Front. Microbiol.* 10, 1137. <https://doi.org/10.3389/fmicb.2019.01137>.
- Smith, P.L., Lowe, J.B., 1994. Molecular cloning of a murine N-acetylgalactosamine transferase cDNA that determines expression of the T lymphocyte-specific CT oligosaccharide differentiation antigen. *J. Biol. Chem.* 269, 15162–15171.
- Smith-Brown, P., Morrison, M., Krause, L., Davies, P.S.W., 2016. Mothers secretor status affects development of children's microbiota composition and function: a pilot study. *PLoS One* 11, e0161211. <https://doi.org/10.1371/journal.pone.0161211>.
- Smyth, D.J., Cooper, J.D., Howson, J.M.M., Clarke, P., Downes, K., Mistry, T., Stevens, H., Walker, N.M., Todd, J.A., 2011. FUT2 nonsecretor status links type 1 diabetes susceptibility and resistance to infection. *Diabetes* 60, 3081–3084. <https://doi.org/10.2337/db11-0638>.
- Soejima, M., Fujimoto, R., Agusa, T., Iwata, H., Fujihara, J., Takeshita, H., Minh, T.B., Trang, P.T.K., Viet, P.H., Nakajima, T., Yoshimoto, J., Tanabe, S., Koda, Y., 2012. Genetic variation of FUT2 in a Vietnamese population: identification of two novel Se enzyme-inactivating mutations. *Transfusion* 52, 1268–1275. <https://doi.org/10.1111/j.1537-2995.2011.03485.x>.
- Stahl, M., Fris, L.M., Nothaft, H., Liu, X., Li, J., Szymanski, C.M., Stintzi, A., 2011. L-fucose utilization provides *Campylobacter jejuni* with a competitive advantage. *Proc. Natl. Acad. Sci. U. S. A.* 108, 7194–7199. <https://doi.org/10.1073/pnas.1014125108>.
- Stepleton, A., Nudelman, E., Clausen, H., Hakomori, S., Stamm, W.E., 1992. Binding of uropathogenic *Escherichia coli* R45 to glycolipids extracted from vaginal epithelial cells is dependent on histo-blood-group secretor status. *J. Clin. Invest.* 90, 965–972. <https://doi.org/10.1172/JCI115973>.
- Staubach, F., Künnel, S., Baines, A.C., Yee, A., McGee, B.M., Bäckhed, F., Baines, J.F., Johnsen, J.M., 2012. Expression of the blood-group-related glycosyltransferase B4galnt2 influences the intestinal microbiota in mice. *ISME J.* 6, 1345–1355. <https://doi.org/10.1038/ismej.2011.204>.
- Storry, J.R., Castilho, L., Chen, Q., Daniels, G., Denomme, G., Flegel, W.A., Gassner, C., de Haas, M., Hyland, C., Keller, M., Lomas-Francis, C., Moulds, J.M., Nogues, N., Olson, M.L., Peyrard, T., van der Schoot, C.E., Tani, Y., Thornton, N., Wagner, F., Wendel, S., Westhoff, C., Yahalom, V., 2016. International society of blood transfusion working party on red cell immunogenetics and terminology: report of the Seoul and London meetings. *ISBT Sci. Ser.* 11, 118–122. <https://doi.org/10.1111/voxs.12280>.
- Suwandi, A., Galeev, A., Riedel, R., Sharma, S., Seeger, K., Sterzenbach, T., Garcia Pastor, L., Boyle, E.C., Gal-Mor, O., Hensel, M., Casadesús, J., Baines, J.F., Grassl, G. A., 2019. Stx fimbriae-fucose interaction increases *Salmonella*-induced intestinal inflammation and prolongs colonization. *PLoS Pathog.* 15, e1007915. <https://doi.org/10.1371/journal.ppat.1007915>.
- Tailford, L.E., Crost, E.H., Kavanaugh, D., Juge, N., 2015. Mucin glycan foraging in the human gut microbiome. *Front. Genet.* 6, 81. <https://doi.org/10.3389/fgene.2015.00081>.
- Taylor, S.L., Woodman, R.J., Chen, A.C., Burr, L.D., Gordon, D.L., McGuckin, M.A., Wesselingh, S., Rogers, G.B., 2017. FUT2 genotype influences lung function, exacerbation frequency and airway microbiota in non-CF bronchiectasis. *Thorax* 72, 304–310. <https://doi.org/10.1136/thoraxjnli-2016-208775>.
- Taylor, S.L., McGuckin, M.A., Wesselingh, S., Rogers, G.B., 2018. Infection's sweet tooth: how glycans mediate infection and disease susceptibility. *Trends Microbiol.* 26, 92–101. <https://doi.org/10.1016/j.tim.2017.09.011>.
- Tollefson, K., Kornfeld, R., 1983. The B4 lectin from *Vicia villosa* seeds interacts with N-acetylgalactosamine residues alpha-linked to serine or threonine residues in cell surface glycoproteins. *J. Biol. Chem.* 258, 5172–5176.
- Tong, M., McHardy, I., Ruegger, P., Goudarzi, M., Kashyap, P.C., Haritunians, T., Li, X., Graeber, T.G., Schwager, E., Huttenhower, C., Fornace, A.J., Sonnenburg, J.L., McGovern, D.P.B., Borneman, J., Braun, J., 2014. Reprograming of gut microbiome energy metabolism by the FUT2 Crohn's disease risk polymorphism. *ISME J.* 8, 2193–2206. <https://doi.org/10.1038/ismej.2014.64>.
- Torres, A.G., Zhou, X., Kaper, J.B., 2005. Adherence of diarrheagenic *Escherichia coli* strains to epithelial cells. *Infect. Immun.* 73, 18–29. <https://doi.org/10.1128/IAI.73.1.18-29.2005>.
- Turpin, W., Bedrani, L., Espin-Garcia, O., Xu, W., Silverberg, M.S., Smith, M.I., Guttmann, D.S., Griffiths, A., Moayedi, P., Panaccione, R., Huynh, H., Steinhart, H., Aumais, G., Shestopaloff, K., Dieleman, L.A., Turner, D., Paterson, A.D., Croitoru, K., 2018. FUT2 genotype and secretory status are not associated with fecal microbial composition and inferred function in healthy subjects. *Gut Microbes* 9, 357–368. <https://doi.org/10.1080/19490976.2018.1445956>.
- Ubeda, C., Djukovic, A., Isaac, S., 2017. Roles of the intestinal microbiota in pathogen protection. *Clin. Transl. Immunology* 6, e128. <https://doi.org/10.1038/cti.2017.2>.
- Uchiyama, R., Chassaing, B., Zhang, B., Gewirtz, A.T., 2014. Antibiotic treatment suppresses rotavirus infection and enhances specific humoral immunity. *J. Infect. Dis.* 210, 171–182. <https://doi.org/10.1093/infdis/jiu037>.
- Vallier, M., Abou Chakra, M., Hindersin, L., Linnenbrink, M., Traulsen, A., Baines, J.F., 2017. Evaluating the maintenance of disease-associated variation at the blood group-related gene B4galnt2 in house mice. *BMC Evol. Biol.* 17, 187. <https://doi.org/10.1186/s12862-017-1035-7>.
- van der Hoof, J.J., Alghefari, W., Watson, E., Everest, P., Morton, F.R., Burgess, K.E.V., Smith, D.G.E., 2018. Unexpected differential metabolic responses of *Campylobacter jejuni* to the abundant presence of glutamate and fucose. *Metabolomics* 14, 144. <https://doi.org/10.1007/s11306-018-1438-5>.
- Wacklin, P., Mäkiyükkö, H., Alakulppi, N., Nikkilä, J., Tenkanen, H., Räbinä, J., Partanen, J., Aranko, K., Mättö, J., 2011. Secretor genotype (FUT2 gene) is strongly associated with the composition of Bifidobacteria in the human intestine. *PLoS One* 6, e20113. <https://doi.org/10.1371/journal.pone.0020113>.
- Wagner, C., Hensel, M., 2011. Adhesive mechanisms of *Salmonella enterica*. *Adv. Exp. Med. Biol.* 715, 17–34. https://doi.org/10.1007/978-94-007-0940-9_2.
- Walsh, C., Lane, J.A., van Sinderen, D., Hickey, R.M., 2020. Human milk oligosaccharides: shaping the infant gut microbiota and supporting health. *J. Funct. Foods* 72, 104074. <https://doi.org/10.1016/j.jff.2020.104074>.
- Warren, J.R., Marshall, B., 1983. Unidentified curved Bacilli on gastric epithelium in active chronic gastritis. *Lancet* 1273–1275. [https://doi.org/10.1016/S0140-6736\(83\)92719-8](https://doi.org/10.1016/S0140-6736(83)92719-8). Originally published as Volume 1, Issue 8336 321.
- Weening, E.H., Barker, J.D., Laarakker, M.C., Humphries, A.D., Tsolis, R.M., Bäumler, A. J., 2005. The *Salmonella enterica* serotype typhimurium lpf, bcf, stb, std, and sth fimbrial operons are required for intestinal persistence in mice. *Infect. Immun.* 73, 3358–3366. <https://doi.org/10.1128/IAI.73.6.3358-3366.2005>.

- Weichert, S., Jennewein, S., Hüfner, E., Weiss, C., Borkowski, J., Putze, J., Schrotten, H., 2013. Bioengineered 2'-fucosyllactose and 3-fucosyllactose inhibit the adhesion of *Pseudomonas aeruginosa* and enteric pathogens to human intestinal and respiratory cell lines. *Nutr. Res.* 33, 831–838. <https://doi.org/10.1016/j.nutres.2013.07.009>.
- Wong, H.H., Fung, K., Nicholls, J.M., 2019. MDCK-B4GalNT2 cells disclose a α 2,3-sialic acid requirement for the 2009 pandemic H1N1 A/California/04/2009 and NA aid entry of A/WSN/33. *Emerg. Microbes Infect.* 8, 1428–1437. <https://doi.org/10.1080/22221751.2019.1665971>.
- Wrzosek, L., Miquel, S., Noordine, M.-L., Bouet, S., Chevalier-Curt, M.J., Robert, V., Philippe, C., Bridonneau, C., Cherbuy, C., Robbe-Masselot, C., Langella, P., Thomas, M., 2013. Bacteroides thetaiotaomicron and *Faecalibacterium prausnitzii* influence the production of mucus glycans and the development of goblet cells in the colonic epithelium of a gnotobiotic model rodent. *BMC Biol.* 11, 61. <https://doi.org/10.1186/1741-7007-11-61>.
- Wu, H., Rebello, O., Crost, E.H., Owen, C.D., Walpole, S., Bennati-Granier, C., Ndeh, D., Monaco, S., Hicks, T., Colvile, A., Urbanowicz, P.A., Walsh, M.A., Angulo, J., Spencer, D.I.R., Juge, N., 2020. Fucosidases from the human gut symbiont *Ruminococcus gnavus*. *Cell. Mol. Life Sci.* <https://doi.org/10.1007/s0018-020-03514-x>.
- Yu, Z.-T., Chen, C., Kling, D.E., Liu, B., McCoy, J.M., Merighi, M., Heidtman, M., Newburg, D.S., 2013. The principal fucosylated oligosaccharides of human milk exhibit prebiotic properties on cultured infant microbiota. *Glycobiology* 23, 169–177. <https://doi.org/10.1093/glycob/cws138>.
- Yu, Z.-T., Nanthakumar, N.N., Newburg, D.S., 2016. The human milk oligosaccharide 2'-Fucosyllactose quenches campylobacter jejuni-induced inflammation in human epithelial cells HEp-2 and HT-29 and in mouse intestinal mucosa. *J. Nutr.* 146, 1980–1990. <https://doi.org/10.3945/jn.116.230706>.
- Yue, M., Rankin, S.C., Blanchet, R.T., Nulton, J.D., Edwards, R.A., Schifferli, D.M., 2012. Diversification of the *Salmonella* fimbriae: a model of macro- and microevolution. *PLoS One* 7, e38596. <https://doi.org/10.1371/journal.pone.0038596>.
- Zhao, C., Cooper, D.K.C., Dai, Y., Hara, H., Cai, Z., Mou, L., 2018. The Sda and Cad glycan antigens and their glycosyltransferase, β 1,4GalNAcT-II, in xenotransplantation. *Xenotransplantation* 25, e12386. <https://doi.org/10.1111/xcia.12386>.
- Zhao, J., Yang, Y., Huang, H., Li, D., Gu, D., Lu, X., Zhang, Z., Liu, L., Liu, T., Liu, Y., He, Y., Sun, B., Wei, M., Yang, G., Wang, X., Zhang, L., Zhou, X., Xing, M., Wang, P., G., 2020. Relationship between the ABO blood group and the coronavirus disease 2019 (COVID-19) susceptibility. *Clin. Infect. Dis.* <https://doi.org/10.1093/cid/ciaa1150>.

Chapter 2: Role of *B4galnt2* and Microbial Diversity in Colonization Resistance against *Salmonella* Typhimurium

Introduction

Microbial populations, referred to as microbiota, comprise a diverse group of microorganisms including bacteria, archaea, fungi, protozoa, and viruses, which inhabit distinct host niches. The composition and diversity of these populations changes across different biological sites, as well as time (Greenhalgh et al., 2016; Kennedy and Chang, 2020). Many factors can modulate the microbiota diversity, including microbial interactions, environmental influences, and host genetic background (Ahn and Hayes, 2021; Blekhman et al., 2015; Coyte and Rakoff-Nahoum, 2019).

The gastrointestinal tract represents one of the largest interfaces between host, environment, and microbiome, harboring from 10^7 microorganisms in the upper small intestine to 10^{14} in the human colon (Sender et al., 2016). The abundance and diversity of the microbiota exhibits a non-uniform spatial distribution along the entire intestinal tract, with discernible variations between the luminal and mucosal environments (Lkhagva et al., 2021; Wu et al., 2020; Zoetendal et al., 2002).

Intestinal microbiota is known to have a strong effect on the health and physiology of their hosts. The microbial communities contribute to the development and homeostasis of the host's immune system (Round and Mazmanian, 2009; Wu and Wu, 2012), as well as to the morphogenesis and maturation of the gastrointestinal tract (Reinhardt et al., 2012; Sommer and Bäckhed, 2013). Another important aspect of the intestinal microbiota's functionality is protection against invading pathogens, known as colonization resistance (Ducarmon et al., 2019). The mechanism by which the microbiota confer colonization resistance could be direct, such as the release of a variety of metabolites, including bacteriocins (Heilbronner et al., 2021), and secondary bile acids (Ducarmon et al., 2019; Fuchs, 2023; Winston and Theriot, 2016). Another important group of metabolites are short-chain fatty acids (SCFAs), which are produced through fermentation of nondigestible carbohydrates by the microbiota (Ducarmon et al., 2019; Fuchs, 2023; Louis and Flint, 2017). SCFAs play a pivotal role in preventing the growth and invasion of pathogenic bacteria (Zhan et al., 2022), either through direct mechanisms (Roe et al., 2002), or indirectly by modulating the host immune response (Koh et al., 2016). Another significant means of colonization resistance is in the competition for nutrients, where the resident microbiota compete with invading pathogens for limited

resources (Ducarmon et al., 2019; Fuchs, 2023). This competition includes the battle for macronutrients such as carbon (Fabich et al., 2008) or amino acids (Momose et al., 2008), as well as micro-nutrients like iron (Deriu et al., 2013) or zinc (Behnsen et al., 2021, Ducarmon et al., 2019; Fuchs, 2023). Changes in the microbiome communities, termed dysbiosis, have been linked to the development and progression of several autoimmune diseases, such as chronic inflammatory bowel disease (Shan et al., 2022) or ulcerative colitis (Shen et al., 2018), as well as pathogenic infections (Sehgal and Khanna, 2021).

The gastrointestinal tract of humans and other mammals is covered by a glycosylated mucus layer that plays an important role in facilitating food passage, mediating cell signaling pathways, establishing a physical barrier between host and microbial communities, and actively participating in host-microbe interactions (Grondin et al., 2020). As the first point of interaction between the host and intestinal microbes, glycans are known to contribute to the abundance and composition of the commensal microbiota (Koropatkin et al., 2012). Host glycans can interact directly with microbiota, serving as both a nutrient source and attachment site (Koropatkin et al., 2012; Sonnenburg et al., 2005; Tailford et al., 2015).

The glycosylation pattern of the mammalian intestine is influenced by numerous genes, among which is the *B4galnt2* (Beta-1,4-N-Acetyl-Galactosaminyltransferase 2), a blood-group related protein-coding gene with variability in its expression pattern in mouse tissues (Vallier, 2017). The wild-type allele of *B4galnt2*, found in the C57BL/6J (B6) laboratory mouse strain, is expressed in the gastrointestinal tract. An alternative allele variant of the *B4galnt2* gene, first discovered in the RIIIS/J (R3) mouse strain, is expressed in the vascular endothelium, which leads to the degradation of von Willebrand factor, a key component in the coagulation process (Vallier, 2017). Accordingly, expression of this alternative allele leads to a bleeding phenotype similar to von Willebrand disease (Johnsen et al., 2008; Mohlke et al., 1999; Vallier, 2017). Previous studies have shown that the *B4galnt2* gene shows signatures of long-term balancing selection in wild mouse populations, suggesting an evolutionary trade-off where the cost of prolonged bleeding times may confer resistance to pathogens (Johnsen et al., 2009; Linnenbrink et al., 2011; Vallier, 2017). In a follow-up study, Vallier et al., used a new pathometagenomic approach and discovered an association between resistance to the infection with *Morganella morganii*, an intestinal pathogen, and the expression of the

RIIS/J allele in the blood vessels of wild mice (Vallier et al., 2023). In addition to the wild mouse populations, mice with genetically engineered endothelial tissue-specific expression of *B4galnt2* on the one hand showed partial protection against the pathogen in a *Salmonella* Typhimurium infection model. On the other hand, intestinal expression of *B4galnt2* is associated with elevated susceptibility to *Salmonella*, leading to increased intestinal inflammatory cytokines and immune cell infiltration (Rausch et al., 2015). This association between *B4galnt2* expression patterns and colonization resistance to *Salmonella* is mediated by *B4galnt2*-associated microbiota, as demonstrated by fecal transfer experiments conducted between different *B4galnt2*-expressing genotypes (Rausch et al., 2015).

Salmonella enterica serovar Typhimurium is a gram-negative, facultative anaerobic, non-spore-forming bacterium, belonging to the family Enterobacteriaceae (Fàbrega and Vila, 2013). Recognized as an important pathogen affecting both humans and other animals, *Salmonella* Typhimurium usually originates from contaminated food or water, although sporadic zoonotic transmission has been documented (Andino and Hanning, 2015; Tauni and Osterlund, 2000). This bacterium, which primarily infects the gastrointestinal tract, has become an important model organism for studying host-pathogen interactions (Andino and Hanning, 2015). In order to establish a successful infection in model organisms, *Salmonella* must overcome the colonization resistance conferred by the commensal microbiota (Stecher, 2015).

Notably, germ-free mice, which lack any commensal microbiota, are fully susceptible to *Salmonella* Typhimurium infection (Collins and Carter, 1978; Fuchs, 2023; Stecher et al., 2005). In addition, historical evidence dating back to the 1950s has shown that the administration of antibiotics, in particular streptomycin, can significantly increase the susceptibility to *Salmonella* infection (Bohnhoff et al., 1954). Subsequently, streptomycin administration became an integral part of the standard *Salmonella* infection model (Barthel et al., 2003). A single high dose of streptomycin disrupts the gut microbiota and facilitates successful colonization by pathogenic bacteria in a similar, but not identical manner to germ-free mice (Fuchs, 2023; Stecher et al., 2005).

Rausch et al. used streptomycin treatment to break the colonization resistance of the commensal microbiota and successfully infected mice of varying *B4galnt2* genotypes with *Salmonella* (Rausch et al., 2015). Their research highlighted the influence of tissue

specific *B4galnt2* expression on susceptibility to *Salmonella* Typhimurium infection. Interestingly, the results of the study suggest that the observed effect is not solely dependent on tissue specific *B4galnt2* expression. Rather, the expression of *B4galnt2* itself shapes the composition of the commensal microbiota, which in interaction with streptomycin influences the outcome of the *Salmonella* infection (Rausch et al., 2015).

The overall research aim of this study is to unravel the complex interplay between *B4galnt2*-associated gut microbiota, streptomycin treatment and the success of *Salmonella* infection. Specifically, this study builds on the previous work (Rausch et al., 2015) through the addition of shotgun metagenomic sequencing data, and investigates both their taxonomic and functional profiles at three stages: (i) prior to any treatment, (ii) post-antibiotic administration, and (iii) following the *Salmonella* Typhimurium infection. The aim is to identify distinct taxonomic and functional markers associated with the partial protection against *Salmonella* infection conferred by differential *B4galnt2* expression.

Materials and methods

A previous study (Rausch et al., 2015) investigated the role of the host *B4galnt2* expression and susceptibility to *Salmonella* infection. To test this, genetically engineered mice with tissue specific *B4galnt2* expression were challenged with *Salmonella* Typhimurium. Mice were bred to carry the desired combinations of alleles: with intestinal expression of *B4galnt2* ($B4^{+/-}$), and without ($B4^{-/-}$), as well as vascular endothelium expression, derived from the RIIS/J-derived *Mvwf1* bacterial artificial chromosome transgene (Tg^+), and without (Tg^-) (Johnsen et al., 2008; Rausch et al., 2015). Mice were kept in individually ventilated cages, under specific pathogen-free conditions, and fed with standard chow diet (ssniff, Soest, Germany). All animal experiments were performed at the animal facility of the University of Kiel (CAU), Germany. Experimental procedures were carried out in accordance with the ethical guidelines of the Animal Care Committee of the Ministry of Energy, Agriculture, the Environment and Rural Areas of Schleswig-Holstein, Germany, and the study was approved by the Ethics Committee (protocol: V312-72241.123-3 and V312-7224.123-3) (Rausch et al., 2015).

Mice aged 10-14 weeks were given a single dose of streptomycin (20 mg per mouse) by gavage (Barthel et al., 2003; Rausch et al., 2015). Mice were infected with *Salmonella enterica* serovar Typhimurium SL1344 24 hours after antibiotic treatment (Hoiseth and Stocker, 1981). Fecal samples were collected before antibiotic administration, following a single dose of streptomycin, and after the infection with *S. Typhimurium* (Figure 1, Supplementary Table 1) (Rausch et al., 2015).

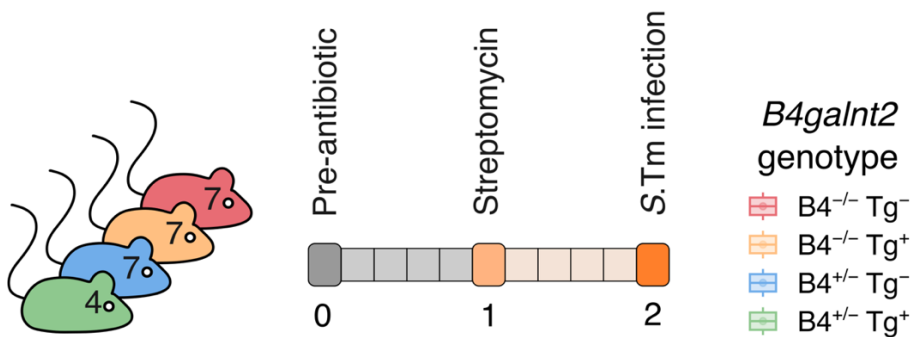


Figure 1: Experimental design of the study.

Total DNA was extracted from the samples using the PowerSoil DNA Kit (MO Bio Laboratories, Carlsbad, CA). The 27F and 338R primer set was used in initial study to amplify the V1-V2 hypervariable region of the bacterial 16S rRNA gene (Rausch et al., 2015).

The current study incorporated advances in sequencing technologies, specifically shotgun metagenomic sequencing performed on the Illumina NextSeq platform. This method allowed for improved resolution, accuracy and a more comprehensive analysis of the microbial communities.

Sequencing data pre-processing was performed using KneadData (v0.7.10), which integrates the tools FastQC (v0.12.1) for quality checking, Trimmomatic (v0.39) (Bolger et al., 2014) for quality filtering, and Bowtie2 (v1.2.2) (Langmead and Salzberg, 2012) for the host sequence decontamination. Briefly, raw reads were trimmed using a sliding window trimming approach (SLIDINGWINDOW:5:20), and then reads shorter than 100 bp were discarded. In the next step, Bowtie2 was implemented to detect and remove host reads present in each sample, by mapping the reads against the C57BL/6 mouse reference genome (GCA_001632555.1 assembly). The ratio of host reads to the remaining reads was used as an approximation to measure bacterial load.

Taxonomic profiles at the genus and species level were obtained using Kraken v2.1.2 (confidence 0.05) and Bracken v2.2, using the PlusPFP database (PlusPFP_2022_09_08) containing bacterial, archaeal, viral, plasmid, fungal, protozoan and plant indices (Lu et al., 2017; Wood and Salzberg, 2014). Eukaryotic reads were removed prior to functional analysis, using the extract_kraken_reads.py script as part of the Kraken v2.1.2 package. Only bacterial and archaeal reads were used for the downstream analysis.

The resulting microbial feature table and metadata tables were imported into R using the biomformat v1.26.0 and phyloseq v1.42.0 packages (McMurdie and Paulson, 2017; McMurdie and Holmes, 2013). Samples with at least 50000 Kraken2/Bracken classified reads were kept for taxonomic analysis. Taxa relative sequence abundances were filtered, requiring each taxa to have an average abundance of at least 0.005 % per sample.

Alpha diversity was calculated using the Shannon index for community diversity, the Simpson index for community evenness and the number of taxa observed at the genus level using the microbiome R package v1.20.0 (Lahti, Shetty et al., 2017).

Beta diversity metrics based on presence or absence – Jaccard, and relative abundance – Bray-Curtis were calculated using the vegan package v2.6-4 in R (Dixon, 2003). Principal Coordinate Analysis (PCoA) was used to explore and visualize the relationship between samples of different genotypes using the Jaccard and Bray-Curtis distance matrices implemented in the microViz package (Barnett et al., 2021). The PERMANOVA test, part of adonis2, implemented in the vegan package, was used to test for the differences in microbial composition between the genotypes at each timepoint. The significance of PERMANOVA was determined using 9999 permutations and results were considered significant if the p-value was less than 0.05.

Differences in relative taxa abundances between *B4galnt2* genotypes were identified using the linear discriminant analysis effect size (LEfSe) method (Segata et al., 2011). The LEfSe uses the nonparametric Kruskal-Wallis test for identifying taxa that have significantly distinct abundances across groups and time points, and linear discriminant analysis (LDA) for determining effect size for each taxa. The threshold of the logarithmic linear discriminant analysis (LDA) score for discriminative features was set at 2.0, with a significance level of $p_{val} < 0.05$.

Spearman's correlation coefficient was used to determine the correlation between the relative abundances of the Lachnospiraceae family members and the inflammation score, Shannon index, Simpson index, and relative abundance of *Salmonella* reads after infection. The heatmaps were generated using the ggplot package (v3.4.4) in R (Wickham, 2016).

Functional profiling of the merged paired-end reads was performed using the HMP Unified Metabolic Analysis Network 3 (HUMAnN3 v3.6) pipeline with default settings and screened against the UniRef90 database (Beghini et al., 2021). Samples with at least 200000 paired sequences were kept for functional analysis. To quantify differences between pathway abundances by *B4galnt2* genotypes and adjust for covariate - sex, Microbiome Multivariable Associations with Linear Models - MaAsLin2 (v1.12.0) was employed (Mallick et al., 2021). P-values were adjusted using the Benjamini-Hochberg procedure (FDR) for each group, or time point.

Results

Rausch et al. conducted a study using a *Salmonella* Typhimurium colitis model and found that the loss of intestinal expression of *B4galnt2* reduces susceptibility to infection (Rausch et al., 2015). This effect was closely associated with changes in the composition and diversity of the intestinal microbiota, which predicts reduced inflammation and resistance to *Salmonella* Typhimurium infection. Furthermore, the expression of *B4galnt2* in blood vessels also affected susceptibility to *Salmonella* and colonization success (Rausch et al., 2015). Our study utilized advanced sequencing techniques to provide a more detailed analysis of microbial community dynamics.

A cohort of 25 mice, consisting of 7 $B4^{-/-}$ Tg⁻, 7 $B4^{+/-}$ Tg⁻, 7 $B4^{-/-}$ Tg⁺, and 4 $B4^{+/-}$ Tg⁺ mice, were treated with streptomycin at a dose of 20 mg per mouse (Barthel et al., 2003; Rausch et al., 2015). The mice were then infected with *Salmonella* Typhimurium SL1344 (Hoiseth and Stocker, 1981). Fecal samples were collected at each time point (Figure 1, Supplementary Table 1) (Rausch et al., 2015). DNA was extracted from the fecal samples and sequenced on the NextSeq platform. A total of 1,342,554,348 reads were generated, with an average of 17,900,725 reads per sample after sequencing. After quality filtering and removal of host reads, the average number of reads per sample was 7,874,453.

Significant differences were observed between B4 genotypes ($p_{val} = 0.00052$) in the relative abundance of mouse reads after the streptomycin treatment, functioning as an approximation for bacterial load (Figure 2). Furthermore, the proportion of mouse reads following the antibiotic treatment was positively correlated with the inflammation scores after the *Salmonella* infection ($r_s = 0.41$; $p_{val} = 0.042$)

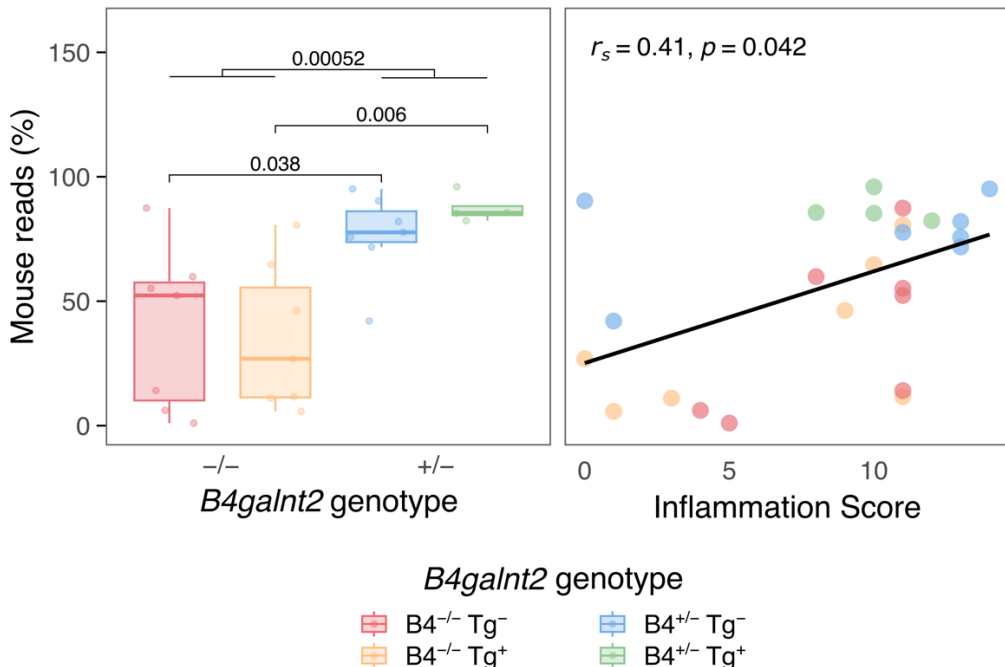


Figure 2: Relative abundance of mouse reads following the streptomycin treatment as an approximation of bacterial load: between different *B4galnt2* genotypes, and inflammation scores after *Salmonella* infection.

At the Phylum level, the overall fecal microbiome composition was found to be comparable between *B4galnt2* genotypes, with Bacteroidetes ($83.84 \pm 13.97\%$) as the dominant phylum, and members of the Muribaculaceae family ($63.27 \pm 19.65\%$) being the most dominant family, before any treatment (Figure 3, Supplementary Table 2, Supplementary Table 3). Following the streptomycin treatment, there was a significant shift in microbial composition, across all *B4galnt2*-genotype groups. The shift in the microbiome composition was characterized by an increase in the relative abundance of the Deferribacteres phylum ($53.16 \pm 36.05\%$) and the Mucispirillaceae family ($53.16 \pm 36.05\%$) reads. Infection with *Salmonella* Typhimurium resulted in additional shifts in the microbiome compositions. Notably, reads belonging to *Salmonella* and its family, Enterobacteriaceae, emerged as dominant in most of the samples, with an average of $62.68 \pm 30.07\%$ reads per sample.

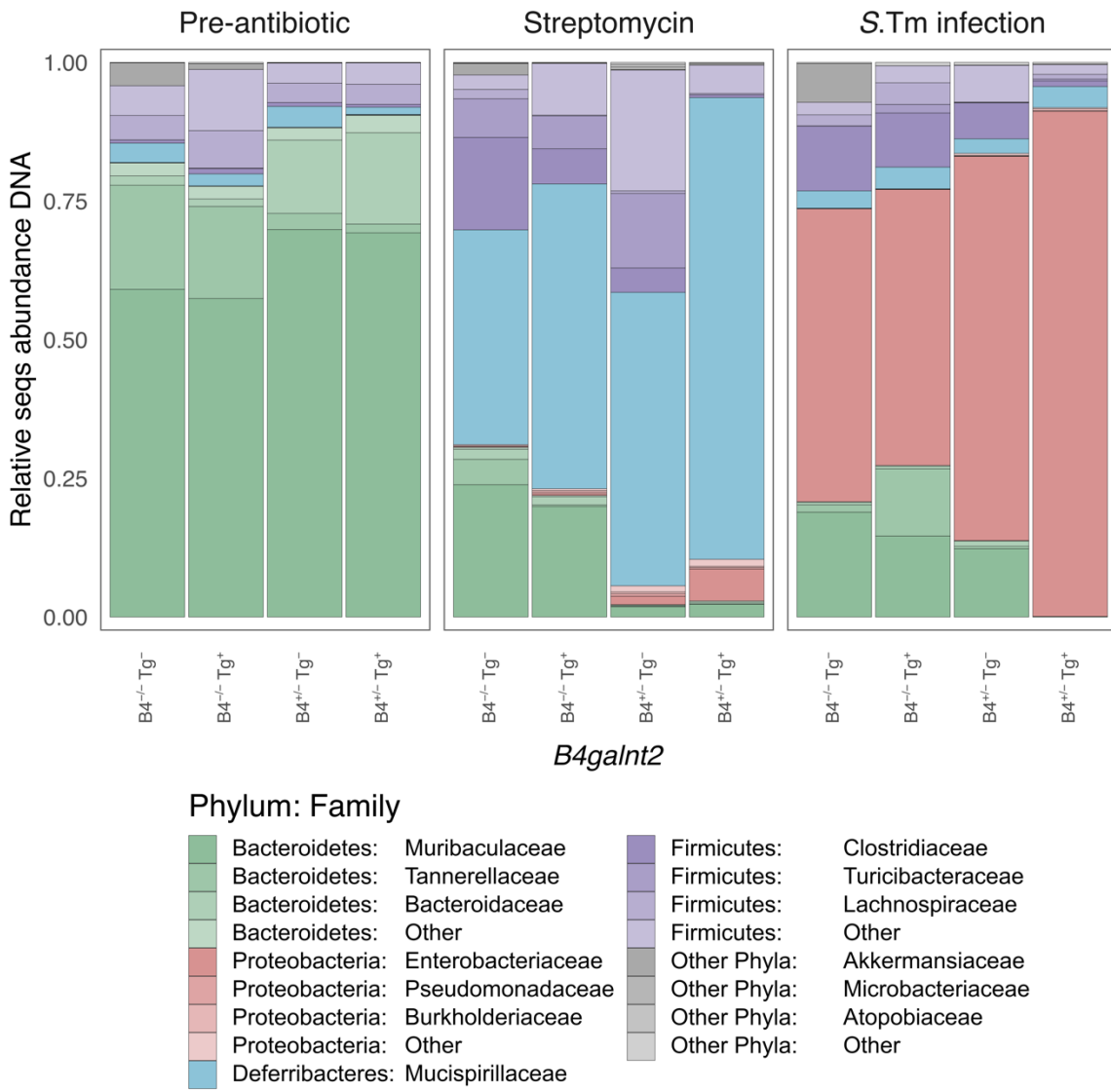


Figure 3: Fecal microbiome composition dynamics: Relative sequence abundance in *B4galnt2*-associated microbial communities at the phylum and family levels.

The assessment of microbial diversity within and between mice genotypes was conducted by calculating alpha and beta indices at the genus level. Alpha indices, including observed taxa, Simpson index, and Shannon index, and beta indices, Bray-Curtis and Jaccard, were used. Prior to streptomycin treatment, there were no statistically significant differences between the different B4 groups measured by alpha diversity indices. No significant correlations were found between the inflammation score, *Salmonella* relative abundance post-infection, and alpha diversity indices.

The number of genera observed was not significantly different between genotypes after the streptomycin treatment ($p_{val} = 0.45$) (Figure 4). However, when comparing the

number of genera observed after *Salmonella* Typhimurium infection , the B4^{-/-} mouse group showed a significantly higher number of genera observed compared to the B4^{+/+} mice ($p_{val} = 0.048$). The number of observed taxa after infection was negatively associated with the inflammation score ($r_s = -0.64$, $p_{val} = 0.00058$). A similar, but not significant trend was also observed after streptomycin treatment ($r_s = -0.36$, $p_{val} = 0.086$). The total number of identified taxa was also negatively correlated with the relative abundance of *Salmonella* after the infection at both timepoints after the antibiotic treatment ($r_s = -0.58$, $p_{val} = 0.0029$), and after the infection with *Salmonella* ($r_s = -0.92$, $p_{val} < 0.00001$).

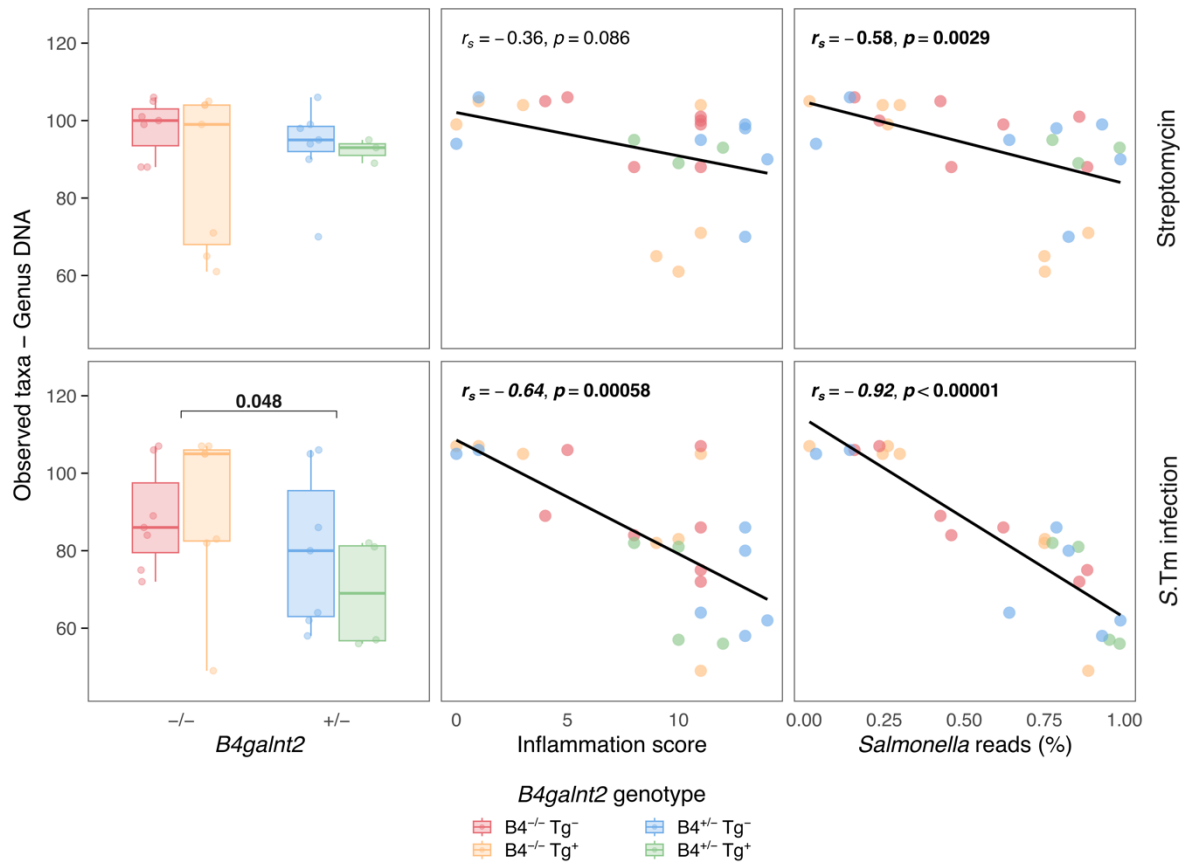


Figure 4: Correlation between *B4galnt2* genotypes, inflammation score, *Salmonella* relative abundance after infection and observed taxa at streptomycin and *S.Tm* infection timepoints.

The Simpson diversity index, used to measure the microbial community richness and evenness, showed a similar trend, with differences between genotypes observed at the time point after the antibiotic treatment ($p_{val} = 0.026$) (Figure 5). The inflammation score was also found to be correlated with the Simpson index following *Salmonella* infection ($r_s = -0.51$, $p_{val} = 0.0088$). Furthermore, the Simpson index showed a significant correlation with the relative abundance of *Salmonella* reads after the infection at both

timepoints, following the administration of streptomycin ($r_s = -0.49$, $p_{val} = 0.015$) and infection ($r_s = -0.59$, $p_{val} = 0.0025$).

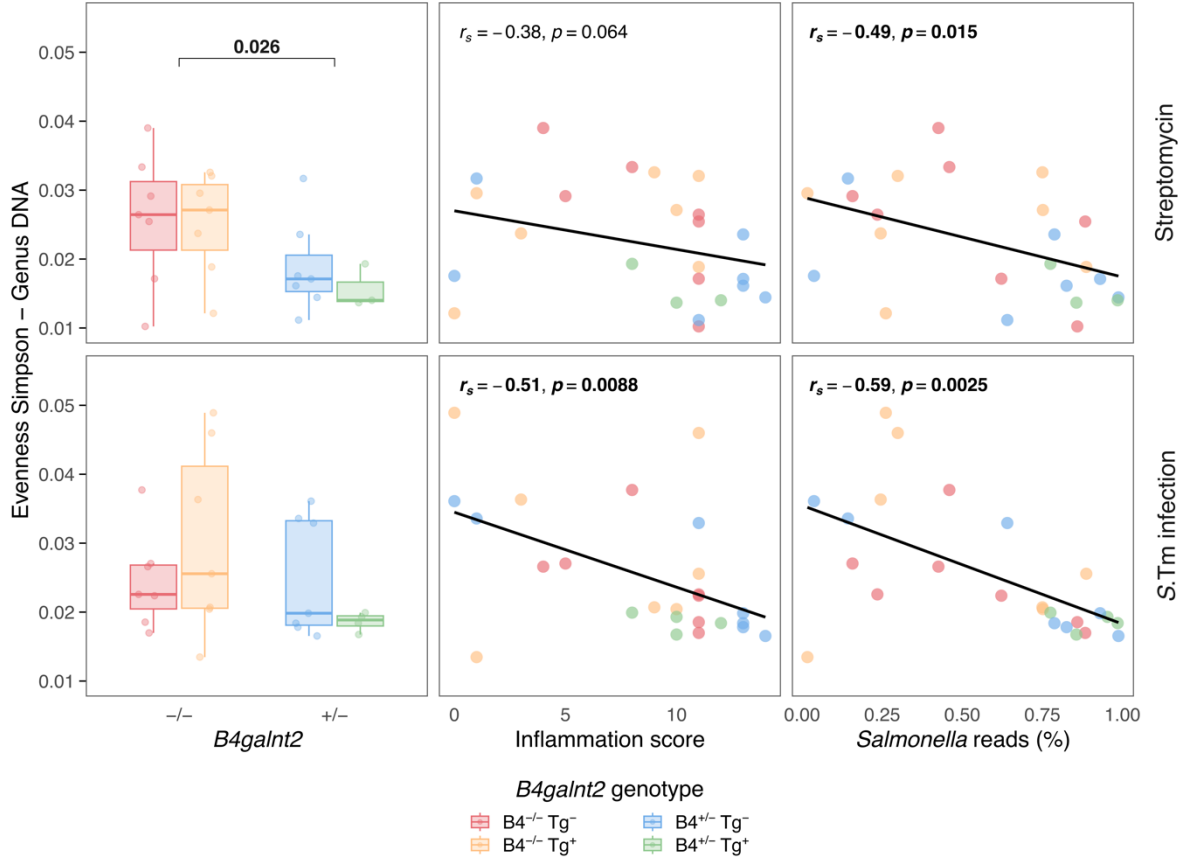


Figure 5: Correlation between *B4galnt2* genotypes, inflammation score, *Salmonella* relative abundance after infection and Simpson index at streptomycin and S.Tm infection timepoints.

The Shannon diversity index did not show any significant differences between the *B4galnt2* genotypes at any timepoint. Similar to other alpha indices, a significant negative correlation was found between the Shannon index and both the inflammation score, and *Salmonella* reads abundance (Supplementary Figure 1).

To assess the dynamics of microbial composition, the loss, gained, and persisted taxa were tracked between the antibiotic and infection timepoints within the same mouse (Figure 6). A significant loss of taxa was observed between B4 genotypes ($p_{val} = 0.02$). No changes were identified in the number of taxa that persisted ($p_{val} = 0.22$) or were newly gained ($p_{val} = 0.34$) between genotypes.

A positive correlation was identified between the number of lost taxa and both the inflammation score ($r_s = 0.64; p_{val} = 0.00077$) and the relative abundance of *Salmonella* reads following infection ($r_s = 0.83; p_{val} < 0.00001$). Conversely, a significant negative correlation was observed for the number of persisted taxa between these timepoint (Inflammation score: $r_s = -0.6; p_{val} = 0.0018$; *Salmonella* reads: $r_s = -0.84; p_{val} < 0.00001$).

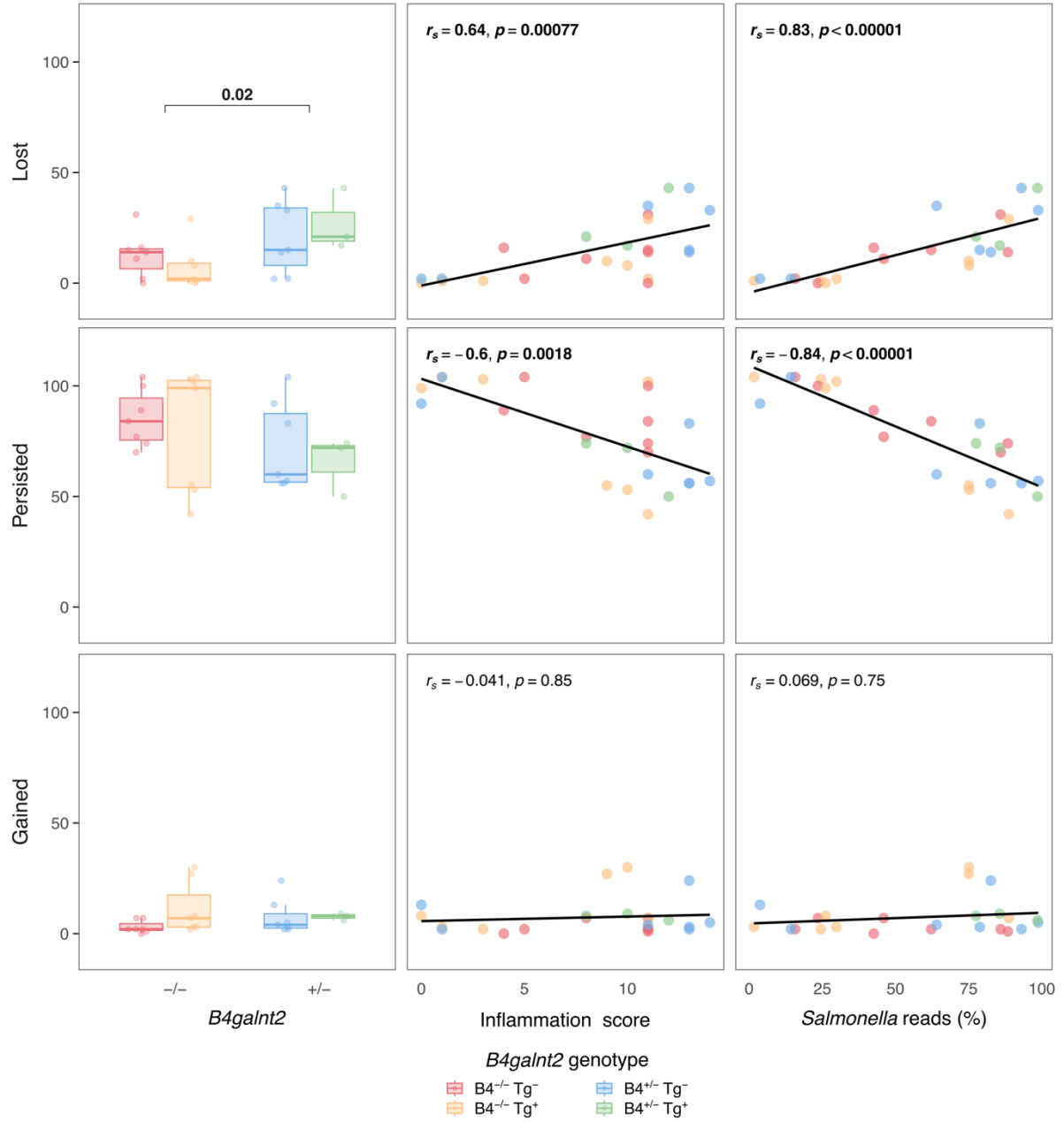


Figure 6: Number of lost, gained and persisted taxa between streptomycin and *S.Tm* infection timepoints: comparison between *B4galnt2* genotypes, spearman correlation – inflammation score and relative abundance of *Salmonella* reads after infection.

The Jaccard distance was used as a metric to quantify the dissimilarities between microbial communities based on the presence or absence of taxa (Figure 7, Supplementary Table 4). Significant differences were detected between B4 genotypes across all time points: prior to streptomycin treatment (PERMANOVA, $R^2 = 0.1158$; $p_{val} = 0.0115$), post-antibiotic treatment (PERMANOVA, $R^2 = 0.0878$; $p_{val} = 0.0313$), and following infection with *Salmonella* Typhimurium (PERMANOVA, $R^2 = 0.1000$; $p_{val} = 0.0206$). Moreover, significant differences were found in inflammation scores (PERMANOVA, $R^2 = 0.1874$; $p_{val} = 0.0011$) following *Salmonella* infection.

Similar observations were made using the Bray-Curtis distance, which takes into account both the presence or absence of taxa and their relative abundance (Supplementary Table 5). Significant differences were detected between B4 genotypes prior to treatment with antibiotics (PERMANOVA, $R^2 = 0.3211$; $p_{val} = 0.0002$), as well as in inflammation scores and sex after the infection with *Salmonella*.

To identify the taxa that drive the differentiation between B4 genotypes, linear discriminant effect size (LEFSe) analysis (Segata et al., 2011) was conducted. The results showed statistically significant differences in 22 bacterial genera between the *B4galnt2* genotypes (Table 1). Prior to antibiotic treatment, most of the Bacteroidia Class members, along with its six genera (*Bacteroides*, *Barnesiella*, *Muribaculum*, *Phocaeicola*, *Prevotella*, and *Sodalisphilus*) had significantly higher abundances in the B4⁺⁻ group. In contrast, the B4^{-/-} groups showed enrichments in the two genera *Acutalibacter* and *Parabacteroides*. After the streptomycin treatment *Parabacteroides* was the sole marker for the B4^{-/-} group, whereas the B4⁺⁻ had a diverse group of significantly abundant genera, including *Acinetobacter*, *Alistipes*, *Diaphorobacter*, *Lactobacillus*, *Olsenella*, *Pantoea*, *Parolsenella*, and *Turicibacter*. Following the *Salmonella* infection, markers for the B4^{-/-} mice comprised two Clostridia members (*Blautia* and *Ruthenibacterium*) and one member of the Erysipelotrichia class (*Faecalibaculum*). In contrast, the B4⁺⁻ mouse groups exhibited enrichments in *Proteus*, *Pseudomonas*, and *Yersinia* of the Gammaproteobacteria Class.

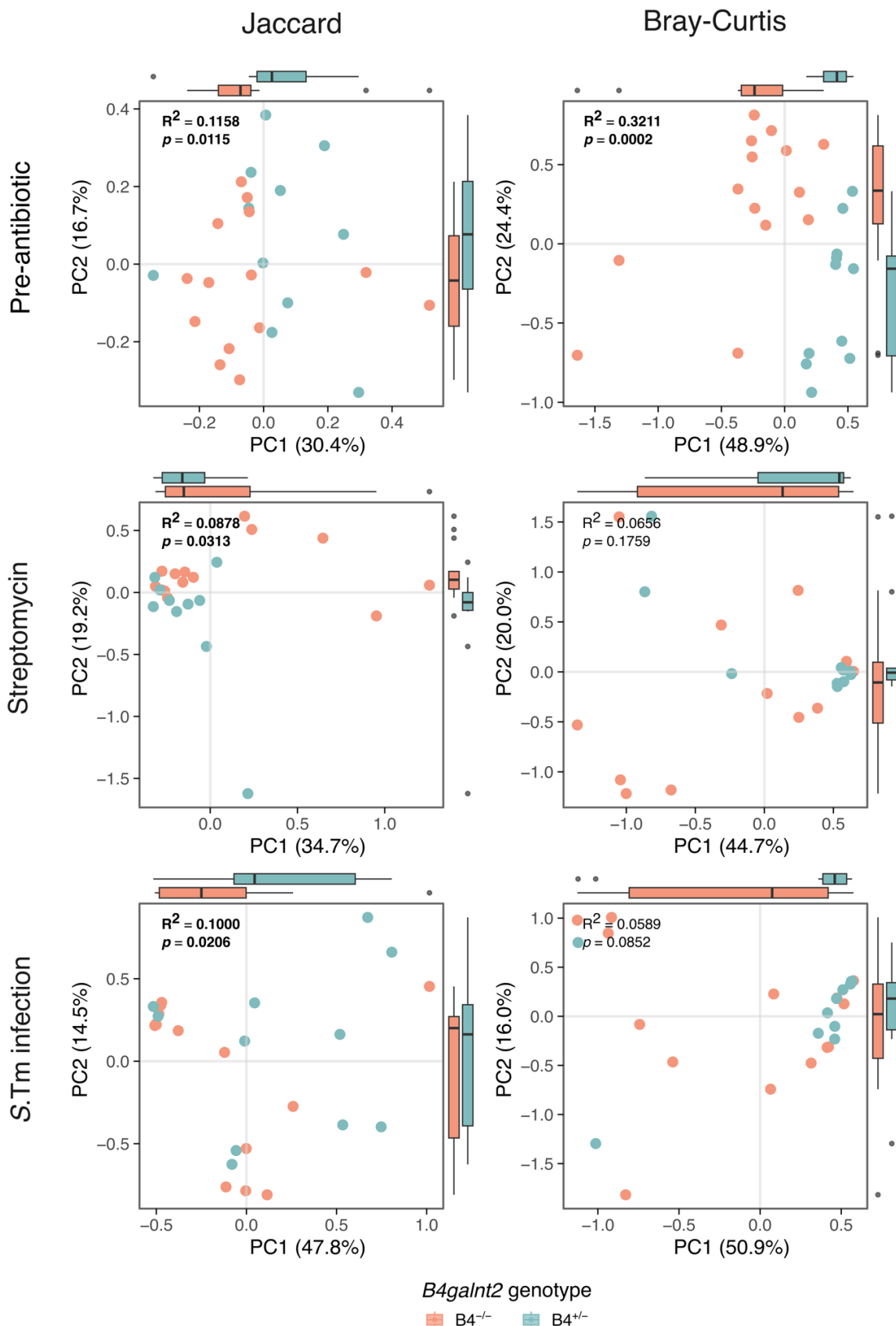


Figure 7: PCoA plot of the fecal microbiome among B4 genotypes at the genus level per timepoint, based on Jaccard and Bray-Curtis indices. The PERMANOVA R^2 and p values for the B4 variable are displayed at the top of each figure.

Table 1: Differentially abundant genera between *B4galnt2* mice groups at different time points

Time	Group	ef_lda	p_val	Class	Family	Genus
Pre-antibiotic	B4 ^{-/-}	4.17	0.03276	Clostridia	Oscillospiraceae	<i>Acutalibacter</i>
	B4 ^{+/-}	5.07	0.00002	Bacteroidia	Bacteroidaceae	<i>Bacteroides</i>
	B4 ^{+/-}	2.81	0.01857	Bacteroidia	Barnesiellaceae	<i>Barnesiella</i>
	B4 ^{+/-}	5.23	0.00020	Bacteroidia	Muribaculaceae	<i>Muribaculum</i>
	B4 ^{-/-}	5.18	0.00010	Bacteroidia	Tannerellaceae	<i>Parabacteroides</i>
	B4 ^{+/-}	4.18	0.00002	Bacteroidia	Bacteroidaceae	<i>Phocaeicola</i>
	B4 ^{+/-}	3.55	0.00004	Bacteroidia	Prevotellaceae	<i>Prevotella</i>
	B4 ^{+/-}	3.20	0.00013	Bacteroidia	Muribaculaceae	<i>Sodaliphilus</i>
Streptomycin	B4 ^{+/-}	3.61	0.00011	Gammaproteobacteria	Moraxellaceae	<i>Acinetobacter</i>
	B4 ^{+/-}	2.74	0.03504	Bacteroidia	Rikenellaceae	<i>Alistipes</i>
	B4 ^{+/-}	3.17	0.01636	Betaproteobacteria	Comamonadaceae	<i>Diaphorobacter</i>
	B4 ^{+/-}	3.20	0.03027	Bacilli	Lactobacillaceae	<i>Lactobacillus</i>
	B4 ^{+/-}	3.24	0.01900	Coriobacteriia	Atopobiaceae	<i>Olsenella</i>
	B4 ^{+/-}	3.04	0.02608	Gammaproteobacteria	Erwiniaceae	<i>Pantoea</i>
	B4 ^{-/-}	4.56	0.00104	Bacteroidia	Tannerellaceae	<i>Parabacteroides</i>
	B4 ^{+/-}	3.29	0.02078	Coriobacteriia	Atopobiaceae	<i>Parolsenella</i>
	B4 ^{+/-}	5.00	0.00341	Erysipelotrichia	Turicibacteraceae	<i>Turicibacter</i>
S.Tm infection	B4 ^{-/-}	3.44	0.04281	Clostridia	Lachnospiraceae	<i>Blautia</i>
	B4 ^{-/-}	3.03	0.01898	Erysipelotrichia	Erysipelotrichaceae	<i>Faecalibaculum</i>
	B4 ^{+/-}	3.11	0.03276	Gammaproteobacteria	Morganellaceae	<i>Proteus</i>
	B4 ^{+/-}	2.79	0.03750	Gammaproteobacteria	Pseudomonadaceae	<i>Pseudomonas</i>
	B4 ^{-/-}	3.56	0.04225	Clostridia	Oscillospiraceae	<i>Ruthenibacterium</i>
	B4 ^{+/-}	3.14	0.00056	Gammaproteobacteria	Yersiniaceae	<i>Yersinia</i>

In the analysis of important factors influencing the success of *Salmonella* infection, particular emphasis was put on the analysis of the Lachnospiraceae family and its members, as according to Eberl et al., members of the Lachnospiraceae family play an important role in colonization resistance to *Salmonella* Typhimurium infection (Eberl et al., 2021). Before antibiotic treatment and post-*Salmonella* infection timepoints, a significant positive correlation was observed between the relative sequence abundance of members within the Lachnospiraceae family and alpha diversity indices (Shannon and Simpson). After the streptomycin treatment, *Blautia* was the only taxa that showed a significant positive correlation between its relative abundance and Shannon diversity

index. Furthermore, a significant negative correlation was identified between the relative abundances of most of the Lachnospiraceae members and both inflammation scores and the relative abundance of *Salmonella* reads following the infection (Figure 8).

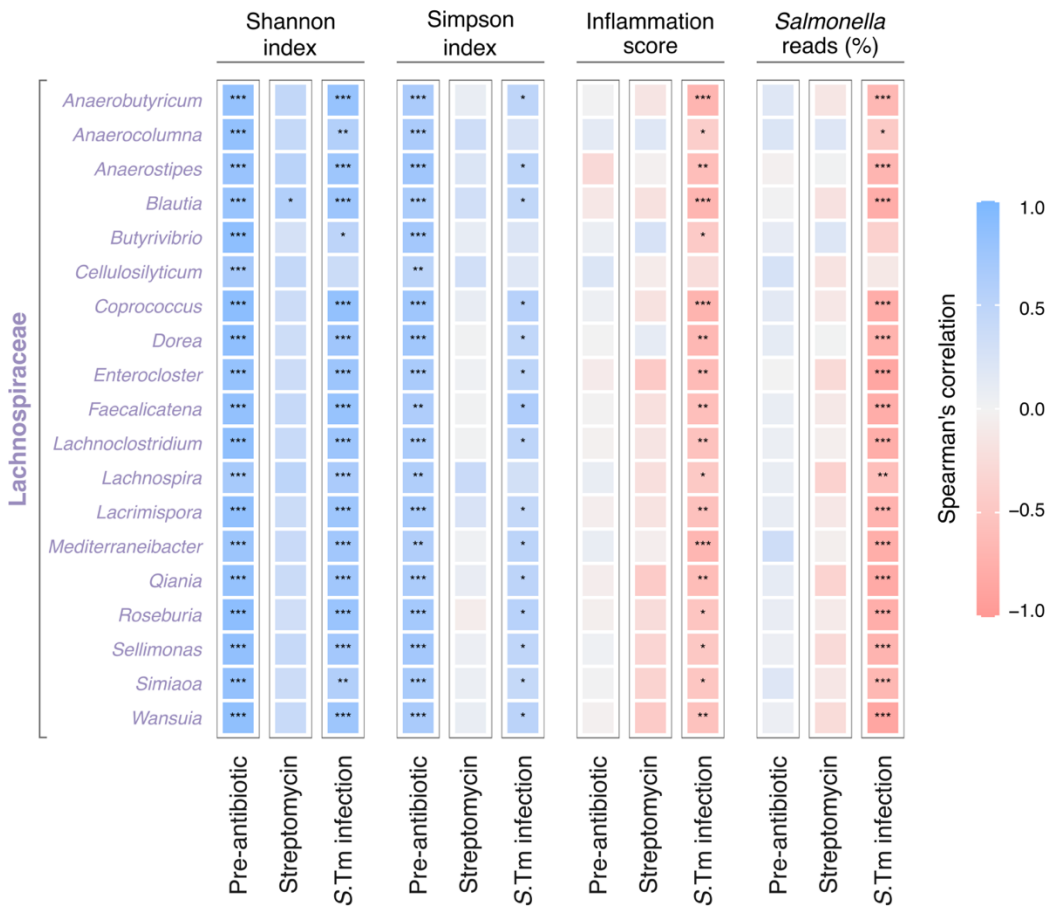


Figure 8: Spearman correlation between relative sequence abundance of the Lachnospiraceae family members and key parameters: Shannon index, Simpson index, inflammation score, and relative abundance of *Salmonella* reads following *S.Tm* infection. The color represents the r_s values (Spearman's correlation). Only significant p adjusted values are presented ($p_{adj}^{***} < 0.001$; $p_{adj}^{**} < 0.01$; $p_{adj}^* < 0.05$).

Next, to predict functional profiles of the fecal microbiota and provide more novel additional insight than that available to Rausch et al. 2015, which was limited to 16S rRNA gene sequencing, the HUMAN3 workflow was used (Beghini et al., 2021). Principal Coordinate analysis (PCoA) showed significant differences in functional composition on the pathway level between B4 genotypes before the streptomycin treatment for both Jaccard (PERMANOVA, $R^2 = 0.1902$; $p_{val} = 0.0002$) and Bray-Curtis (PERMANOVA, $R^2 = 0.1656$; $p_{val} = 0.0031$) indices, and following the *Salmonella* infection for the Bray-Curtis (PERMANOVA, $R^2 = 0.1147$; $p_{val} = 0.0081$) index (Figure 9, Supplementary Table 6, Supplementary Table 7).

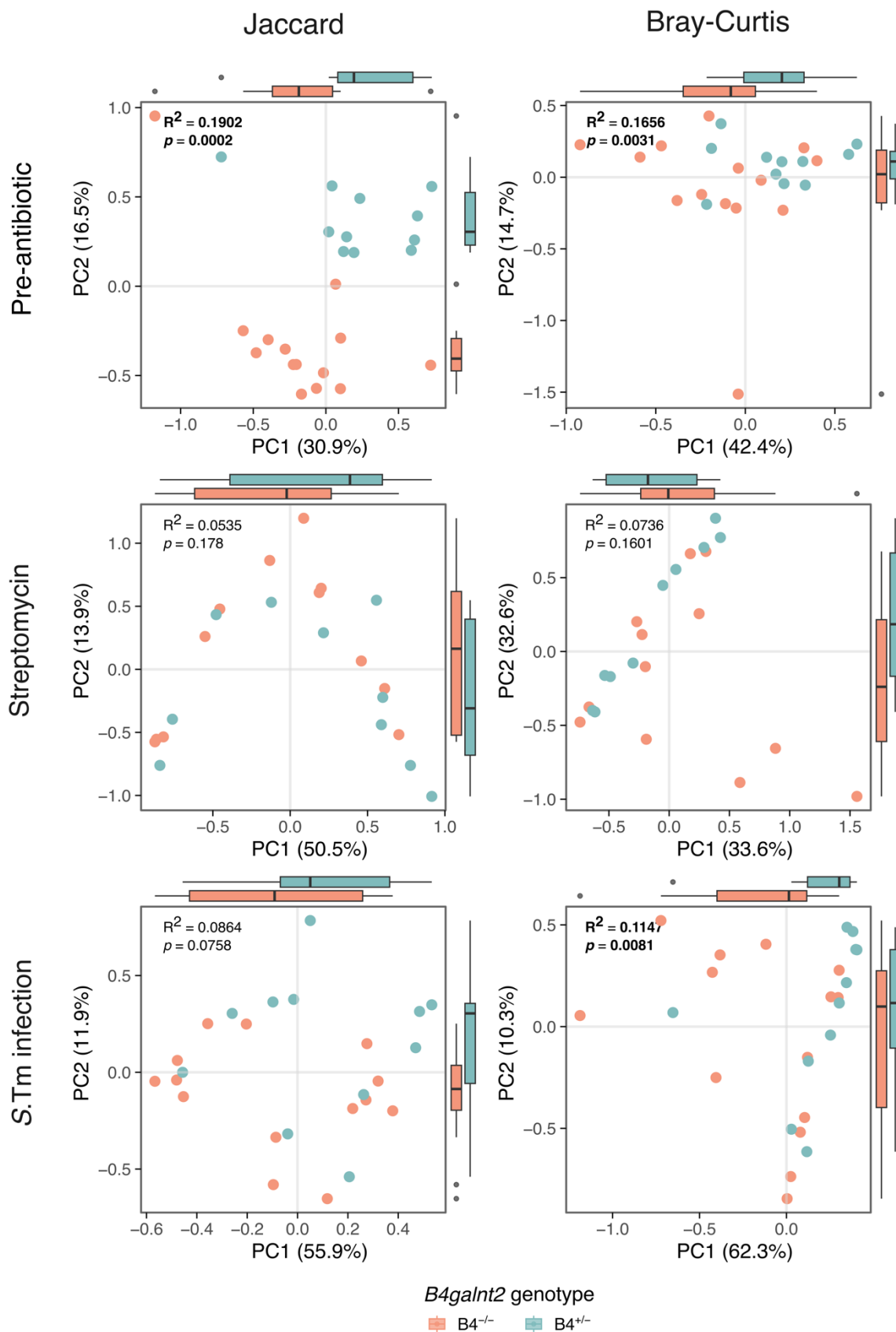


Figure 9: PCoA plot of the fecal microbiome among B4 genotypes at the pathway abundance level per timepoint, based on Jaccard and Bray-Curtis indices. The PERMANOVA R^2 and p values for the B4 variable are displayed at the top of each figure.

Next, to identify pathways that were significantly different between *B4galnt2* genotypes, Microbiome Multivariable Association with Linear Models (MaAsLin2) analysis was used (Mallick et al., 2021), which also adjusted for covariates of sex (Figure 10, Supplementary Table 8, Supplementary Table 9).

Competition for nutrients is one of the main strategies used by the resident microbiota to combat invading pathogens. Therefore, pathways for utilizing various substrates such as carbohydrates, carboxylates, nucleosides and nucleotides, amines and polyamines, and amino acids as sources of nutrients and energy were investigated in more detail. Prior to antibiotic treatment, 29 pathways involved in substrate degradation were enriched. Of these, 21 (72.41%) were enriched in the *B4^{-/-}* group, and 8 (27.59%) were enriched in the *B4^{+/-}* group. There were no significant differences in the pathways involved in the degradation of substrates for energy and nutrients between the Tg groups.

Notably, FUCCAT-PWY (fucose degradation), PWY-7242 (D-fructuronate degradation), and P161-PWY (acetylene degradation (anaerobic)), associated with *B4^{-/-}* prior to antibiotic administration, were correlated with an elevated proportion of *Salmonella* reads after infection, indicating potential utilization by the pathogen. After treatment with streptomycin, these pathways were found to be correlated with reduced inflammation scores. However, after infection, these pathways were associated with elevated inflammation scores, indicating that they might play an important role in *Salmonella* colonization and infection (Figure 11).

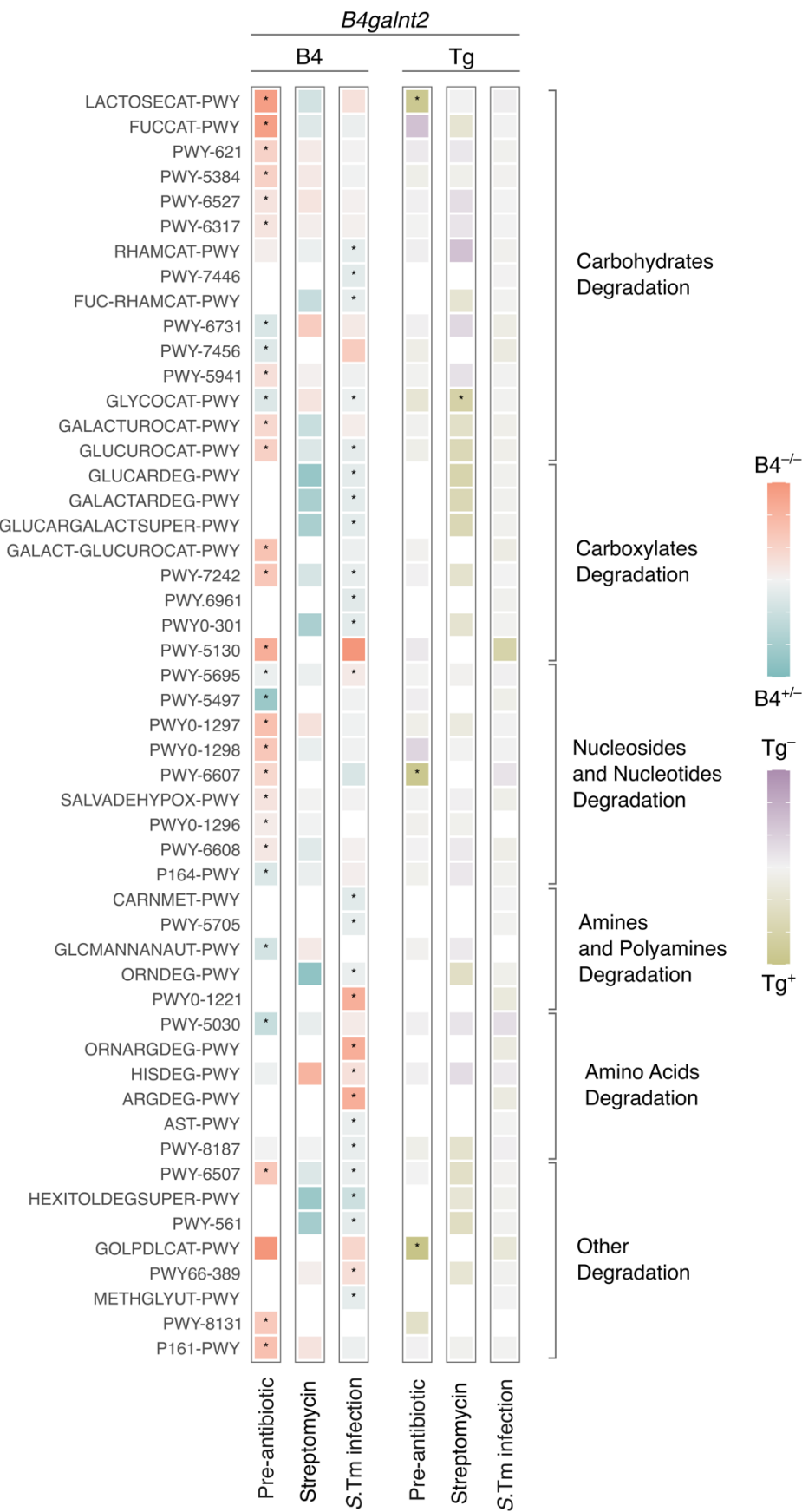


Figure 10: Significantly different pathways involved in the degradation of various substrates detected in the comparison of B4^{-/-} versus B4^{+/-}, and Tg⁻ versus Tg⁺. Stars represent a $q_{val} < 0.25$.

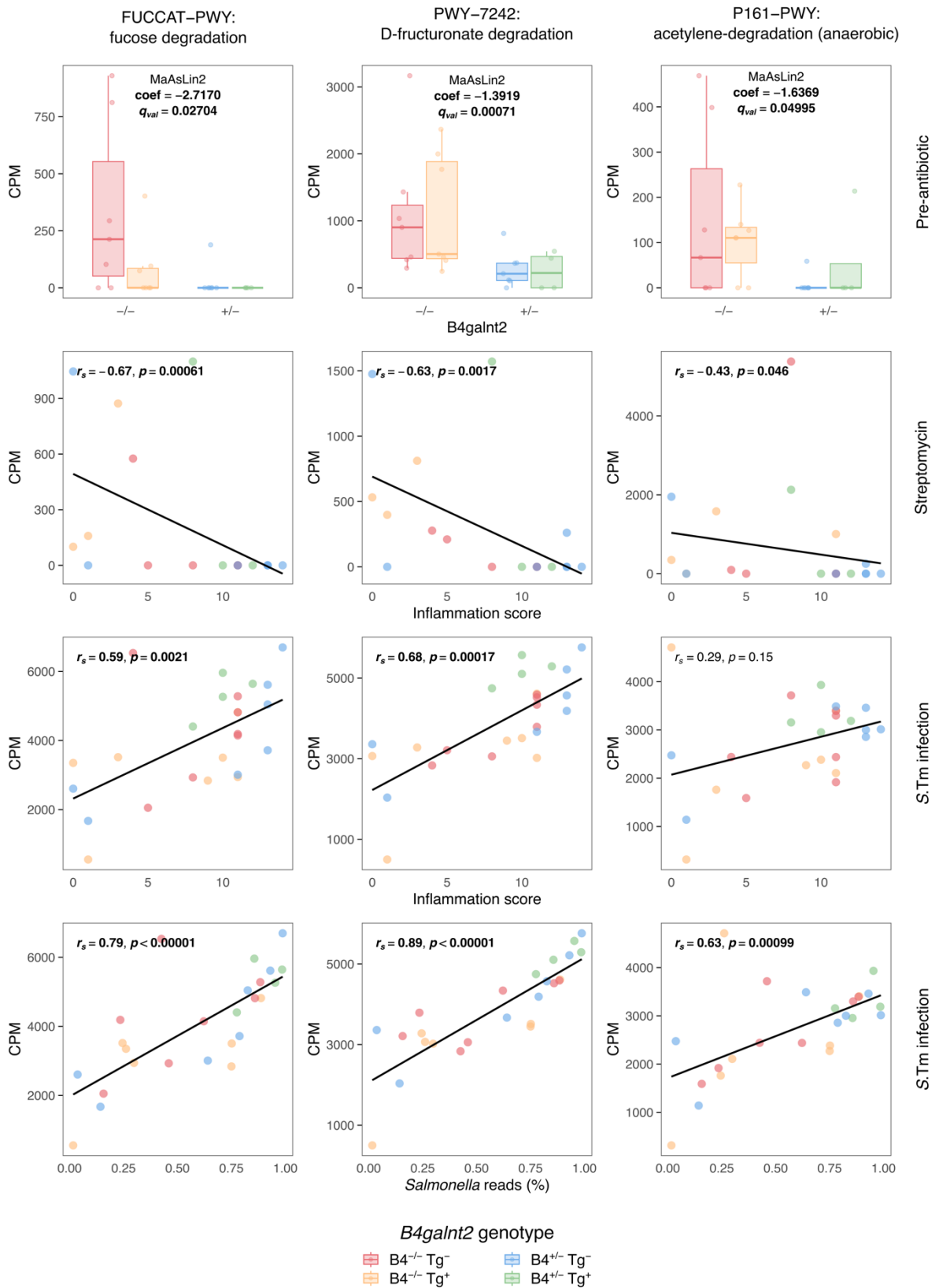


Figure 11: Correlation of FUCCAT-PWY, PWY-7242, and P161-PWY between B4 genotypes, inflammation score, and *Salmonella* relative abundance at specific time points.

Discussion

Host-associated microbial communities play an important role in defending against intestinal pathogens, known as colonization resistance. This protection involves various mechanisms, such as direct microbe-microbe interactions, the production of antimicrobial substances, and competition for nutrients (Ducarmon et al., 2019). However, disruptions of the microbiota, such as antibiotic use, can weaken colonization resistance and provide opportunities for pathogens to cause infections. Intestinal pathogens, such as *Salmonella* Typhimurium, have evolved numerous strategies to compete with intestinal microbes and the host (Ducarmon et al., 2019).

The distinctive patterns of tissue-specific *B4galnt2* expression patterns, as demonstrated in a previous study, were identified as influential factors shaping the composition of host microbial communities (Staubach et al., 2012). Furthermore, these different expression patterns were shown to affect host susceptibility and immunological responses upon infection with *Salmonella* Typhimurium (Rausch et al., 2015). These studies indicate the influence of *B4galnt2*-associated microbial communities in providing partial protection against *Salmonella* infection. To further expand on these findings, a more comprehensive analysis was conducted through higher resolution shotgun metagenomic sequencing and analysis of the fecal samples obtained from the Rausch 2015 study.

The current study revealed notable differences between *B4galnt2*-associated microbial communities prior to any treatment, as well as alterations in these communities in response to streptomycin treatment and subsequent infection with *Salmonella* Typhimurium, largely confirming, and also expanding upon earlier results based on 16S rRNA gene sequencing (Rausch et al. 2015). The diversity of host microbiota has been linked to increased ability to defend against pathogens and provide colonization resistance (Spragge et al., 2023).

Differences in alpha diversity were observed between *B4galnt2*-associated microbial communities after streptomycin treatment and subsequent *Salmonella* infection, exhibiting reduced complexity in the *B4⁺⁻* group. The lower diversity microbiome was correlated with elevated inflammation scores and a higher proportion of *Salmonella* reads at both the post-antibiotic treatment and infection time points.

According to Stecher et al., mice with a low complexity gut microbiota were more susceptible to *Salmonella* gut infection and colitis (Stecher et al., 2010).

Increased protection against the pathogen colonization and infection is driven by the presence of diverse microbial communities. Furthermore, greater colonization resistance is observed when certain combinations of species are present together rather than in isolation. It is important to note that the availability and utilization of nutrients between the microbiome and the infecting pathogen play a pivotal role in this context (Spragge et al., 2023).

In the current study, we identified genus *Blautia*, a member of the Lachnospiraceae family and an anaerobic bacterium commonly found within the intestine of many mammals (Furuya et al., 2010; Kaneuchi et al., 1976; Park et al., 2012), as one of the biomarkers of the B4^{-/-} mouse group following *Salmonella* infection. Experiments showed that all *Blautia* strains can utilize glucose, in addition to other diverse carbohydrates including sucrose, fructose, lactose, maltose and many others. Alavi et al., found that microbiota with higher relative proportions of *Blautia obeum* was significantly correlated with reduced *Vibrio cholerae* colonization in their *V. cholerae* infection experiments (Alavi et al., 2020).

According to Schubert et al., higher relative proportions of the Lachnospiraceae family, along with other taxa such as Porphyromonadaceae, *Lactobacillus*, and *Alistipes*, are associated with increased colonization resistance against pathogenic bacteria, such as *C. difficile* (Schubert et al., 2015). Our study found positive correlations between higher relative abundances of members of the Lachnospiraceae family, increased microbial diversity, reduced inflammation scores, and a lower proportion of *Salmonella* reads following infection. The depletion of Clostridia, induced by streptomycin, results in reduced butyrate production, increased epithelial oxygenation, and exacerbation of *Salmonella enterica* serovar Typhimurium expansion, as documented by (Rivera-Chávez et al., 2016). Eberl et al. reported that members of the Lachnospiraceae family, along with other intestinal microbiome constituent *E. coli*, contribute to colonization resistance against *Salmonella* Typhimurium infection (Eberl et al., 2021).

Our analysis based on Maaslin2 identified several significant pathways, including an increase in the relative abundance of substrate degradation pathways associated with the B4^{-/-}genotype. The absence of *B4galnt2* expression in the intestinal environment

shapes the microbiota to have a higher diversity of potential to utilize carbohydrates and other substrates as nutrients or sources of energy. The commensal microbiota provides colonization resistance through nutrient competition (Ducarmon et al., 2019). A diverse microbiota that can utilize a variety of nutrient sources may thus reduce the availability of nutrients that are required by the invading pathogen.

Fucose plays an important role in the pathogenesis of *Salmonella* infection, facilitating bacterial adherence and colonization in the intestine. The bacteria's Std fimbriae bind to α terminal (1,2)-fucose residues on host cells, which mediates bacterial adherence and invasion (Suwandi et al., 2019). This process leads to increased intestinal inflammation in fucosylated (*Fut2^{+/−}*) mice compared to non-fucosylated (*Fut2^{−/−}*) ones (Suwandi et al., 2019). The fucose degradation pathway was found to be enriched in microbiota associated with the absence of *B4galnt2* gut expression at the pre-treatment time point. This suggests that it may provide colonization resistance by competition for available nutrients.

In conclusion, this study examines the impact of *B4galnt2* expression patterns on host microbial community dynamics and susceptibility to *Salmonella*. Deep sequencing of fecal samples revealed significant differences in microbial communities associated with *B4galnt2* expression before and after streptomycin treatment and subsequent *Salmonella* infection. After streptomycin treatment, there was a reduction in microbial diversity, which was correlated with an increase in inflammation and *Salmonella* abundance. The genus *Blautia* emerged as a marker in *Salmonella*-infected mice lacking intestinal *B4galnt2* expression, and it was associated with reduced inflammation. Furthermore, the increased substrate degradation pathways in intestinal *B4galnt2* deficient mice suggest a potential mechanism for increased nutrient competition and colonization resistance. Overall, these findings demonstrate the significance of the interplay between host genetics, microbial diversity, and nutrient availability in mediating colonization resistance against *Salmonella* Typhimurium.

Supplementary information

Supplementary Table 1: Metadata

Sample ID	Mouse ID	Treatment	Sex	B4	Tg	Inflammation score
GG1_S1	GG03_1	Pre-antibiotic	Female	B4 ^{-/-}	Tg ⁺	3
GG12_S9	GG04_16	Pre-antibiotic	Male	B4 ^{-/-}	Tg ⁺	11
GG13_S10	GG04_1	Pre-antibiotic	Male	B4 ^{-/-}	Tg ⁻	11
GG14_S11	GG04_2	Pre-antibiotic	Male	B4 ^{-/-}	Tg ⁺	9
GG15_S12	GG04_3	Pre-antibiotic	Male	B4 ^{-/-}	Tg ⁻	8
gg16_S1	GG04_4	Pre-antibiotic	Male	B4 ^{-/-}	Tg ⁺	10
gg17_S2	GG04_5	Pre-antibiotic	Male	B4 ^{-/-}	Tg ⁻	11
GG2_S2	GG03_10	Pre-antibiotic	Female	B4 ^{-/-}	Tg ⁺	11
gg20_S3	GG05_9	Pre-antibiotic	Male	B4 ^{+/-}	Tg ⁻	14
gg22_S4	GG06_11	Pre-antibiotic	Female	B4 ^{+/-}	Tg ⁺	8
gg23_S5	GG06_12	Pre-antibiotic	Female	B4 ^{+/-}	Tg ⁺	10
gg24_S6	GG06_13	Pre-antibiotic	Female	B4 ^{+/-}	Tg ⁺	10
gg27_S7	GG06_16	Pre-antibiotic	Female	B4 ^{+/-}	Tg ⁻	1
gg28_S8	GG06_17	Pre-antibiotic	Female	B4 ^{+/-}	Tg ⁻	11
gg29_S9	GG06_1	Pre-antibiotic	Male	B4 ^{+/-}	Tg ⁺	12
GG3_S3	GG03_11	Pre-antibiotic	Female	B4 ^{-/-}	Tg ⁺	1
gg30_S10	GG06_4	Pre-antibiotic	Male	B4 ^{+/-}	Tg ⁻	13
gg31_S11	GG06_5	Pre-antibiotic	Male	B4 ^{+/-}	Tg ⁻	13
gg32_S12	GG06_6	Pre-antibiotic	Male	B4 ^{+/-}	Tg ⁻	0
gg33_S13	GG06_7	Pre-antibiotic	Male	B4 ^{+/-}	Tg ⁻	13
GG4_S4	GG03_12	Pre-antibiotic	Female	B4 ^{-/-}	Tg ⁻	5
GG5_S5	GG03_3	Pre-antibiotic	Female	B4 ^{-/-}	Tg ⁻	11
GG6_S6	GG03_4	Pre-antibiotic	Female	B4 ^{-/-}	Tg ⁻	11
GG8_S7	GG03_7	Pre-antibiotic	Female	B4 ^{-/-}	Tg ⁻	4
GG9_S8	GG04_12	Pre-antibiotic	Male	B4 ^{-/-}	Tg ⁺	0
G03_1_d0_S13	GG03_1	Streptomycin	Female	B4 ^{-/-}	Tg ⁺	3
G03_10_d0_S14	GG03_10	Streptomycin	Female	B4 ^{-/-}	Tg ⁺	11
G03_11_d0_S15	GG03_11	Streptomycin	Female	B4 ^{-/-}	Tg ⁺	1
G04_12_d0_S11	GG04_12	Streptomycin	Male	B4 ^{-/-}	Tg ⁺	0
G04_16_d0_S9	GG04_16	Streptomycin	Male	B4 ^{-/-}	Tg ⁺	11
G04_2_d0_S10	GG04_2	Streptomycin	Male	B4 ^{-/-}	Tg ⁺	9
G04_4_d0_S12	GG04_4	Streptomycin	Male	B4 ^{-/-}	Tg ⁺	10
GG03_12_d0_S2	GG03_12	Streptomycin	Female	B4 ^{-/-}	Tg ⁻	5
GG03_3_d0_S3	GG03_3	Streptomycin	Female	B4 ^{-/-}	Tg ⁻	11
GG03_4_d0_S4	GG03_4	Streptomycin	Female	B4 ^{-/-}	Tg ⁻	11
GG03_7_d0_S1	GG03_7	Streptomycin	Female	B4 ^{-/-}	Tg ⁻	4
GG04_1_d0_S6	GG04_1	Streptomycin	Male	B4 ^{-/-}	Tg ⁻	11

Sample ID	Mouse ID	Treatment	Sex	B4	Tg	Inflammation score
GG04_3_d0_S7	GG04_3	Streptomycin	Male	B4 ^{-/-}	Tg ⁻	8
GG04_5_d0_S5	GG04_5	Streptomycin	Male	B4 ^{-/-}	Tg ⁻	11
GG05_9_d0_S8	GG05_9	Streptomycin	Male	B4 ^{+/-}	Tg ⁻	14
GG06_1_d0_S16	GG06_1	Streptomycin	Male	B4 ^{+/-}	Tg ⁺	12
GG06_11_d0_S17	GG06_11	Streptomycin	Female	B4 ^{+/-}	Tg ⁺	8
GG06_12_d0_S18	GG06_12	Streptomycin	Female	B4 ^{+/-}	Tg ⁺	10
GG06_13_d0_S19	GG06_13	Streptomycin	Female	B4 ^{+/-}	Tg ⁺	10
GG06_16_d0_S20	GG06_16	Streptomycin	Female	B4 ^{+/-}	Tg ⁻	1
GG06_17_d0_S21	GG06_17	Streptomycin	Female	B4 ^{+/-}	Tg ⁻	11
GG06_4_d0_S22	GG06_4	Streptomycin	Male	B4 ^{+/-}	Tg ⁻	13
GG06_5_d0_S23	GG06_5	Streptomycin	Male	B4 ^{+/-}	Tg ⁻	13
GG06_6_d0_S24	GG06_6	Streptomycin	Male	B4 ^{+/-}	Tg ⁻	0
GG06_7_d0_S25	GG06_7	Streptomycin	Male	B4 ^{+/-}	Tg ⁻	13
G03_1_d1_S13	GG03_1	S.Tm infection	Female	B4 ^{-/-}	Tg ⁺	3
G03_10_d1_S14	GG03_10	S.Tm infection	Female	B4 ^{-/-}	Tg ⁺	11
G03_11_d1_S15	GG03_11	S.Tm infection	Female	B4 ^{-/-}	Tg ⁺	1
G04_12_d1_S11	GG04_12	S.Tm infection	Male	B4 ^{-/-}	Tg ⁺	0
G04_16_d1_S9	GG04_16	S.Tm infection	Male	B4 ^{-/-}	Tg ⁺	11
G04_2_d1_S10	GG04_2	S.Tm infection	Male	B4 ^{-/-}	Tg ⁺	9
G04_4_d1_S12	GG04_4	S.Tm infection	Male	B4 ^{-/-}	Tg ⁺	10
GG03_12_d1_S2	GG03_12	S.Tm infection	Female	B4 ^{-/-}	Tg ⁻	5
GG03_3_d1_S3	GG03_3	S.Tm infection	Female	B4 ^{-/-}	Tg ⁻	11
GG03_4_d1_S4	GG03_4	S.Tm infection	Female	B4 ^{-/-}	Tg ⁻	11
GG03_7_d1_S1	GG03_7	S.Tm infection	Female	B4 ^{-/-}	Tg ⁻	4
GG04_1_d1_S6	GG04_1	S.Tm infection	Male	B4 ^{-/-}	Tg ⁻	11
GG04_3_d1_S7	GG04_3	S.Tm infection	Male	B4 ^{-/-}	Tg ⁻	8
GG04_5_d1_S5	GG04_5	S.Tm infection	Male	B4 ^{-/-}	Tg ⁻	11
GG05_9_d1_S8	GG05_9	S.Tm infection	Male	B4 ^{+/-}	Tg ⁻	14
GG06_1_d1_S16	GG06_1	S.Tm infection	Male	B4 ^{+/-}	Tg ⁺	12
GG06_11_d1_S17	GG06_11	S.Tm infection	Female	B4 ^{+/-}	Tg ⁺	8
GG06_12_d1_S18	GG06_12	S.Tm infection	Female	B4 ^{+/-}	Tg ⁺	10
GG06_13_d1_S19	GG06_13	S.Tm infection	Female	B4 ^{+/-}	Tg ⁺	10
GG06_16_d1_S20	GG06_16	S.Tm infection	Female	B4 ^{+/-}	Tg ⁻	1
GG06_17_d1_S21	GG06_17	S.Tm infection	Female	B4 ^{+/-}	Tg ⁻	11
GG06_4_d1_S22	GG06_4	S.Tm infection	Male	B4 ^{+/-}	Tg ⁻	13
GG06_5_d1_S23	GG06_5	S.Tm infection	Male	B4 ^{+/-}	Tg ⁻	13
GG06_6_d1_S24	GG06_6	S.Tm infection	Male	B4 ^{+/-}	Tg ⁻	0
GG06_7_d1_S25	GG06_7	S.Tm infection	Male	B4 ^{+/-}	Tg ⁻	13

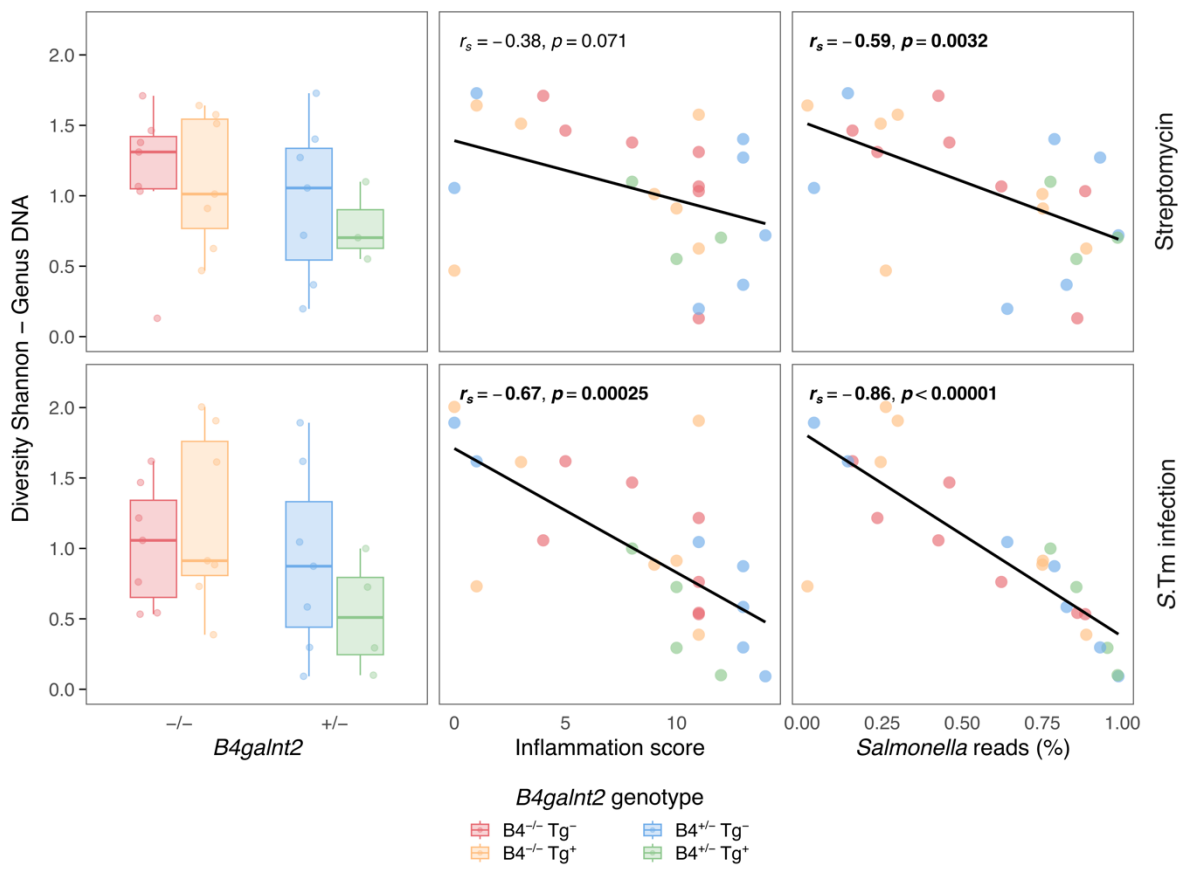
Supplementary Table 2: Microbial phyla abundance in mice before, after streptomycin treatment, and after *Salmonella* infection.

Taxa	Pre-antibiotic		Streptomycin		S.Tm infection	
	Mean	Std.dev	Mean	Std.dev	Mean	Std.dev
Bacteroidetes	83.8424	13.9714	16.3283	27.9492	17.3523	30.3855
Firmicutes	11.6244	11.0294	26.8851	32.7778	13.9263	13.7249
Deferribacteres	2.8548	3.7914	53.1632	36.0463	3.3200	4.5915
Proteobacteria	0.0889	0.0643	2.4324	4.3703	63.0062	30.1204
Verrucomicrobia	1.4634	3.5207	0.6356	2.9029	1.9611	9.7824
Actinobacteria	0.0683	0.0579	0.5118	1.0201	0.0483	0.0645
Crenarchaeota	0.0255	0.0694	0.0054	0.0166	0.2273	0.3993
Euryarchaeota	0.0324	0.0348	0.0384	0.0993	0.1585	0.3299

Supplementary Table 3: Microbial family abundance in mice before, after streptomycin treatment, and after *Salmonella* infection.

Taxa	Pre-antibiotic		Streptomycin		S.Tm infection	
	Mean	Std.dev	Mean	Std	Mean	Std.dev
Muribaculaceae	63.2676	19.6490	13.6127	25.4228	12.8451	24.4962
Mucispirillaceae	2.8548	3.7914	53.1632	36.0463	3.3200	4.5915
Enterobacteriaceae	0.0235	0.0592	1.2427	3.8933	62.6840	30.0684
Tannerellaceae	10.9805	13.9319	1.4454	6.1176	3.8933	16.5023
Clostridiaceae	0.7004	0.7656	8.0492	17.2707	7.9811	10.9761
Turicibacteraceae	0.0256	0.0436	7.6897	21.4326	0.5089	2.1195
Peptostreptococcaceae	0.1051	0.1032	3.8431	14.9238	1.9701	5.2052
Oscillospiraceae	3.5794	4.2669	2.9781	9.3285	0.5460	1.2809
Akkermansiaceae	1.4634	3.5207	0.6356	2.9029	1.9611	9.7824
Bacteroidaceae	7.1824	7.3446	1.0606	1.9085	0.5139	1.1620
Lachnospiraceae	4.6873	4.5967	0.6897	2.2153	1.8082	4.0765
Lactobacillaceae	1.2427	1.8709	2.4500	3.6718	0.4461	0.6093
Rikenellaceae	1.9418	1.8533	0.0570	0.0633	0.0112	0.0289
Enterococcaceae	0.1906	0.2102	0.5781	1.1886	0.4500	0.8980
Erysipelotrichaceae	0.6292	0.7267	0.1318	0.2527	0.1414	0.3626
Eubacteriales Family XIII	0.0151	0.0389	0.2163	0.7684	0.0044	0.0203
Prevotellaceae	0.2944	0.2017	0.0819	0.1465	0.0576	0.1282
Burkholderiaceae	0.0003	0.0002	0.2455	0.3402	0.1124	0.1540
Pseudomonadaceae	0.0120	0.0068	0.3087	0.3932	0.0629	0.0669
Microbacteriaceae	0.0023	0.0017	0.2296	0.5184	0.0346	0.0620
Atopobiaceae	0.0057	0.0071	0.1619	0.5744	0.0036	0.0067
Eubacteriales Order	0.3114	0.3737	0.0173	0.0352	0.0046	0.0095
Paenibacillaceae	0.0309	0.0254	0.0860	0.3119	0.0350	0.1150

Taxa	Pre-antibiotic		Streptomycin		S.Tm infection	
	Mean	Std.dev	Mean	Std	Mean	Std.dev
Sulfolobaceae	0.0031	0.0099	0.0033	0.0127	0.1750	0.3503
Moraxellaceae	0.0039	0.0043	0.1805	0.2703	0.0156	0.0222
Methanobacteriaceae	0.0297	0.0356	0.0304	0.0906	0.0792	0.2175
Yersiniaceae	0.0007	0.0025	0.0287	0.1064	0.0600	0.2082
Erwiniaceae	0.0041	0.0050	0.1825	0.1924	0.0068	0.0092
Methanocaldococcaceae	0.0027	0.0059	0.0080	0.0257	0.0793	0.2579
Morganellaceae	0.0002	0.0006	0.0120	0.0394	0.0527	0.2487
Comamonadaceae	0.0014	0.0011	0.1218	0.1983	0.0059	0.0073
Caldisphaeraceae	0.0014	0.0065	0.0021	0.0096	0.0523	0.2118
Bacillaceae	0.0065	0.0041	0.0641	0.1308	0.0088	0.0134
Eubacteriaceae	0.0706	0.0666	0.0082	0.0219	0.0071	0.0243
Odoribacteraceae	0.0621	0.0974	0.0101	0.0128	0.0027	0.0058
Staphylococcaceae	0.0033	0.0021	0.0675	0.0914	0.0086	0.0081
Barnesiellaceae	0.0535	0.0382	0.0189	0.0337	0.0113	0.0252
Coriobacteriaceae	0.0022	0.0028	0.0348	0.1208	0.0009	0.0016
Eggerthellaceae	0.0281	0.0305	0.0301	0.0668	0.0022	0.0043
Xanthomonadaceae	0.0021	0.0022	0.0485	0.1025	0.0020	0.0031
Desulfovibrionaceae	0.0181	0.0249	0.0232	0.0506	0.0003	0.0009
Bifidobacteriaceae	0.0135	0.0137	0.0164	0.0512	0.0024	0.0057
Desulfurococcaceae	0.0210	0.0690	0.0000	0.0000	0.0000	0.0000
Porphyromonadaceae	0.0265	0.0097	0.0055	0.0101	0.0048	0.0109
Streptococcaceae	0.0147	0.0122	0.0128	0.0107	0.0054	0.0108
Sutterellaceae	0.0161	0.0310	0.0040	0.0129	0.0000	0.0000
Streptomycetaceae	0.0100	0.0074	0.0115	0.0275	0.0009	0.0016
Nitrobacteraceae	0.0061	0.0040	0.0193	0.0264	0.0011	0.0012
Pasteurellaceae	0.0003	0.0003	0.0151	0.0340	0.0023	0.0035
Flavobacteriaceae	0.0056	0.0033	0.0128	0.0216	0.0038	0.0075
Propionibacteriaceae	0.0023	0.0017	0.0176	0.0272	0.0020	0.0019
Dysgonomonadaceae	0.0039	0.0026	0.0110	0.0232	0.0026	0.0050
Hymenobacteraceae	0.0194	0.0074	0.0045	0.0047	0.0033	0.0086
Christensenellaceae	0.0114	0.0108	0.0032	0.0055	0.0006	0.0015
Weeksellaceae	0.0048	0.0022	0.0077	0.0109	0.0027	0.0042
Corynebacteriaceae	0.0041	0.0027	0.0098	0.0103	0.0016	0.0022



Supplementary Figure 1: Correlation between *B4galnt2* genotypes, Inflammation score, *Salmonella* relative abundance after infection and Shannon index at streptomycin and *S.Tm* infection timepoints

Supplementary Table 4: PERMANOVA - Effect size (R2) of *B4galnt2* and confounding factors on Jaccard index at the genus level

	Pre-antibiotic		Streptomycin		<i>S.Tm</i> infection	
	R ²	p _{val}	R ²	p _{val}	R ²	p _{val}
B4	0.1158	0.0115	0.0878	0.0313	0.1000	0.0206
Transgene	0.0322	0.4837	0.0460	0.3078	0.0473	0.1634
B4/Transgene	0.0807	0.0628	0.0292	0.6442	0.0245	0.5063
Inflammation_score	0.0297	0.5176	0.0503	0.2512	0.1874	0.0011
Sex	0.0065	0.9063	0.0739	0.0908	0.0466	0.1757
B4:Inflammation score	0.0281	0.5494	0.0411	0.4011	0.0142	0.8177
B4:Sex	0.0876	0.0409	0.0410	0.4049	0.0671	0.0714
Transgene:Sex	0.0149	0.7862	0.0359	0.5015	0.0251	0.4936
B4/Transgene:Sex	0.0846	0.0542	0.0428	0.3402	0.0324	0.3419

Supplementary Table 5: PERMANOVA - Effect size (R2) of *B4galnt2* and confounding factors on Bray-Curtis index at the genus level

	Pre-antibiotic		Streptomycin		<i>S.Tm</i> infection	
	R ²	p _{val}	R ²	p _{val}	R ²	p _{val}
B4	0.3211	0.0002	0.0656	0.1759	0.0589	0.0852
Transgene	0.0179	0.6886	0.0397	0.4263	0.0141	0.7620
B4/Transgene	0.0109	0.8456	0.0076	0.9797	0.0458	0.1417
Inflammation_score	0.0113	0.8333	0.0413	0.3946	0.2853	0.0004
Sex	0.0242	0.5406	0.1073	0.0474	0.0803	0.0399
B4:Inflammation score	0.0227	0.5739	0.0127	0.9214	0.0239	0.4518
B4:Sex	0.0241	0.5314	0.0600	0.2278	0.0435	0.1803
Transgene:Sex	0.0383	0.3321	0.0514	0.2748	0.0187	0.6017
B4/Transgene:Sex	0.0307	0.4240	0.0239	0.7063	0.0158	0.6795

Supplementary Table 6: PERMANOVA - Effect size (R2) of *B4galnt2* and confounding factors on Jaccard index at the pathway abundances level

	Pre-antibiotic		Streptomycin		<i>S.Tm</i> infection	
	R ²	p _{val}	R ²	p _{val}	R ²	p _{val}
B4	0.1902	0.0002	0.0535	0.178	0.0864	0.0758
Transgene	0.0663	0.083	0.0718	0.1044	0.0302	0.4379
B4/Transgene	0.0294	0.6152	0.0235	0.6376	0.0209	0.6315
Inflammation_score	0.0172	0.9171	0.2025	0.0025	0.0327	0.4043
Sex	0.0322	0.5276	0.0329	0.426	0.1815	0.0067
B4:Inflammation score	0.0254	0.7196	0.0195	0.7579	0.0228	0.5832
B4:Sex	0.0278	0.6407	0.0251	0.5997	0.0308	0.4283
Transgene:Sex	0.022	0.8129	0.0996	0.0417	0.0449	0.2501
B4/Transgene:Sex	0.0292	0.5984	0.0346	0.3976	0.0127	0.8725

Supplementary Table 7: PERMANOVA - Effect size (R2) of *B4galnt2* and confounding factors on Bray-Curtis index at the pathway abundances level

	Pre-antibiotic		Streptomycin		<i>S.Tm</i> infection	
	R ²	p _{val}	R ²	p _{val}	R ²	p _{val}
B4	0.1656	0.0031	0.0736	0.1601	0.1147	0.0081
Transgene	0.0241	0.4997	0.0356	0.5608	0.0098	0.7963
B4/Transgene	0.0234	0.5304	0.0211	0.7901	0.0587	0.0735
Inflammation_score	0.0223	0.5584	0.0915	0.0884	0.1965	0.0015
Sex	0.0564	0.1345	0.0718	0.1761	0.1638	0.0021
B4:Inflammation score	0.0636	0.1028	0.0285	0.6568	0.0171	0.4903
B4:Sex	0.0435	0.2217	0.041	0.4588	0.039	0.1668

	Pre-antibiotic		Streptomycin		<i>S.Tm</i> infection	
	R ²	p _{val}	R ²	p _{val}	R ²	p _{val}
Transgene:Sex	0.0262	0.4682	0.0842	0.1071	0.0152	0.5637
B4/Transgene:Sex	0.106	0.0246	0.0188	0.8385	0.033	0.2192

Supplementary Table 8: Differential abundance of degradation pathways between B4 groups

Pathway	Group	Coef	q _{val}	Treatment
PWY-5130	B4 ^{-/-}	-2.2095	0.00002	Pre-antibiotic
PWY-5030	B4 ^{+/-}	1.1640	0.00009	Pre-antibiotic
PWY-7242	B4 ^{-/-}	-1.3919	0.00071	Pre-antibiotic
GALACTUROCAT-PWY	B4 ^{-/-}	-0.8439	0.00071	Pre-antibiotic
GLUCUROCAT-PWY	B4 ^{-/-}	-1.1095	0.00153	Pre-antibiotic
PWY-6507	B4 ^{-/-}	-1.3645	0.00170	Pre-antibiotic
PWY-6317	B4 ^{-/-}	-0.4709	0.00291	Pre-antibiotic
GLCMANNANAUT-PWY	B4 ^{+/-}	0.8259	0.00670	Pre-antibiotic
PWY-5941	B4 ^{-/-}	-0.6177	0.01654	Pre-antibiotic
PWY-6527	B4 ^{-/-}	-0.4800	0.02600	Pre-antibiotic
GALACT-GLUCUROCAT-PWY	B4 ^{-/-}	-1.5447	0.02677	Pre-antibiotic
FUCCAT-PWY	B4 ^{-/-}	-2.7170	0.02704	Pre-antibiotic
LACTOSECAT-PWY	B4 ^{-/-}	-2.7371	0.02972	Pre-antibiotic
PWY0-1298	B4 ^{-/-}	-1.3962	0.03012	Pre-antibiotic
PWY-5497	B4 ^{+/-}	2.3007	0.03398	Pre-antibiotic
PWY-6731	B4 ^{+/-}	0.6637	0.03416	Pre-antibiotic
PWY-5384	B4 ^{-/-}	-1.0791	0.03955	Pre-antibiotic
P161-PWY	B4 ^{-/-}	-1.6369	0.04995	Pre-antibiotic
PWY0-1297	B4 ^{-/-}	-1.6435	0.05443	Pre-antibiotic
PWY-7456	B4 ^{+/-}	0.5301	0.10052	Pre-antibiotic
PWY-6607	B4 ^{-/-}	-0.8665	0.10640	Pre-antibiotic
SALVADEHYPOX-PWY	B4 ^{-/-}	-0.4875	0.11253	Pre-antibiotic
PWY-8131	B4 ^{-/-}	-1.3341	0.12510	Pre-antibiotic
PWY0-1296	B4 ^{-/-}	-0.2378	0.15234	Pre-antibiotic
PWY-6608	B4 ^{-/-}	-0.3572	0.17163	Pre-antibiotic
PWY-621	B4 ^{-/-}	-1.0375	0.17516	Pre-antibiotic
PWY-5695	B4 ^{+/-}	0.1818	0.17516	Pre-antibiotic
P164-PWY	B4 ^{+/-}	0.6172	0.17516	Pre-antibiotic
GLYCOCAT-PWY	B4 ^{+/-}	0.5915	0.20429	Pre-antibiotic
RHAMCAT-PWY	B4 ^{-/-}	-0.1789	0.50670	Pre-antibiotic
HISDEG-PWY	B4 ^{+/-}	0.1301	0.54986	Pre-antibiotic
PWY-8187	B4 ^{+/-}	0.0122	0.98228	Pre-antibiotic
GOLPDLCAT-PWY	B4 ^{-/-}	-22.2028	0.99890	Pre-antibiotic
HISDEG-PWY	B4 ^{-/-}	-2.0372	0.34548	Streptomycin

Pathway	Group	Coef	q_{val}	Treatment
GALACTARDEG-PWY	B4 ⁺⁻	1.9185	0.34548	Streptomycin
GLUCARGALACTSUPER-PWY	B4 ⁺⁻	1.9185	0.34548	Streptomycin
HEXITOLDEGSUPER-PWY	B4 ⁺⁻	2.2981	0.34548	Streptomycin
GLUCARDEG-PWY	B4 ⁺⁻	2.3891	0.34548	Streptomycin
ORNDEG-PWY	B4 ⁺⁻	2.5728	0.34548	Streptomycin
PWY-561	B4 ⁺⁻	2.0464	0.35590	Streptomycin
PWY-6731	B4 ⁺⁻	-1.2312	0.43509	Streptomycin
PWY0-301	B4 ⁺⁻	1.8890	0.44059	Streptomycin
PWY-5695	B4 ⁺⁻	0.1864	0.44361	Streptomycin
GALACTUROCAT-PWY	B4 ⁺⁻	1.1073	0.51186	Streptomycin
PWY-7242	B4 ⁺⁻	0.7596	0.59382	Streptomycin
FUC-RHAMCAT-PWY	B4 ⁺⁻	1.1761	0.59382	Streptomycin
PWY-6507	B4 ⁺⁻	0.5771	0.68206	Streptomycin
PWY-6527	B4 ⁺⁻	-0.4569	0.73559	Streptomycin
PWY-6608	B4 ⁺⁻	0.4868	0.75440	Streptomycin
PWY0-1297	B4 ⁺⁻	-0.5581	0.75828	Streptomycin
GLUCUROCAT-PWY	B4 ⁺⁻	0.5832	0.82773	Streptomycin
LACTOSECAT-PWY	B4 ⁺⁻	0.8597	0.82773	Streptomycin
PWY-5384	B4 ⁺⁻	-0.3185	0.86133	Streptomycin
FUCCAT-PWY	B4 ⁺⁻	0.5382	0.86133	Streptomycin
P161-PWY	B4 ⁺⁻	-0.4840	0.87692	Streptomycin
GLYCOCAT-PWY	B4 ⁺⁻	-0.4546	0.87872	Streptomycin
GLCMANNANAUT-PWY	B4 ⁺⁻	-0.2913	0.88066	Streptomycin
PWY-621	B4 ⁺⁻	-0.2560	0.92545	Streptomycin
PWY-6317	B4 ⁺⁻	-0.1760	0.94734	Streptomycin
RHAMCAT-PWY	B4 ⁺⁻	0.1788	0.94892	Streptomycin
P164-PWY	B4 ⁺⁻	0.2058	0.94892	Streptomycin
PWY0-1298	B4 ⁺⁻	0.2443	0.94892	Streptomycin
PWY-5030	B4 ⁺⁻	0.2725	0.94892	Streptomycin
PWY66-389	B4 ⁺⁻	-0.1714	0.95662	Streptomycin
PWY-5941	B4 ⁺⁻	-0.0848	0.96976	Streptomycin
PWY-8187	B4 ⁺⁻	0.0259	0.97954	Streptomycin
PWY0-1296	B4 ⁺⁻	0.0269	0.97954	Streptomycin
SALVADEHYPOX-PWY	B4 ⁺⁻	-0.0160	0.98731	Streptomycin
PWY-561	B4 ⁺⁻	0.3765	0.04415	S.Tm infection
GALACTARDEG-PWY	B4 ⁺⁻	0.3992	0.04415	S.Tm infection
GLUCARGALACTSUPER-PWY	B4 ⁺⁻	0.3992	0.04415	S.Tm infection
PWY-6961	B4 ⁺⁻	0.4659	0.05186	S.Tm infection
RHAMCAT-PWY	B4 ⁺⁻	0.3455	0.09262	S.Tm infection
GLUCARDEG-PWY	B4 ⁺⁻	0.3721	0.09262	S.Tm infection
PWY0-301	B4 ⁺⁻	0.3958	0.09262	S.Tm infection
CARNMET-PWY	B4 ⁺⁻	0.4493	0.09262	S.Tm infection

Pathway	Group	Coef	<i>q_{val}</i>	Treatment
PWY-5705	B4 ⁺⁻	0.3288	0.09325	S.Tm infection
PWY-7446	B4 ⁺⁻	0.4288	0.10316	S.Tm infection
FUC-RHAMCAT-PWY	B4 ⁺⁻	0.3177	0.11468	S.Tm infection
ARGDEG-PWY	B4 ⁺⁻	-2.2242	0.12261	S.Tm infection
ORNARGDEG-PWY	B4 ⁺⁻	-2.2242	0.12261	S.Tm infection
HISDEG-PWY	B4 ⁺⁻	-0.5733	0.12261	S.Tm infection
PWY-5695	B4 ⁺⁻	-0.2847	0.12261	S.Tm infection
GLUCUROCAT-PWY	B4 ⁺⁻	0.3541	0.13749	S.Tm infection
METHGLYUT-PWY	B4 ⁺⁻	0.3376	0.14835	S.Tm infection
PWY-7242	B4 ⁺⁻	0.2781	0.16349	S.Tm infection
AST-PWY	B4 ⁺⁻	0.2224	0.16448	S.Tm infection
PWY-8187	B4 ⁺⁻	0.2786	0.20001	S.Tm infection
PWY-6507	B4 ⁺⁻	0.2524	0.20708	S.Tm infection
GLYCOCAT-PWY	B4 ⁺⁻	0.1737	0.22839	S.Tm infection
PWY66-389	B4 ⁺⁻	-0.6451	0.23475	S.Tm infection
PWY0-1221	B4 ⁺⁻	-2.1950	0.23766	S.Tm infection
ORNDEG-PWY	B4 ⁺⁻	0.2188	0.23766	S.Tm infection
HEXITOLDEGSUPER-PWY	B4 ⁺⁻	1.0158	0.24952	S.Tm infection
PWY-7456	B4 ⁺⁻	-1.2412	0.29270	S.Tm infection
FUCCAT-PWY	B4 ⁺⁻	0.1992	0.35259	S.Tm infection
P161-PWY	B4 ⁺⁻	0.1506	0.43022	S.Tm infection
PWY-5941	B4 ⁺⁻	0.0820	0.46826	S.Tm infection
LACTOSECAT-PWY	B4 ⁺⁻	-0.5636	0.49758	S.Tm infection
PWY-6317	B4 ⁺⁻	-0.1101	0.49758	S.Tm infection
PWY0-1297	B4 ⁺⁻	0.0746	0.50265	S.Tm infection
GOLPDLCAT-PWY	B4 ⁺⁻	-0.9207	0.53865	S.Tm infection
PWY-6527	B4 ⁺⁻	-0.0939	0.62335	S.Tm infection
PWY-6607	B4 ⁺⁻	0.6980	0.70187	S.Tm infection
GALACTUROCAT-PWY	B4 ⁺⁻	-0.2106	0.71389	S.Tm infection
PWY-6731	B4 ⁺⁻	-0.3087	0.72404	S.Tm infection
PWY0-1298	B4 ⁺⁻	0.0563	0.72404	S.Tm infection
PWY-5030	B4 ⁺⁻	-0.2562	0.79111	S.Tm infection
P164-PWY	B4 ⁺⁻	-0.1547	0.84181	S.Tm infection
GALACT-GLUCUROCAT-PWY	B4 ⁺⁻	0.1510	0.85439	S.Tm infection
PWY-6608	B4 ⁺⁻	-0.1062	0.86855	S.Tm infection
PWY-5384	B4 ⁺⁻	0.0604	0.88047	S.Tm infection
PWY-5497	B4 ⁺⁻	0.0642	0.91950	S.Tm infection
PWY-621	B4 ⁺⁻	-0.0216	0.97180	S.Tm infection
SALVADEHYPOX-PWY	B4 ⁺⁻	-0.0203	0.97895	S.Tm infection
PWY-5130	B4 ⁺⁻	-67.2889	0.99854	S.Tm infection

Supplementary Table 9: Differential abundance of degradation pathways between Tg groups

Pathway	Group	Coef	<i>q</i>_{val}	Treatment
PWY-6607	Tg ⁺	2.9728	0.02429	Pre-antibiotic
LACTOSECAT-PWY	Tg ⁺	2.9170	0.09555	Pre-antibiotic
GOLPDLCAT-PWY	Tg ⁺	3.1981	0.21959	Pre-antibiotic
GLYCOCAT-PWY	Tg ⁺	0.8755	0.41544	Pre-antibiotic
FUCCAT-PWY	Tg ⁻	-1.5086	0.43923	Pre-antibiotic
PWY-8131	Tg ⁺	1.2517	0.49388	Pre-antibiotic
PWY0-1298	Tg ⁻	-0.9019	0.49388	Pre-antibiotic
PWY-7456	Tg ⁺	0.3535	0.68662	Pre-antibiotic
PWY0-1296	Tg ⁺	0.1915	0.68662	Pre-antibiotic
GLUCUROCAT-PWY	Tg ⁺	0.2968	0.69649	Pre-antibiotic
PWY-8187	Tg ⁺	0.3028	0.69649	Pre-antibiotic
PWY-5130	Tg ⁻	-0.3172	0.87653	Pre-antibiotic
PWY-5384	Tg ⁺	0.2934	0.88629	Pre-antibiotic
GALACTUROCAT-PWY	Tg ⁺	0.1233	0.92530	Pre-antibiotic
RHAMCAT-PWY	Tg ⁻	-0.1278	0.95119	Pre-antibiotic
GLCMANNANAUT-PWY	Tg ⁺	0.1068	0.97386	Pre-antibiotic
HISDEG-PWY	Tg ⁻	-0.0862	0.97386	Pre-antibiotic
P164-PWY	Tg ⁺	0.1660	0.97386	Pre-antibiotic
PWY-621	Tg ⁻	-0.2779	0.97386	Pre-antibiotic
PWY-6527	Tg ⁻	-0.0766	0.97386	Pre-antibiotic
PWY0-1297	Tg ⁺	0.2825	0.97386	Pre-antibiotic
PWY-5030	Tg ⁻	-0.0933	0.97748	Pre-antibiotic
PWY-5941	Tg ⁺	0.0832	0.97748	Pre-antibiotic
GALACT-GLUCUROCAT-PWY	Tg ⁺	0.1140	0.99996	Pre-antibiotic
P161-PWY	Tg ⁻	-0.0654	0.99996	Pre-antibiotic
PWY-5497	Tg ⁻	-0.1481	0.99996	Pre-antibiotic
PWY-5695	Tg ⁺	0.0305	0.99996	Pre-antibiotic
PWY-6317	Tg ⁺	0.0243	0.99996	Pre-antibiotic
PWY-6507	Tg ⁻	-0.0071	0.99996	Pre-antibiotic
PWY-6608	Tg ⁻	-0.0176	0.99996	Pre-antibiotic
PWY-6731	Tg ⁻	-0.0870	0.99996	Pre-antibiotic
PWY-7242	Tg ⁻	-0.0562	0.99996	Pre-antibiotic
SALVADEHYPOX-PWY	Tg ⁺	0.0669	0.99996	Pre-antibiotic
GLYCOCAT-PWY	Tg ⁺	2.2528	0.22462	Streptomycin
GLUCARDEG-PWY	Tg ⁺	2.0753	0.29085	Streptomycin
PWY-8187	Tg ⁺	1.1037	0.31613	Streptomycin
RHAMCAT-PWY	Tg ⁻	-1.5170	0.31613	Streptomycin
PWY-6507	Tg ⁺	1.2698	0.33086	Streptomycin

Pathway	Group	Coef	q_{val}	Treatment
GALACTARDEG-PWY	Tg ⁺	1.8318	0.37206	Streptomycin
GLUCARGALACTSUPER-PWY	Tg ⁺	1.8318	0.37206	Streptomycin
GLUCUROCAT-PWY	Tg ⁺	1.7638	0.37206	Streptomycin
GALACTUROCAT-PWY	Tg ⁺	1.2596	0.52432	Streptomycin
PWY-7242	Tg ⁺	1.0860	0.52432	Streptomycin
PWY-561	Tg ⁺	1.4180	0.68350	Streptomycin
PWY66-389	Tg ⁺	0.9063	0.70073	Streptomycin
PWY-6527	Tg ⁻	-0.6405	0.70226	Streptomycin
ORNDEG-PWY	Tg ⁺	1.3527	0.71693	Streptomycin
FUC-RHAMCAT-PWY	Tg ⁺	0.9581	0.73415	Streptomycin
FUCCAT-PWY	Tg ⁺	0.9523	0.73415	Streptomycin
HISDEG-PWY	Tg ⁻	-0.6709	0.73415	Streptomycin
PWY-5695	Tg ⁺	0.1195	0.73415	Streptomycin
PWY-5941	Tg ⁻	-0.5303	0.73415	Streptomycin
PWY-6731	Tg ⁻	-0.8120	0.73415	Streptomycin
PWY0-301	Tg ⁺	1.0163	0.75418	Streptomycin
PWY-6317	Tg ⁻	-0.4246	0.76092	Streptomycin
PWY0-1297	Tg ⁺	0.5546	0.76488	Streptomycin
HEXITOLDEGSUPER-PWY	Tg ⁺	0.8728	0.76590	Streptomycin
PWY-621	Tg ⁻	-0.3415	0.83196	Streptomycin
GLCMANNANAUT-PWY	Tg ⁻	-0.2772	0.84362	Streptomycin
P164-PWY	Tg ⁻	-0.3342	0.84362	Streptomycin
PWY-6608	Tg ⁻	-0.2854	0.84502	Streptomycin
PWY0-1296	Tg ⁺	0.1649	0.84502	Streptomycin
PWY-5030	Tg ⁻	-0.4362	0.84759	Streptomycin
PWY-5384	Tg ⁺	0.2351	0.84759	Streptomycin
P161-PWY	Tg ⁺	0.1486	0.95393	Streptomycin
SALVADEHYPOX-PWY	Tg ⁻	-0.0829	0.98350	Streptomycin
LACTOSECAT-PWY	Tg ⁻	-0.0384	0.98890	Streptomycin
PWY0-1298	Tg ⁺	0.0163	0.98890	Streptomycin
ARGDEG-PWY	Tg ⁺	0.5314	0.98090	S.Tm infection
AST-PWY	Tg ⁺	0.0240	0.98090	S.Tm infection
CARNMET-PWY	Tg ⁺	0.0085	0.98090	S.Tm infection
FUC-RHAMCAT-PWY	Tg ⁺	0.0778	0.98090	S.Tm infection
FUCCAT-PWY	Tg ⁻	-0.0410	0.98090	S.Tm infection
GALACT-GLUCUROCAT-PWY	Tg ⁺	0.4447	0.98090	S.Tm infection
GALACTARDEG-PWY	Tg ⁺	0.1542	0.98090	S.Tm infection
GALACTUROCAT-PWY	Tg ⁺	0.2743	0.98090	S.Tm infection
GLUCARDEG-PWY	Tg ⁺	0.1428	0.98090	S.Tm infection
GLUCARGALACTSUPER-PWY	Tg ⁺	0.1542	0.98090	S.Tm infection
GLUCUROCAT-PWY	Tg ⁺	0.2604	0.98090	S.Tm infection
GLYCOCAT-PWY	Tg ⁺	0.0926	0.98090	S.Tm infection

Pathway	Group	Coef	<i>q_val</i>	Treatment
GOLPDLCAT-PWY	Tg ⁺	0.7757	0.98090	S.Tm infection
HEXITOLDEGSUPER-PWY	Tg ⁺	0.1691	0.98090	S.Tm infection
HISDEG-PWY	Tg ⁻	-0.2895	0.98090	S.Tm infection
LACTOSECAT-PWY	Tg ⁻	-0.1654	0.98090	S.Tm infection
METHGLYUT-PWY	Tg ⁻	-0.0126	0.98090	S.Tm infection
ORNARGDEG-PWY	Tg ⁺	0.5314	0.98090	S.Tm infection
ORNDEG-PWY	Tg ⁺	0.2301	0.98090	S.Tm infection
P161-PWY	Tg ⁺	0.0560	0.98090	S.Tm infection
P164-PWY	Tg ⁺	0.1484	0.98090	S.Tm infection
PWY-5030	Tg ⁻	-0.6184	0.98090	S.Tm infection
PWY-5130	Tg ⁺	2.1600	0.98090	S.Tm infection
PWY-5384	Tg ⁺	0.1060	0.98090	S.Tm infection
PWY-5497	Tg ⁺	0.2912	0.98090	S.Tm infection
PWY-561	Tg ⁺	0.1234	0.98090	S.Tm infection
PWY-5695	Tg ⁻	-0.1043	0.98090	S.Tm infection
PWY-5705	Tg ⁺	0.0956	0.98090	S.Tm infection
PWY-5941	Tg ⁺	0.0675	0.98090	S.Tm infection
PWY-621	Tg ⁺	0.1576	0.98090	S.Tm infection
PWY-6317	Tg ⁺	0.0094	0.98090	S.Tm infection
PWY-6507	Tg ⁺	0.1105	0.98090	S.Tm infection
PWY-6527	Tg ⁺	0.0144	0.98090	S.Tm infection
PWY-6607	Tg ⁻	-0.4700	0.98090	S.Tm infection
PWY-6608	Tg ⁺	0.3285	0.98090	S.Tm infection
PWY-6731	Tg ⁺	0.4106	0.98090	S.Tm infection
PWY-6961	Tg ⁺	0.1599	0.98090	S.Tm infection
PWY-7242	Tg ⁺	0.0106	0.98090	S.Tm infection
PWY-7446	Tg ⁺	0.0368	0.98090	S.Tm infection
PWY-7456	Tg ⁺	0.5263	0.98090	S.Tm infection
PWY-8187	Tg ⁻	-0.1109	0.98090	S.Tm infection
PWY0-1221	Tg ⁺	0.6453	0.98090	S.Tm infection
PWY0-1297	Tg ⁻	-0.0331	0.98090	S.Tm infection
PWY0-1298	Tg ⁻	-0.0250	0.98090	S.Tm infection
PWY0-301	Tg ⁺	0.0741	0.98090	S.Tm infection
PWY66-389	Tg ⁺	0.1254	0.98090	S.Tm infection
RHAMCAT-PWY	Tg ⁺	0.1721	0.98090	S.Tm infection
SALVADEHYPOX-PWY	Tg ⁺	0.3040	0.98090	S.Tm infection

References

- Ahn, J., Hayes, R.B., 2021. Environmental Influences on the Human Microbiome and Implications for Noncommunicable Disease. *Annu. Rev. Public Health* 42, 277–292. <https://doi.org/10.1146/annurev-publhealth-012420-105020>
- Alavi, S., Mitchell, J.D., Cho, J.Y., Liu, R., Macbeth, J.C., Hsiao, A., 2020. Interpersonal Gut Microbiome Variation Drives Susceptibility and Resistance to Cholera Infection. *Cell* 181, 1533-1546.e13. <https://doi.org/10.1016/j.cell.2020.05.036>
- Andino, A., Hanning, I., 2015. *Salmonella enterica* : Survival, Colonization, and Virulence Differences among Serovars. *Sci. World J.* 2015, 1–16. <https://doi.org/10.1155/2015/520179>
- Barnett, D., Arts, I., Penders, J., 2021. microViz: an R package for microbiome data visualization and statistics. *J. Open Source Softw.* 6, 3201. <https://doi.org/10.21105/joss.03201>
- Barthel, M., Hapfelmeier, S., Quintanilla-Martínez, L., Kremer, M., Rohde, M., Hogardt, M., Pfeffer, K., Rüssmann, H., Hardt, W.-D., 2003. Pretreatment of Mice with Streptomycin Provides a *Salmonella enterica* Serovar Typhimurium Colitis Model That Allows Analysis of Both Pathogen and Host. *Infect. Immun.* 71, 2839–2858. <https://doi.org/10.1128/IAI.71.5.2839-2858.2003>
- Beghini, F., McIver, L.J., Blanco-Míguez, A., Dubois, L., Asnicar, F., Maharjan, S., Mailyan, A., Manghi, P., Scholz, M., Thomas, A.M., Valles-Colomer, M., Weingart, G., Zhang, Y., Zolfo, M., Huttenhower, C., Franzosa, E.A., Segata, N., 2021. Integrating taxonomic, functional, and strain-level profiling of diverse microbial communities with bioBakery 3. *eLife* 10, e65088. <https://doi.org/10.7554/eLife.65088>
- Behnsen, J., Zhi, H., Aron, A.T., Subramanian, V., Santus, W., Lee, M.H., Gerner, R.R., Petras, D., Liu, J.Z., Green, K.D., Price, S.L., Camacho, J., Hillman, H., Tjokrosurjo, J., Montaldo, N.P., Hoover, E.M., Treacy-Abarca, S., Gilston, B.A., Skaar, E.P., Chazin, W.J., Garneau-Tsodikova, S., Lawrenz, M.B., Perry, R.D., Nuccio, S.-P., Dorrestein, P.C., Raffatellu, M., 2021. Siderophore-mediated zinc acquisition enhances enterobacterial colonization of the inflamed gut. *Nat. Commun.* 12, 7016. <https://doi.org/10.1038/s41467-021-27297-2>
- Blekhman, R., Goodrich, J.K., Huang, K., Sun, Q., Bukowski, R., Bell, J.T., Spector, T.D., Keinan, A., Ley, R.E., Gevers, D., Clark, A.G., 2015. Host genetic variation impacts microbiome composition across human body sites. *Genome Biol.* 16, 191. <https://doi.org/10.1186/s13059-015-0759-1>

- Bohnhoff, M., Drake, B.L., Miller, C.P., 1954. Effect of Streptomycin on Susceptibility of Intestinal Tract to Experimental *Salmonella* Infection. *Exp. Biol. Med.* 86, 132–137. <https://doi.org/10.3181/00379727-86-21030>
- Bolger, A.M., Lohse, M., Usadel, B., 2014. Trimmomatic: a flexible trimmer for Illumina sequence data. *Bioinformatics* 30, 2114–2120. <https://doi.org/10.1093/bioinformatics/btu170>
- Collins, F.M., Carter, P.B., 1978. Growth of salmonellae in orally infected germfree mice. *Infect. Immun.* 21, 41–47. <https://doi.org/10.1128/iai.21.1.41-47.1978>
- Coyte, K.Z., Rakoff-Nahoum, S., 2019. Understanding Competition and Cooperation within the Mammalian Gut Microbiome. *Curr. Biol.* 29, R538–R544. <https://doi.org/10.1016/j.cub.2019.04.017>
- Deriu, E., Liu, J.Z., Pezeshki, M., Edwards, R.A., Ochoa, R.J., Contreras, H., Libby, S.J., Fang, F.C., Raffatellu, M., 2013. Probiotic Bacteria Reduce *Salmonella* Typhimurium Intestinal Colonization by Competing for Iron. *Cell Host Microbe* 14, 26–37. <https://doi.org/10.1016/j.chom.2013.06.007>
- Dixon, P., 2003. VEGAN, a package of R functions for community ecology. *J. Veg. Sci.* 14, 927–930. <https://doi.org/10.1111/j.1654-1103.2003.tb02228.x>
- Ducarmon, Q.R., Zwittink, R.D., Hornung, B.V.H., Van Schaik, W., Young, V.B., Kuijper, E.J., 2019. Gut Microbiota and Colonization Resistance against Bacterial Enteric Infection. *Microbiol. Mol. Biol. Rev.* 83, e00007-19. <https://doi.org/10.1128/MMBR.00007-19>
- Eberl, C., Weiss, A.S., Jochum, L.M., Durai Raj, A.C., Ring, D., Hussain, S., Herp, S., Meng, C., Kleigrewe, K., Gigl, M., Basic, M., Stecher, B., 2021. *E. coli* enhance colonization resistance against *Salmonella* Typhimurium by competing for galactitol, a context-dependent limiting carbon source. *Cell Host Microbe* 29, 1680–1692.e7. <https://doi.org/10.1016/j.chom.2021.09.004>
- Fabich, A.J., Jones, S.A., Chowdhury, F.Z., Cernosek, A., Anderson, A., Smalley, D., McHargue, J.W., Hightower, G.A., Smith, J.T., Autieri, S.M., Leatham, M.P., Lins, J.J., Allen, R.L., Laux, D.C., Cohen, P.S., Conway, T., 2008. Comparison of Carbon Nutrition for Pathogenic and Commensal *Escherichia coli* Strains in the Mouse Intestine. *Infect. Immun.* 76, 1143–1152. <https://doi.org/10.1128/IAI.01386-07>
- Fàbrega, A., Vila, J., 2013. *Salmonella enterica* Serovar Typhimurium Skills To Succeed in the Host: Virulence and Regulation. *Clin. Microbiol. Rev.* 26, 308–341. <https://doi.org/10.1128/CMR.00066-12>

- Fuchs, L.M., 2023. Identification of carbon and nitrogen sources promoting *Salmonella* Typhimurium gut colonization. ETH Zurich. <https://doi.org/10.3929/ETHZ-B-000642973>
- Furuya, H., Ide, Y., Hamamoto, M., Asanuma, N., Hino, T., 2010. Isolation of a novel bacterium, *Blautia glucerasei* sp. nov., hydrolyzing plant glucosylceramide to ceramide. Arch. Microbiol. 192, 365–372. <https://doi.org/10.1007/s00203-010-0566-8>
- Greenhalgh, K., Meyer, K.M., Aagaard, K.M., Wilmes, P., 2016. The human gut microbiome in health: establishment and resilience of microbiota over a lifetime. Environ. Microbiol. 18, 2103–2116. <https://doi.org/10.1111/1462-2920.13318>
- Grondin, J.A., Kwon, Y.H., Far, P.M., Haq, S., Khan, W.I., 2020. Mucins in Intestinal Mucosal Defense and Inflammation: Learning From Clinical and Experimental Studies. Front. Immunol. 11, 2054. <https://doi.org/10.3389/fimmu.2020.02054>
- Heilbronner, S., Krismer, B., Brötz-Oesterhelt, H., Peschel, A., 2021. The microbiome-shaping roles of bacteriocins. Nat. Rev. Microbiol. 19, 726–739. <https://doi.org/10.1038/s41579-021-00569-w>
- Hoiseth, S.K., Stocker, B.A.D., 1981. Aromatic-dependent *Salmonella typhimurium* are non-virulent and effective as live vaccines. Nature 291, 238–239. <https://doi.org/10.1038/291238a0>
- Johnsen, J.M., Teschke, M., Pavlidis, P., McGee, B.M., Tautz, D., Ginsburg, D., Baines, J.F., 2009. Selection on cis-regulatory variation at *B4galnt2* and its influence on von Willebrand factor in house mice. Mol. Biol. Evol. 26, 567–578. <https://doi.org/10.1093/molbev/msn284>
- Johnsen, J.M., Levy, G.G., Westrick, R.J., Tucker, P.K., Ginsburg, D., 2008. The endothelial-specific regulatory mutation, *Mwgf1*, is a common mouse founder allele. Mamm. Genome 19, 32–40. <https://doi.org/10.1007/s00335-007-9079-4>
- Kaneuchi, C., Benno, Y., Mitsuoka, T., 1976. *Clostridium coccoides*, a New Species from the Feces of Mice. Int. J. Syst. Bacteriol. 26, 482–486. <https://doi.org/10.1099/00207713-26-4-482>
- Kennedy, M.S., Chang, E.B., 2020. The microbiome: Composition and locations, in: Progress in Molecular Biology and Translational Science. Elsevier, pp. 1–42. <https://doi.org/10.1016/bs.pmbts.2020.08.013>
- Koh, A., De Vadder, F., Kovatcheva-Datchary, P., Bäckhed, F., 2016. From Dietary Fiber to Host Physiology: Short-Chain Fatty Acids as Key Bacterial Metabolites. Cell 165, 1332–1345. <https://doi.org/10.1016/j.cell.2016.05.041>

- Koropatkin, N.M., Cameron, E.A., Martens, E.C., 2012. How glycan metabolism shapes the human gut microbiota. *Nat. Rev. Microbiol.* 10, 323–335. <https://doi.org/10.1038/nrmicro2746>
- Lahti, Shetty et al., 2017. microbiome. <https://doi.org/10.18129/B9.BIOC.MICROBIOME>
- Langmead, B., Salzberg, S.L., 2012. Fast gapped-read alignment with Bowtie 2. *Nat. Methods* 9, 357–359. <https://doi.org/10.1038/nmeth.1923>
- Linnenbrink, M., Johnsen, J.M., Montero, I., Brzezinski, C.R., Harr, B., Baines, J.F., 2011. Long-Term Balancing Selection at the Blood Group-Related Gene *B4galnt2* in the Genus *Mus* (Rodentia; Muridae). *Mol. Biol. Evol.* 28, 2999–3003. <https://doi.org/10.1093/molbev/msr150>
- Lkhagva, E., Chung, H.-J., Hong, J., Tang, W.H.W., Lee, S.-I., Hong, S.-T., Lee, S., 2021. The regional diversity of gut microbiome along the GI tract of male C57BL/6 mice. *BMC Microbiol.* 21, 44. <https://doi.org/10.1186/s12866-021-02099-0>
- Louis, P., Flint, H.J., 2017. Formation of propionate and butyrate by the human colonic microbiota. *Environ. Microbiol.* 19, 29–41. <https://doi.org/10.1111/1462-2920.13589>
- Lu, J., Breitwieser, F.P., Thielen, P., Salzberg, S.L., 2017. Bracken: estimating species abundance in metagenomics data. *PeerJ Comput. Sci.* 3, e104. <https://doi.org/10.7717/peerj-cs.104>
- Mallick, H., Rahnavard, A., McIver, L.J., Ma, S., Zhang, Y., Nguyen, L.H., Tickle, T.L., Weingart, G., Ren, B., Schwager, E.H., Chatterjee, S., Thompson, K.N., Wilkinson, J.E., Subramanian, A., Lu, Y., Waldron, L., Paulson, J.N., Franzosa, E.A., Bravo, H.C., Huttenhower, C., 2021. Multivariable association discovery in population-scale meta-omics studies. *PLOS Comput. Biol.* 17, e1009442. <https://doi.org/10.1371/journal.pcbi.1009442>
- McMurdie, P., Paulson, J., 2017. biomformat. <https://doi.org/10.18129/B9.BIOC.BIOMFORMAT>
- McMurdie, P.J., Holmes, S., 2013. phyloseq: An R Package for Reproducible Interactive Analysis and Graphics of Microbiome Census Data. *PLoS ONE* 8, e61217. <https://doi.org/10.1371/journal.pone.0061217>
- Mohlke, K.L., Purkayastha, A.A., Westrick, R.J., Smith, P.L., Petryniak, B., Lowe, J.B., Ginsburg, D., 1999. Mvwf, a Dominant Modifier of Murine von Willebrand Factor, Results from Altered Lineage-Specific Expression of a Glycosyltransferase. *Cell* 96, 111–120. [https://doi.org/10.1016/S0092-8674\(00\)80964-2](https://doi.org/10.1016/S0092-8674(00)80964-2)

- Momose, Y., Hirayama, K., Itoh, K., 2008. Competition for proline between indigenous *Escherichia coli* and *E. coli* O157:H7 in gnotobiotic mice associated with infant intestinal microbiota and its contribution to the colonization resistance against *E. coli* O157:H7. Antonie Van Leeuwenhoek 94, 165–171. <https://doi.org/10.1007/s10482-008-9222-6>
- Park, S.-K., Kim, M.-S., Roh, S.W., Bae, J.-W., 2012. *Blautia stercoris* sp. nov., isolated from human faeces. Int. J. Syst. Evol. Microbiol. 62, 776–779. <https://doi.org/10.1099/ijsm.0.031625-0>
- Rausch, P., Steck, N., Suwandi, A., Seidel, J.A., Künzel, S., Bhullar, K., Basic, M., Bleich, A., Johnsen, J.M., Vallance, B.A., Baines, J.F., Grassl, G.A., 2015. Expression of the Blood-Group-Related Gene *B4galnt2* Alters Susceptibility to *Salmonella* Infection. PLOS Pathog. 11, e1005008. <https://doi.org/10.1371/journal.ppat.1005008>
- Reinhardt, C., Bergentall, M., Greiner, T.U., Schaffner, F., Östergren-Lundén, G., Petersen, L.C., Ruf, W., Bäckhed, F., 2012. Tissue factor and PAR1 promote microbiota-induced intestinal vascular remodelling. Nature 483, 627–631. <https://doi.org/10.1038/nature10893>
- Rivera-Chávez, F., Zhang, L.F., Faber, F., Lopez, C.A., Byndloss, M.X., Olsan, E.E., Xu, G., Velazquez, E.M., Lebrilla, C.B., Winter, S.E., Bäumler, A.J., 2016. Depletion of Butyrate-Producing Clostridia from the Gut Microbiota Drives an Aerobic Luminal Expansion of *Salmonella*. Cell Host Microbe 19, 443–454. <https://doi.org/10.1016/j.chom.2016.03.004>
- Roe, A.J., O'Byrne, C., McLaggan, D., Booth, I.R., 2002. Inhibition of *Escherichia coli* growth by acetic acid: a problem with methionine biosynthesis and homocysteine toxicity. Microbiology 148, 2215–2222. <https://doi.org/10.1099/00221287-148-7-2215>
- Round, J.L., Mazmanian, S.K., 2009. The gut microbiota shapes intestinal immune responses during health and disease. Nat. Rev. Immunol. 9, 313–323. <https://doi.org/10.1038/nri2515>
- Schubert, A.M., Sinani, H., Schloss, P.D., 2015. Antibiotic-Induced Alterations of the Murine Gut Microbiota and Subsequent Effects on Colonization Resistance against *Clostridium difficile*. mBio 6, e00974-15. <https://doi.org/10.1128/mBio.00974-15>
- Segata, N., Izard, J., Waldron, L., Gevers, D., Miropolsky, L., Garrett, W.S., Huttenhower, C., 2011. Metagenomic biomarker discovery and explanation. Genome Biol. 12, R60. <https://doi.org/10.1186/gb-2011-12-6-r60>

- Sehgal, K., Khanna, S., 2021. Gut microbiome and *Clostridoides difficile* infection: a closer look at the microscopic interface. Ther. Adv. Gastroenterol. 14, 175628482199473. <https://doi.org/10.1177/1756284821994736>
- Sender, R., Fuchs, S., Milo, R., 2016. Revised Estimates for the Number of Human and Bacteria Cells in the Body. PLOS Biol. 14, e1002533. <https://doi.org/10.1371/journal.pbio.1002533>
- Shan, Y., Lee, M., Chang, E.B., 2022. The Gut Microbiome and Inflammatory Bowel Diseases. Annu. Rev. Med. 73, 455–468. <https://doi.org/10.1146/annurev-med-042320-021020>
- Shen, Z.-H., Zhu, C.-X., Quan, Y.-S., Yang, Z.-Y., Wu, S., Luo, W.-W., Tan, B., Wang, X.-Y., 2018. Relationship between intestinal microbiota and ulcerative colitis: Mechanisms and clinical application of probiotics and fecal microbiota transplantation. World J. Gastroenterol. 24, 5–14. <https://doi.org/10.3748/wjg.v24.i1.5>
- Sommer, F., Bäckhed, F., 2013. The gut microbiota — masters of host development and physiology. Nat. Rev. Microbiol. 11, 227–238. <https://doi.org/10.1038/nrmicro2974>
- Sonnenburg, J.L., Xu, J., Leip, D.D., Chen, C.-H., Westover, B.P., Weatherford, J., Buhler, J.D., Gordon, J.I., 2005. Glycan Foraging in Vivo by an Intestine-Adapted Bacterial Symbiont. Science 307, 1955–1959. <https://doi.org/10.1126/science.1109051>
- Spragge, F., Bakkeren, E., Jahn, M.T., B. N. Araujo, E., Pearson, C.F., Wang, X., Pankhurst, L., Cunrath, O., Foster, K.R., 2023. Microbiome diversity protects against pathogens by nutrient blocking. Science 382, eadj3502. <https://doi.org/10.1126/science.adj3502>
- Staubach, F., Künzel, S., Baines, A.C., Yee, A., McGee, B.M., Bäckhed, F., Baines, J.F., Johnsen, J.M., 2012. Expression of the blood-group-related glycosyltransferase *B4galnt2* influences the intestinal microbiota in mice. ISME J. 6, 1345–1355. <https://doi.org/10.1038/ismej.2011.204>
- Stecher, B., 2015. The Roles of Inflammation, Nutrient Availability and the Commensal Microbiota in Enteric Pathogen Infection. Microbiol. Spectr. 3, 3.3.12. <https://doi.org/10.1128/microbiolspec.MBP-0008-2014>
- Stecher, B., Chaffron, S., Käppeli, R., Hapfelmeier, S., Freedrich, S., Weber, T.C., Kirundi, J., Suar, M., McCoy, K.D., Von Mering, C., Macpherson, A.J., Hardt, W.-D., 2010. Like Will to Like: Abundances of Closely Related Species Can Predict Susceptibility to Intestinal Colonization by Pathogenic and Commensal Bacteria. PLoS Pathog. 6, e1000711. <https://doi.org/10.1371/journal.ppat.1000711>

- Stecher, B., Macpherson, A.J., Hapfelmeier, S., Kremer, M., Stallmach, T., Hardt, W.-D., 2005. Comparison of *Salmonella enterica* Serovar Typhimurium Colitis in Germfree Mice and Mice Pretreated with Streptomycin. *Infect. Immun.* 73, 3228–3241. <https://doi.org/10.1128/IAI.73.6.3228-3241.2005>
- Suwandi, A., Galeev, A., Riedel, R., Sharma, S., Seeger, K., Sterzenbach, T., García Pastor, L., Boyle, E.C., Gal-Mor, O., Hensel, M., Casadesús, J., Baines, J.F., Grassl, G.A., 2019. Std fimbriae-fucose interaction increases *Salmonella*-induced intestinal inflammation and prolongs colonization. *PLOS Pathog.* 15, e1007915. <https://doi.org/10.1371/journal.ppat.1007915>
- Tailford, L.E., Crost, E.H., Kavanaugh, D., Juge, N., 2015. Mucin glycan foraging in the human gut microbiome. *Front. Genet.* 6. <https://doi.org/10.3389/fgene.2015.00081>
- Tauni, M.A., Osterlund, A., 2000. Outbreak of *Salmonella typhimurium* in cats and humans associated with infection in wild birds. *J. Small Anim. Pract.* 41, 339–341. <https://doi.org/10.1111/j.1748-5827.2000.tb03214.x>
- Vallier, M., 2017. Characterization of pathogen-driven selection at B4galnt2 in house mice. Christian-Albrechts-Universität, Kiel.
- Vallier, M., Suwandi, A., Ehrhardt, K., Belheouane, M., Berry, D., Čepić, A., Galeev, A., Johnsen, J.M., Grassl, G.A., Baines, J.F., 2023. Pathometagenomics reveals susceptibility to intestinal infection by *Morganella* to be mediated by the blood group-related *B4galnt2* gene in wild mice. *Gut Microbes* 15, 2164448. <https://doi.org/10.1080/19490976.2022.2164448>
- Wickham, H., 2016. *ggplot2: Elegant Graphics for Data Analysis*, 2nd ed. 2016. ed, Use R! Springer International Publishing : Imprint: Springer, Cham. <https://doi.org/10.1007/978-3-319-24277-4>
- Winston, J.A., Theriot, C.M., 2016. Impact of microbial derived secondary bile acids on colonization resistance against *Clostridium difficile* in the gastrointestinal tract. *Anaerobe* 41, 44–50. <https://doi.org/10.1016/j.anaerobe.2016.05.003>
- Wood, D.E., Salzberg, S.L., 2014. Kraken: ultrafast metagenomic sequence classification using exact alignments. *Genome Biol.* 15, R46. <https://doi.org/10.1186/gb-2014-15-3-r46>
- Wu, H.-J., Wu, E., 2012. The role of gut microbiota in immune homeostasis and autoimmunity. *Gut Microbes* 3, 4–14. <https://doi.org/10.4161/gmic.19320>

Wu, M., Li, P., Li, J., An, Y., Wang, M., Zhong, G., 2020. The Differences between Luminal Microbiota and Mucosal Microbiota in Mice. *J. Microbiol. Biotechnol.* 30, 287–295.
<https://doi.org/10.4014/jmb.1908.08037>

Zhan, Z., Tang, H., Zhang, Y., Huang, X., Xu, M., 2022. Potential of gut-derived short-chain fatty acids to control enteric pathogens. *Front. Microbiol.* 13, 976406.
<https://doi.org/10.3389/fmicb.2022.976406>

Zoetendal, E.G., Von Wright, A., Vilpponen-Salmela, T., Ben-Amor, K., Akkermans, A.D.L., De Vos, W.M., 2002. Mucosa-Associated Bacteria in the Human Gastrointestinal Tract Are Uniformly Distributed along the Colon and Differ from the Community Recovered from Feces. *Appl. Environ. Microbiol.* 68, 3401–3407.
<https://doi.org/10.1128/AEM.68.7.3401-3407.2002>

Chapter 3: The role of *B4galnt2* in shaping the outcome of antibiotic treatment

Introduction

The gastrointestinal tract carries a highly diverse and complex community of microorganisms known as intestinal microbiota. This community plays an important role in nutrient metabolism, immune system development, and protection against invading pathogens (Ducarmon et al., 2019; Round and Mazmanian, 2009; Rowland et al., 2018; Wu and Wu, 2012). The composition of intestinal microbiota can rapidly change after exposure to antibiotics, affecting host health and homeostasis (Strati et al., 2021). Gut microbiota alterations pose a significant threat to increased susceptibility to intestinal infections (Bailey, 2012; Lange et al., 2016). These infections may arise from newly colonizing pathogens or from sudden overgrowth of opportunistic microbes already present in healthy microbiota (Kesavelu and Jog, 2023). Changes in microbiota composition following antibiotic treatment are associated with the development of antibiotic-associated diarrhea (AAD) and pathogen proliferation, including *Clostridium difficile*, *Klebsiella oxytoca*, and *Staphylococcus aureus* (Ackermann et al., 2005; Gravet et al., 1999; Kesavelu and Jog, 2023; Philbrick and Ernst, 2007). After the antibiotic treatment ends, the microbiota has the ability to return to a composition similar to its pre-antibiotic state. The success of recovery is influenced by various factors, such as the type and duration of the antibiotic treatment, diet, age, and other factors (Antonopoulos et al., 2009; FitzGerald et al., 2022; Laubitz et al., 2021; Palleja et al., 2018).

Mouse infection models have shown that the gut microbiota plays an important role in protecting against enteric pathogens. Mice with intact microbial communities exhibit a partial resistance to *Salmonella* infections, highlighting the protective function of conventional gut microbiota (Barthel et al., 2003). Changes in dietary composition, such as a decrease in fiber content and an increase in fat intake, have been linked to an elevated gut colonization by *Salmonella* Typhimurium or *Escherichia coli*. This colonization has been associated with changes in the composition of the gut microbiota (Fuchs, 2023; Wotzka et al., 2019). Furthermore, it has been observed that germ-free mice are fully susceptible to *Salmonella* Typhimurium infection (Fuchs, 2023; Stecher et al., 2005). Mice subjected to antibiotic treatment, including streptomycin, ampicillin, kanamycin, or vancomycin, have been shown to display increased susceptibility to *Salmonella* infection (Bakkeren et al., 2022; Barthel et al., 2003; Ferreira et al., 2011;

Fuchs, 2023; Sekirov et al., 2008; Woo et al., 2008). Antibiotic pretreatment induces changes in both taxonomic composition and functional profiles of gut microbiota (Theriot et al., 2014). Streptomycin is a commonly used antibiotic that disrupts host microbiota in animal models. It reduces colonization resistance and allows successful infection in the *Salmonella enterica* serovar Typhimurium colitis model (Barthel et al., 2003; Fuchs, 2023; Rausch et al., 2015). Administration of a single oral dose of 20 mg of streptomycin one day prior to infection facilitates successful colonization by *Salmonella* Typhimurium (Barthel et al., 2003; Fuchs, 2023; Rausch et al., 2015; Walker et al., 2023). These findings highlight the complex relationship between host microbiota, antibiotic-induced dysbiosis, and susceptibility to enteric pathogens.

Streptomycin (STR) is an aminoglycoside antibiotic that was first isolated from the gram-positive bacterium *Streptomyces griseus* by Selman Waksman and colleagues in the 1940s (Waksman et al., 1946). It is commonly used in clinical settings due to its effectiveness against both gram-positive and gram-negative pathogens. The use of aminoglycoside antibiotics dates back to the 1940s when it was first applied as a treatment for *Mycobacterium tuberculosis*. Since then, it has been used to combat a wide range of microbial agents, including *Yersinia pestis*, *Francisella tularensis*, *Brucella*, and others (Maurin and Raoult, 2001). Aminoglycoside antibiotics function by disrupting ribosomal protein synthesis. Specifically, streptomycin binds to the 30S ribosomal subunit of bacteria, inhibiting the process of protein synthesis and thereby hindering the production of essential bacterial proteins.

In order to investigate the impact of the host blood group-related gene *B4galnt2* on the success of *Salmonella* infection, Rausch et al., used streptomycin to reduce colonization resistance in the *Salmonella* Typhimurium model (Rausch et al., 2015). The tissue-specific expression of *B4galnt2* (Beta-1,4-N-Acetyl-Galactosaminyltransferase 2) is an important factor in shaping the glycosylation pattern of the mammalian gastrointestinal tract (Mohlke et al., 1999; Vallier, 2017). The gene's differential expression in the intestine is known to affect the composition of the gut microbiota (Staubach et al., 2012; Vallier, 2017), and the interaction between *B4galnt2*-associated microbial communities and streptomycin treatment influences the outcome of *Salmonella* infection, where the loss of *B4galnt2* gut expression reduces susceptibility to the infection (Rausch et al., 2015). The mechanism by which *B4galnt2* genotype leads to

this microbiota-dependent phenotype is however unclear. Thus, the aim of this study is to investigate the impact of glycosyltransferase *B4galnt2* expression on the composition and function of the commensal microbiota in greater, multi-omic detail (amplicon, shotgun metagenomic and metatranscriptomic sequencing), and in conjunction with its response and recovery after antibiotic treatment using a greater diversity of antibiotics.

Accordingly, in addition to streptomycin, we included kanamycin and vancomycin to test the generality of the observations of Rausch et al. (Rausch et al., 2015). Kanamycin A (KAN) is an aminoglycoside antibiotic that was first isolated in the 1950s from *Streptomyces kanamyceticus* (Umezawa et al., 1957), and similar to other aminoglycoside antibiotics, it works by binding to the bacterial 30S ribosomal subunit, causing misreading of t-RNA and halting protein synthesis. In the *Salmonella*-induced colitis model, kanamycin was used to disrupt colonization resistance (Woo et al., 2008). Vancomycin (VAN), in contrast, is a glycopeptide antibiotic obtained from the bacterium *Streptomyces orientalis* (Griffith, 1984). It targets cell wall biosynthesis by forming hydrogen bonds with the D-alanyl-D-alanine (D-Ala-D-Ala) peptide motif of the peptidoglycan precursor, preventing the incorporation of N-acetylmuramic acid (NAM) and N-acetylglucosamine (NAG) peptide subunits into the peptidoglycan matrix (Reynolds, 1989). Furthermore, vancomycin is known to modify the permeability of bacterial cell membranes and RNA synthesis (Wilhelm, 1991). Vancomycin has been utilized to break colonization resistance and facilitate *Salmonella enterica* serovar Typhimurium infection (Sekirov et al., 2008).

Materials and methods

Animals and housing

Experiments were conducted at the animal facility of the Max Planck Institute for Evolutionary Biology in Plön, Germany. Mice were maintained, and experiments were performed in accordance with FELASA guidelines and German animal welfare law (Tierschutzgesetz § 11; permits from Veterinäramt Kreis Plön: PLÖ-0004697 and Ministerium für Landwirtschaft, ländliche Räume, Europa und Verbraucherschutz: 96-8/17). The C57BL/6J *B4galnt2^{+/−}* and *B4galnt2^{−/−}* mice were raised and housed together as littermates under specific pathogen-free conditions. The mice were kept in open cages and fed with Altromin 1324 standard diet. The cages were changed every two weeks, and the light cycle in the mouse room was 12 hours bright/12 hours dark phase.

Experimental design and antibiotic treatment

The mice were grouped into cages according to their *B4galnt2* genotype and were acclimatized for two weeks prior to treatment. Mice were divided into 8 groups, with control groups for each genotype. Each group consisted of seven mice.

Three types of antibiotics, streptomycin (20 mg) (Barthel et al., 2003; Rausch et al., 2015), kanamycin (10 mg) (Woo et al., 2008), and vancomycin (40 mg) (Ferreira et al., 2011; Sekirov et al., 2008), were administered in a high dose by oral gavage, diluted in 100µl of water. In addition to the treatment groups, a control group of mice was also set up (100 µL of water). Fecal samples were collected before and after antibiotic treatment on the following days: -4, 0, 1, 2, 3, 4, 10, and 15 (Figure 1). To avoid the influence of circadian rhythms on the host and microbiota, fecal samples were collected at the same time at each time point.

Simultaneous DNA and RNA extraction, 16s rRNA gene (DNA) and transcript (RNA) amplification, and amplicon sequencing

Simultaneous extraction of DNA and RNA from fecal pellets was performed using the Qiagen AllPrep DNA/RNA Kit (Qiagen, Hilden, Germany). The samples were

homogenized in 600 µL of RLT buffer (Qiagen) with a Lysing Matrix E tube (MPBio) and Precellys (3 x 15 s). DNase I Solution (Stemcell technologies) was used to treat the RNA extracts and remove any DNA contamination. The cDNA was synthesized from RNA using the High-Capacity cDNA Reverse Transcription kit (Thermo Fisher Scientific), following the manufacturer's instructions. The hypervariable region V1-V2 of the 16S rRNA gene was amplified using universal bacterial primers 27F (5'-AGAGTTGATCCTGGCTCAG-3') and 338R (5'-TGCTGCCTCCGTAGGAGT-3') (Lee et al., 2023). The PCR amplification was carried out using the following thermocycling protocol: an initial denaturation at 98°C for 3 minutes, followed by 30 cycles consisting of denaturation at 98°C for 9 seconds, annealing at 55°C for 1 minute, and extension at 72°C for 1 minute, with a final extension step at 72°C for 10 minutes. The resulting PCR products were quantified using GelDoc XR+ (BioRad) and pooled in equimolar proportions. The ZymoBIOMICS Microbial Community DNA Standard containing 8 bacterial and 2 fungal species was amplified and used as a sequencing quality control, and the libraries were sequenced on the Illumina MiSeq platform using the v2 kit (2 x 250 bp).

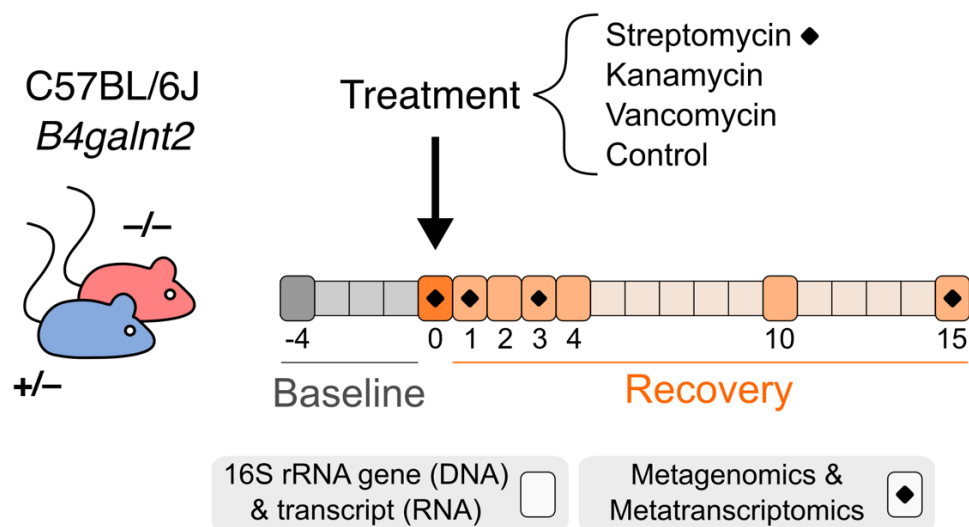


Figure 1. Outline of animal experiment

16S rRNA gene (DNA) and transcript (RNA) processing and analysis

Raw reads were demultiplexed using bcl2fastq allowing no mismatches in the barcodes. Subsequently, demultiplexed paired-end FASTQ files were subjected to quality filtration and taxonomic assignment using Qiime2 version 2023.05 (Bolyen et al., 2019).

Briefly, denoising, chimera removal, and identification of representative sequences were performed using DADA2 (Callahan et al., 2016). Taxonomic annotation of representative sequences for Amplicon Sequence Variants (ASVs) was accomplished utilizing the SILVA database (v 138) and a pre-trained Naive Bayes classifier (Bokulich et al., 2018; Quast et al., 2012). The ASV sequences were used to construct a tree for phylogenetic diversity analyses. Prior to tree construction, a multiple sequence alignment was generated using MAFFT (Katoh, 2002), after which all highly variable and uninformative alignment columns were masked. The unrooted phylogenetic tree was constructed using FastTree (Price et al., 2009) from the masked alignments. The tree was subsequently rooted at the midpoint of the longest tip-to-tip distance in the unrooted tree.

The resulting ASV feature table, phylogenetic tree, and reference sequences from Qiime2 were imported into R along with the metadata table using the qiime2R and phyloseq packages (Bisanz, 2018; McMurdie and Holmes, 2013). The ASVs observed in only one sample were removed. Rarefaction curve analysis was used to estimate the completeness of microbial sampling, and a depth of 4500 sequences was selected.

Metagenomics and metatranscriptomics

Metagenomic sequencing libraries were constructed using the NexteraXT technology, as described by the manufacturer (Illumina). The libraries were sequenced using the Illumina NextSeq 550 System High-Output kit.

For selected RNA samples, ribodepletion was performed using the QIAseq FastSelect -5S/16S/23S Kit (Qiagen), and the Illumina TruSeq protocol was used to prepare the RNA-Seq library. The 56 RNA samples were run on the Illumina NovaSeq at 100bp, single end.

The preprocessing of metagenomic and metatranscriptomic sequencing data was carried out using KneadData (v0.7.10). KneadData includes FastQC (v0.12.1) for quality assessment, Trimmomatic (v0.39) (Bolger et al., 2014) for quality filtering, and Bowtie2 (v1.2.2) (Langmead and Salzberg, 2012) for host sequence decontamination.

Metagenomics taxonomic profiles were generated using Kraken v2.1.2 (confidence level 0.05) and Bracken v2.2 with the PlusPFP database (PlusPFP_2022_09_08), which includes bacterial, archaeal, viral, plasmid, fungal,

protozoan, and plant indices (Lu et al., 2017; Wood and Salzberg, 2014). The resulting microbiota abundances and associated metadata tables were imported into R using the biomformat v1.26.0 and phyloseq v1.42.0 packages (McMurdie and Paulson, 2017; McMurdie and Holmes, 2013). Samples with at least 500000 Kraken2/Bracken classified reads were kept for taxonomic analysis. The relative sequence abundances of taxa were filtered, requiring that each taxon have an average abundance of at least 0.0025% per sample.

The HMP Unified Metabolic Analysis Network 3 (HUMAnN3 v3.6) pipeline was used to generate functional profiles for both metagenome and metatranscriptome data sets (Beghini et al., 2021).

Antibiotic resistance genes abundance profiling

Short reads were queried for antibiotic resistance genes using DeepARG (v1.0.2) with default settings (identity cutoff for sequence alignment – 50, E-value cutoff – 1e-10, alignment read overlap – 0.8) (Arango-Argoty et al., 2018).

Microbial dynamics analysis

For alpha diversity analysis, ASV richness, Shannon diversity index, and Faith's phylogenetic diversity (Faith, 1992) were calculated for each *B4galnt2* genotype and time point, and Mann–Whitney–Wilcoxon test was used to compare groups.

To explore the community structure and to visualize the clustering of samples based on their compositional similarities, Principal Coordinate Analysis (PCoA) was performed using the phyoseq v1.42.0 package (McMurdie and Holmes, 2013). To compare microbiota communities across genotypes and time points, while considering potential sex effects, Adonis permutational multivariate analysis of variance (PERMANOVA) was used on Bray-Curtis, Jaccard, and both weighted and unweighted Unifrac distances with 9999 permutations, implemented in the vegan package v2.6-4 in R (Dixon, 2003).

Microbiome Multivariable Associations with Linear Models - MaAsLin2 (v1.12.0) was used to quantify differences in functional and ARG profiles by *B4galnt2* genotype and to adjust for the covariate sex (Mallick et al., 2021).

R software (v4.2.2) and the rstatix package (v0.7.2) were used for statistical analysis. Graphs were generated using the ggplot2 package (v3.4.4) (Wickham, 2016). Spearman correlation was utilized to examine associations between continuous variables. The Mann–Whitney–Wilcoxon test (Mann and Whitney, 1947; Wilcoxon, 1945) was employed to assess relationships between continuous and categorical variables. Correction for multiple testing was performed using the false discovery rate (FDR) method for each treatment, group, or time point, when appropriate (Benjamini and Hochberg, 1995).

Results

To evaluate the longitudinal dynamics of recovery from antibiotic treatment according to *B4galnt2* genotype, n=28 *B4galnt2*^{-/-} and n=28 *B4galnt2*^{+/+} were randomly assigned to one of four treatment groups: control (Ctrl), streptomycin (STR), kanamycin (KAN), and vancomycin (VAN) groups. The antibiotics were administered in a single oral gavage with streptomycin (20 mg) (Barthel et al., 2003; Rausch et al., 2015), kanamycin (10 mg) (Woo et al., 2008), and vancomycin (40 mg) (Ferreira et al., 2011; Sekirov et al., 2008) per mouse. Fecal samples were collected before, during and after the antibiotic treatment (Figure 1). Total DNA and RNA were then extracted from these samples for further analysis.

16S rRNA gene (DNA) and transcript (RNA) amplicon analysis

The relative microbial abundances were quantified using the 16S rRNA gene (DNA) amplicon, while the activity of microbial communities was quantified using the 16S rRNA transcript (RNA) amplicon (Belheouane et al., 2020).

To ensure standardization between 16S rRNA libraries, ZymoBIOMICS Microbial Community DNA Standard was used in each sequencing library (Supplementary Figure 1). Rarefaction analysis was performed to evaluate the sufficiency of the sequencing depth, and a depth of 4500 reads was selected (Supplementary Figure 2).

16S rRNA gene (DNA) sequencing of the fecal microbiota revealed that prior to antibiotic treatment, the samples consisted primarily of the two dominant phyla, Bacteroidetes (STR -4: $41.89 \pm 16.9\%$; STR 0: $37.34 \pm 13.68\%$) and Firmicutes (STR -4: $55.71 \pm 14.78\%$; STR 0: $61.75 \pm 13.18\%$) (Figure 2). The microbiota's response to streptomycin treatment exhibited similar trends for both *B4galnt2* groups. After streptomycin administration, there was a significant decrease in the Firmicutes phylum by day 1 ($18.55 \pm 8.95\%$), accompanied by a relative increase in Bacteroidetes ($80.54 \pm 9.36\%$). Recovery began in both genotypes by day 2, eventually returning to pre-antibiotic levels by day 10.

Similar dynamics were observed in kanamycin-treated mice, with slightly faster recovery (Figure 2). In contrast, vancomycin treatment had the opposite effect on gut

microbiota composition. One day after antibiotic treatment, the relative abundance of Bacteroidetes was minimal ($0.39 \pm 0.98\%$), while Firmicutes accounted for the majority of the microbial population ($99.36 \pm 0.93\%$). However, by the day 10, the relative abundance of Bacteroidetes had returned to pre-antibiotic levels ($41.16 \pm 13.67\%$).

Fecal microbiota activity, as measured by 16S rRNA transcript (RNA) amplicon sequencing, showed comparable profiles to the 16S rRNA gene (DNA) amplicon sequencing, with higher relative proportions of Firmicutes (Supplementary Figure 3).

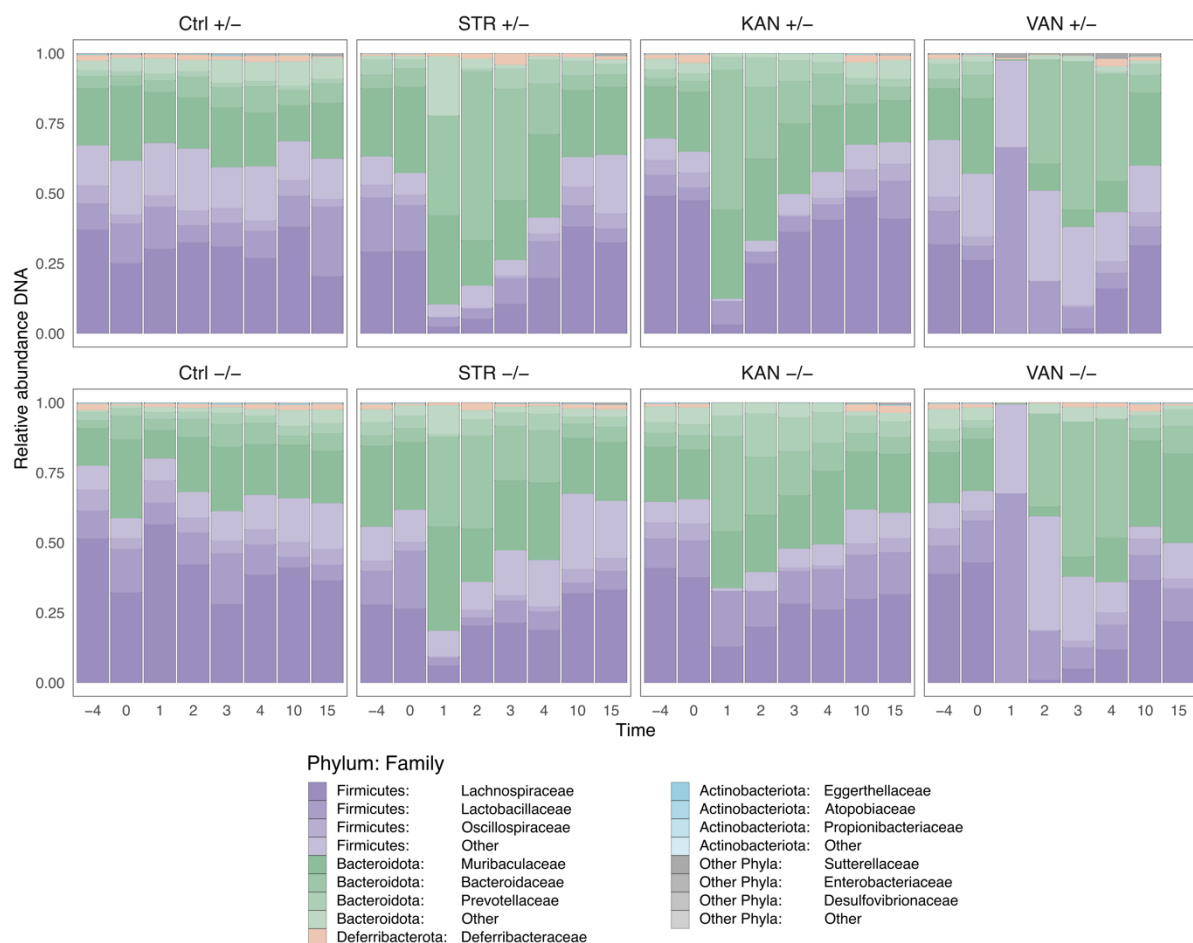


Figure 2: Fecal microbiome composition dynamics based on 16S rRNA gene (DNA) sequencing: Relative sequence abundance in *B4galnt2*-associated microbial communities at the phylum and family levels.

The alpha diversity of 16S rRNA samples was measured by the number of observed ASVs and the phylogenetic diversity (PD) index. Both *B4galnt2* groups showed a decrease in these indices after streptomycin treatment (Figure 3). Analysis of ASV abundances per mouse within each experimental group showed no statistically

significant differences in abundance between the *B4galnt2* groups at any time point. Additionally, no significant differences were observed between the *B4galnt2* groups for the phylogenetic diversity index. A comparison was made between the treated groups and their respective control or baseline cohorts. The results showed that *B4galnt2*^{-/-} mice had a faster recovery trajectory compared to *B4galnt2*^{+/−} mice. This phenomenon was notably evident when assessing both 16S rRNA gene (DNA) and transcript (RNA) levels. However, this differential recovery pattern was not consistently observed in the other antibiotic treatment groups (Supplementary Figure 4, Supplementary Figure 5).

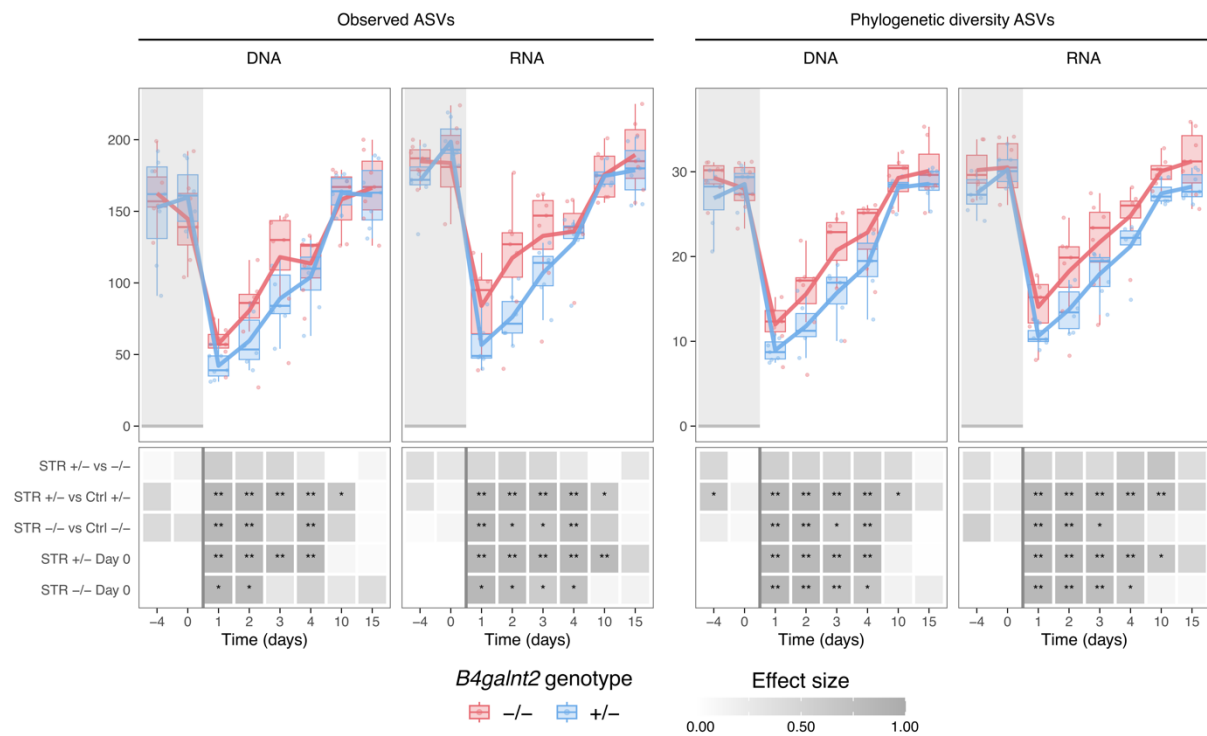


Figure 3: ASV richness and phylogenetic diversity (PD) in the streptomycin treated mice at the 16S rRNA gene (DNA) and transcript (RNA) levels. Stars denote significance: * $p_{adj} < 0.05$, ** $p_{adj} < 0.01$, *** $p_{adj} < 0.001$

These dynamics were also observed on the 16S rRNA gene (DNA) and transcript (RNA) levels in both PCoA plots based on Bray-Curtis and weighted Unifrac distance metrics (Figure 4, Supplementary Figures 6, 7, 8). Both the *B4galnt2*^{+/−} and *B4galnt2*^{-/-} groups clustered together at baseline. After the administration of streptomycin on day one, both groups experienced a significant shift compared to baseline. As observed in the alpha diversity metrics, the *B4galnt2*^{+/−} group recovered slowly until day 10 when it reached levels comparable to the baseline. In contrast, the *B4galnt2*^{-/-} mice displayed faster recovery rates, starting on day 2.

Kanamycin treatment resulted in a microbiota response comparable to that of streptomycin treatment, but the recovery rates did not differ according to *B4galnt2* genotype (Supplementary Figures 9, 10, 11, 12). Treatment with vancomycin resulted in more significant changes in microbiota communities after treatment when compared to its respective baseline, similar to kanamycin, without differences in recovery rates according to *B4galnt2* genotype (Supplementary Figures 13, 14, 15, 16).

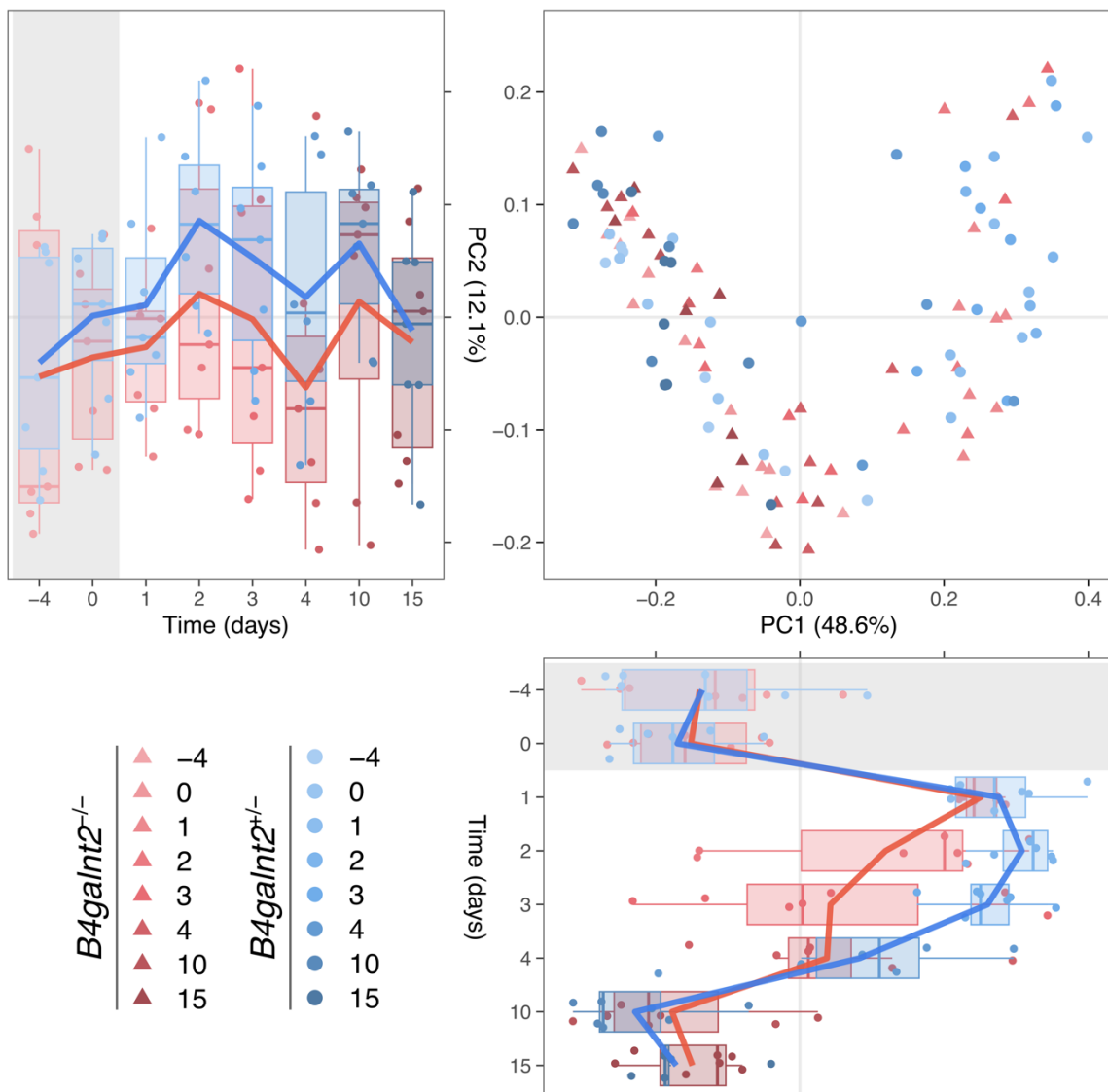


Figure 4: Principal Coordinates Analysis (PCoA) plot of samples before, during and after the streptomycin treatment based on weighted UniFrac (W-UniFrac) distances at the 16S rRNA transcript (RNA) level. The distribution of samples by *B4galnt2* groups and time is shown along the first and second axes of the PCoA plot.

The statistical significance of the observed patterns for streptomycin treatment was assessed using permutational multivariate analysis of variance (PERMANOVA) with

Bray-Curtis and weighted UniFrac distances, taking into account potential sex effects. Direct comparison between the two genotypes revealed statistically significant differences only at the 16S rRNA gene (DNA) level at day 10 post-treatment (Bray–Curtis: PERMANOVA, $R^2 = 0.1288$; $p_{adj} = 0.0360$; W-Unifrac: PERMANOVA, $R^2 = 0.1540$; $p_{adj} = 0.0208$). When comparing the *B4galnt2* groups with their respective controls, both groups exhibited significant changes after treatment. Notably, the *B4galnt2*^{-/-} cohort demonstrated a significantly faster recovery rate at both the 16S rRNA gene (DNA) and transcript (RNA) levels (Figure 5, Supplementary Table 1). A similar trend was observed for both Bray-Curtis and weighted UniFrac distances at the 16S rRNA transcript (RNA) level when comparing the *B4galnt2* mice to their corresponding baseline cohorts.

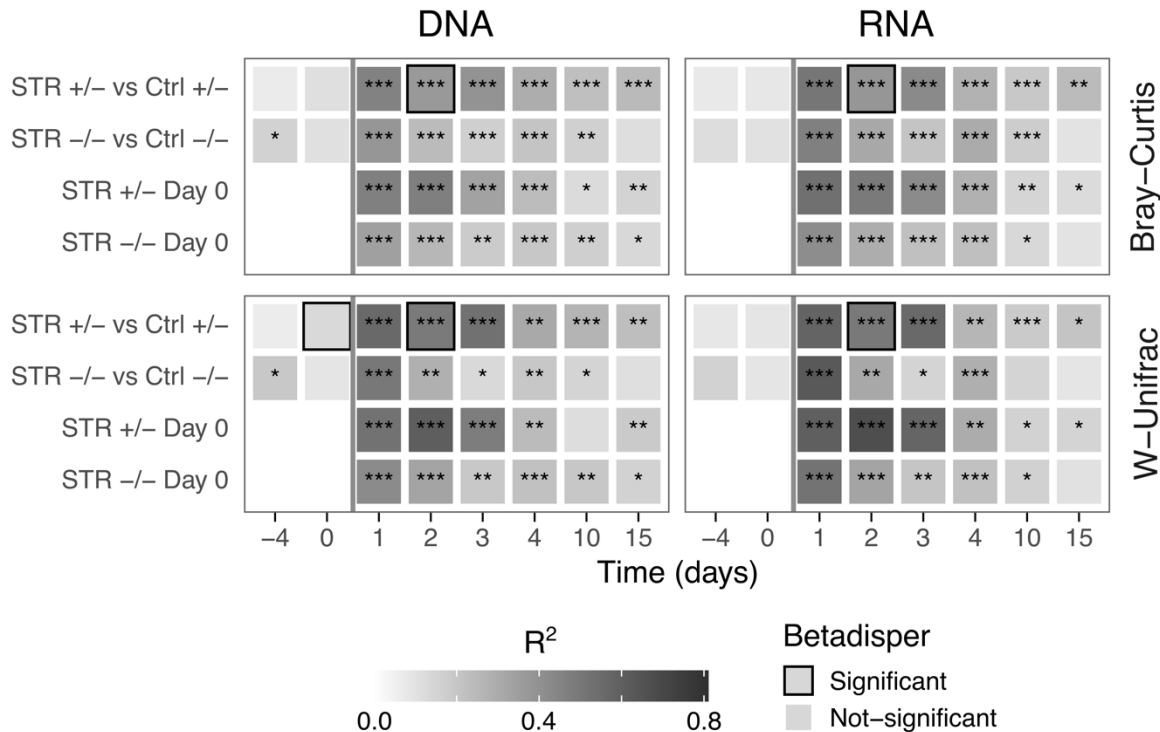


Figure 5: Significance and effect size estimates for PERMANOVA and Betadisper analysis for differences in the streptomycin treated mice at 16S rRNA gene (DNA) and transcript (RNA) levels between *B4galnt2* genotypes. Stars denote significance: * $p_{adj} < 0.05$, ** $p_{adj} < 0.01$, *** $p_{adj} < 0.001$.

Mice treated with kanamycin showed a similar recovery trend to the streptomycin group when compared to controls, with faster recovery in *B4galnt2*^{-/-} mice. However, unlike the streptomycin group, kanamycin-treated mice did not exhibit differential recovery between genotypes when compared to their respective baseline at both 16S

rRNA gene (DNA) and transcript (RNA) levels (Supplementary Figure 17, Supplementary Table 2).

No significant differences in recovery rates were observed between the *B4galnt2* groups in vancomycin-treated mice at both the 16S rRNA gene (DNA) and transcript (RNA) levels, when compared to their respective controls or to the baseline (Supplementary Figure 18, Supplementary Table 3).

Metagenomics – Taxonomic profiling

Samples before (day 0) and immediately after (day 1) streptomycin treatment, as well as early (day 3) and late (day 15) recovery time points, were selected for further in-depth analysis using metagenomics and metatranscriptomics approaches.

At the metagenomics level, the phylum-level composition was similar to that of the 16S rRNA gene (DNA) profiles before treatment. The Bacteroidetes ($38.71 \pm 28.34\%$) and Firmicutes ($57.79 \pm 26.39\%$) phyla accounted for most of the sequence relative abundances (Figure 6). After the antibiotic treatment, there was a decrease in the relative abundance of Firmicutes ($4.72 \pm 4.39\%$), which showed relative recovery on day 3 ($25.16 \pm 19.94\%$). By day 15, the relative abundances of Bacteroidetes ($41.58 \pm 24.55\%$) and Firmicutes ($50.73 \pm 20.19\%$) had returned to pre-antibiotic levels for both *B4galnt2* treated groups.

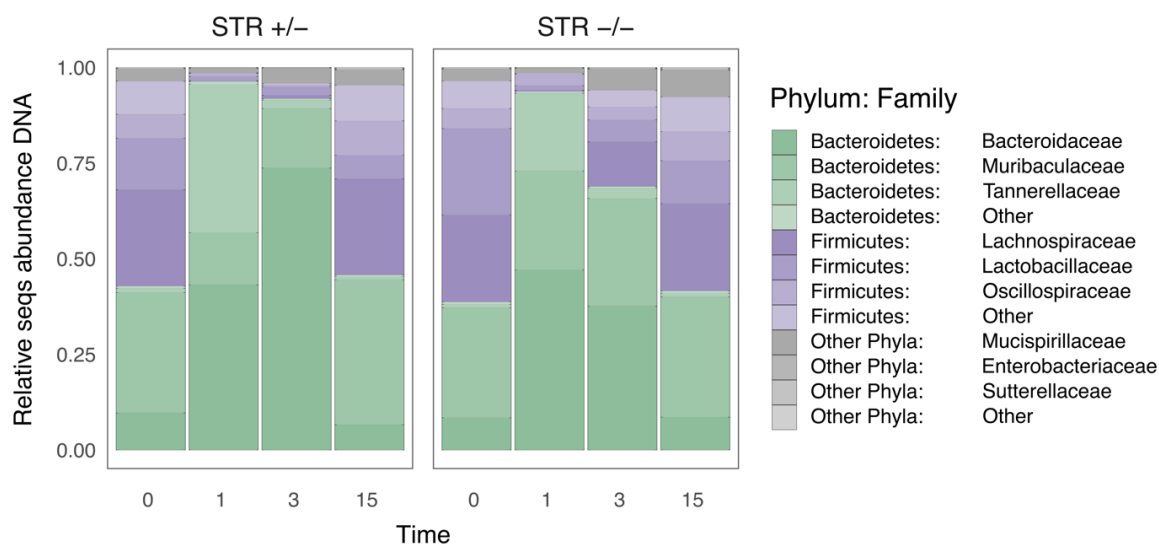


Figure 6: Fecal microbiome composition dynamics based on metagenomics (MGX) sequencing: Relative sequence abundance in *B4galnt2*-associated microbial communities at the phylum and family levels.

Alpha diversity analysis was performed on the metagenomics samples to assess the diversity of *B4galnt2* groups before, during, and after the streptomycin treatment using richness, Shannon, and Simpson diversity indices. The administration of streptomycin on day 0 resulted in a significant and immediate reduction in microbial species richness and diversity by day 1. On the third day, *B4galnt2*^{-/-} mice showed a recovery of microbiota diversity to pre-antibiotic levels, while *B4galnt2*^{+/−} mice achieved full recovery on the fifteenth day following the treatment (Figure 7).

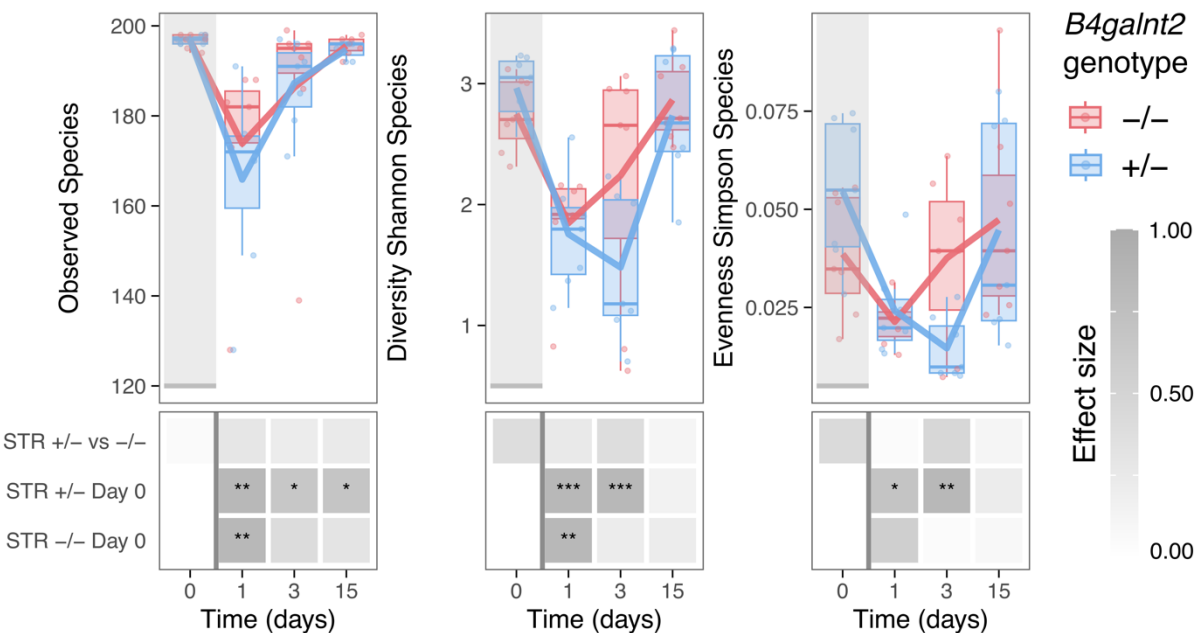


Figure 7: Species richness, Shannon and Simpson diversity indices in the streptomycin treated mice at the metagenomics (MGX) level. Stars denote significance: * $p_{adj} < 0.05$, ** $p_{adj} < 0.01$, *** $p_{adj} < 0.001$.

Prior to streptomycin treatment, the metagenomic samples of both *B4galnt2* groups clustered together (Figure 8, Table 1). One day after the antibiotic treatment, the microbial communities underwent a significant shift. By the third day following antibiotic treatment, the individual communities began to recover to their initial state. The *B4galnt2*^{-/-} group exhibited a faster recovery when compared to their baseline level (STR *+/-* vs Day 0: PERMANOVA, $R^2 = 0.6204$; $p_{adj} = 0.0005$; STR *-/-* vs Day 0: PERMANOVA, $R^2 = 0.1124$; $p_{adj} = 0.1124$). By day 15, both *B4galnt2*-associated microbiota groups had clustered back with their respective baseline levels.

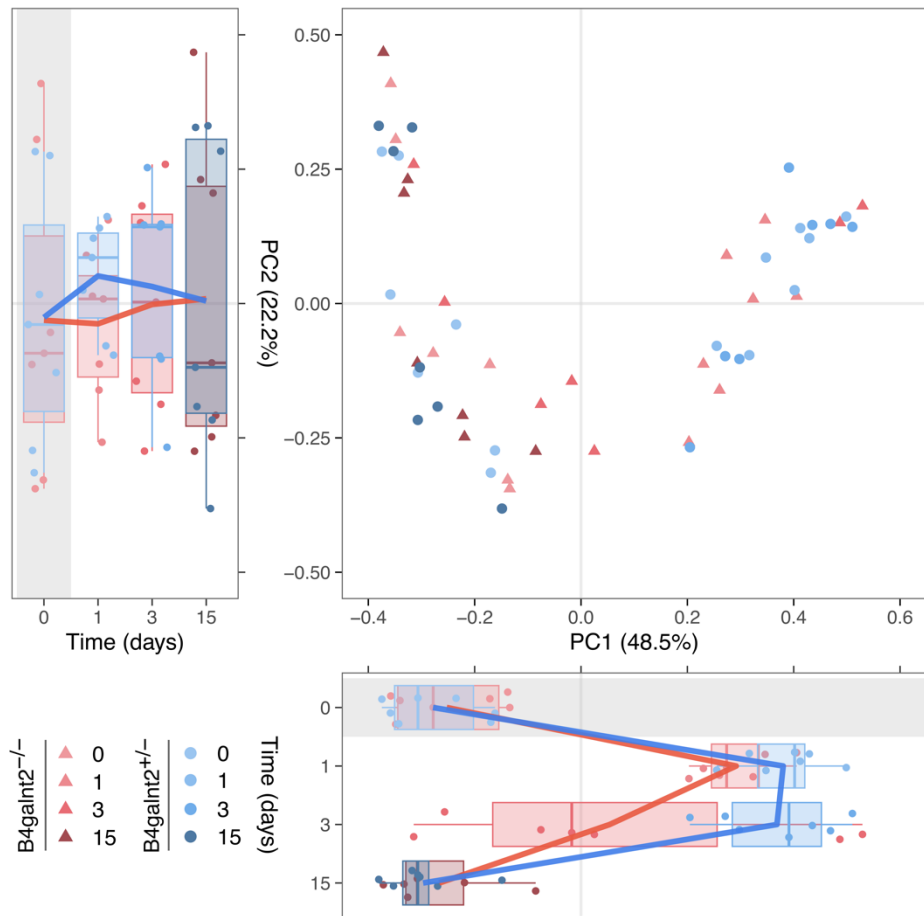


Figure 8: Principal Coordinates Analysis (PCoA) plot of samples before, during and after the streptomycin treatment (STR) based on Bray-Curtis distances at the metagenomics (MGX) level. The distribution of samples by *B4galnt2* groups and time is shown along the first and second axes of the PCoA plot.

Table 1: PERMANOVA and Betadisper results of species relative abundances based on Bray–Curtis distances for the streptomycin treated mice at metagenomics (MGX) level:

Time	STR +/- vs Day 0			STR -/- vs Day 0		
	p _{adj}	R ²	Dispersion	p _{adj}	R ²	Dispersion
1	0.0005	0.6536	0.3451	0.0006	0.3979	0.5607
3	0.0005	0.6204	0.5320	0.1124	0.1642	0.5550
15	0.4200	0.0523	0.6348	0.8230	0.0275	0.8058

To identify specific taxonomic signatures associated with the *B4galnt2* genotype and streptomycin treatment, bacterial communities of both genotypes at metagenome level were compared using Maaslin2 (Mallick et al., 2021). A total of 141 species and 85 genera were found to be associated with differential *B4galnt2* gut expression throughout the experiment (Figure 9, Supplementary Figure 19).



Figure 9: Differently abundant species between *B4galnt2* groups at different time points. Stars represent a $q_{val} < 0.25$.

The species that were differentially abundant were mostly specific to the early recovery stage and were enriched in the *B4galnt2^{-/-}* mice. Most of these species belong to the Firmicutes phylum, including the Lachnospiraceae and Oscillospiraceae families. Notable bacteria with potential probiotic functions included members of the *Blautia* genus (Liu et al., 2021; Osbelt et al., 2021), *Enterococcus faecalis* (Al Atya et al., 2015; Osbelt et al., 2021), *Enterocloster clostridioformis* (Beresford-Jones et al., 2023; Osbelt et al., 2021), *Coprococcus eutactus* (Yang et al., 2023), *Roseburia intestinalis* (Zhang et al., 2022), *Roseburia hominis* (Patterson et al., 2017), *Bifidobacterium longum* (Zhang et al., 2019), *Lactobacillus intestinalis* (Wang et al., 2023), *Akkermansia muciniphila* (Cheng and Xie, 2021), among others. Additionally, twelve species, all belonging to the *Bacteroides* genus, were found to be specific to early recovery in the *B4galnt2^{+/+}* group, on day 3 following streptomycin treatment.

Metagenomics and Metatranscriptomics – Functional profiling:

Functional profiling of shotgun metagenomics and metatranscriptomics sequences was performed using Humann3 (Beghini et al., 2021). The results of PERMANOVA based on Bray-Curtis distances of the KEGG Ortholog groups showed that *B4galnt2^{-/-}* mice recovered faster by day 3 after the streptomycin treatment on the metagenome level (Table 2). At the metatranscriptome level, *B4galnt2^{-/-}* mice recovered by day 3, while *B4galnt2^{+/+}* mice showed significant differences even after 15 days after the streptomycin treatment.

Table 2: PERMANOVA and Betadisper results of the KEGG Ortholog groups based on Bray–Curtis distances for the streptomycin treated mice at metagenomics (MGX) and metatranscriptomic (MTX) levels:

Time	STR +/- vs Day 0			STR -/- vs Day 0			MGX
	p _{adj}	R ²	Dispersion	p _{adj}	R ²	Dispersion	
1	0.0006	0.7151	0.0286	0.0018	0.6322	0.2144	MGX
3	0.0006	0.6197	0.0371	0.3512	0.1564	0.2417	
15	0.6652	0.0255	0.9060	0.7938	0.0207	0.9480	
1	0.0005	0.6169	0.0001	0.0027	0.4459	0.0815	MTX
3	0.0005	0.6364	0.1694	0.1947	0.1383	0.2043	
15	0.0011	0.4219	0.8399	0.2360	0.1077	0.1627	

Maaslin2 (Mallick et al., 2021) was used for differential abundance analysis, which revealed significant differences between *B4galnt2* mice in 400 out of 2774 KEGG ortholog groups in at least one of the time points. Among the significant KEGG ortholog groups, genes encoding flagellin and motility associated proteins were more enriched in a metatranscriptomic (MTX) *B4galnt2^{-/-}* samples following antibiotic treatment (Figure 10).

Antibiotic resistance genes in gut microbiota:

The differences in relative abundances of antibiotic resistance genes (ARGs) between *B4galnt2* groups before and after the streptomycin treatment were analyzed using Maaslin2 (Mallick et al., 2021). Before treatment, the relative abundance of total antibiotic resistance genes (ARGs) was on average $0.216 \pm 0.095\%$ in metagenomic samples and $0.028 \pm 0.01\%$ in metatranscriptomic samples. After treatment, the relative abundance of ARGs decreased in metagenomic samples ($0.119 \pm 0.141\%$), while no significant differences were observed in metatranscriptome samples ($0.022 \pm 0.005\%$). By the third day after streptomycin treatment, the abundance of antibiotic resistance genes in metagenomic samples had returned to pre-treatment levels (day 3: $0.200 \pm 0.144\%$; day 15: $0.208 \pm 0.180\%$). The relative abundance of ARG transcripts on day 3 however showed a significant increase ($0.041 \pm 0.019\%$) compared to previous time points, but returned to baseline by day 15 ($0.029 \pm 0.012\%$). Multidrug and mupirocin class resistance genes were enriched in the *B4galnt2^{+/−}* mice in metagenomic samples (MGX) before antibiotic treatment (Figure 11A, Supplementary Table 4). Following streptomycin treatment, an enrichment of genes associated with resistance to diaminopyrimidine, fosmidomycin, multidrug, nucleoside, peptide, polymyxin, rifamycin, and tetracycline classes of antibiotics was observed in *B4galnt2^{-/-}* mice. No differences were found between *B4galnt2* expression groups in relation to aminoglycoside class related resistance genes on a metagenomic level.

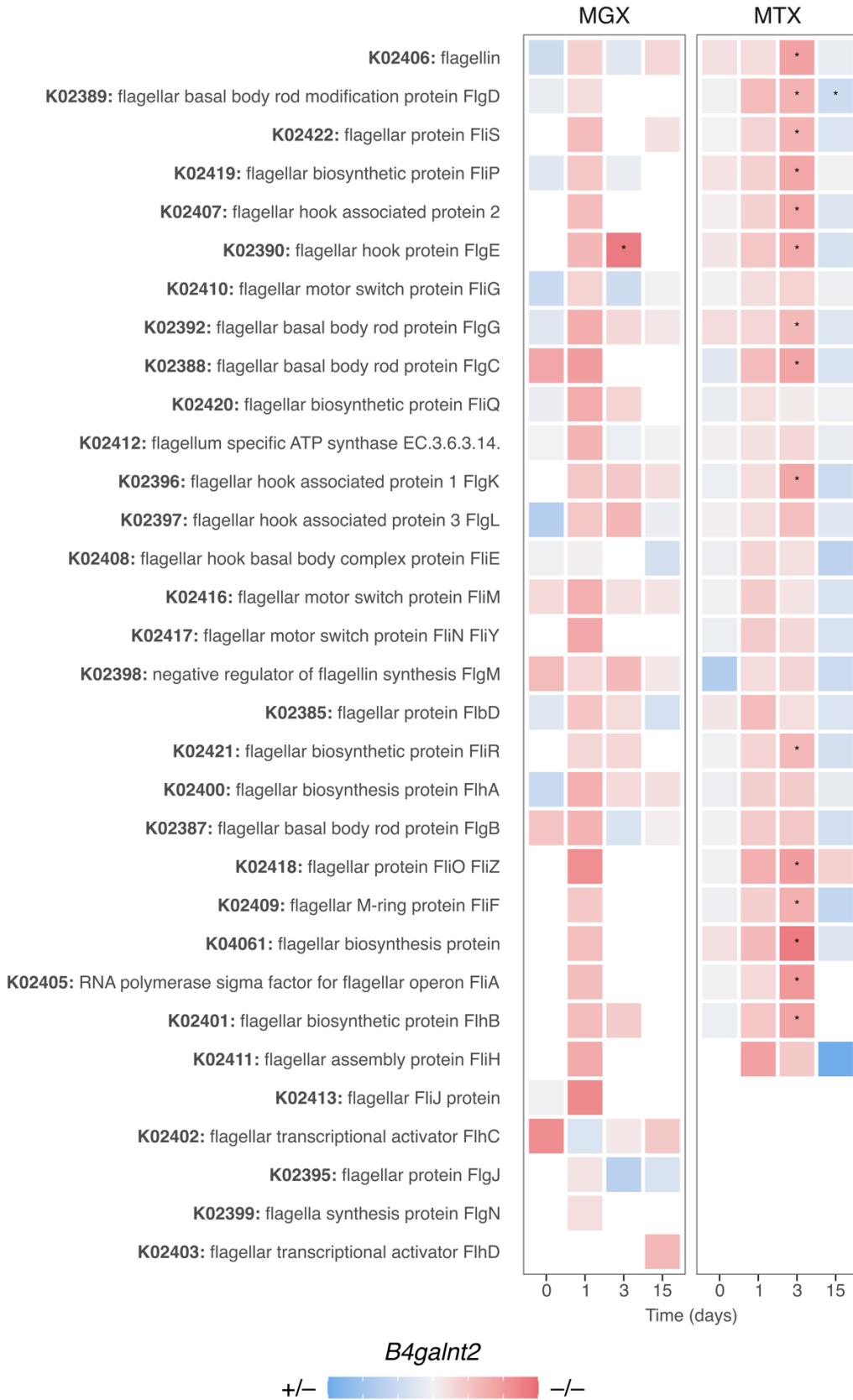


Figure 10: Differential KEGG ortholog groups involved in flagellin and motility functions between *B4galnt2*^{+/−} and *B4galnt2*^{−/−} mice in metagenomics (MGX) and metatranscriptomics (MTX) samples. Stars represent a $q_{val} < 0.25$.

Differences in aminoglycoside, glycopeptide, MLS, multidrug, mupirocin, and unclassified class related resistance genes were observed on the metatranscriptome level (MTX) during early recovery (days 1 and 3) after streptomycin treatment in the *B4galnt2*^{-/-} group. Fosmidomycin resistance was enriched in *B4galnt2*^{+/−} mice on day 3, and aminoglycoside, beta-lactam, multidrug, and unclassified class of ARGs were observed during the later recovery phase (day 15) after treatment (Figure 11A, Supplementary Table 5). Upon analyzing specific antibiotic resistance genes on the metatranscriptome level, it was found that aminoglycoside nucleotidyltransferase genes *aadA* and *aadE* were enriched in *B4galnt2*^{-/-} mice immediately after streptomycin treatment (day 1). Additionally, there was a significant difference in transcript levels of *aadA* during late recovery (day 15) with enrichment in *B4galnt2*^{+/−} mice (Figure 11B, Supplementary Table 6).

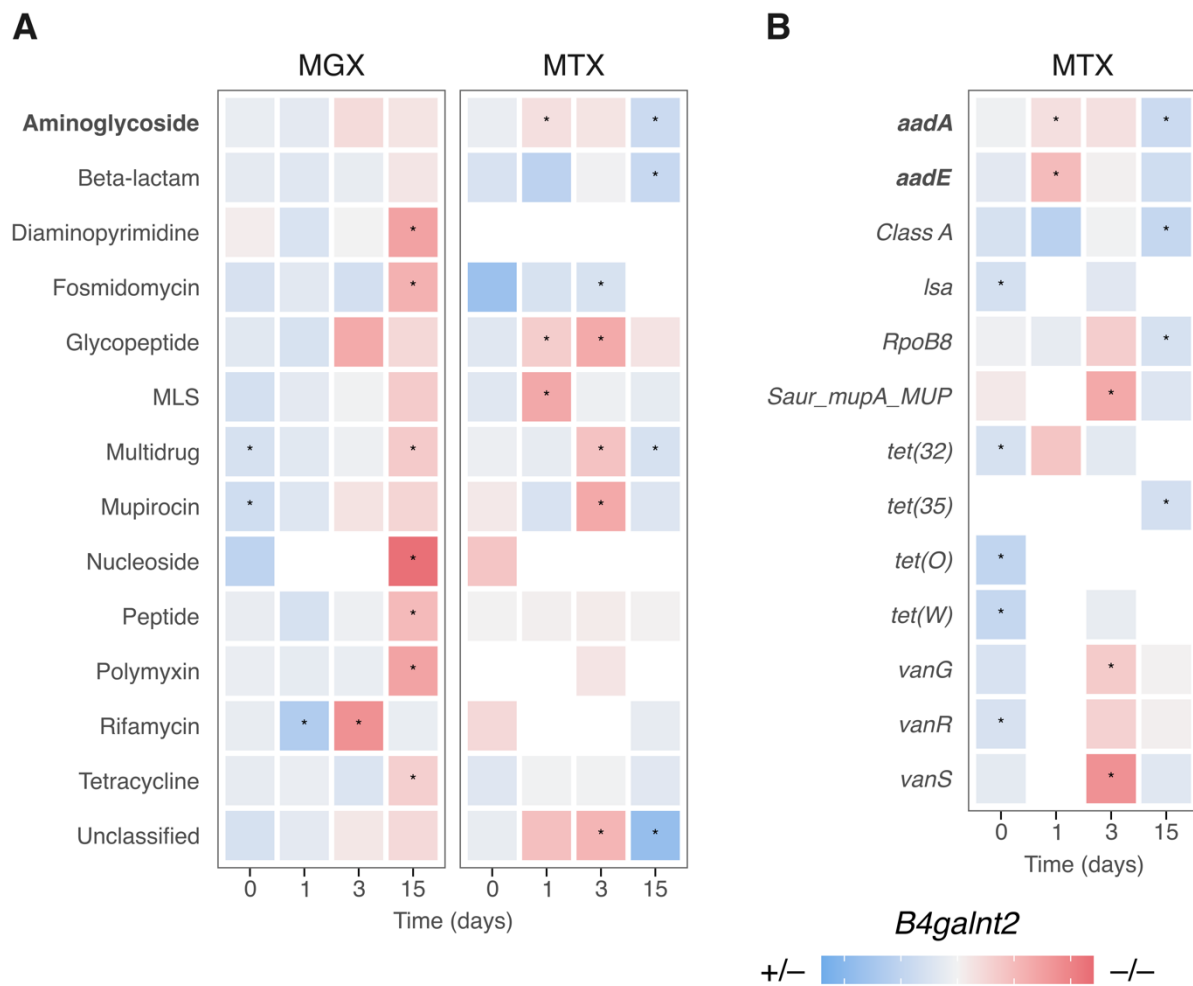


Figure 11: Differential abundance of antibiotic resistance gene classes on MGX and MTX levels (A), and differential abundance of antibiotic resistance genes on MTX level (B). Stars represent a $q_{val} < 0.25$.

Discussion

This study investigates the effect of intestinal *B4galnt2* expression on the response of gut microbiota to antibiotic treatment, specifically streptomycin. Previous studies have shown that antibiotic treatment significantly disrupts intestinal microbiota, with gradual recovery of microbial communities after treatment cessation (Ng et al., 2019; Palleja et al., 2018). Streptomycin has been used in various experimental models to investigate the impact of microbiota dysbiosis and its role in colonization resistance (Garner et al., 2009; Hentges et al., 1990; Miller and Bohnhoff, 1963; Stecher et al., 2005; Suar et al., 2006; Van Der Waaij et al., 1972). The administration of a high dose of this antibiotic leads to the microbiota dysbiosis, which in turn disrupts colonization resistance and facilitates the colonization of enteric pathogens (Barthel et al., 2003; Stecher et al., 2005). Conversely, the treatment of mice with a single low dose of streptomycin (1 mg) does not increase susceptibility to *Salmonella* infection (Bohnhoff et al., 1954).

Rausch et al. used streptomycin to disrupt commensal microbiota resistance, which enabled *Salmonella* Typhimurium infection in mice with varying *B4galnt2* expression phenotypes (Rausch et al., 2015). The investigation highlighted the crucial role of tissue-specific *B4galnt2* expression in modulating susceptibility to *Salmonella* Typhimurium infection. As stated in the study and further explored in Chapter 1, the observed effect is not solely dependent on tissue-specific *B4galnt2* expression. Instead, *B4galnt2* expression itself affects the composition of the commensal microbiota, which, in combination with streptomycin treatment, influences the outcome of *Salmonella* infection. Our study found that the absence of intestinal *B4galnt2* expression accelerated the recovery of microbial communities after the end of streptomycin treatment. However, this phenomenon was not observed with other antibiotics.

Similar to this study, previous research has shown that vancomycin significantly impacts the intestinal microbiota, resulting in an increase in the relative abundance of Firmicutes and a decrease in Bacteroidetes and Proteobacteria (Hung et al., 2019). However, despite the relative increase of Firmicutes, mice treated with vancomycin showed a decrease in the Clostridiales order and the families Lachnospiraceae, Prevotellaceae, and Rikenellaceae (Candon et al., 2015). No significant differences were

observed in the microbiota response to vancomycin or in recovery between *B4galnt2* genotypes.

Previous studies have reported a relative decline in Firmicutes and a rise in Bacteroidetes following the streptomycin treatment (Tamada et al., 2022; Thompson et al., 2015). This study similarly noted a decrease in Firmicutes. However, it found that the population of Firmicutes, particularly within the Lachnospiraceae, Oscillospiraceae, and Lactobacillaceae families, was restored more quickly during the early recovery phase in *B4galnt2^{-/-}* mice. *Enterococcus faecalis*, *Enterocloster clostridioformis*, and members of the *Blautia* genus were notable probiotic species associated with early recovery of *B4galnt2^{-/-}* mice. These species, in cooperation with *Klebsiella oxytoca*, were required to confer resistance against the pathogen *Klebsiella pneumoniae* MDR1, by competing for carbon sources (Osbelt et al., 2021). *Enterocloster clostridioformis* and *Blautia coccoides*, together with *E. coli* are important mediators of colonization resistance in *Salmonella* Typhimurium infection in OMM¹² mice. In this protective context, these members of the Lachnospiraceae family consume free sugars and play an essential role in protecting against pathogens (Eberl et al., 2021). A previous study on vancomycin-resistant *Enterococcus faecium* (VRE) infection described cooperative behavior among commensal species in protection against enteropathogens (Caballero et al., 2017). *Enterocloster bolteae* and *Blautia producta* were found to restore colonization resistance against infection and clear VRE from the intestines of mice (Caballero et al., 2017). Additionally, *Enterocloster bolteae* was identified as a biomarker of early recovery in *B4galnt2^{-/-}* mice.

Another differentially abundant probiotic bacterium, specific for early recovery of *B4galnt2^{-/-}* mice, is *Akkermansia muciniphila*. Pretreatment of mice with this bacterium has been linked to a decreased susceptibility to *Salmonella* Typhimurium infection (Liu et al., 2023). Live *Akkermansia muciniphila* reduces bacterial burden by promoting gut barrier gene expression and the secretion of antimicrobial peptides. Additionally, pasteurized *Akkermansia muciniphila* treatment also ameliorates *Salmonella* Typhimurium infection through inflammasome activation (Liu et al., 2023). *Bifidobacterium longum*, another bacterium associated with the recovery in *B4galnt2^{-/-}* mice, has been associated with improved survival of *C. difficile* infected mice, due to its production of organic acids and decrease in pH (Yun et al., 2017).

Roseburia intestinalis, an anaerobic bacterium, is also associated with the recovery of *B4galnt2^{-/-}* mice. *R. intestinalis* modulates immune responses, increases levels of interleukin (IL)-17 secretion, and promotes Treg differentiation, ameliorating colitis in DSS- and TNBS-induced mouse models of colitis (Luo et al., 2019; Zhu et al., 2018). In colitis models, *R. intestinalis* flagellin induces the expression of the long noncoding RNA HIF1A-AS2, which may modulate intestinal inflammation (Quan et al., 2018). Furthermore, *R. intestinalis*-derived flagellin ameliorates colitis by decreasing the serum levels of proinflammatory cytokines, and inhibiting the activation of the nucleotide-binding oligomerization segment-like receptor family 3 (NLRP3) inflammasome via miR-223-3p/NLRP3 signaling (Wu et al., 2020).

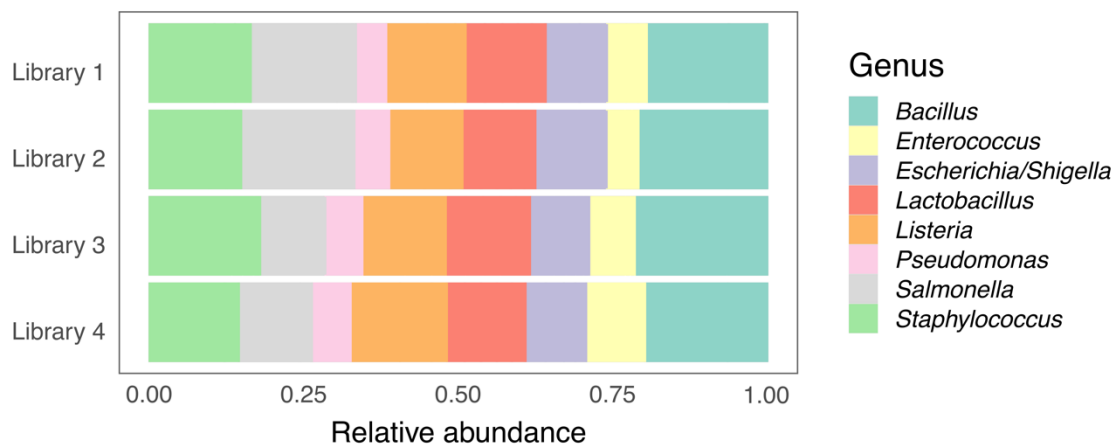
The flagellum is a locomotive organelle responsible for bacterial motility (Macnab and Aizawa, 1984). Swimming motility is a type of movement characterized by the rotation of flagella to move through aqueous environments (Zegadło et al., 2023). In complex environments, such as the mammalian gut, bacteria commonly associate with mucosal surfaces. These bacteria can use various motility mechanisms for movement, including swarming and surfing (Wadhwa and Berg, 2022). Swarming is a type of bacterial movement that involves the collective and coordinated motion of densely packed cells on semi-solid surfaces (Jose and Singh, 2020). Recent studies suggest that intestinal stress and microbiota dysbiosis may lead to an increase in the swarming phenotype of bacteria, which could potentially help alleviate intestinal inflammation (De et al., 2021). Swarming motility has been linked to increased resistance to antibiotics and antimicrobial agents in several species, including *Pseudomonas aeruginosa*, *Escherichia coli*, *Serratia marcescens*, *Burkholderia thailandensis*, *Bacillus subtilis*, and *Salmonella enterica* (Kim et al., 2003; Kim and Surette, 2003; Lai et al., 2009; Overhage et al., 2008). Surfing motility, which was first observed in *P. aeruginosa*, is dependent on the presence of the glycoprotein mucin (Yeung et al., 2012). Surfing-like phenotype is associated with broad-spectrum antibiotic resistance, including aminoglycosides (Sun et al., 2018a, 2018b; Yeung et al., 2012). Furthermore, a transcriptomic analysis of *Escherichia coli*'s response to nine classes of antibiotics, including kanamycin as a representative of the aminoglycoside antibiotics, revealed that genes responsible for regulating flagellar assembly were upregulated after kanamycin treatment, indicating an increase in motility (Bie et al., 2023). In the present study, motility related proteins showed differential expression profiles following the streptomycin treatment with elevated levels of flagellin

and flagellin related proteins in *B4galnt2*^{-/-} mice indicating a potential swarming and/or surfing motility phenotype.

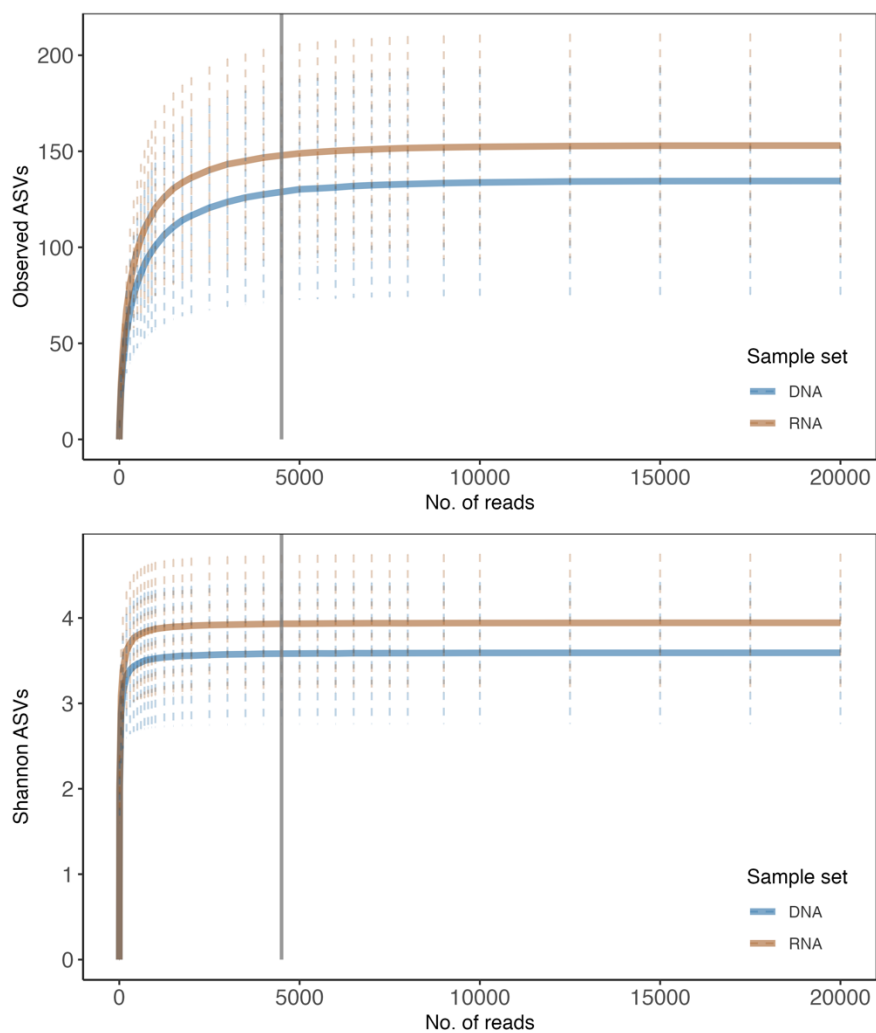
The results of the differential abundance analysis of antibiotic resistance profiles indicate that streptomycin has a variable impact on the abundance of antibiotic resistance genes and transcripts. After streptomycin treatment, a set of differently abundant antibiotic-resistant genes, unrelated to the used antibiotic, were enriched in either of the two *B4galnt2* genotypes at the metagenomic level. However, no significant differences were observed in the genes that confer resistance to the aminoglycoside class of antibiotics. In contrast, the transcriptome response was more specific. The aminoglycoside resistance genes *aadA* and *aadE* were specific for early recovery in *B4galnt2*^{-/-} mice, and *aadA* for late recovery in *B4galnt2*^{+/+} group. Aminoglycoside (3'')(9) adenylyltransferase *AadA*, belonging to the ANT(3'')-Ia family, O-adenylates position 3'' of streptomycin and position 9 of spectinomycin (Hollingshead and Vapnek, 1985; Ramirez and Tolmasky, 2010).

In conclusion, this study investigates how different patterns of intestinal *B4galnt2* expression affect microbiome dynamics following antibiotic treatment, focusing on the detailed analysis of its recovery. The analysis of fecal samples revealed a differential response of tissue-specific *B4galnt2*-associated microbiota to streptomycin treatment, with faster recovery in *B4galnt2*^{-/-} mice. During early recovery, many beneficial species, including *Akkermansia muciniphila*, *Enterocloster clostridioformis*, and *Blautia* members, were enriched in *B4galnt2*^{-/-} mice, which could explain the partial protection against *Salmonella* infection, described in the previous study and Chapter 1 (Eberl et al., 2021; Liu et al., 2023; Rausch et al., 2015). Possible mechanisms behind the faster recovery could be multifactorial, including specialized bacterial motility associated with antimicrobial protection, facilitated by the flagellum, and antibiotic resistance genes such as *aadA* and *aadE*.

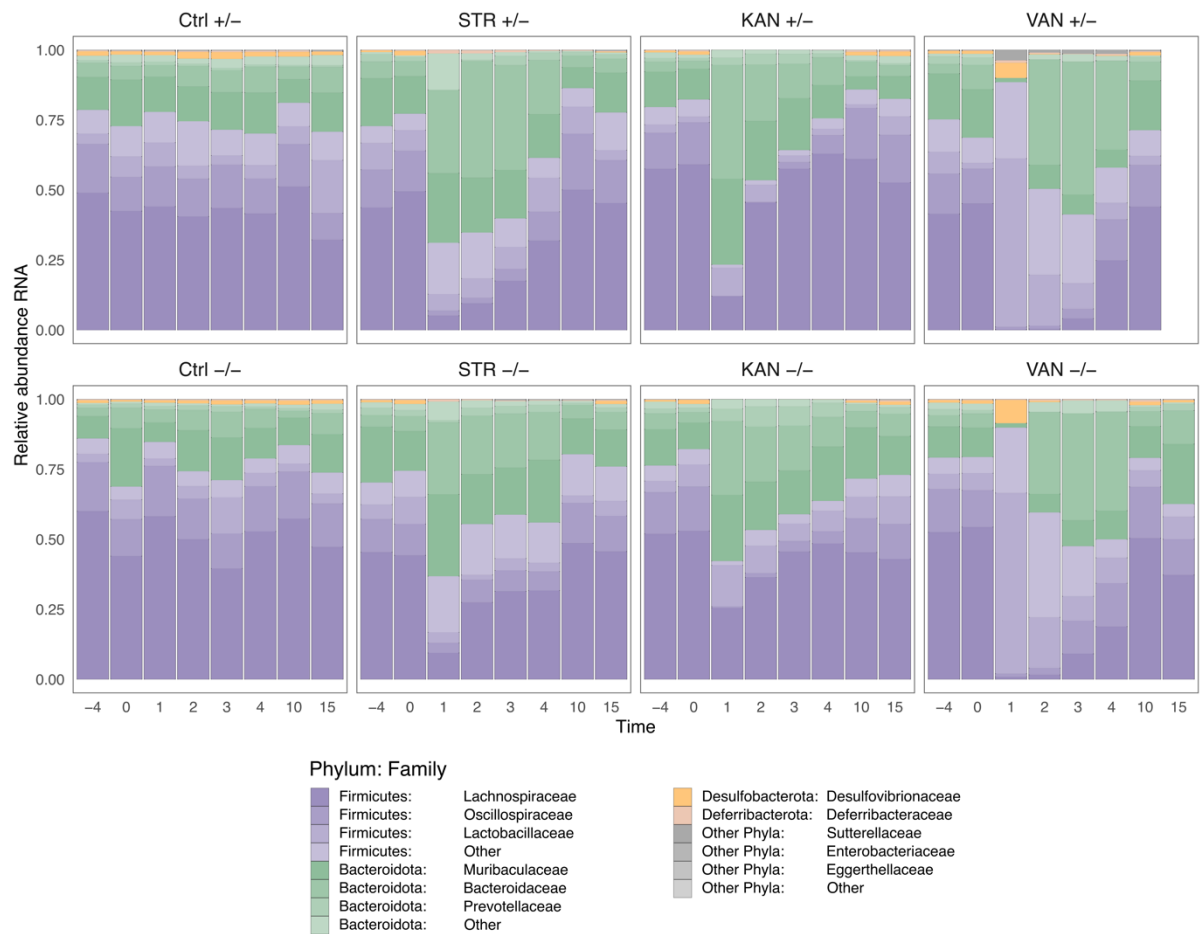
Supplementary information



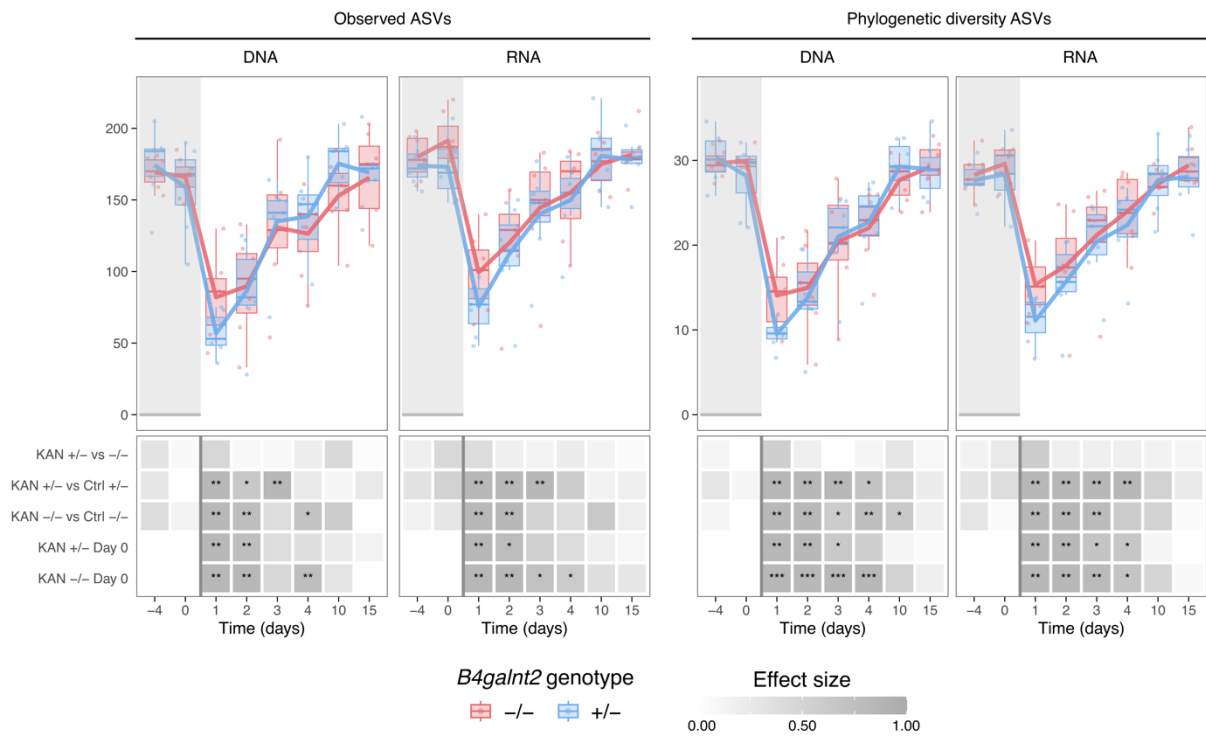
Supplementary Figure 1: Analysis of a mock community as a positive sequencing control.



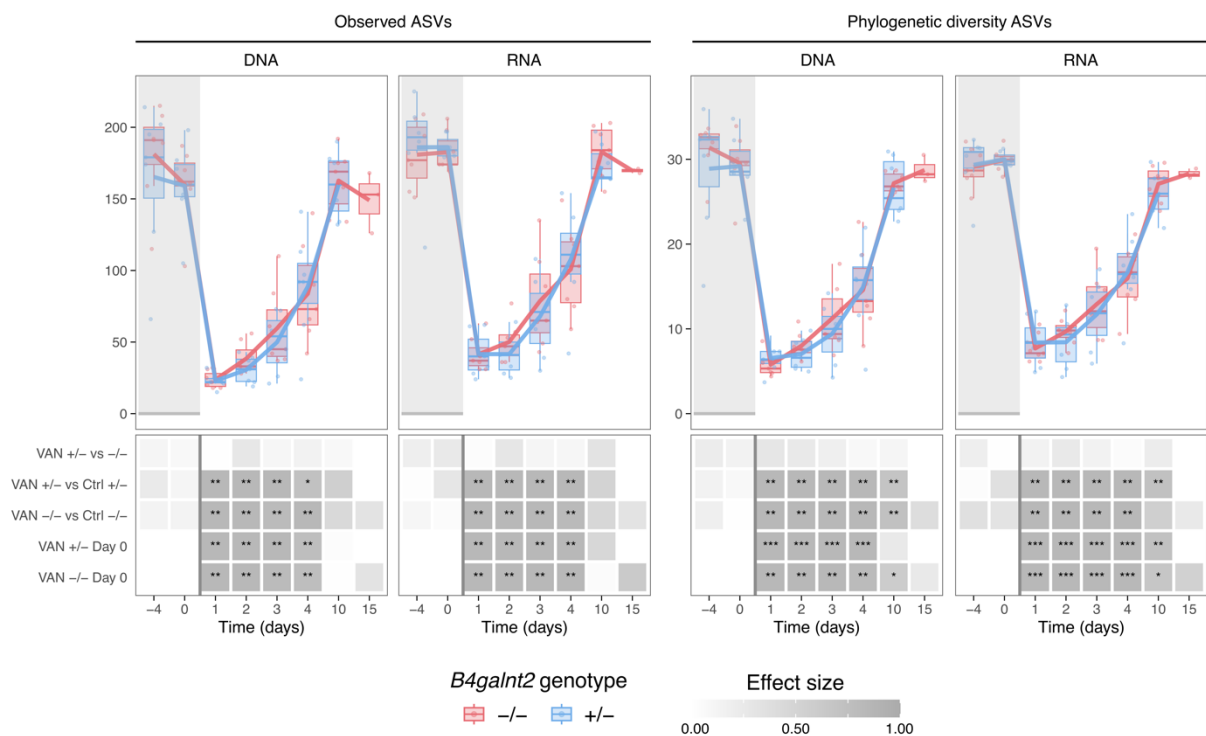
Supplementary Figure 2: Rarefaction curves based on number of observed ASVs, and Shannon index.



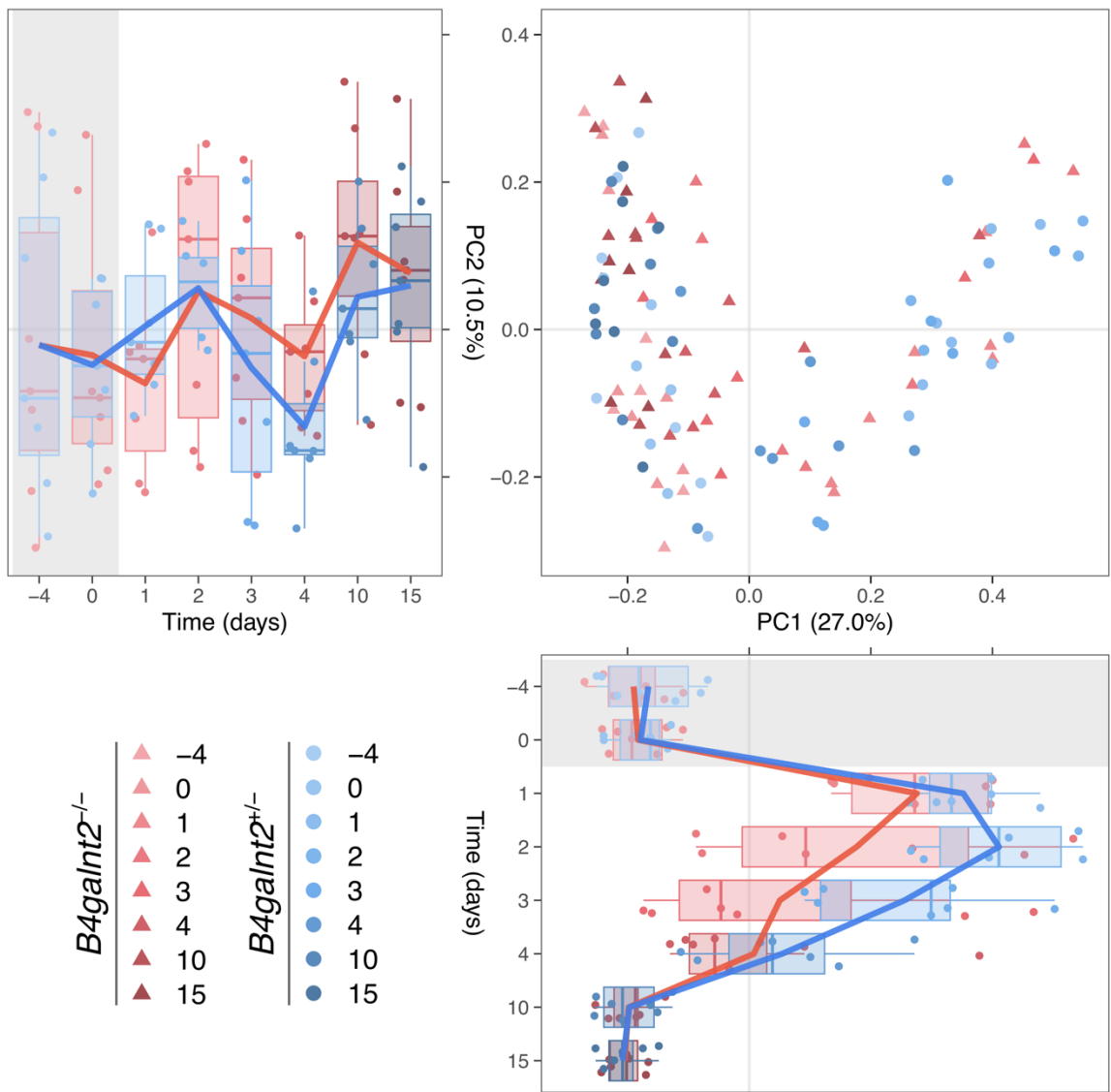
Supplementary Figure 3: Fecal microbiome composition dynamics based on 16S rRNA transcript (RNA) sequencing: Relative sequence abundance in *B4galnt2*-associated microbial communities at the phylum and family levels.

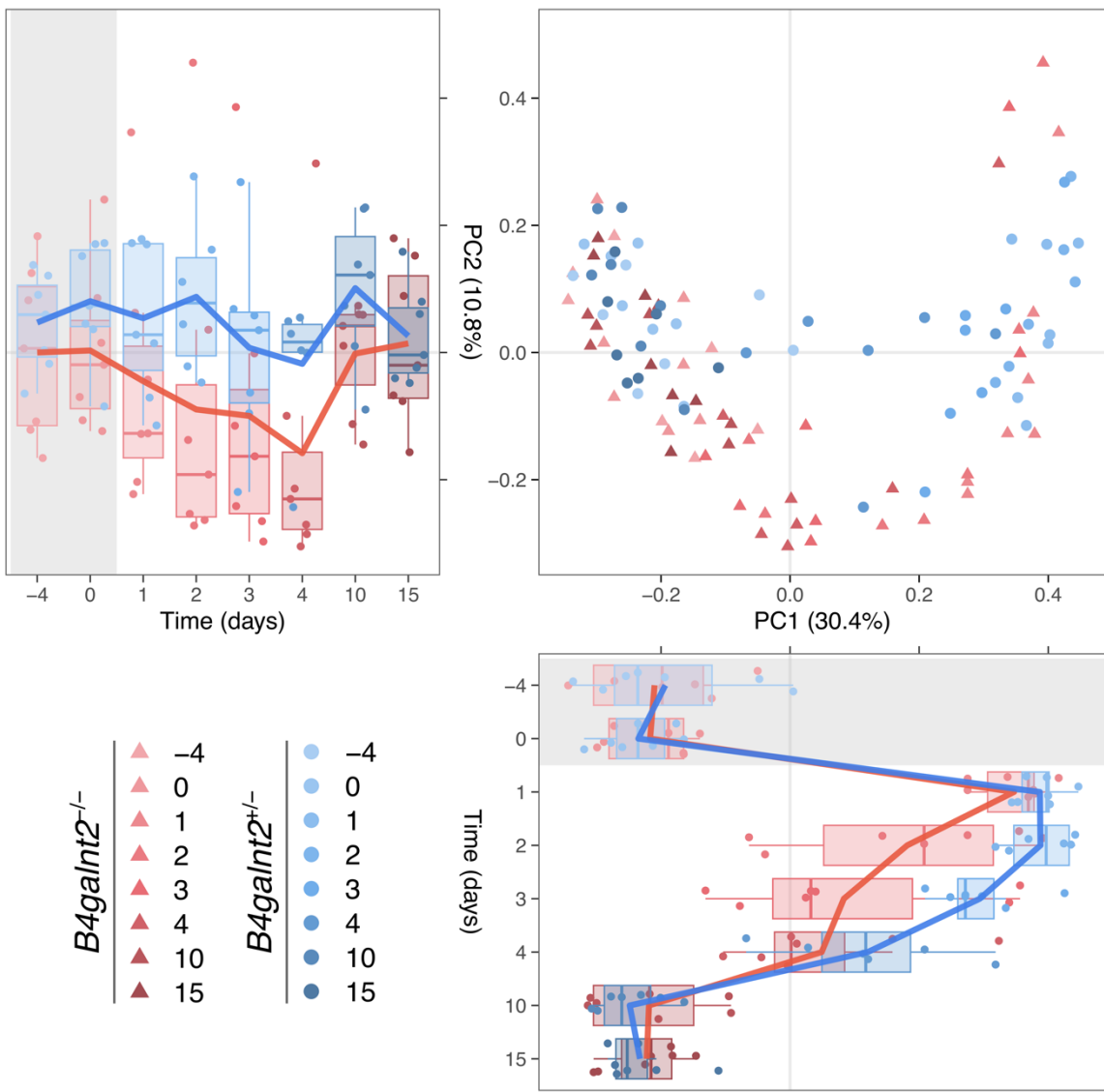


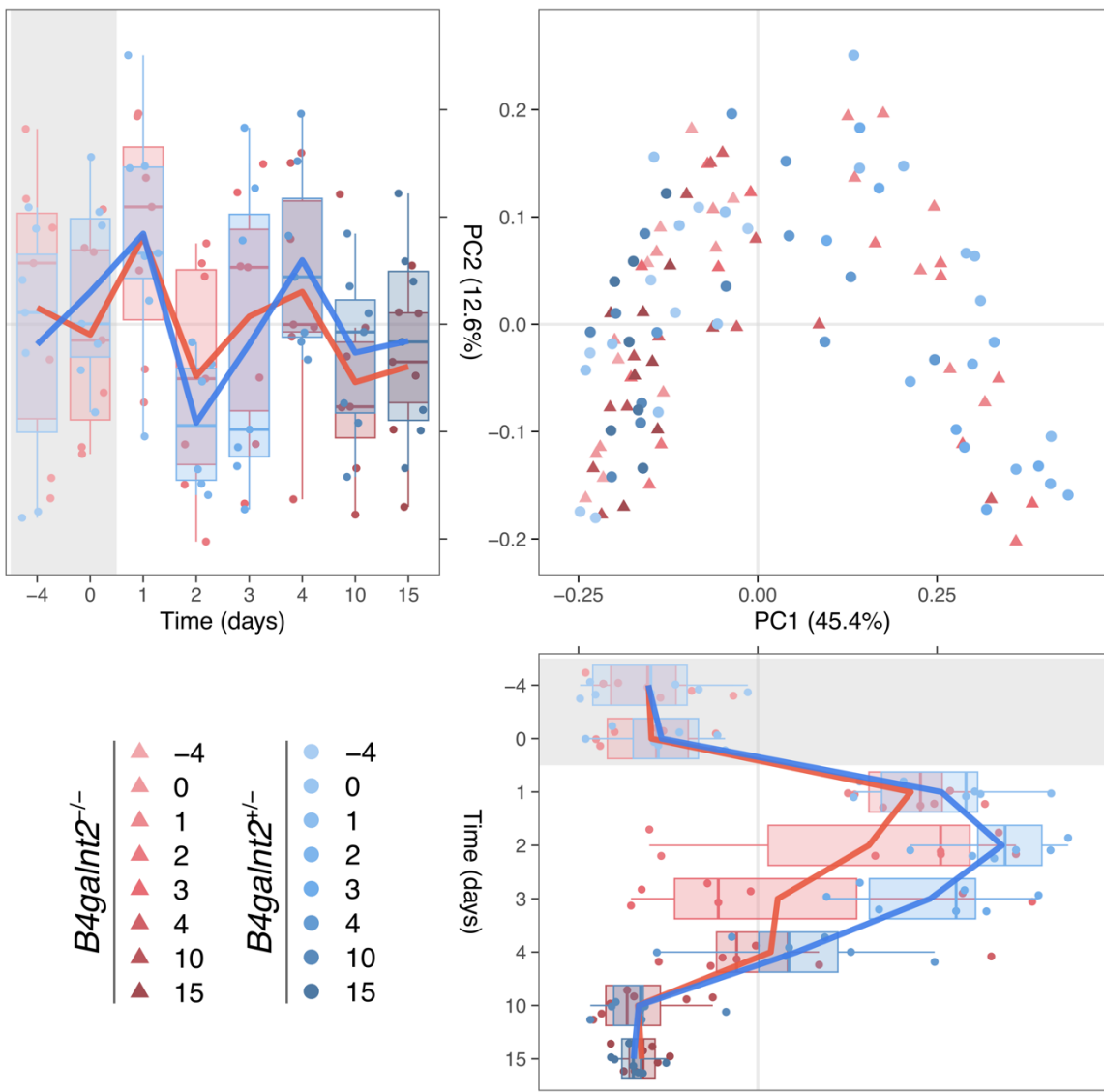
Supplementary Figure 4: ASV richness and phylogenetic diversity (PD) in the kanamycin treated mice at the 16S rRNA gene (DNA) and transcript (RNA) levels; Stars denote significance: * $p_{adj} < 0.05$, ** $p_{adj} < 0.01$, *** $p_{adj} < 0.001$.



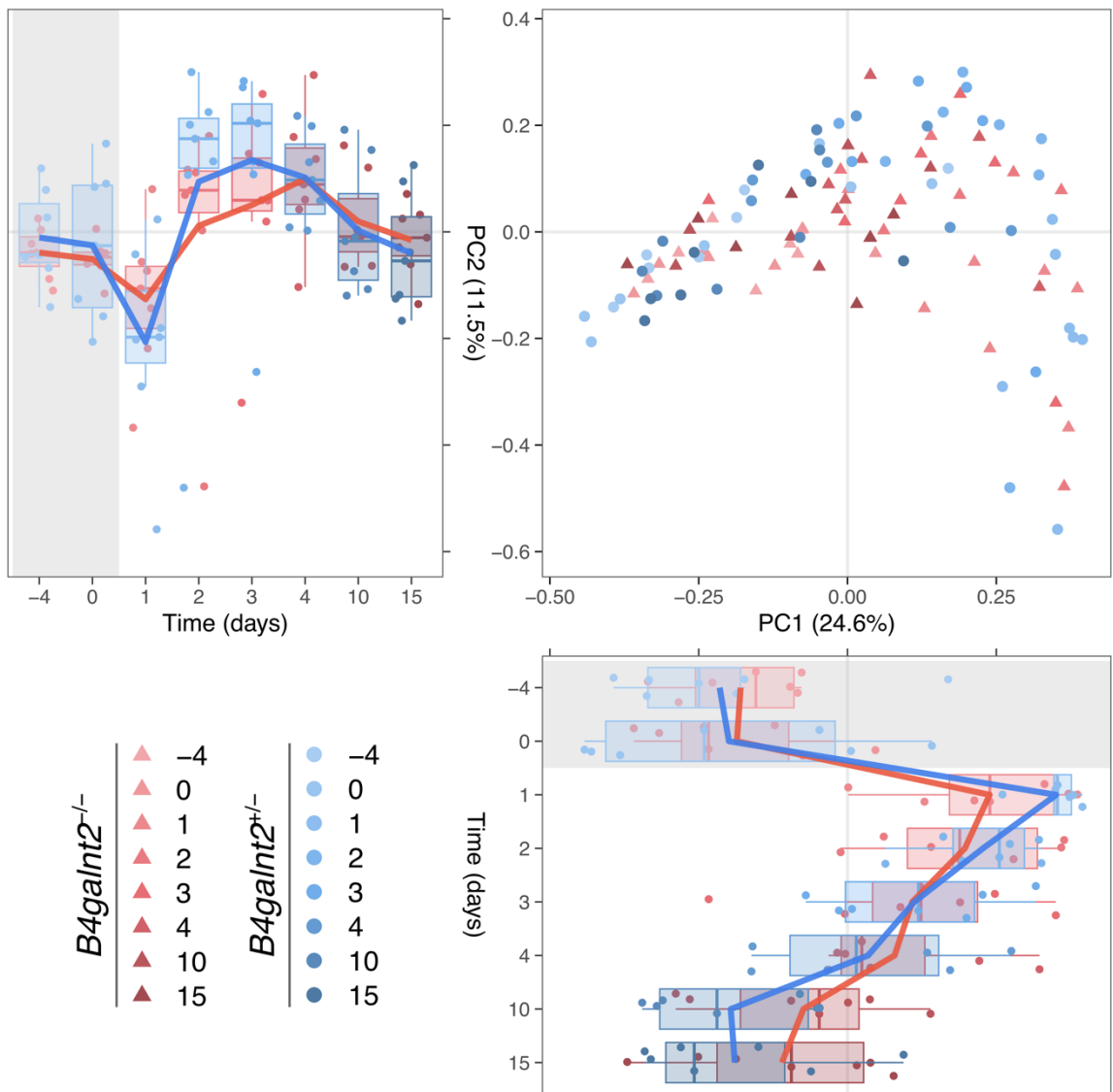
Supplementary Figure 5: ASV richness and phylogenetic diversity (PD) in the vancomycin treated mice at the 16S rRNA gene (DNA) and transcript (RNA) levels; Stars denote significance: * $p_{adj} < 0.05$, ** $p_{adj} < 0.01$, *** $p_{adj} < 0.001$.



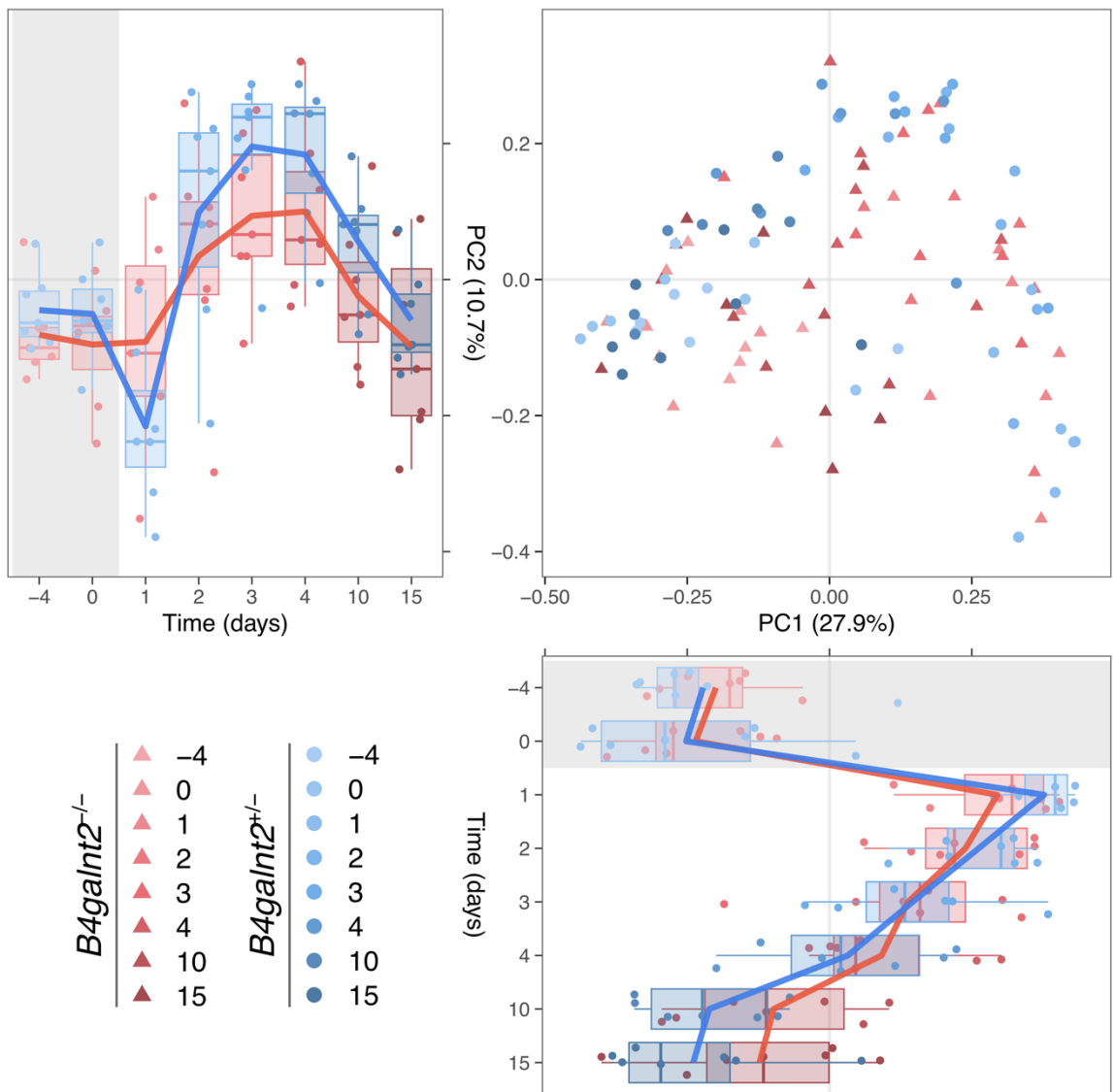




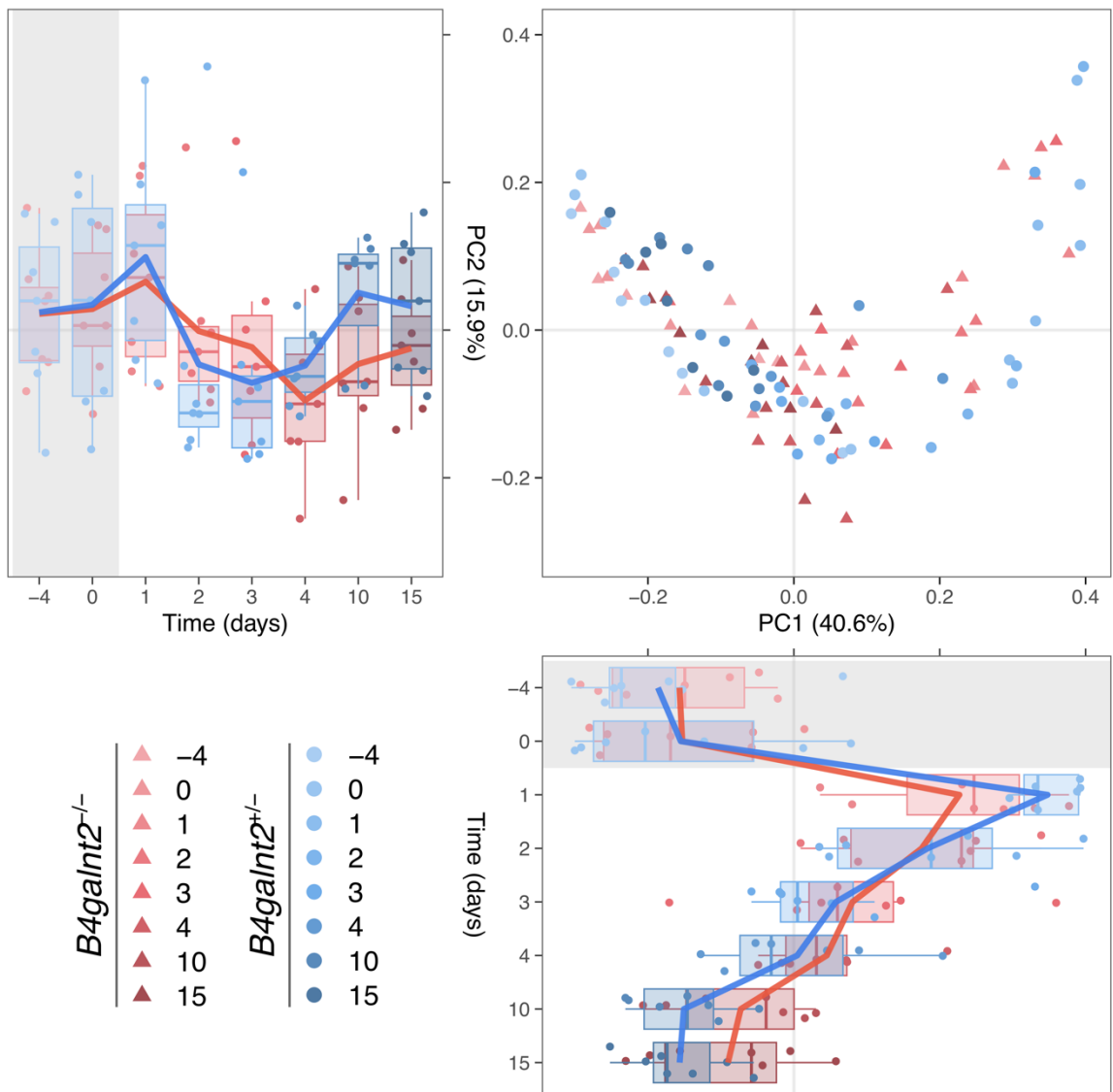
Supplementary Figure 8: Principal Coordinates Analysis (PCoA) plot of samples before, during and after the streptomycin treatment (STR) based on weighted UniFrac (W-UniFrac) distances at the 16S rRNA gene (DNA) level. The distribution of samples by *B4galnt2* groups and time is shown along the first and second axes of the PCoA plot.



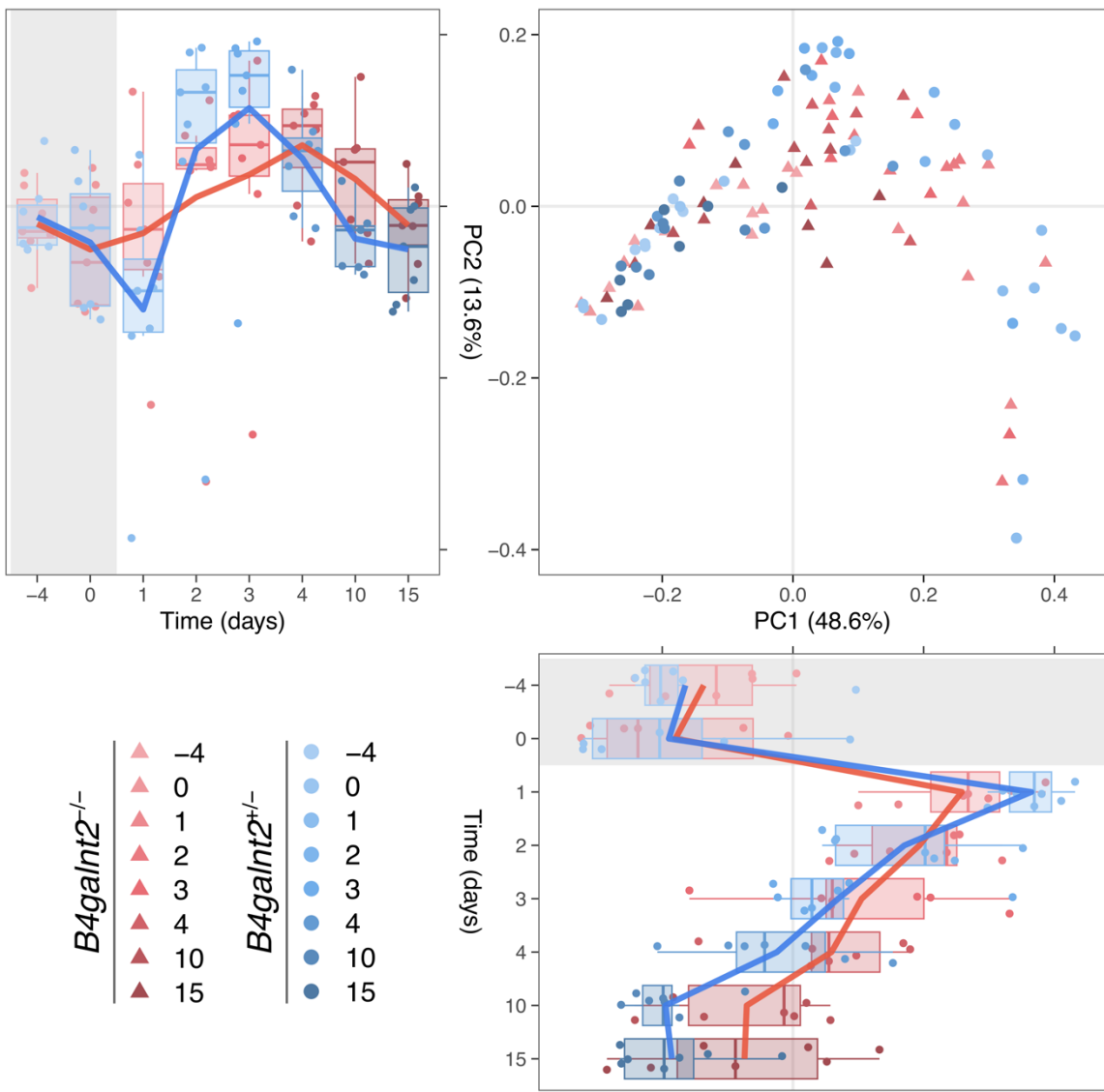
Supplementary Figure 9: Principal Coordinates Analysis (PCoA) plot of samples before, during and after the kanamycin treatment (KAN) based on Bray-Curtis distances at the 16S rRNA gene (DNA) level. The distribution of samples by *B4galnt2* groups and time is shown along the first and second axes of the PCoA plot.

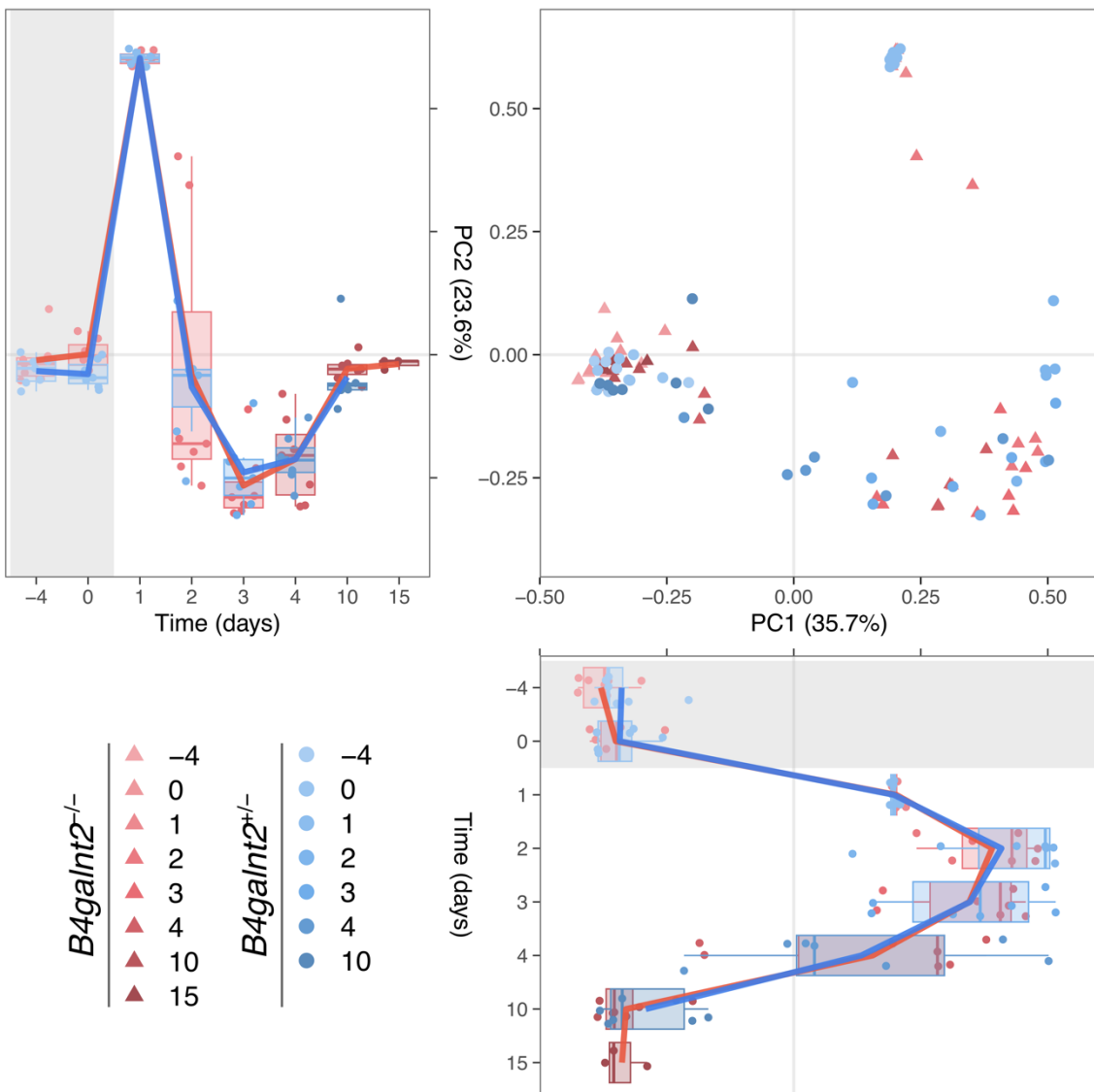


Supplementary Figure 10: Principal Coordinates Analysis (PCoA) plot of samples before, during and after the kanamycin treatment (KAN) based on Bray-Curtis distances at the 16S rRNA transcript (RNA) level. The distribution of samples by *B4galnt2* groups and time is shown along the first and second axes of the PCoA plot.

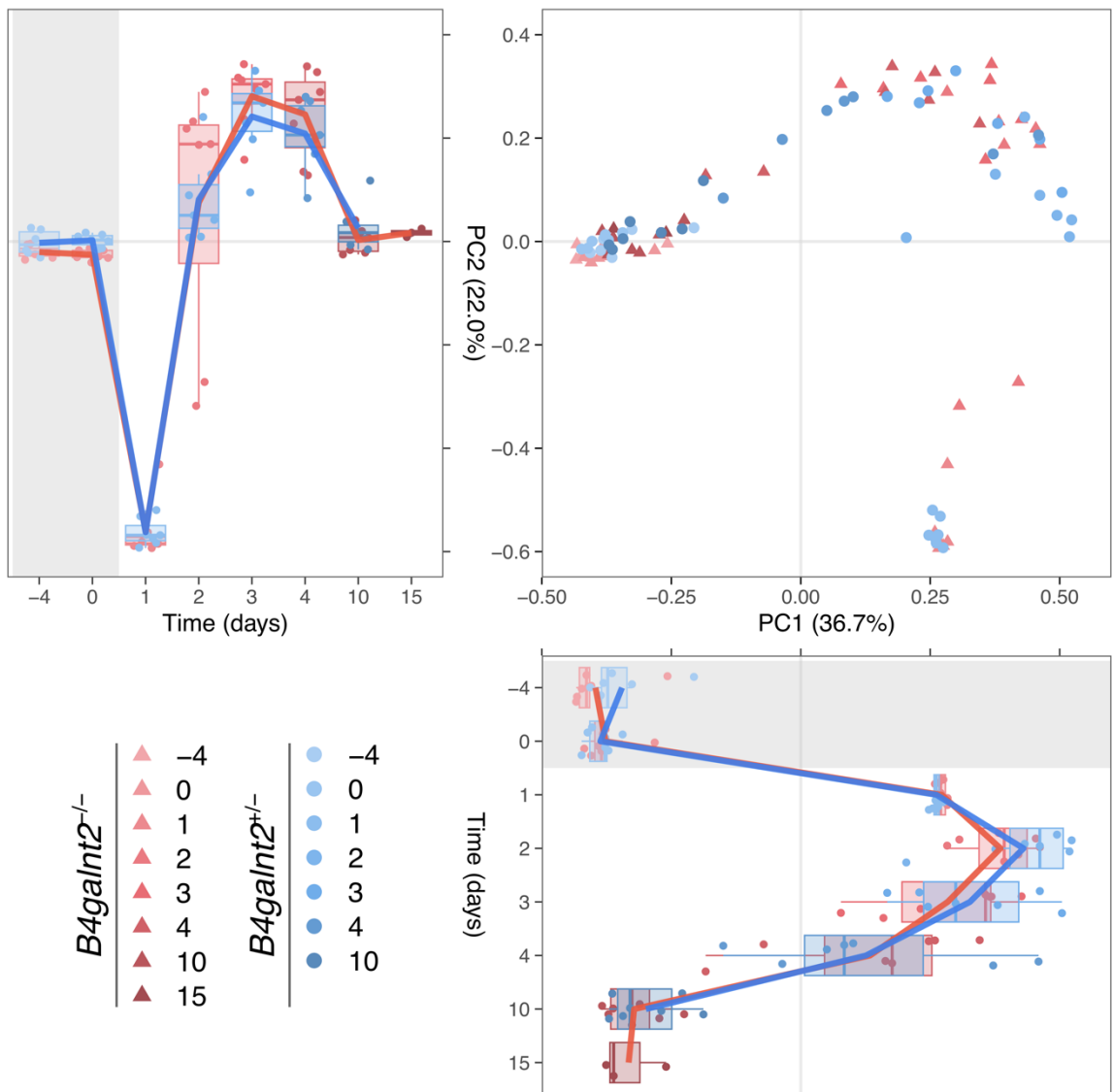


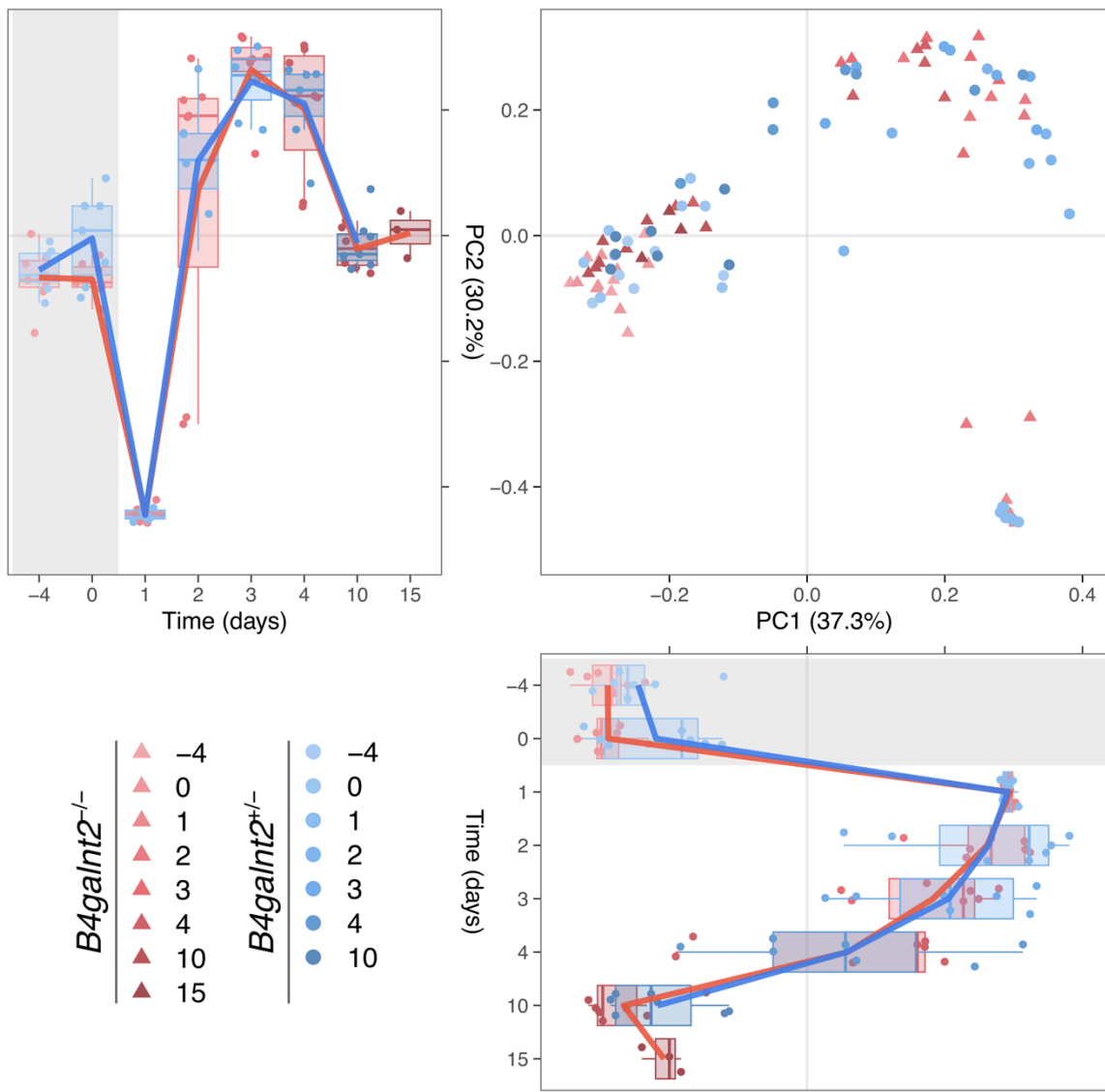
Supplementary Figure 11: Principal Coordinates Analysis (PCoA) plot of samples before, during and after the kanamycin treatment (KAN) based on weighted Unifrac (W-UniFrac) distances at the 16S rRNA gene (DNA) level. The distribution of samples by *B4galnt2* groups and time is shown along the first and second axes of the PCoA plot.

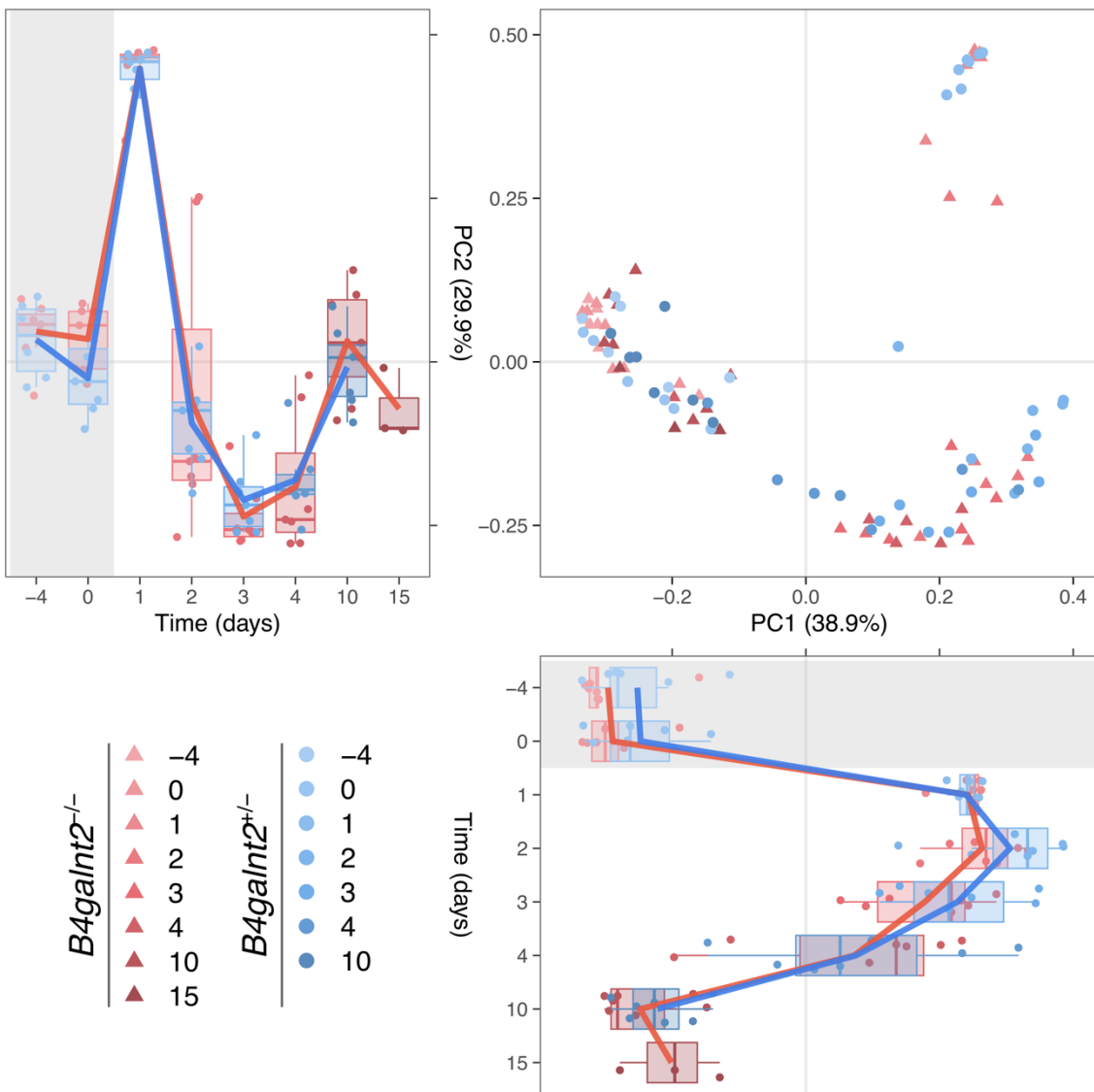




Supplementary Figure 13: Principal Coordinates Analysis (PCoA) plot of samples before, during and after the vancomycin treatment (VAN) based on Bray-Curtis distances at the 16S rRNA gene (DNA) level. The distribution of samples by *B4galnt2* groups and time is shown along the first and second axes of the PCoA plot.





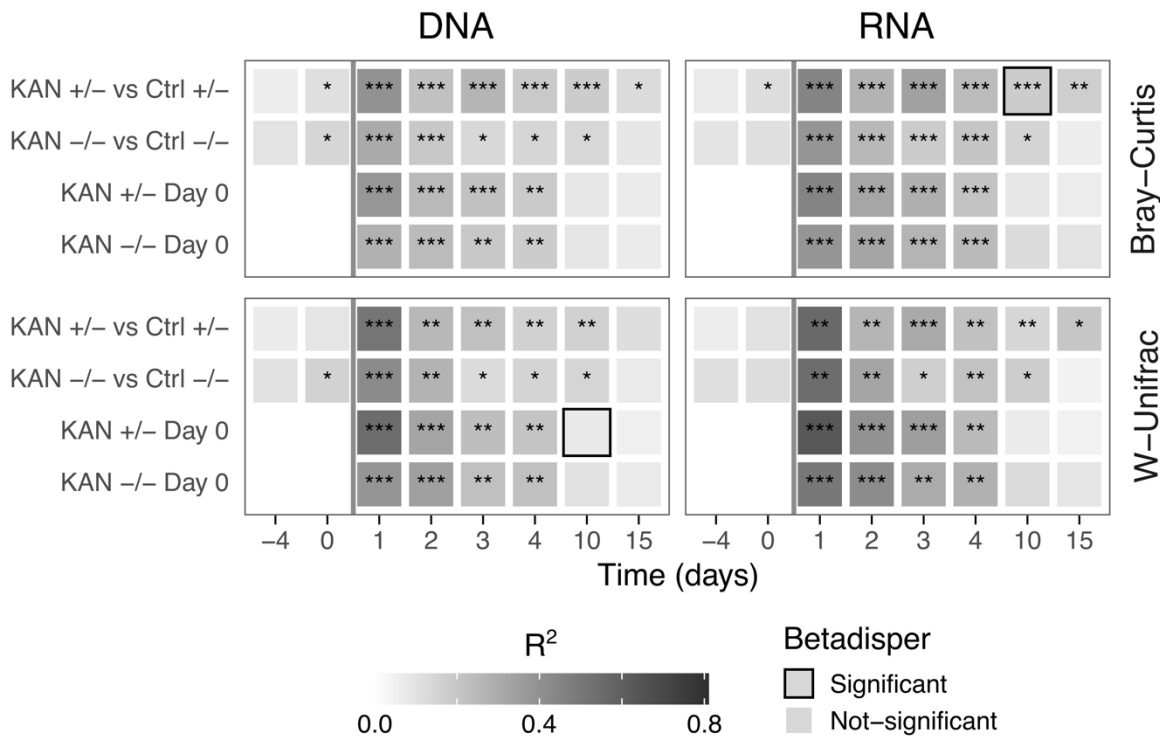


Supplementary Figure 16: Principal Coordinates Analysis (PCoA) plot of samples before, during and after the vancomycin treatment (VAN) based on weighted UniFrac (W-UniFrac) distances at the 16S rRNA transcript (RNA) level. The distribution of samples by *B4galnt2* groups and time is shown along the first and second axes of the PCoA plot.

Supplementary Table 1: PERMANOVA and Betadisper results based on Bray–Curtis and W–Unifrac distances for the streptomycin treated mice at 16S rRNA gene (DNA) and transcript (RNA) levels:

Level	Time	Feature	Bray–Curtis			W–Unifrac		
			p _{adj}	R ²	Dispersion	p _{adj}	R ²	Dispersion
DNA	-4	STR +/- vs -/-	0.4399	0.0657	0.5435	0.7042	0.0525	0.4223
DNA	0	STR +/- vs -/-	0.3073	0.0832	0.3864	0.5499	0.0695	0.2107
DNA	1	STR +/- vs -/-	0.4319	0.0683	0.4769	0.7724	0.0340	0.5650
DNA	2	STR +/- vs -/-	0.2662	0.1313	0.0657	0.3560	0.1703	0.1040
DNA	3	STR +/- vs -/-	0.3073	0.0832	0.7190	0.5309	0.0784	0.4500
DNA	4	STR +/- vs -/-	0.2662	0.0969	0.9785	0.5309	0.0703	0.8090
DNA	10	STR +/- vs -/-	0.0360	0.1288	0.2067	0.0208	0.1540	0.0846
DNA	15	STR +/- vs -/-	0.2662	0.0896	0.9262	0.5309	0.0617	0.8501
DNA	-4	STR -/- vs Ctrl -/-	0.0243	0.1609	0.5640	0.0262	0.1973	0.5398
DNA	0	STR -/- vs Ctrl -/-	0.0688	0.1090	0.5310	0.1574	0.0923	0.5798
DNA	1	STR -/- vs Ctrl -/-	0.0003	0.3832	0.8783	0.0008	0.5027	0.6303
DNA	2	STR -/- vs Ctrl -/-	0.0003	0.2429	0.6856	0.0067	0.2838	0.8864
DNA	3	STR -/- vs Ctrl -/-	0.0008	0.1721	0.9781	0.0453	0.1350	0.9638
DNA	4	STR -/- vs Ctrl -/-	0.0003	0.2117	0.2823	0.0012	0.1983	0.3025
DNA	10	STR -/- vs Ctrl -/-	0.0013	0.1678	0.4025	0.0342	0.1539	0.3739
DNA	15	STR -/- vs Ctrl -/-	0.0954	0.1155	0.1594	0.1574	0.1127	0.1443
DNA	-4	STR +/- vs Ctrl +/-	0.4016	0.0709	0.9677	0.4432	0.0662	0.6945
DNA	0	STR +/- vs Ctrl +/-	0.0814	0.1135	0.1245	0.0543	0.1357	0.0338
DNA	1	STR +/- vs Ctrl +/-	0.0003	0.4600	0.4005	0.0006	0.5624	0.1711
DNA	2	STR +/- vs Ctrl +/-	0.0002	0.3721	0.0167	0.0005	0.4914	0.0025
DNA	3	STR +/- vs Ctrl +/-	0.0004	0.3956	0.3244	0.0004	0.5311	0.6086
DNA	4	STR +/- vs Ctrl +/-	0.0002	0.2956	0.3990	0.0016	0.3093	0.1836
DNA	10	STR +/- vs Ctrl +/-	0.0002	0.2291	0.6780	0.0004	0.2692	0.5168
DNA	15	STR +/- vs Ctrl +/-	0.0002	0.2477	0.8661	0.0020	0.2312	0.9443
DNA	1	STR -/- Day 0	0.0002	0.3440	0.9193	0.0003	0.4242	0.7654
DNA	2	STR -/- Day 0	0.0002	0.2574	0.3069	0.0004	0.3314	0.7451
DNA	3	STR -/- Day 0	0.0024	0.1857	0.7731	0.0022	0.1961	0.8333
DNA	4	STR -/- Day 0	0.0002	0.1992	0.5690	0.0003	0.2226	0.5812
DNA	10	STR -/- Day 0	0.0065	0.1714	0.6603	0.0022	0.1989	0.5896
DNA	15	STR -/- Day 0	0.0291	0.1375	0.3465	0.0196	0.1589	0.2912
DNA	1	STR +/- Day 0	0.0005	0.4711	0.8130	0.0010	0.5265	0.7898
DNA	2	STR +/- Day 0	0.0004	0.4723	0.3464	0.0009	0.6088	0.0505
DNA	3	STR +/- Day 0	0.0004	0.3390	0.4712	0.0009	0.4823	0.7785

Level	Time	Feature	Bray-Curtis			W-Unifrac		
			p _{adj}	R ²	Dispersion	p _{adj}	R ²	Dispersion
DNA	4	STR +/- Day 0	0.0004	0.2398	0.7702	0.0011	0.2425	0.8424
DNA	10	STR +/- Day 0	0.0313	0.1267	0.4656	0.0853	0.1193	0.2122
DNA	15	STR +/- Day 0	0.0078	0.1562	0.7720	0.0032	0.1892	0.8786
RNA	-4	STR +/- vs -/-	0.7028	0.0558	0.7614	0.8360	0.0393	0.5431
RNA	0	STR +/- vs -/-	0.2876	0.0812	0.5730	0.5355	0.0684	0.2348
RNA	1	STR +/- vs -/-	0.5439	0.0589	0.6608	0.8360	0.0362	0.8035
RNA	2	STR +/- vs -/-	0.2288	0.1446	0.3470	0.3936	0.1991	0.1504
RNA	3	STR +/- vs -/-	0.2288	0.1190	0.5523	0.4648	0.1159	0.1447
RNA	4	STR +/- vs -/-	0.2876	0.0882	0.4683	0.5355	0.0691	0.5222
RNA	10	STR +/- vs -/-	0.2288	0.1044	0.3683	0.4648	0.0960	0.3322
RNA	15	STR +/- vs -/-	0.2876	0.0881	0.6913	0.5355	0.0660	0.4325
RNA	-4	STR -/- vs Ctrl -/-	0.0856	0.1215	0.3742	0.0937	0.1589	0.2452
RNA	0	STR -/- vs Ctrl -/-	0.0704	0.1074	0.6154	0.2141	0.0911	0.8248
RNA	1	STR -/- vs Ctrl -/-	0.0003	0.4710	0.9203	0.0008	0.6267	0.9688
RNA	2	STR -/- vs Ctrl -/-	0.0003	0.3129	0.7159	0.0091	0.3133	0.3995
RNA	3	STR -/- vs Ctrl -/-	0.0003	0.2122	0.8932	0.0378	0.1512	0.9794
RNA	4	STR -/- vs Ctrl -/-	0.0003	0.3041	0.6464	0.0008	0.2874	0.6348
RNA	10	STR -/- vs Ctrl -/-	0.0003	0.1781	0.4750	0.0781	0.1516	0.6332
RNA	15	STR -/- vs Ctrl -/-	0.1379	0.1003	0.2939	0.2754	0.0899	0.3191
RNA	-4	STR +/- vs Ctrl +/ -	0.3077	0.0779	0.6391	0.2255	0.0847	0.7331
RNA	0	STR +/- vs Ctrl +/ -	0.2725	0.0830	0.2192	0.2158	0.0900	0.0827
RNA	1	STR +/- vs Ctrl +/ -	0.0003	0.5084	0.5592	0.0005	0.5804	0.5783
RNA	2	STR +/- vs Ctrl +/ -	0.0003	0.3839	0.0175	0.0006	0.4970	0.0038
RNA	3	STR +/- vs Ctrl +/ -	0.0003	0.4316	0.6049	0.0005	0.5618	0.3842
RNA	4	STR +/- vs Ctrl +/ -	0.0003	0.2789	0.4466	0.0064	0.2607	0.7665
RNA	10	STR +/- vs Ctrl +/ -	0.0003	0.1961	0.5503	0.0005	0.1878	0.9079
RNA	15	STR +/- vs Ctrl +/ -	0.0016	0.2454	0.9023	0.0108	0.2118	0.6320
RNA	1	STR -/- Day 0	0.0002	0.4199	0.9874	0.0003	0.5213	0.4298
RNA	2	STR -/- Day 0	0.0002	0.2974	0.5550	0.0004	0.3302	0.7494
RNA	3	STR -/- Day 0	0.0002	0.2248	0.6064	0.0018	0.2076	0.4992
RNA	4	STR -/- Day 0	0.0002	0.2289	0.8350	0.0003	0.2233	0.8986
RNA	10	STR -/- Day 0	0.0114	0.1367	0.3538	0.0380	0.1617	0.5369
RNA	15	STR -/- Day 0	0.0924	0.0989	0.9262	0.1110	0.1059	0.7319
RNA	1	STR +/- Day 0	0.0006	0.5340	0.7760	0.0006	0.6014	0.7977
RNA	2	STR +/- Day 0	0.0006	0.4911	0.7181	0.0006	0.6748	0.5599
RNA	3	STR +/- Day 0	0.0006	0.4256	0.6852	0.0006	0.5775	0.5396
RNA	4	STR +/- Day 0	0.0006	0.2804	0.1433	0.0027	0.3003	0.1206
RNA	10	STR +/- Day 0	0.0046	0.1480	0.2099	0.0195	0.1594	0.2583
RNA	15	STR +/- Day 0	0.0284	0.1269	0.8871	0.0195	0.1525	0.8511



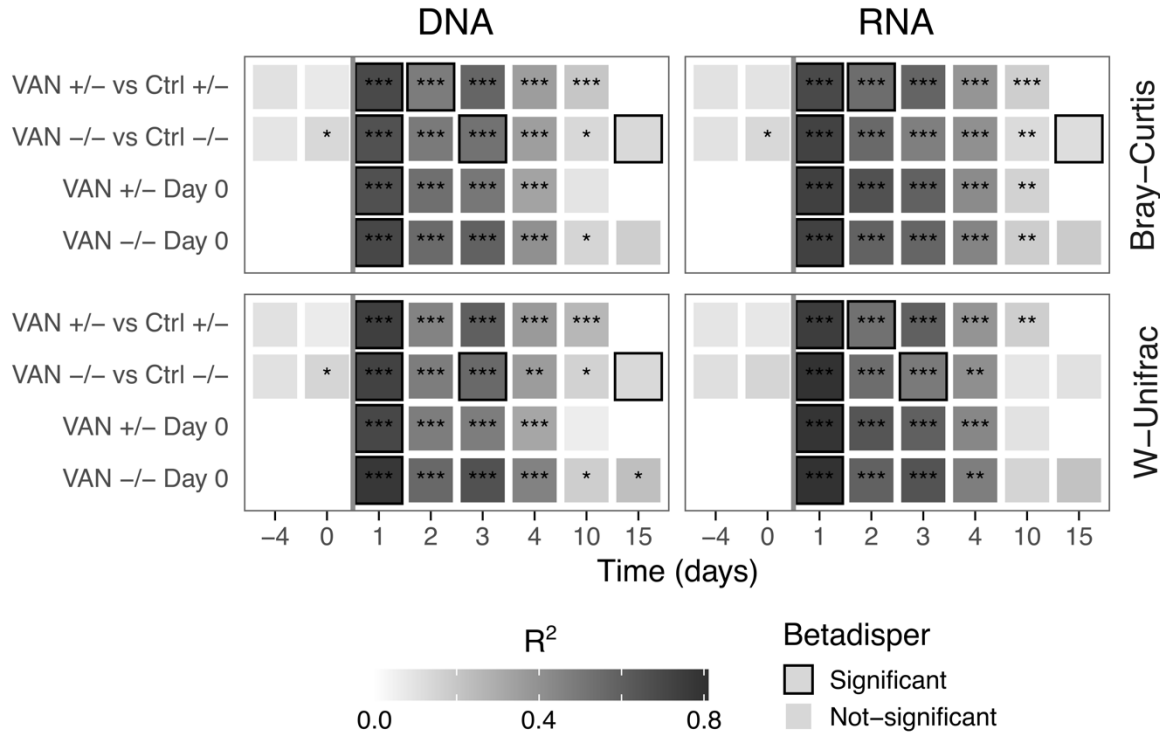
Supplementary Figure 17: Significance and effect size estimates for PERMANOVA and Betadisper analysis for differences in the kanamycin treated mice at 16S rRNA gene (DNA) and transcript (RNA) levels between *B4galnt2* genotypes; Stars denote significance: $*p_{adj} < 0.05$, $**p_{adj} < 0.01$, $***p_{adj} < 0.001$.

Supplementary Table 2: PERMANOVA and Betadisper results based on Bray–Curtis and W–Unifrac distances for the kanamycin treated mice at 16S rRNA gene (DNA) and transcript (RNA) levels:

Level	Time	Feature	Bray–Curtis			W–Unifrac		
			p_{adj}	R ²	Dispersion	p_{adj}	R ²	Dispersion
DNA	-4	KAN +/- vs -/-	0.1507	0.0941	0.9482	0.2371	0.0816	0.8988
DNA	0	KAN +/- vs -/-	0.0883	0.1109	0.1693	0.2371	0.0848	0.7447
DNA	1	KAN +/- vs -/-	0.0604	0.1540	0.3211	0.0548	0.1905	0.1824
DNA	2	KAN +/- vs -/-	0.3517	0.0822	0.7813	0.4691	0.0717	0.9125
DNA	3	KAN +/- vs -/-	0.1915	0.0938	0.5951	0.4691	0.0679	0.5441
DNA	4	KAN +/- vs -/-	0.0883	0.1081	0.9079	0.2371	0.1055	0.4685
DNA	10	KAN +/- vs -/-	0.0232	0.1628	0.8733	0.0548	0.1760	0.0228
DNA	15	KAN +/- vs -/-	0.0883	0.1181	0.8954	0.2371	0.1036	0.6748

Level	Time	Feature	Bray-Curtis			W-Unifrac		
			p _{adj}	R ²	Dispersion	p _{adj}	R ²	Dispersion
DNA	-4	KAN -/- vs Ctrl -/-	0.1112	0.0999	0.9342	0.1267	0.1011	0.9180
DNA	0	KAN -/- vs Ctrl -/-	0.0250	0.1463	0.2908	0.0412	0.1608	0.3699
DNA	1	KAN -/- vs Ctrl -/-	0.0008	0.3065	0.9863	0.0008	0.4262	0.8349
DNA	2	KAN -/- vs Ctrl -/-	0.0008	0.1952	0.8541	0.0012	0.2747	0.3751
DNA	3	KAN -/- vs Ctrl -/-	0.0110	0.1371	0.9907	0.0413	0.1266	0.9527
DNA	4	KAN -/- vs Ctrl -/-	0.0110	0.1463	0.4383	0.0328	0.1524	0.3001
DNA	10	KAN -/- vs Ctrl -/-	0.0269	0.1421	0.7309	0.0499	0.1484	0.4408
DNA	15	KAN -/- vs Ctrl -/-	0.2268	0.0880	0.4774	0.4129	0.0723	0.2955
DNA	-4	KAN +/- vs Ctrl +/-	0.4204	0.0644	0.9883	0.2414	0.0720	0.8201
DNA	0	KAN +/- vs Ctrl +/-	0.0443	0.1140	0.6090	0.1384	0.0924	0.6366
DNA	1	KAN +/- vs Ctrl +/-	0.0003	0.3992	0.7024	0.0008	0.5135	0.3068
DNA	2	KAN +/- vs Ctrl +/-	0.0008	0.2223	0.6109	0.0020	0.2566	0.3144
DNA	3	KAN +/- vs Ctrl +/-	0.0003	0.2662	0.3695	0.0013	0.2268	0.9522
DNA	4	KAN +/- vs Ctrl +/-	0.0008	0.1923	0.8773	0.0080	0.1647	0.5922
DNA	10	KAN +/- vs Ctrl +/-	0.0003	0.1804	0.2571	0.0013	0.1681	0.9366
DNA	15	KAN +/- vs Ctrl +/-	0.0479	0.1262	0.4017	0.0841	0.1188	0.6849
DNA	1	KAN -/- Day 0	0.0003	0.2825	0.2755	0.0006	0.3855	0.6689
DNA	2	KAN -/- Day 0	0.0003	0.2434	0.5089	0.0006	0.3469	0.9745
DNA	3	KAN -/- Day 0	0.0020	0.1985	0.4595	0.0077	0.2237	0.7133
DNA	4	KAN -/- Day 0	0.0020	0.1803	0.8035	0.0024	0.2253	0.8650
DNA	10	KAN -/- Day 0	0.2820	0.0918	0.7241	0.2119	0.1044	0.9025
DNA	15	KAN -/- Day 0	0.4455	0.0700	0.8482	0.3885	0.0733	0.7899
DNA	1	KAN +/- Day 0	0.0002	0.3814	0.2008	0.0006	0.5497	0.4366
DNA	2	KAN +/- Day 0	0.0002	0.2515	0.7509	0.0006	0.3303	0.9550
DNA	3	KAN +/- Day 0	0.0002	0.2207	0.3588	0.0018	0.2329	0.6006
DNA	4	KAN +/- Day 0	0.0024	0.1900	0.3263	0.0042	0.2118	0.4299
DNA	10	KAN +/- Day 0	0.1159	0.0850	0.2306	0.1682	0.0770	0.0473
DNA	15	KAN +/- Day 0	0.1754	0.0719	0.2702	0.2912	0.0574	0.2445
RNA	-4	KAN +/- vs -/-	0.1397	0.0969	0.6010	0.3038	0.0873	0.9678
RNA	0	KAN +/- vs -/-	0.1275	0.0953	0.2399	0.4717	0.0548	0.9957
RNA	1	KAN +/- vs -/-	0.0432	0.1768	0.4845	0.0420	0.2164	0.6810
RNA	2	KAN +/- vs -/-	0.2738	0.0863	0.7589	0.4717	0.0686	0.8690
RNA	3	KAN +/- vs -/-	0.1465	0.0983	0.6127	0.4429	0.0824	0.4102
RNA	4	KAN +/- vs -/-	0.1260	0.1054	0.6173	0.3038	0.1019	0.6007
RNA	10	KAN +/- vs -/-	0.0216	0.1475	0.4657	0.0328	0.2103	0.4223
RNA	15	KAN +/- vs -/-	0.0877	0.1203	0.6090	0.2323	0.1185	0.2348
RNA	-4	KAN -/- vs Ctrl -/-	0.1954	0.0947	0.7306	0.1229	0.1129	0.4717
RNA	0	KAN -/- vs Ctrl -/-	0.0939	0.1133	0.9383	0.1229	0.1206	0.6418
RNA	1	KAN -/- vs Ctrl -/-	0.0004	0.3862	0.6788	0.0016	0.5445	0.4332

Level	Time	Feature	Bray-Curtis			W-Unifrac		
			<i>p_{adj}</i>	R ²	Dispersion	<i>p_{adj}</i>	R ²	Dispersion
RNA	2	KAN -/- vs Ctrl -/-	0.0004	0.2535	0.8626	0.0016	0.3242	0.9301
RNA	3	KAN -/- vs Ctrl -/-	0.0004	0.1813	0.7719	0.0188	0.1704	0.8224
RNA	4	KAN -/- vs Ctrl -/-	0.0004	0.2078	0.9936	0.0075	0.2195	0.9121
RNA	10	KAN -/- vs Ctrl -/-	0.0142	0.1508	0.6756	0.0472	0.1771	0.9560
RNA	15	KAN -/- vs Ctrl -/-	0.5750	0.0631	0.8923	0.7445	0.0451	0.8530
RNA	-4	KAN +/- vs Ctrl +/-	0.3339	0.0726	0.8028	0.2929	0.0642	0.5380
RNA	0	KAN +/- vs Ctrl +/-	0.0313	0.1187	0.2756	0.1081	0.1041	0.9669
RNA	1	KAN +/- vs Ctrl +/-	0.0003	0.4518	0.6478	0.0012	0.5619	0.5302
RNA	2	KAN +/- vs Ctrl +/-	0.0002	0.2718	0.6529	0.0029	0.2679	0.5739
RNA	3	KAN +/- vs Ctrl +/-	0.0002	0.3403	0.4057	0.0008	0.3077	0.9771
RNA	4	KAN +/- vs Ctrl +/-	0.0002	0.2426	0.1422	0.0029	0.2222	0.9287
RNA	10	KAN +/- vs Ctrl +/-	0.0002	0.1829	0.0494	0.0029	0.1463	0.6854
RNA	15	KAN +/- vs Ctrl +/-	0.0061	0.1745	0.4967	0.0104	0.2025	0.8671
RNA	1	KAN -/- Day 0	0.0002	0.3886	0.6511	0.0006	0.5020	0.2111
RNA	2	KAN -/- Day 0	0.0002	0.3267	0.9025	0.0006	0.4202	0.5994
RNA	3	KAN -/- Day 0	0.0002	0.2686	0.7386	0.0023	0.3049	0.8848
RNA	4	KAN -/- Day 0	0.0002	0.2475	0.8850	0.0014	0.2803	0.9692
RNA	10	KAN -/- Day 0	0.0626	0.1255	0.7912	0.1313	0.1290	0.3705
RNA	15	KAN -/- Day 0	0.1488	0.0990	0.7326	0.2472	0.0906	0.9758
RNA	1	KAN +/- Day 0	0.0002	0.4537	0.0780	0.0002	0.6309	0.4261
RNA	2	KAN +/- Day 0	0.0002	0.3214	0.7705	0.0002	0.3981	0.7868
RNA	3	KAN +/- Day 0	0.0002	0.2860	0.2868	0.0002	0.3526	0.4862
RNA	4	KAN +/- Day 0	0.0002	0.2159	0.7116	0.0029	0.2491	0.8404
RNA	10	KAN +/- Day 0	0.1312	0.0856	0.7146	0.2650	0.0718	0.1713
RNA	15	KAN +/- Day 0	0.2217	0.0680	0.2555	0.4741	0.0491	0.3319



Supplementary Figure 18: Significance and effect size estimates for PERMANOVA and Betadisper analysis for differences in the vancomycin treated mice at 16S rRNA gene (DNA) and transcript (RNA) levels between *B4galnt2* genotypes; Stars denote significance: * $p_{adj} < 0.05$, ** $p_{adj} < 0.01$, *** $p_{adj} < 0.001$.

Supplementary Table 3: PERMANOVA and Betadisper results based on Bray–Curtis and W–Unifrac distances for the vancomycin treated mice at 16S rRNA gene (DNA) and transcript (RNA) levels:

Level	Time	Feature	Bray–Curtis			W–Unifrac		
			p_{adj}	R ²	Dispersion	p_{adj}	R ²	Dispersion
DNA	-4	VAN +/- vs -/-	0.2822	0.0977	0.2215	0.2295	0.1109	0.1441
DNA	0	VAN +/- vs -/-	0.1365	0.1327	0.2092	0.0140	0.1827	0.2424
DNA	1	VAN +/- vs -/-	0.2822	0.1002	0.8672	0.2295	0.0976	0.7444
DNA	2	VAN +/- vs -/-	0.7340	0.0352	0.9587	0.7354	0.0313	0.8154
DNA	3	VAN +/- vs -/-	0.2822	0.1012	0.5734	0.2295	0.1118	0.3820
DNA	4	VAN +/- vs -/-	0.3619	0.0737	0.5713	0.4363	0.0626	0.9592
DNA	10	VAN +/- vs -/-	0.2822	0.0830	0.7873	0.1736	0.1150	0.5089
DNA	-4	VAN -/- vs Ctrl -/-	0.1932	0.0929	0.3887	0.1325	0.1061	0.3578
DNA	0	VAN -/- vs Ctrl -/-	0.0300	0.1374	0.2823	0.0424	0.1474	0.2690
DNA	1	VAN -/- vs Ctrl -/-	0.0006	0.6615	0.0001	0.0005	0.7275	0.0001

Level	Time	Feature	Bray-Curtis			W-Unifrac		
			p _{adj}	R ²	Dispersion	p _{adj}	R ²	Dispersion
DNA	2	VAN -/- vs Ctrl -/-	0.0006	0.4915	0.1540	0.0005	0.4826	0.4082
DNA	3	VAN -/- vs Ctrl -/-	0.0006	0.5261	0.0281	0.0005	0.5619	0.0166
DNA	4	VAN -/- vs Ctrl -/-	0.0006	0.3543	0.5507	0.0014	0.3589	0.4968
DNA	10	VAN -/- vs Ctrl -/-	0.0138	0.1381	0.8965	0.0424	0.1580	0.2048
DNA	15	VAN -/- vs Ctrl -/-	0.1932	0.1353	0.0228	0.2324	0.1327	0.0228
DNA	-4	VAN +/- vs Ctrl +/-	0.0974	0.1064	0.6336	0.1345	0.1043	0.3716
DNA	0	VAN +/- vs Ctrl +/-	0.1894	0.0769	0.7736	0.2473	0.0705	0.8377
DNA	1	VAN +/- vs Ctrl +/-	0.0004	0.6959	0.0001	0.0002	0.7426	0.0001
DNA	2	VAN +/- vs Ctrl +/-	0.0007	0.4868	0.0376	0.0007	0.4554	0.0819
DNA	3	VAN +/- vs Ctrl +/-	0.0004	0.5779	0.4782	0.0002	0.6013	0.6668
DNA	4	VAN +/- vs Ctrl +/-	0.0004	0.3579	0.2992	0.0004	0.3683	0.8540
DNA	10	VAN +/- vs Ctrl +/-	0.0004	0.2039	0.1838	0.0002	0.2582	0.2374
DNA	1	VAN -/- Day 0	0.0003	0.7052	0.0010	0.0006	0.7795	0.0049
DNA	2	VAN -/- Day 0	0.0003	0.5560	0.4315	0.0006	0.5677	0.8941
DNA	3	VAN -/- Day 0	0.0006	0.5943	0.0983	0.0006	0.6643	0.0812
DNA	4	VAN -/- Day 0	0.0006	0.4084	0.9825	0.0006	0.4609	0.8758
DNA	10	VAN -/- Day 0	0.0115	0.1498	0.3372	0.0127	0.1753	0.8517
DNA	15	VAN -/- Day 0	0.0722	0.1758	0.0555	0.0434	0.2307	0.1073
DNA	1	VAN +/- Day 0	0.0001	0.6659	0.0001	0.0001	0.7071	0.0001
DNA	2	VAN +/- Day 0	0.0001	0.5358	0.0864	0.0001	0.4808	0.2296
DNA	3	VAN +/- Day 0	0.0001	0.5048	0.0618	0.0001	0.4793	0.1303
DNA	4	VAN +/- Day 0	0.0001	0.3326	0.9825	0.0001	0.3228	0.4212
DNA	10	VAN +/- Day 0	0.0767	0.0941	0.9160	0.1909	0.0643	0.5002
RNA	-4	VAN +/- vs -/-	0.2880	0.1031	0.4117	0.3568	0.1097	0.2864
RNA	0	VAN +/- vs -/-	0.2177	0.1068	0.7204	0.1139	0.1351	0.8893
RNA	1	VAN +/- vs -/-	0.1855	0.1434	0.2596	0.1029	0.1784	0.4287
RNA	2	VAN +/- vs -/-	0.6988	0.0441	0.6142	0.6962	0.0401	0.5294
RNA	3	VAN +/- vs -/-	0.2478	0.1205	0.8262	0.1139	0.1521	0.5101
RNA	4	VAN +/- vs -/-	0.3379	0.0782	0.4940	0.4729	0.0605	0.9988
RNA	10	VAN +/- vs -/-	0.2880	0.0793	0.9363	0.3975	0.0782	0.7829
RNA	-4	VAN -/- vs Ctrl -/-	0.1515	0.1007	0.9429	0.1783	0.1116	0.9293
RNA	0	VAN -/- vs Ctrl -/-	0.0219	0.1379	0.4294	0.0906	0.1494	0.4374
RNA	1	VAN -/- vs Ctrl -/-	0.0004	0.7259	0.0001	0.0004	0.7988	0.0052
RNA	2	VAN -/- vs Ctrl -/-	0.0004	0.5600	0.3530	0.0004	0.5439	0.8518
RNA	3	VAN -/- vs Ctrl -/-	0.0008	0.4745	0.1167	0.0005	0.4924	0.0488
RNA	4	VAN -/- vs Ctrl -/-	0.0008	0.4060	0.9029	0.0024	0.4100	0.8766
RNA	10	VAN -/- vs Ctrl -/-	0.0083	0.1263	0.2165	0.2670	0.0884	0.5705
RNA	15	VAN -/- vs Ctrl -/-	0.2647	0.1192	0.0268	0.3594	0.1064	0.1255
RNA	-4	VAN +/- vs Ctrl +/-	0.1438	0.1027	0.9075	0.2011	0.0924	0.7501

Level	Time	Feature	Bray-Curtis			W-Unifrac		
			p _{adj}	R ²	Dispersion	p _{adj}	R ²	Dispersion
RNA	0	VAN +/- vs Ctrl +/-	0.0908	0.0986	0.2095	0.1559	0.0835	0.2598
RNA	1	VAN +/- vs Ctrl +/-	0.0004	0.6972	0.0001	0.0005	0.7490	0.0013
RNA	2	VAN +/- vs Ctrl +/-	0.0006	0.5466	0.0003	0.0007	0.5273	0.0175
RNA	3	VAN +/- vs Ctrl +/-	0.0004	0.5807	0.6666	0.0005	0.6006	0.9531
RNA	4	VAN +/- vs Ctrl +/-	0.0004	0.3879	0.1948	0.0005	0.3919	0.9366
RNA	10	VAN +/- vs Ctrl +/-	0.0004	0.1736	0.2092	0.0063	0.1743	0.3978
RNA	1	VAN -/- Day 0	0.0003	0.7340	0.0001	0.0006	0.8016	0.0025
RNA	2	VAN -/- Day 0	0.0003	0.5899	0.5438	0.0006	0.5965	0.8521
RNA	3	VAN -/- Day 0	0.0006	0.5783	0.4851	0.0008	0.6526	0.4273
RNA	4	VAN -/- Day 0	0.0006	0.4543	0.7131	0.0011	0.4757	0.6208
RNA	10	VAN -/- Day 0	0.0014	0.1761	0.0886	0.0659	0.1511	0.1980
RNA	15	VAN -/- Day 0	0.0511	0.1868	0.1461	0.0759	0.2181	0.3695
RNA	1	VAN +/- Day 0	0.0001	0.7358	0.0001	0.0001	0.7918	0.0001
RNA	2	VAN +/- Day 0	0.0001	0.6634	0.1636	0.0001	0.6457	0.6010
RNA	3	VAN +/- Day 0	0.0001	0.5946	0.5755	0.0001	0.5987	0.7926
RNA	4	VAN +/- Day 0	0.0001	0.4249	0.0686	0.0001	0.4433	0.4720
RNA	10	VAN +/- Day 0	0.0023	0.1611	0.0995	0.0526	0.1031	0.3162



Supplementary Figure 19: Differently abundant genera between *B4galnt2* mice groups at different time points; Stars represent a $q_{val} < 0.25$.

Supplementary Table 4: Differential abundance of antibiotic resistance gene classes on metagenomics level:

ARG Class	Group	Coef	<i>p</i> _{val}	<i>q</i> _{val}	Time
Aminoglycoside	+/-	0.1814	0.64393	0.74300	0
Beta-lactam	+/-	0.2711	NA	NA	0
Diaminopyrimidine	-/-	-0.1054	0.79637	0.79637	0
Fosmidomycin	+/-	0.5574	NA	NA	0
Glycopeptide	+/-	0.3479	0.35836	0.64175	0
MLS	+/-	0.6232	NA	NA	0
Multidrug	+/-	0.5744	0.00273	0.04097	0
Mupirocin	+/-	0.7084	0.00869	0.06520	0
Nucleoside	+/-	1.0498	0.08589	0.42946	0
Peptide	+/-	0.1947	0.42783	0.64175	0
Polymyxin	+/-	0.1753	0.49504	0.67506	0
Rifamycin	+/-	0.2055	0.62234	0.74300	0
Tetracycline	+/-	0.2203	0.42609	0.64175	0
Unclassified	+/-	0.5718	NA	NA	0
Aminoglycoside	+/-	0.2916	0.39709	0.56727	1
Beta-lactam	+/-	0.3678	0.08043	0.38086	1
Diaminopyrimidine	+/-	0.5067	0.11426	0.38086	1
Fosmidomycin	+/-	0.3343	0.23304	0.56432	1
Glycopeptide	+/-	0.5494	0.33218	0.56432	1
MLS	+/-	0.2991	NA	NA	1
Multidrug	+/-	0.3515	0.33859	0.56432	1
Mupirocin	+/-	0.4175	NA	NA	1
Peptide	+/-	0.5693	NA	NA	1
Polymyxin	+/-	0.2432	NA	NA	1
Rifamycin	+/-	1.3103	0.00648	0.06482	1
Tetracycline	+/-	0.1729	0.76505	0.85005	1
Unclassified	+/-	0.2988	NA	NA	1
Aminoglycoside	-/-	-0.4294	NA	NA	3
Beta-lactam	+/-	0.2045	0.62080	0.79080	3
Diaminopyrimidine	+/-	0.0095	0.98250	0.98250	3
Fosmidomycin	+/-	0.6449	0.15710	0.66768	3
Glycopeptide	-/-	-1.3217	0.02979	0.25323	3
MLS	+/-	0.0327	0.92490	0.98250	3
Multidrug	+/-	0.1083	0.73702	0.83529	3
Mupirocin	-/-	-0.2806	NA	NA	3
Peptide	+/-	0.0959	NA	NA	3
Polymyxin	+/-	0.1824	0.60581	0.79080	3
Rifamycin	-/-	-1.7746	0.00707	0.12019	3
Tetracycline	+/-	0.4744	0.14416	0.66768	3

ARG Class	Group	Coef	p _{val}	q _{val}	Time
Unclassified	-/-	-0.2078	0.57559	0.79080	3
Aminoglycoside	-/-	-0.2659	0.46807	0.49560	15
Beta-lactam	-/-	-0.2343	NA	NA	15
Diaminopyrimidine	-/-	-1.4706	0.00284	0.01023	15
Fosmidomycin	-/-	-1.1954	0.00868	0.02604	15
Glycopeptide	-/-	-0.4805	0.29598	0.38055	15
MLS	-/-	-0.7135	0.14327	0.25788	15
Multidrug	-/-	-0.7329	0.07189	0.18487	15
Mupirocin	-/-	-0.5355	0.29044	0.38055	15
Nucleoside	-/-	-2.3288	0.00231	0.01023	15
Peptide	-/-	-1.0327	0.00118	0.01023	15
Polymyxin	-/-	-1.4473	0.00100	0.01023	15
Rifamycin	+/-	0.1785	NA	NA	15
Tetracycline	-/-	-0.6382	0.00277	0.01023	15
Unclassified	-/-	-0.4510	0.35617	0.41655	15

Supplementary Table 5: Differential abundance of antibiotic resistance gene classes on metatranscriptomics level:

ARG Class	Group	Coef	p _{val}	q _{val}	Time
Aminoglycoside	+/-	0.1625	0.49363	0.94516	0
Beta-lactam	+/-	0.5429	NA	NA	0
Fosmidomycin	+/-	1.6829	NA	NA	0
Glycopeptide	+/-	0.3805	0.16302	0.65934	0
MLS	+/-	0.3628	NA	NA	0
Multidrug	+/-	0.1288	0.73513	0.94516	0
Mupirocin	-/-	-0.1781	0.60479	0.94516	0
Nucleoside	-/-	-0.8210	0.21978	0.65934	0
Peptide	-/-	-0.0164	NA	NA	0
Rifamycin	-/-	-0.4794	NA	NA	0
Tetracycline	+/-	0.4024	0.15011	0.65934	0
Unclassified	+/-	0.2155	0.68300	0.94516	0
Aminoglycoside	-/-	-0.3429	0.01354	0.05415	1
Beta-lactam	+/-	1.0779	NA	NA	1
Fosmidomycin	+/-	0.5465	0.32888	0.50469	1
Glycopeptide	-/-	-0.6828	0.06049	0.16132	1
MLS	-/-	-1.3521	0.01167	0.05415	1
Multidrug	+/-	0.2333	NA	NA	1
Mupirocin	+/-	0.5447	0.24664	0.49327	1
Peptide	-/-	-0.0659	NA	NA	1
Tetracycline	+/-	0.0335	0.90416	0.90416	1

ARG Class	Group	Coef	p _{val}	q _{val}	Time
Unclassified	-/-	-0.9332	0.37852	0.50469	1
Aminoglycoside	-/-	-0.2637	NA	NA	3
Beta-lactam	+/-	0.0510	0.92354	0.92354	3
Fosmidomycin	+/-	0.5561	0.10304	0.24682	3
Glycopeptide	-/-	-1.3265	0.00019	0.00105	3
MLS	+/-	0.1051	NA	NA	3
Multidrug	-/-	-0.8860	0.00002	0.00019	3
Mupirocin	-/-	-1.3405	0.00070	0.00257	3
Peptide	-/-	-0.1374	NA	NA	3
Polymyxin	-/-	-0.2513	0.74122	0.90593	3
Tetracycline	+/-	0.0462	0.85953	0.92354	3
Unclassified	-/-	-1.1143	0.11219	0.24682	3
Aminoglycoside	+/-	0.7994	0.00000	0.00002	15
Beta-lactam	+/-	0.8681	0.01135	0.06242	15
Glycopeptide	-/-	-0.2713	0.62780	0.69057	15
MLS	+/-	0.2434	0.48875	0.59736	15
Multidrug	+/-	0.5802	0.03776	0.10384	15
Mupirocin	+/-	0.4366	0.23050	0.36222	15
Peptide	-/-	-0.0384	NA	NA	15
Rifamycin	+/-	0.2232	0.75254	0.75254	15
Tetracycline	+/-	0.3559	0.38566	0.53028	15
Unclassified	+/-	1.7918	0.02046	0.07501	15

Supplementary Table 6: Differential abundance of antibiotic resistance genes on metatranscriptomics level:

ARG	Group	Coef	p _{val}	q _{val}	Time
aadA	+/-	0.0807	0.79676	0.93187	0
aadE	+/-	0.3198	NA	NA	0
Class A	+/-	0.5687	NA	NA	0
lsa	+/-	0.6199	0.00183	0.01188	0
RpoB8	+/-	0.0902	0.80102	0.93187	0
Saur_mupA_MUP	-/-	-0.1819	0.52987	0.93187	0
tet(32)	+/-	0.5695	0.02425	0.08731	0
tet(O)	+/-	0.9917	0.00175	0.01188	0
tet(W)	+/-	0.9113	0.00198	0.01188	0
vanG	+/-	0.5259	NA	NA	0
vanR	+/-	0.5624	0.01523	0.06854	0
vanS	+/-	0.2823	0.33387	0.75122	0
aadA	-/-	-0.3434	0.01986	0.07236	1
aadE	-/-	-1.0116	0.02412	0.07236	1

ARG	Group	Coef	p_{val}	q_{val}	Time
<i>Class A</i>	+/-	1.1210	NA	NA	1
<i>RpoB8</i>	+/-	0.2350	0.35416	0.53125	1
<i>tet(32)</i>	-/-	-0.8329	0.16328	0.32657	1
<i>aadA</i>	-/-	-0.3227	NA	NA	3
<i>aadE</i>	-/-	-0.0580	0.89305	0.99008	3
<i>Class A</i>	+/-	0.0316	0.95392	0.99008	3
<i>lsa</i>	+/-	0.3594	NA	NA	3
<i>RpoB8</i>	-/-	-0.6764	NA	NA	3
<i>Saur_mupA_MUP</i>	-/-	-1.3405	0.00070	0.00385	3
<i>tet(32)</i>	+/-	0.3107	0.53722	0.84420	3
<i>tet(W)</i>	+/-	0.2008	0.72426	0.99008	3
<i>vanG</i>	-/-	-0.7219	0.03291	0.12066	3
<i>vanR</i>	-/-	-0.6000	0.12526	0.34448	3
<i>vanS</i>	-/-	-1.7651	0.00030	0.00335	3
<i>aadA</i>	+/-	0.8021	0.00000	0.00005	15
<i>aadE</i>	+/-	0.7215	0.20725	0.42259	15
<i>Class A</i>	+/-	0.9170	0.03271	0.14080	15
<i>RpoB8</i>	+/-	0.5803	0.03840	0.14080	15
<i>Saur_mupA_MUP</i>	+/-	0.4366	0.23050	0.42259	15
<i>tet(35)</i>	+/-	0.6335	0.07903	0.21733	15
<i>vanG</i>	-/-	-0.0368	0.96504	0.96504	15
<i>vanR</i>	-/-	-0.0663	0.87635	0.96504	15
<i>vanS</i>	+/-	0.3774	0.39004	0.61292	15

References

- Ackermann, G., Thomalla, S., Ackermann, F., Schaumann, R., Rodloff, A.C., Ruf, B.R., 2005. Prevalence and characteristics of bacteria and host factors in an outbreak situation of antibiotic-associated diarrhoea. *Journal of Medical Microbiology* 54, 149–153. <https://doi.org/10.1099/jmm.0.45812-0>
- Al Atya, A.K., Drider-Hadiouche, K., Ravallac, R., Silvain, A., Vachee, A., Drider, D., 2015. Probiotic potential of *Enterococcus faecalis* strains isolated from meconium. *Front. Microbiol.* 6. <https://doi.org/10.3389/fmicb.2015.00227>
- Antonopoulos, D.A., Huse, S.M., Morrison, H.G., Schmidt, T.M., Sogin, M.L., Young, V.B., 2009. Reproducible Community Dynamics of the Gastrointestinal Microbiota following Antibiotic Perturbation. *Infect Immun* 77, 2367–2375. <https://doi.org/10.1128/IAI.01520-08>
- Arango-Argoty, G., Garner, E., Pruden, A., Heath, L.S., Vikesland, P., Zhang, L., 2018. DeepARG: a deep learning approach for predicting antibiotic resistance genes from metagenomic data. *Microbiome* 6, 23. <https://doi.org/10.1186/s40168-018-0401-z>
- Bailey, M.T., 2012. The contributing role of the intestinal microbiota in stressor-induced increases in susceptibility to enteric infection and systemic immunomodulation. *Hormones and Behavior* 62, 286–294. <https://doi.org/10.1016/j.yhbeh.2012.02.006>
- Bakkeren, E., Güll, E., Huisman, J.S., Steiger, Y., Rocker, A., Hardt, W.-D., Diard, M., 2022. Impact of horizontal gene transfer on emergence and stability of cooperative virulence in *Salmonella* Typhimurium. *Nat Commun* 13, 1939. <https://doi.org/10.1038/s41467-022-29597-7>
- Barthel, M., Hapfelmeier, S., Quintanilla-Martínez, L., Kremer, M., Rohde, M., Hogardt, M., Pfeffer, K., Rüssmann, H., Hardt, W.-D., 2003. Pretreatment of Mice with Streptomycin Provides a *Salmonella enterica* Serovar Typhimurium Colitis Model That Allows Analysis of Both Pathogen and Host. *Infect Immun* 71, 2839–2858. <https://doi.org/10.1128/IAI.71.5.2839-2858.2003>
- Beghini, F., McIver, L.J., Blanco-Míguez, A., Dubois, L., Asnicar, F., Maharjan, S., Mailyan, A., Manghi, P., Scholz, M., Thomas, A.M., Valles-Colomer, M., Weingart, G., Zhang, Y., Zolfo, M., Huttenhower, C., Franzosa, E.A., Segata, N., 2021. Integrating taxonomic, functional, and strain-level profiling of diverse microbial communities with bioBakery 3. *eLife* 10, e65088. <https://doi.org/10.7554/eLife.65088>

Belheouane, M., Vallier, M., Čepić, A., Chung, C.J., Ibrahim, S., Baines, J.F., 2020. Assessing similarities and disparities in the skin microbiota between wild and laboratory populations of house mice. *The ISME Journal* 14, 2367–2380. <https://doi.org/10.1038/s41396-020-0690-7>

Benjamini, Y., Hochberg, Y., 1995. Controlling the False Discovery Rate: A Practical and Powerful Approach to Multiple Testing. *Journal of the Royal Statistical Society: Series B (Methodological)* 57, 289–300. <https://doi.org/10.1111/j.2517-6161.1995.tb02031.x>

Beresford-Jones, B.S., Suyama, S., Clare, S., Soderholm, A., Xia, W., Sardar, P., Harcourt, K., Lawley, T.D., Pedicord, V.A., 2023. *Enterocloster clostridioformis* induces host intestinal epithelial responses that protect against *Salmonella* infection (preprint). *Microbiology*. <https://doi.org/10.1101/2023.07.20.549886>

Bie, L., Zhang, M., Wang, J., Fang, M., Li, L., Xu, H., Wang, M., 2023. Comparative Analysis of Transcriptomic Response of *Escherichia coli* K-12 MG1655 to Nine Representative Classes of Antibiotics. *Microbiol Spectr* 11, e00317-23. <https://doi.org/10.1128/spectrum.00317-23>

Bisanz, J.E., 2018. qiime2R: Importing QIIME2 artifacts and associated data into R sessions.

Bohnhoff, M., Drake, B.L., Miller, C.P., 1954. Effect of Streptomycin on Susceptibility of Intestinal Tract to Experimental *Salmonella* Infection. *Experimental Biology and Medicine* 86, 132–137. <https://doi.org/10.3181/00379727-86-21030>

Bokulich, N.A., Kaehler, B.D., Rideout, J.R., Dillon, M., Bolyen, E., Knight, R., Huttenly, G.A., Gregory Caporaso, J., 2018. Optimizing taxonomic classification of marker-gene amplicon sequences with QIIME 2's q2-feature-classifier plugin. *Microbiome* 6, 90. <https://doi.org/10.1186/s40168-018-0470-z>

Bolger, A.M., Lohse, M., Usadel, B., 2014. Trimmomatic: a flexible trimmer for Illumina sequence data. *Bioinformatics* 30, 2114–2120. <https://doi.org/10.1093/bioinformatics/btu170>

Bolyen, E., Rideout, J.R., Dillon, M.R., Bokulich, N.A., Abnet, C.C., Al-Ghalith, G.A., Alexander, H., Alm, E.J., Arumugam, M., Asnicar, F., Bai, Y., Bisanz, J.E., Bittinger, K., Brejnrod, A., Brislawn, C.J., Brown, C.T., Callahan, B.J., Caraballo-Rodríguez, A.M., Chase, J., Cope, E.K., Da Silva, R., Diener, C., Dorrestein, P.C., Douglas, G.M., Durall, D.M., Duvallet, C., Edwardson, C.F., Ernst, M., Estaki, M., Fouquier, J., Gauglitz, J.M., Gibbons, S.M., Gibson, D.L., Gonzalez, A., Gorlick, K., Guo, J., Hillmann, B., Holmes, S., Holste, H., Huttenhower, C., Huttenly, G.A., Janssen, S., Jarmusch, A.K., Jiang, L.,

Kaehler, B.D., Kang, K.B., Keefe, C.R., Keim, P., Kelley, S.T., Knights, D., Koester, I., Koscioletk, T., Kreps, J., Langille, M.G.I., Lee, J., Ley, R., Liu, Y.-X., Loftfield, E., Lozupone, C., Maher, M., Marotz, C., Martin, B.D., McDonald, D., McIver, L.J., Melnik, A.V., Metcalf, J.L., Morgan, S.C., Morton, J.T., Naimey, A.T., Navas-Molina, J.A., Nothias, L.F., Orchania, S.B., Pearson, T., Peoples, S.L., Petras, D., Preuss, M.L., Pruesse, E., Rasmussen, L.B., Rivers, A., Robeson, M.S., Rosenthal, P., Segata, N., Shaffer, M., Shiffer, A., Sinha, R., Song, S.J., Spear, J.R., Swafford, A.D., Thompson, L.R., Torres, P.J., Trinh, P., Tripathi, A., Turnbaugh, P.J., Ul-Hasan, S., Van Der Hooft, J.J.J., Vargas, F., Vázquez-Baeza, Y., Vogtmann, E., Von Hippel, M., Walters, W., Wan, Y., Wang, M., Warren, J., Weber, K.C., Williamson, C.H.D., Willis, A.D., Xu, Z.Z., Zaneveld, J.R., Zhang, Y., Zhu, Q., Knight, R., Caporaso, J.G., 2019. Reproducible, interactive, scalable and extensible microbiome data science using QIIME 2. *Nat Biotechnol* 37, 852–857. <https://doi.org/10.1038/s41587-019-0209-9>

Caballero, S., Kim, S., Carter, R.A., Leiner, I.M., Sušac, B., Miller, L., Kim, G.J., Ling, L., Pamer, E.G., 2017. Cooperating Commensals Restore Colonization Resistance to Vancomycin-Resistant *Enterococcus faecium*. *Cell Host & Microbe* 21, 592-602.e4. <https://doi.org/10.1016/j.chom.2017.04.002>

Callahan, B.J., McMurdie, P.J., Rosen, M.J., Han, A.W., Johnson, A.J.A., Holmes, S.P., 2016. DADA2: High-resolution sample inference from Illumina amplicon data. *Nat Methods* 13, 581–583. <https://doi.org/10.1038/nmeth.3869>

Candon, S., Perez-Arroyo, A., Marquet, C., Valette, F., Foray, A.-P., Pelletier, B., Milani, C., Ventura, M., Bach, J.-F., Chatenoud, L., 2015. Antibiotics in Early Life Alter the Gut Microbiome and Increase Disease Incidence in a Spontaneous Mouse Model of Autoimmune Insulin-Dependent Diabetes. *PLoS ONE* 10, e0125448. <https://doi.org/10.1371/journal.pone.0125448>

Cheng, D., Xie, M.Z., 2021. A review of a potential and promising probiotic candidate—*Akkermansia muciniphila*. *J Appl Microbiol* 130, 1813–1822. <https://doi.org/10.1111/jam.14911>

De, A., Chen, W., Li, H., Wright, J.R., Lamendella, R., Lukin, D.J., Szymczak, W.A., Sun, K., Kelly, L., Ghosh, S., Kearns, D.B., He, Z., Jobin, C., Luo, X., Byju, A., Chatterjee, S., San Yeoh, B., Vijay-Kumar, M., Tang, J.X., Prajapati, M., Bartnikas, T.B., Mani, S., 2021. Bacterial Swarmers Enriched During Intestinal Stress Ameliorate Damage. *Gastroenterology* 161, 211–224. <https://doi.org/10.1053/j.gastro.2021.03.017>

Dixon, P., 2003. VEGAN, a package of R functions for community ecology. *J Vegetation Science* 14, 927–930. <https://doi.org/10.1111/j.1654-1103.2003.tb02228.x>

- Ducarmon, Q.R., Zwittink, R.D., Hornung, B.V.H., Van Schaik, W., Young, V.B., Kuijper, E.J., 2019. Gut Microbiota and Colonization Resistance against Bacterial Enteric Infection. *Microbiol Mol Biol Rev* 83, e00007-19. <https://doi.org/10.1128/MMBR.00007-19>
- Eberl, C., Weiss, A.S., Jochum, L.M., Durai Raj, A.C., Ring, D., Hussain, S., Herp, S., Meng, C., Kleigrewie, K., Gigl, M., Basic, M., Stecher, B., 2021. *E. coli* enhance colonization resistance against *Salmonella* Typhimurium by competing for galactitol, a context-dependent limiting carbon source. *Cell Host & Microbe* 29, 1680-1692.e7. <https://doi.org/10.1016/j.chom.2021.09.004>
- Faith, D.P., 1992. Conservation evaluation and phylogenetic diversity. *Biological Conservation* 61, 1–10. [https://doi.org/10.1016/0006-3207\(92\)91201-3](https://doi.org/10.1016/0006-3207(92)91201-3)
- Ferreira, R.B.R., Gill, N., Willing, B.P., Antunes, L.C.M., Russell, S.L., Croxen, M.A., Finlay, B.B., 2011. The Intestinal Microbiota Plays a Role in *Salmonella*-Induced Colitis Independent of Pathogen Colonization. *PLoS ONE* 6, e20338. <https://doi.org/10.1371/journal.pone.0020338>
- FitzGerald, J., Patel, S., Eckenerger, J., Guillemard, E., Veiga, P., Schäfer, F., Walter, J., Claesson, M.J., Derrien, M., 2022. Improved gut microbiome recovery following drug therapy is linked to abundance and replication of probiotic strains. *Gut Microbes* 14, 2094664. <https://doi.org/10.1080/19490976.2022.2094664>
- Fuchs, L.M., 2023. Identification of carbon and nitrogen sources promoting *Salmonella* Typhimurium gut colonization. ETH Zurich. <https://doi.org/10.3929/ETHZ-B-000642973>
- Garner, C.D., Antonopoulos, D.A., Wagner, B., Duhamel, G.E., Keresztes, I., Ross, D.A., Young, V.B., Altier, C., 2009. Perturbation of the Small Intestine Microbial Ecology by Streptomycin Alters Pathology in a *Salmonella enterica* Serovar Typhimurium Murine Model of Infection. *Infect Immun* 77, 2691–2702. <https://doi.org/10.1128/IAI.01570-08>
- Gravet, A., Rondeau, M., Harf-Monteil, C., Grunenberger, F., Monteil, H., Scheftel, J.-M., Prévost, G., 1999. Predominant *Staphylococcus aureus* Isolated from Antibiotic-Associated Diarrhea Is Clinically Relevant and Produces Enterotoxin A and the Bicomponent Toxin LukE-LukD. *J Clin Microbiol* 37, 4012–4019. <https://doi.org/10.1128/JCM.37.12.4012-4019.1999>
- Griffith, R.S., 1984. Vancomycin use--an historical review. *Journal of Antimicrobial Chemotherapy* 14, 1–5. https://doi.org/10.1093/jac/14.suppl_D.1

- Hentges, D.J., Pongpech, P., Que, J.U., 1990. Hypothesis: How Streptomycin Treatment Compromises Colonisation Resistance Against Enteric Pathogens in Mice. *Microbial Ecology in Health and Disease* 3, 105–111. <https://doi.org/10.3109/08910609009140124>
- Hollingshead, S., Vapnek, D., 1985. Nucleotide sequence analysis of a gene encoding a streptomycin/spectinomycin adenyltransferase. *Plasmid* 13, 17–30. [https://doi.org/10.1016/0147-619X\(85\)90052-6](https://doi.org/10.1016/0147-619X(85)90052-6)
- Hung, L.Y., Boonma, P., Unterweger, P., Parathan, P., Haag, A., Luna, R.A., Bornstein, J.C., Savidge, T.C., Foong, J.P.P., 2019. Neonatal Antibiotics Disrupt Motility and Enteric Neural Circuits in Mouse Colon. *Cellular and Molecular Gastroenterology and Hepatology* 8, 298-300.e6. <https://doi.org/10.1016/j.jcmgh.2019.04.009>
- Jose, R., Singh, V., 2020. Swarming in Bacteria: A Tale of Plasticity in Motility Behavior. *J Indian Inst Sci* 100, 515–524. <https://doi.org/10.1007/s41745-020-00177-2>
- Katoh, K., 2002. MAFFT: a novel method for rapid multiple sequence alignment based on fast Fourier transform. *Nucleic Acids Research* 30, 3059–3066. <https://doi.org/10.1093/nar/gkf436>
- Kesavelu, D., Jog, P., 2023. Current understanding of antibiotic-associated dysbiosis and approaches for its management. *Therapeutic Advances in Infection* 10, 204993612311544. <https://doi.org/10.1177/20499361231154443>
- Kim, W., Killam, T., Sood, V., Surette, M.G., 2003. Swarm-Cell Differentiation in *Salmonella enterica* Serovar Typhimurium Results in Elevated Resistance to Multiple Antibiotics. *J Bacteriol* 185, 3111–3117. <https://doi.org/10.1128/JB.185.10.3111-3117.2003>
- Kim, W., Surette, M.G., 2003. Swarming populations of *Salmonella* represent a unique physiological state coupled to multiple mechanisms of antibiotic resistance. *Biol. Proced. Online* 5, 189–196. <https://doi.org/10.1251/bpo61>
- Lai, S., Tremblay, J., Déziel, E., 2009. Swarming motility: a multicellular behaviour conferring antimicrobial resistance. *Environmental Microbiology* 11, 126–136. <https://doi.org/10.1111/j.1462-2920.2008.01747.x>
- Lange, K., Buerger, M., Stallmach, A., Bruns, T., 2016. Effects of Antibiotics on Gut Microbiota. *Dig Dis* 34, 260–268. <https://doi.org/10.1159/000443360>
- Langmead, B., Salzberg, S.L., 2012. Fast gapped-read alignment with Bowtie 2. *Nat Methods* 9, 357–359. <https://doi.org/10.1038/nmeth.1923>

- Laubitz, D., Typpo, K., Midura-Kiela, M., Brown, C., Barberán, A., Ghishan, F.K., Kiela, P.R., 2021. Dynamics of Gut Microbiota Recovery after Antibiotic Exposure in Young and Old Mice (A Pilot Study). *Microorganisms* 9, 647. <https://doi.org/10.3390/microorganisms9030647>
- Lee, H.B., Jeong, D.H., Cho, B.C., Park, J.S., 2023. Comparative analyses of eight primer sets commonly used to target the bacterial 16S rRNA gene for marine metabarcoding-based studies. *Front. Mar. Sci.* 10, 1199116. <https://doi.org/10.3389/fmars.2023.1199116>
- Liu, J., Liu, Hongli, Liu, Huanhuan, Teng, Y., Qin, N., Ren, X., Xia, X., 2023. Live and pasteurized *Akkermansia muciniphila* decrease susceptibility to *Salmonella* Typhimurium infection in mice. *Journal of Advanced Research* S2090123223000905. <https://doi.org/10.1016/j.jare.2023.03.008>
- Liu, X., Mao, B., Gu, J., Wu, J., Cui, S., Wang, G., Zhao, J., Zhang, H., Chen, W., 2021. *Blautia* — a new functional genus with potential probiotic properties? *Gut Microbes* 13, 1875796. <https://doi.org/10.1080/19490976.2021.1875796>
- Lu, J., Breitwieser, F.P., Thielen, P., Salzberg, S.L., 2017. Bracken: estimating species abundance in metagenomics data. *PeerJ Computer Science* 3, e104. <https://doi.org/10.7717/peerj-cs.104>
- Luo, W., Shen, Z., Deng, M., Li, X., Tan, B., Xiao, M., Wu, S., Yang, Z., Zhu, C., Tian, L., Wu, X., Meng, X., Quan, Y., Wang, X., 2019. *Roseburia intestinalis* supernatant ameliorates colitis induced in mice by regulating the immune response. *Mol Med Report*. <https://doi.org/10.3892/mmr.2019.10327>
- Macnab, R.M., Aizawa, S.-I., 1984. Bacterial Motility and the Bacterial Flagellar Motor. *Annu. Rev. Biophys. Bioeng.* 13, 51–83. <https://doi.org/10.1146/annurev.bb.13.060184.000411>
- Mallick, H., Rahnavard, A., McIver, L.J., Ma, S., Zhang, Y., Nguyen, L.H., Tickle, T.L., Weingart, G., Ren, B., Schwager, E.H., Chatterjee, S., Thompson, K.N., Wilkinson, J.E., Subramanian, A., Lu, Y., Waldron, L., Paulson, J.N., Franzosa, E.A., Bravo, H.C., Huttenhower, C., 2021. Multivariable association discovery in population-scale meta-omics studies. *PLoS Comput. Biol.* 17, e1009442. <https://doi.org/10.1371/journal.pcbi.1009442>
- Mann, H.B., Whitney, D.R., 1947. On a Test of Whether one of Two Random Variables is Stochastically Larger than the Other. *Ann. Math. Statist.* 18, 50–60. <https://doi.org/10.1214/aoms/1177730491>

- Maurin, M., Raoult, D., 2001. Use of Aminoglycosides in Treatment of Infections Due to Intracellular Bacteria. *Antimicrob Agents Chemother* 45, 2977–2986. <https://doi.org/10.1128/AAC.45.11.2977-2986.2001>
- McMurdie, P., Paulson, J., 2017. biomformat. <https://doi.org/10.18129/B9.BIOC.BIOMFORMAT>
- McMurdie, P.J., Holmes, S., 2013. phyloseq: An R Package for Reproducible Interactive Analysis and Graphics of Microbiome Census Data. *PLoS ONE* 8, e61217. <https://doi.org/10.1371/journal.pone.0061217>
- Miller, C.P., Bohnhoff, M., 1963. Changes in the mouse's enteric microflora associated with enhanced susceptibility to *Salmonella* infection following streptomycin treatment*. *The Journal of Infectious Diseases* 113, 59–66. <https://doi.org/10.1093/infdis/113.1.59>
- Mohlke, K.L., Purkayastha, A.A., Westrick, R.J., Smith, P.L., Petryniak, B., Lowe, J.B., Ginsburg, D., 1999. Mvwf, a Dominant Modifier of Murine von Willebrand Factor, Results from Altered Lineage-Specific Expression of a Glycosyltransferase. *Cell* 96, 111–120. [https://doi.org/10.1016/S0092-8674\(00\)80964-2](https://doi.org/10.1016/S0092-8674(00)80964-2)
- Ng, K.M., Aranda-Díaz, A., Tropini, C., Frankel, M.R., Van Treuren, W., O'Loughlin, C.T., Merrill, B.D., Yu, F.B., Pruss, K.M., Oliveira, R.A., Higginbottom, S.K., Neff, N.F., Fischbach, M.A., Xavier, K.B., Sonnenburg, J.L., Huang, K.C., 2019. Recovery of the Gut Microbiota after Antibiotics Depends on Host Diet, Community Context, and Environmental Reservoirs. *Cell Host & Microbe* 26, 650-665.e4. <https://doi.org/10.1016/j.chom.2019.10.011>
- Osbelt, L., Wende, M., Almási, É., Derksen, E., Muthukumarasamy, U., Lesker, T.R., Galvez, E.J.C., Pils, M.C., Schalk, E., Chhatwal, P., Färber, J., Neumann-Schaal, M., Fischer, T., Schlüter, D., Strowig, T., 2021. *Klebsiella oxytoca* causes colonization resistance against multidrug-resistant *K. pneumoniae* in the gut via cooperative carbohydrate competition. *Cell Host & Microbe* 29, 1663-1679.e7. <https://doi.org/10.1016/j.chom.2021.09.003>
- Overhage, J., Bains, M., Brazas, M.D., Hancock, R.E.W., 2008. Swarming of *Pseudomonas aeruginosa* Is a Complex Adaptation Leading to Increased Production of Virulence Factors and Antibiotic Resistance. *J Bacteriol* 190, 2671–2679. <https://doi.org/10.1128/JB.01659-07>
- Palleja, A., Mikkelsen, K.H., Forslund, S.K., Kashani, A., Allin, K.H., Nielsen, T., Hansen, T.H., Liang, S., Feng, Q., Zhang, C., Pyl, P.T., Coelho, L.P., Yang, H., Wang, Jian, Typas, A., Nielsen, M.F., Nielsen, H.B., Bork, P., Wang, Jun, Vilsbøll, T., Hansen, T., Knop, F.K.,

Arumugam, M., Pedersen, O., 2018. Recovery of gut microbiota of healthy adults following antibiotic exposure. *Nat Microbiol* 3, 1255–1265. <https://doi.org/10.1038/s41564-018-0257-9>

Patterson, A.M., Mulder, I.E., Travis, A.J., Lan, A., Cerf-Bensussan, N., Gaboriau-Routhiau, V., Garden, K., Logan, E., Delday, M.I., Coutts, A.G.P., Monnais, E., Ferraria, V.C., Inoue, R., Grant, G., Aminov, R.I., 2017. Human Gut Symbiont *Roseburia hominis* Promotes and Regulates Innate Immunity. *Front. Immunol.* 8, 1166. <https://doi.org/10.3389/fimmu.2017.01166>

Philbrick, A.M., Ernst, M.E., 2007. Amoxicillin-Associated Hemorrhagic Colitis in the Presence of *Klebsiella oxytoca*. *Pharmacotherapy* 27, 1603–1607. <https://doi.org/10.1592/phco.27.11.1603>

Price, M.N., Dehal, P.S., Arkin, A.P., 2009. FastTree: Computing Large Minimum Evolution Trees with Profiles instead of a Distance Matrix. *Molecular Biology and Evolution* 26, 1641–1650. <https://doi.org/10.1093/molbev/msp077>

Quan, Y., Song, K., Zhang, Y., Zhu, C., Shen, Z., Wu, S., Luo, W., Tan, B., Yang, Z., Wang, X., 2018. *Roseburia intestinalis* -derived flagellin is a negative regulator of intestinal inflammation. *Biochemical and Biophysical Research Communications* 501, 791–799. <https://doi.org/10.1016/j.bbrc.2018.05.075>

Quast, C., Pruesse, E., Yilmaz, P., Gerken, J., Schweer, T., Yarza, P., Peplies, J., Glöckner, F.O., 2012. The SILVA ribosomal RNA gene database project: improved data processing and web-based tools. *Nucleic Acids Research* 41, D590–D596. <https://doi.org/10.1093/nar/gks1219>

Ramirez, M.S., Tolmasky, M.E., 2010. Aminoglycoside modifying enzymes. *Drug Resistance Updates* 13, 151–171. <https://doi.org/10.1016/j.drup.2010.08.003>

Rausch, P., Steck, N., Suwandi, A., Seidel, J.A., Künzel, S., Bhullar, K., Basic, M., Bleich, A., Johnsen, J.M., Vallance, B.A., Baines, J.F., Grassl, G.A., 2015. Expression of the Blood-Group-Related Gene *B4galnt2* Alters Susceptibility to *Salmonella* Infection. *PLoS Pathog* 11, e1005008. <https://doi.org/10.1371/journal.ppat.1005008>

Reynolds, P.E., 1989. Structure, biochemistry and mechanism of action of glycopeptide antibiotics. *Eur. J. Clin. Microbiol. Infect. Dis.* 8, 943–950. <https://doi.org/10.1007/BF01967563>

Round, J.L., Mazmanian, S.K., 2009. The gut microbiota shapes intestinal immune responses during health and disease. *Nat Rev Immunol* 9, 313–323. <https://doi.org/10.1038/nri2515>

- Rowland, I., Gibson, G., Heinken, A., Scott, K., Swann, J., Thiele, I., Tuohy, K., 2018. Gut microbiota functions: metabolism of nutrients and other food components. *Eur J Nutr* 57, 1–24. <https://doi.org/10.1007/s00394-017-1445-8>
- Sekirov, I., Tam, N.M., Joga, M., Robertson, M.L., Li, Y., Lupp, C., Finlay, B.B., 2008. Antibiotic-Induced Perturbations of the Intestinal Microbiota Alter Host Susceptibility to Enteric Infection. *Infect Immun* 76, 4726–4736. <https://doi.org/10.1128/IAI.00319-08>
- Staubach, F., Künzel, S., Baines, A.C., Yee, A., McGee, B.M., Bäckhed, F., Baines, J.F., Johnsen, J.M., 2012. Expression of the blood-group-related glycosyltransferase *B4galnt2* influences the intestinal microbiota in mice. *ISME J* 6, 1345–1355. <https://doi.org/10.1038/ismej.2011.204>
- Stecher, B., Macpherson, A.J., Hapfelmeier, S., Kremer, M., Stallmach, T., Hardt, W.-D., 2005. Comparison of *Salmonella enterica* Serovar Typhimurium Colitis in Germfree Mice and Mice Pretreated with Streptomycin. *Infect Immun* 73, 3228–3241. <https://doi.org/10.1128/IAI.73.6.3228-3241.2005>
- Strati, F., Pujolassos, M., Burrello, C., Giuffrè, M.R., Lattanzi, G., Caprioli, F., Troisi, J., Facciotti, F., 2021. Antibiotic-associated dysbiosis affects the ability of the gut microbiota to control intestinal inflammation upon fecal microbiota transplantation in experimental colitis models. *Microbiome* 9, 39. <https://doi.org/10.1186/s40168-020-00991-x>
- Suar, M., Jantsch, J., Hapfelmeier, S., Kremer, M., Stallmach, T., Barrow, P.A., Hardt, W.-D., 2006. Virulence of Broad- and Narrow-Host-Range *Salmonella enterica* Serovars in the Streptomycin-Pretreated Mouse Model. *Infect Immun* 74, 632–644. <https://doi.org/10.1128/IAI.74.1.632-644.2006>
- Sun, E., Gill, E.E., Falsafi, R., Yeung, A., Liu, S., Hancock, R.E.W., 2018a. Broad-Spectrum Adaptive Antibiotic Resistance Associated with *Pseudomonas aeruginosa* Mucin-Dependent Surfing Motility. *Antimicrob Agents Chemother* 62, e00848-18. <https://doi.org/10.1128/AAC.00848-18>
- Sun, E., Liu, S., Hancock, R.E.W., 2018b. Surfing Motility: a Conserved yet Diverse Adaptation among Motile Bacteria. *J Bacteriol* 200. <https://doi.org/10.1128/JB.00394-18>
- Tamada, H., Ikuta, K., Makino, Y., Joho, D., Suzuki, T., Kakeyama, M., Matsumoto, M., 2022. Impact of Intestinal Microbiota on Cognitive Flexibility by a Novel Touch Screen Operant System Task in Mice. *Front. Neurosci.* 16, 882339. <https://doi.org/10.3389/fnins.2022.882339>

- Theriot, C.M., Koenigsknecht, M.J., Carlson, P.E., Hatton, G.E., Nelson, A.M., Li, B., Huffnagle, G.B., Z. Li, J., Young, V.B., 2014. Antibiotic-induced shifts in the mouse gut microbiome and metabolome increase susceptibility to *Clostridium difficile* infection. *Nat Commun* 5, 3114. <https://doi.org/10.1038/ncomms4114>
- Thompson, J.A., Oliveira, R.A., Djukovic, A., Ubeda, C., Xavier, K.B., 2015. Manipulation of the Quorum Sensing Signal AI-2 Affects the Antibiotic-Treated Gut Microbiota. *Cell Reports* 10, 1861–1871. <https://doi.org/10.1016/j.celrep.2015.02.049>
- Umezawa, H., Ueda, M., Maeda, K., Yagishita, K., Kondō, S., Okami, Y., Utahara, R., Ōsato, Y., Nitta, K., Takeuchi, T., 1957. Production and Isolation of a New Antibiotic, Kanamycin. https://doi.org/10.11554/antibiotics.a.10.5_181
- Vallier, M., 2017. Characterization of pathogen-driven selection at B4galnt2 in house mice. Christian-Albrechts-Universität, Kiel.
- Van Der Waaij, D., Berghuis, J.M., Lekkerkerk, J.E.C., 1972. Colonization resistance of the digestive tract of mice during systemic antibiotic treatment. *Epidemiol. Infect.* 70, 605–610. <https://doi.org/10.1017/S0022172400022464>
- Wadhwa, N., Berg, H.C., 2022. Bacterial motility: machinery and mechanisms. *Nat Rev Microbiol* 20, 161–173. <https://doi.org/10.1038/s41579-021-00626-4>
- Waksman, S.A., Reilly, H.C., Johnstone, D.B., 1946. Isolation of streptomycin-producing strains of *Streptomyces griseus*. *Journal of bacteriology* 52, 393–397.
- Walker, G.T., Gerner, R.R., Nuccio, S., Raffatellu, M., 2023. Murine Models of *Salmonella* Infection. *Current Protocols* 3, e824. <https://doi.org/10.1002/cpz1.824>
- Wang, Qi-Wen, Jia, D., He, J., Sun, Y., Qian, Y., Ge, Q., Qi, Y., Wang, Qing-Yi, Hu, Y., Wang, Lan, Fang, Y., He, H., Luo, M., Feng, L., Si, J., Song, Z., Wang, Liang-Jing, Chen, S., 2023. *Lactobacillus Intestinalis* Primes Epithelial Cells to Suppress Colitis-Related Th17 Response by Host-Microbe Retinoic Acid Biosynthesis. *Advanced Science* 10, 2303457. <https://doi.org/10.1002/advs.202303457>
- Wickham, H., 2016. *ggplot2: Elegant Graphics for Data Analysis*, 2nd ed. 2016. ed, Use R! Springer International Publishing : Imprint: Springer, Cham. <https://doi.org/10.1007/978-3-319-24277-4>
- Wilcoxon, F., 1945. Individual Comparisons by Ranking Methods. *Biometrics Bulletin* 1, 80. <https://doi.org/10.2307/3001968>
- Wilhelm, M.P., 1991. Vancomycin. *Mayo Clinic Proceedings* 66, 1165–1170. [https://doi.org/10.1016/S0025-6196\(12\)65799-1](https://doi.org/10.1016/S0025-6196(12)65799-1)

- Woo, H., Okamoto, S., Guiney, D., Gunn, J.S., Fierer, J., 2008. A Model of *Salmonella* Colitis with Features of Diarrhea in SLC11A1 Wild-Type Mice. PLoS ONE 3, e1603. <https://doi.org/10.1371/journal.pone.0001603>
- Wood, D.E., Salzberg, S.L., 2014. Kraken: ultrafast metagenomic sequence classification using exact alignments. Genome Biol 15, R46. <https://doi.org/10.1186/gb-2014-15-3-r46>
- Wotzka, S.Y., Kreuzer, M., Maier, L., Arnoldini, M., Nguyen, B.D., Brachmann, A.O., Berthold, D.L., Zünd, M., Hausmann, A., Bakkeren, E., Hoces, D., Gül, E., Beutler, M., Dolowschiak, T., Zimmermann, M., Fuhrer, T., Moor, K., Sauer, U., Typas, A., Piel, J., Diard, M., Macpherson, A.J., Stecher, B., Sunagawa, S., Slack, E., Hardt, W.-D., 2019. *Escherichia coli* limits *Salmonella* Typhimurium infections after diet shifts and fat-mediated microbiota perturbation in mice. Nat Microbiol 4, 2164–2174. <https://doi.org/10.1038/s41564-019-0568-5>
- Wu, H.-J., Wu, E., 2012. The role of gut microbiota in immune homeostasis and autoimmunity. Gut Microbes 3, 4–14. <https://doi.org/10.4161/gmic.19320>
- Wu, X., Pan, S., Luo, W., Shen, Z., Meng, X., Xiao, M., Tan, B., Nie, K., Tong, T., Wang, X., 2020. Roseburia intestinalis-derived flagellin ameliorates colitis by targeting miR-223-3p-mediated activation of NLRP3 inflammasome and pyroptosis. Mol Med Rep. <https://doi.org/10.3892/mmr.2020.11351>
- Yang, R., Shan, S., Shi, J., Li, H., An, N., Li, S., Cui, K., Guo, H., Li, Z., 2023. Coprococcus eutactus , a Potent Probiotic, Alleviates Colitis via Acetate-Mediated IgA Response and Microbiota Restoration. J. Agric. Food Chem. 71, 3273–3284. <https://doi.org/10.1021/acs.jafc.2c06697>
- Yeung, A.T.Y., Parayno, A., Hancock, R.E.W., 2012. Mucin Promotes Rapid Surface Motility in *Pseudomonas aeruginosa*. mBio 3, e00073-12. <https://doi.org/10.1128/mBio.00073-12>
- Yun, B., Song, M., Park, D.-J., Oh, S., 2017. Beneficial Effect of *Bifidobacterium longum* ATCC 15707 on Survival Rate of *Clostridium difficile* Infection in Mice. Korean Journal for Food Science of Animal Resources 37, 368–375. <https://doi.org/10.5851/kosfa.2017.37.3.368>
- Zegadło, K., Gieroń, M., Żarnowiec, P., Durlik-Popińska, K., Kręcisz, B., Kaca, W., Czerwonka, G., 2023. Bacterial Motility and Its Role in Skin and Wound Infections. IJMS 24, 1707. <https://doi.org/10.3390/ijms24021707>
- Zhang, C., Ma, K., Nie, K., Deng, M., Luo, W., Wu, X., Huang, Y., Wang, X., 2022. Assessment of the safety and probiotic properties of *Roseburia intestinalis*: A potential “Next

Generation Probiotic." Front. Microbiol. 13, 973046.
<https://doi.org/10.3389/fmicb.2022.973046>

Zhang, C., Yu, Z., Zhao, J., Zhang, H., Zhai, Q., Chen, W., 2019. Colonization and probiotic function of *Bifidobacterium longum*. Journal of Functional Foods 53, 157–165.
<https://doi.org/10.1016/j.jff.2018.12.022>

Zhu, C., Song, K., Shen, Z., Quan, Y., Tan, B., Luo, W., Wu, S., Tang, K., Yang, Z., Wang, X., 2018. *Roseburia intestinalis* inhibits interleukin-17 excretion and promotes regulatory T cells differentiation in colitis. Mol Med Report.
<https://doi.org/10.3892/mmr.2018.8833>

Chapter 4: The *B4galnt2*-Associated Microbiota Plays a Protective Role in Susceptibility to Intestinal Infections in Wild Mice

Introduction

The microbiota is a complex ecosystem comprising billions of microorganisms that colonize various body sites, including the skin, respiratory tract, urogenital tract, oral cavity, and notably the gastrointestinal tract. These diverse microbial communities have a strong influence on host metabolism, immunity, and susceptibility to pathogens (Nicholson et al., 2012; Panwar et al., 2021; Zheng et al., 2020). Gastrointestinal microbiota, plays important role in maintaining the integrity of the mucosal barrier and modulating immune responses (Belkaid and Hand, 2014; Gieryńska et al., 2022).

The gastrointestinal mucosa is coated by a protective layer of highly glycosylated mucus, which serves not only as a physical barrier separating the host from its microbiota but also as a crucial interface for host-microbiome interactions (Johansson et al., 2011; Koropatkin et al., 2012; Linden et al., 2008). This mucus layer is rich in glycans and is integral to these interactions, influencing the composition and function of the microbiota (Koropatkin et al., 2012; Staubach et al., 2012). These endogenous glycans provide nutrient sources for resident microbes as well as binding sites for many commensal bacteria (Luis and Hansson, 2023; Tailford et al., 2015).

B4galnt2 (Beta-1,4 N-acetyl galactosaminyl transferase 2) is a blood group related glycosyltransferase gene, which exhibits signatures of long-term balancing selection in wild mouse populations (Johnsen et al., 2009; Linnenbrink et al., 2011; Vallier, 2017; Vallier et al., 2023). A 2015 study by Rausch et al. on inbred mouse lab strains demonstrated that this dynamic may arise from a trade-off between susceptibility to a pathogen and the cost of prolonged bleeding, which is associated with the RIIIS/J strain (Rausch et al., 2015). In mice, the RIIIS/J strain has an alternative *B4galnt2* allele that switches *B4galnt2* expression from the gut to blood vessels, altering glycosylation of von Willebrand factor (VWF), which results in faster clearance of VWF and prolonged bleeding time (Mohlke et al., 1999; Vallier, 2017; Vallier et al., 2023). Furthermore, differences in intestinal *B4galnt2* expression are associated with distinct microbial compositions in both lab and wild mice (Rausch et al., 2015; Staubach et al., 2012; Vallier, 2017; Vallier et al., 2023). Moreover, studies on wild mouse populations have identified a correlation between the *B4galnt2* genotype and gastrointestinal inflammation (Vallier, 2017; Vallier et al., 2023). Using 16S rRNA gene-based community profiling, it was found

that the *Morganella morganii* subspecies is associated with the *B4galnt2* gut-expressing mice (C57BL/6J) and gastrointestinal inflammation (Vallier, 2017; Vallier et al., 2023).

This study builds on previous research by incorporating shotgun metagenomic sequencing data and exploring in greater depth both the pathogenic and the beneficial aspects of the *B4galnt2*-associated microbiota. The overall aim is to identify taxonomical markers associated with protection against invading pathogens, which is driven by differential *B4galnt2* expression patterns.

Materials and methods

A previous study investigated the role of *B4galnt2* gene expression and resistance to *M. morganii* in wild mouse populations (Vallier et al., 2023). For this study two hundred and seventeen wild mice were captured around the southwestern French town of Espelette (Vallier et al., 2023). A subset of 46 samples from this dataset, representing different inflammatory statuses, genotypes, sexes, haplogroups and populations, was selected for comprehensive metagenomic analysis in this study (Supplementary Table 1). Body weight, length and sex were recorded for each mouse (Vallier et al., 2023). The mitochondrial D-loop segment was sequenced and aligned to reference sequences to determine haplogroups of wild house mice (Vallier et al., 2023). Microsatellite typing of eighteen neutral autosomal loci was performed using Geneious (v.7.0) and analyzed using STRUCTURE (2.3.4) software as previously described (Belheouane et al., 2020; Vallier et al., 2023).

Samples were processed using the QIAamp PowerFecal Pro DNA Kit (Qiagen). The manufacturer's protocol was followed, with the exception of a modification in the first homogenization step, where the Bead Ruptor 24 Elite (Omni International) was employed. The extracted DNA was processed using the Nextera Library Preparation Kit. Libraries were sequenced using the Illumina NextSeq 550 System High-Output sequencing kit.

Paired raw reads from each sample were filtered for quality and potential mouse contamination by mapping reads to the mouse reference genome (mouse_C57BL) using KneadData version 0.7.10. Relative sequence abundances of each species and genus were generated using Kraken v2.1.2 and Bracken v2.2 tools with the PlusPFP database (Lu et al., 2017; Wood and Salzberg, 2014). Microbiota abundance tables were imported into R using the biomformat v1.26.0 and phyloseq v1.42.0 packages (McMurdie and Paulson, 2017; McMurdie and Holmes, 2013). Samples with at least 49000 species-level and 100000 genus-level Kraken2/Bracken classified reads were kept for taxonomic analysis. Taxa relative sequence abundances were filtered, requiring each taxa to have an average abundance of at least 0.01 % per sample.

Microbial alpha diversity indices, Shannon index, and Simpson index were computed using the microbiome package (Lahti, Shetty et al., 2017). Beta diversity was calculated using Jaccard and Bray-Curtis indices using the vegan package v2.6-4 in R (Dixon, 2003) and summarized using Principal Coordinates Analysis (PCoA) with microViz (Barnett et al., 2021).

Microbiome Multivariable Associations with Linear Models - MaAsLin2 (v1.12.0) was used to quantify differences between taxonomic profiles by *B4galnt2* genotype and to adjust for the covariates of sex and population (Mallick et al., 2021). P-values were adjusted using the Benjamini-Hochberg procedure (FDR) for each group.

Spearman correlations were calculated between taxa relative abundances, inflammation scores, and alpha diversity indices (Shannon and Simpson). Results were visualized using the ggplot2 package (v3.4.4) (Wickham, 2016).

Results

Vallier et al., 2023 conducted a study to investigate the potential link between *B4galnt2* genotype and susceptibility to gastrointestinal pathogens in the wild (Vallier et al., 2023). To identify candidate pathogens whose susceptibility might be mediated by *B4galnt2* genotype, 16S rRNA gene-based community profiling was conducted. *M. morganii* was identified as a potential candidate pathogen, and subsequently confirmed using in vivo models of infection (Vallier et al., 2023). Our study employed an advanced deep sequencing method on a subset of the original data set (Supplementary Table 1), offering a more detailed analysis of microbial pathogens and potential beneficial taxa.

At the phylum level, no significant differences were observed according to *B4galnt2* genotype (Figure 1). The majority of samples were primarily composed of three dominant phyla (Supplementary Table 2), namely Actinobacteria ($13.30 \pm 21.24\%$), Bacteroidetes ($14.16 \pm 23.65\%$), and Firmicutes ($63.23 \pm 31.09\%$), with members of the Lactobacillaceae ($44.70 \pm 33.50\%$) being the most abundant family (Supplementary Table 3).

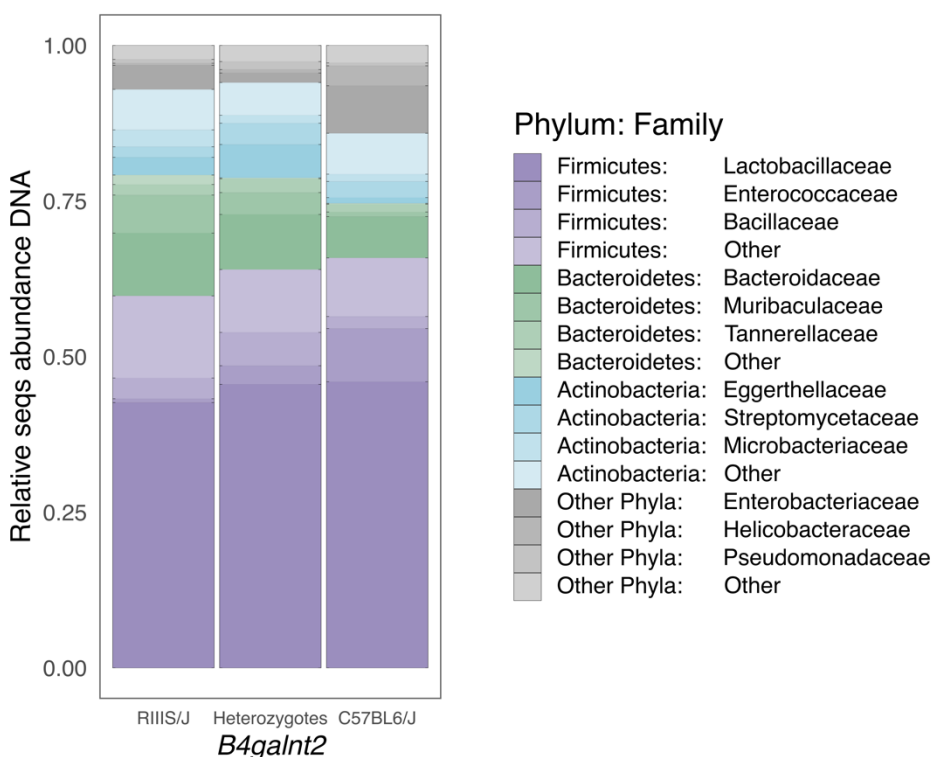


Figure 1: Fecal microbiome composition: Relative sequence abundance in *B4galnt2*-associated microbial communities at the phylum and family levels.

Alpha diversity, measured by Shannon and Simpson indices at both species and genus levels, showed no significant differences according to *B4galnt2* genotype (Kruskal-Wallis test: Shannon index – genus: $p_{val} = 0.37$; Simpson index – genus: $p_{val} = 0.52$; Shannon index – species: $p_{val} = 0.35$; Simpson index – species: $p_{val} = 0.38$) (Supplementary Figure 1).

Spearman's correlation analysis of both alpha diversity metrics was performed against inflammation score for all *B4galnt2* genotypes together and each genotype separately. A significant negative correlation was observed among mice homozygous for the C57BL/6J allele and inflammation score at both the genus (Shannon: $r_s = 0.64, p_{val} = 0.0072$; Simpson: $r_s = 0.56, p_{val} = 0.025$) (Figure 2) and species (Shannon: $r_s = 0.5, p_{val} = 0.053$; Simpson: $r_s = 0.49, p_{val} = 0.025$) levels (Supplementary Figure 2).

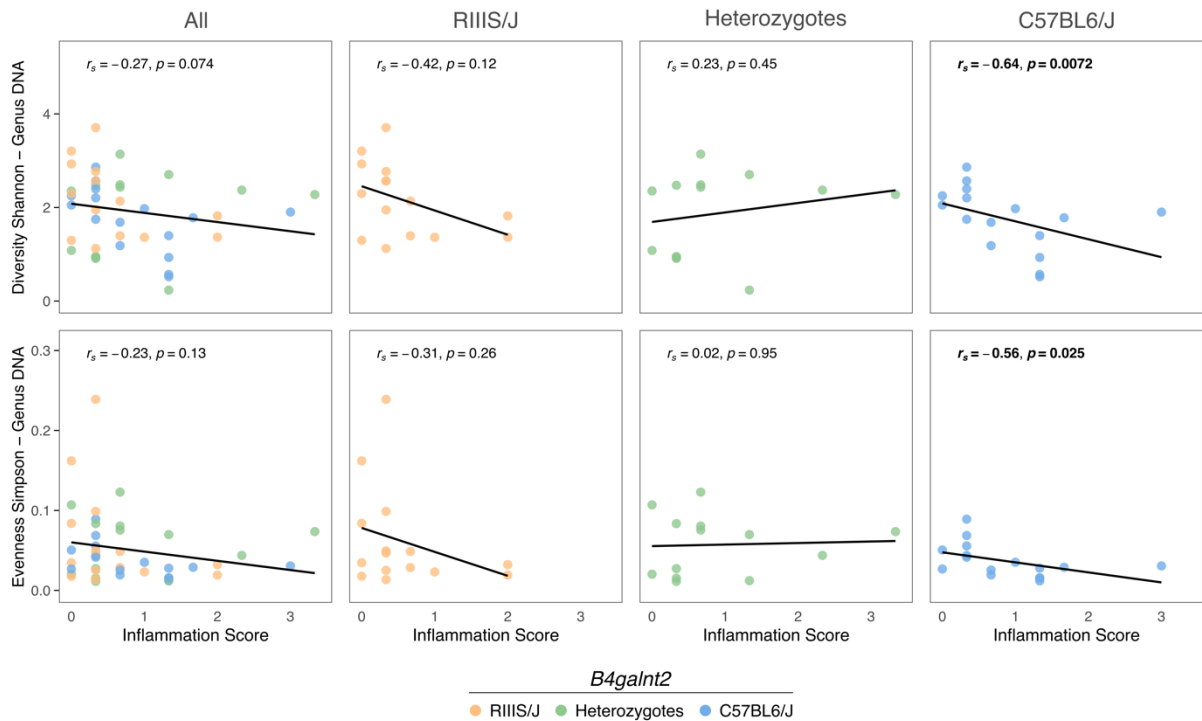


Figure 2: Correlation between Shannon and Simpson indices, and the inflammation score among *B4galnt2* genotype categories at the genus level

For beta diversity, the principal coordinate analysis (PCoA) was conducted using Jaccard and Bray-Curtis distances at the genus and species level, comparing *B4galnt2* genotypes (Supplementary Figures 3 and 4). No significant differences were found for *B4galnt2* background, haplogroup, sex, weight, inflammation status, or score, while population structure showed significant differences (Supplementary Tables 4 and 5).

Microbiome Multivariable Association with Linear Models (MaAsLin2) analysis (Mallick et al., 2021) was performed to identify significantly different taxa between *B4galnt2* genotypes (Figure 3).



Figure 3: Differently abundant species between *B4galnt2* genotypes. Stars represent a $q_{val} < 0.25$.

A total of 128 species were found to be associated with one of the *B4galnt2* genotypes, of which 68 were differentially abundant between mice homozygous for the RIII/J versus C57BL6/J alleles. The analysis confirmed *M. morganii* as the pathogen associated with the C57BL6/J homozygous genotype, similar to the original 16S rRNA gene-based analysis (Vallier et al., 2023). In addition to *M. morganii*, multiple candidate species were revealed, including the known pathogens *Pseudomonas aeruginosa* (Qin et al., 2022), *Serratia liquefaciens* (Rafii, 2014), and *Proteus mirabilis* (Armbruster et al., 2018). In addition to potential pathogens, this analysis revealed potential beneficial microbes associated to the RIII/J homozygous genotype, including Lachnospiraceae member *Sellimonas intestinalis* (Muñoz et al., 2020), *Latilactobacillus sakei* (Liu et al., 2023), and butyrate-producing *Intestinimonas butyriciproducens* (Bui et al., 2016), and *Anaerostipes caccae* (Kadowaki et al., 2023).

The Lachnospiraceae and Enterobacteriaceae families, along with their respective members, were investigated in greater detail. The Enterobacteriaceae family is recognized as comprising common pathogenic taxa, while the Lachnospiraceae family members are known for their role in conferring colonization resistance against invading pathogens (Eberl et al., 2021; Shealy et al., 2021). The majority of the Enterobacteriaceae genera (*Citrobacter*, *Escherichia*, *Klebsiella*, *Raoultella*, and *Shigella*) exhibited a positive correlation with inflammation, while *Citrobacter* and *Shigella* also demonstrated a significant negative correlation with alpha diversity metrics (Figure 4). Conversely, Lachnospiraceae members (*Anaerobutyricum*, *Blautia*, *Coprococcus*, *Enterocloster*, *Faecalicatena*, *Lachnoclostridium*, *Roseburia*, *Sellimonas*, *Simiaoa*, and *Wansuia*) demonstrated a significant positive association with higher alpha diversities. Furthermore, *Dorea*, *Lachnoclostridium*, and *Sellimonas* exhibited a significant negative correlation with the inflammation score (Figure 4).

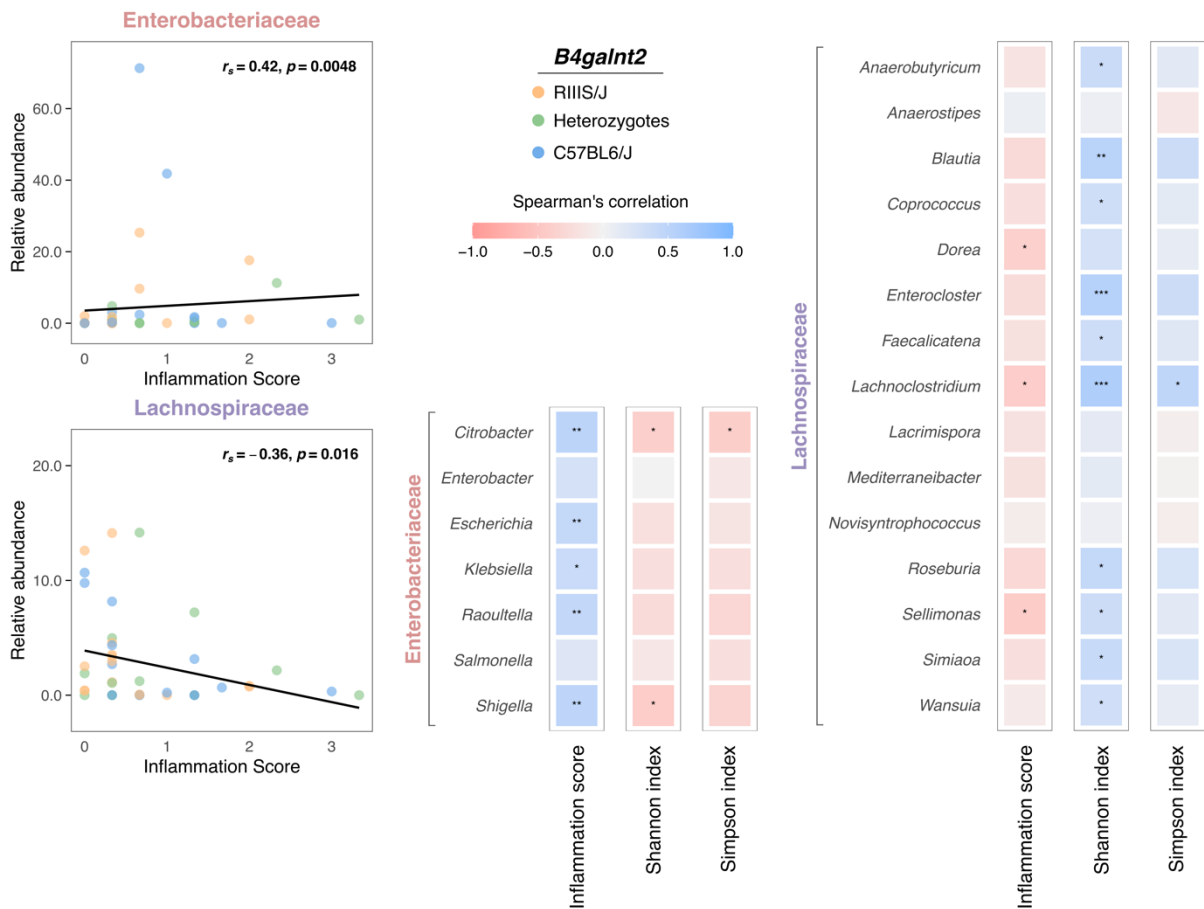


Figure 4: Spearman correlation between inflammation score, Shannon index, Simpson index and relative abundance of Lachnospiraceae and Enterobacteriaceae families and their members. The color represents the r_s values (Spearman's correlation). Stars represent $p_{adj}^{***} < 0.001$; $p_{adj}^{**} < 0.01$; $p_{adj}^* < 0.05$.

Discussion

The results of shotgun metagenomic sequencing data analysis reconfirmed the results from the original 16S rRNA profiling study (Vallier et al., 2023). Despite the lack of significant differences in alpha and beta diversity metrics according to *B4galnt2* genotype, specific microbial biomarkers were identified, underscoring the influence of host genetics on the microbial community structure.

M. morganii, an enteric pathogen initially identified in the original study, was confirmed to be associated with the C57BL6/J homozygous genotype, with differences in susceptibility to this pathogen being mediated by variation in *B4galnt2* gene expression (Vallier et al., 2023). In addition to *M. morganii*, the shotgun metagenomic analysis identified several additional candidate pathogen species associated to the C57BL6/J homozygous genotype. Notably, these included *Pseudomonas aeruginosa*, an opportunistic pathogen implicated in respiratory, and less commonly also gastrointestinal infections (Adlard et al., 1998; Chuang et al., 2017; Qin et al., 2022), *Serratia liquefaciens* (Rafii, 2014), *Proteus mirabilis*, a common cause of urinary tract infections (Armbruster et al., 2018), and *Klebsiella pneumoniae*, a pathogen responsible for lung and bloodstream infections as well as various gastrointestinal tract diseases (Kaur et al., 2018; Martin et al., 2016; Young et al., 2020). The identification of these potential pathogens in C57BL6/J mice underscores the significant influence of *B4galnt2* expression on gastrointestinal microbial composition and pathogenicity, highlighting genotype-driven susceptibility to infection.

In addition to uncovering pathogenic taxa, this study has unveiled a spectrum of potential beneficial bacteria associated with mice homozygous for the RIII/J allele. Among these beneficial taxa is *Sellimonas intestinalis*, a member of the Lachnospiraceae family, and a gram-positive and obligately anaerobic member of the gut microbiota (Seo et al., 2016). *S. intestinalis* has been identified as a potential biomarker of intestinal homeostasis recovery (Muñoz et al., 2020). Notably, this study reveals a significant negative association between *Sellimonas intestinalis* and intestinal inflammation, suggesting potential probiotic characteristics of this bacterium in mitigating inflammatory responses within the gut.

Furthermore, the investigation highlights the presence of butyrate-producing bacteria, *Intestinimonas butyriciproducens* and *Anaerostipes caccae*, as additional beneficial members associated with mice homozygous for the RIII/J allele (Bui et al., 2016; Kadowaki et al., 2023). Butyrate, a short-chain fatty acid, serves as a major source of energy for colonic mucosal cells and plays an important role in regulating host immune responses, maintaining mucosal barrier integrity, and providing protection against invading pathogens (Chen et al., 2019; Furusawa et al., 2013; Roediger, 1990). Depletion of butyrate-producing bacteria can lead to decreased butyrate levels, increased epithelial oxygenation, and weakened colonization resistance, rendering the host more susceptible to infections. This disruption can result in the expansion of pathogenic bacteria such as *Salmonella enterica* serovar Typhimurium (Rivera-Chávez et al., 2016).

In summary, this study validates the initial observations regarding the association between *M. morganii*, *B4galnt2* genotype, and susceptibility to infection. Moreover, it goes deeper into the potential links between *B4galnt2* expression, inflammation, and other potential pathogens within the Enterobacteriaceae family. Additionally, the study underscores the importance of beneficial microbes, particularly members of the Lachnospiraceae family and butyrate-producing bacteria, in conferring partial protection against intestinal pathogens. These findings emphasize the important role of *B4galnt2* gene expression in shaping gut microbiota composition and modulating infection risk, offering valuable insights into the genetic determinants of microbial ecology and host health.

Supplementary information

Supplementary Table 1: Sample metadata:

Sample ID	<i>B4galnt2</i>	Sex	Population	Haplogroup	Inflammation score	Weight (g)	Taxonomic profiling
JJM0909_S1	C57BL6/J	Female	P06	H2	0.00	6.5	Yes
MT1301_S2	C57BL6/J	Female	P12	H8	0.00	6.5	Yes
JJM0207_S3	C57BL6/J	Male	P04	H4	0.33	11	Yes
MJJ0114_S4	C57BL6/J	Male	P08	H11	0.33	12	Yes
MN4104_S5	C57BL6/J	Male	P07	H2	0.33	15	Yes
MT3511_S6	C57BL6/J	Female	P11	H11	0.33	19	Yes
JJM0206_S7	Heterozygotes	Female	P04	H4	0.00	10	Yes
JJM0203B_S8	Heterozygotes	Male	P04	H4	0.67	15.5	Yes
MJJ0107_S9	Heterozygotes	Male	P08	H11	0.33	10	Yes
MJJ0113_S10	Heterozygotes	Male	P08	H11	1.33	13	Yes
MJJ0607_S11	Heterozygotes	Male	P03	H4	0.33	17	Yes
MT3505_S12	Heterozygotes	Female	P11	H4	0.67	14	Yes
MT3510_S13	Heterozygotes	Female	P11	H11	0.67	18	Yes
MN3202_S14	RIIIS/J	Male	P13	H2	0.00	14.5	Yes
MN3211_S15	RIIIS/J	Female	P13	H2	0.00	5.5	Yes
MT0109_S16	RIIIS/J	Female	P02	H8	0.00	20	Yes
MJJ0602_S17	RIIIS/J	Male	P03	H4	1.00	13	Yes
MJJ0611_S18	RIIIS/J	Male	P03	H4	0.33	15	Yes
MN3201_S19	RIIIS/J	Female	P13	H2	0.33	12	No
MN3206_S20	RIIIS/J	Female	P13	H2	0.33	9	Yes
MN3215_S21	RIIIS/J	Male	P13	H2	0.33	10.5	Yes
MT0104_S22	RIIIS/J	Male	P02	H8	0.33	20	Yes
MT0111_S23	RIIIS/J	Male	P02	H8	0.33	8	Yes
MT0114_S24	RIIIS/J	Female	P02	H8	0.33	14	Yes
MT3504_S25	RIIIS/J	Female	P11	H8	2.00	22	Yes
MT3507_S26	RIIIS/J	Male	P11	H8	2.00	16	Yes
MJJ1002_S27	Heterozygotes	Female	P10	H4	0.00	19	Yes
MJJ1001_S28	Heterozygotes	Male	P10	H4	1.33	13.5	Yes
MT1306_S29	Heterozygotes	Female	P12	H8	2.33	17	Yes
JJM0901_S30	C57BL6/J	Male	P06	H8	1.33	16	Yes
JJM0904_S31	C57BL6/J	Female	P06	H2	0.33	9	Yes
JJM0908_S32	C57BL6/J	Male	P06	H2	0.67	8.5	Yes
JJM0910_S33	C57BL6/J	Female	P06	H2	1.33	22	Yes

Sample ID	<i>B4galnt2</i>	Sex	Population	Haplogroup	Inflammation score	Weight (g)	Taxonomic profiling
MN3209_S34	C57BL6/J	Male	P13	H11	1.67	15.5	Yes
MN3205_S35	C57BL6/J	Female	P13	H11	0.67	10.5	Yes
MN2609_S36	Heterozygotes	Female	P05	H4	0.33	14.5	Yes
MJJ0609_S37	RIIIS/J	Male	P03	H4	0.67	14	Yes
MN3214_S38	RIIIS/J	Female	P13	H11	0.67	25.5	Yes
JJM0912_S39	C57BL6/J	Female	P06	H2	0.67	8	No
MJJ0117_S40	C57BL6/J	Male	P08	H11	1.33	16	Yes
MN3204_S41	C57BL6/J	Female	P13	H2	3.00	11.5	Yes
MN3213_S42	C57BL6/J	Male	P13	H2	1.00	11	Yes
MT3513_S43	C57BL6/J	Male	P11	H8	1.33	11	Yes
MJJ0601_S44	Heterozygotes	Male	P03	H4	3.33	8	Yes
MN3210_S45	Heterozygotes	Male	P13	H11	0.33	15	Yes
MN3212_S46	RIIIS/J	Male	P13	H11	0.00	10	Yes
blank_501_S47	NaN	NaN	NaN	NaN	NaN	NaN	No
blank_502_S48	NaN	NaN	NaN	NaN	NaN	NaN	No

Supplementary Table 2: Microbial phyla abundance in mice by *B4galnt2* genotype:

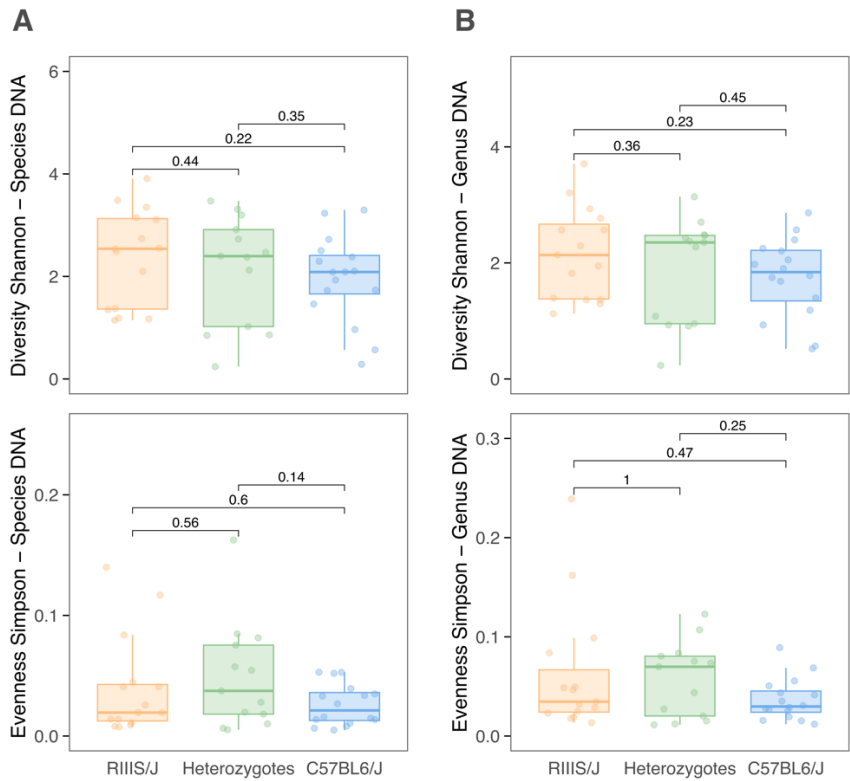
Taxa	RIIIS/J		Heterozygotes		C57BL6/J		All	
	Mean	Std.dev	Mean	Std.dev	Mean	Std.dev	Mean	Std.dev
Firmicutes	59.761	28.966	63.993	31.094	65.864	34.559	63.231	31.090
Bacteroidetes	19.417	27.239	14.724	26.183	8.765	17.403	14.157	23.646
Actinobacteria	13.742	17.955	15.312	22.651	11.252	23.946	13.300	21.237
Proteobacteria	5.954	7.676	5.152	7.321	13.741	25.325	8.549	16.545
Euryarchaeota	1.101	1.632	0.800	1.821	0.198	0.411	0.684	1.416
Deferribacteres	0.025	0.035	0.018	0.043	0.179	0.615	0.079	0.372

Supplementary Table 3: Microbial family abundance in mice by *B4galnt2* genotype:

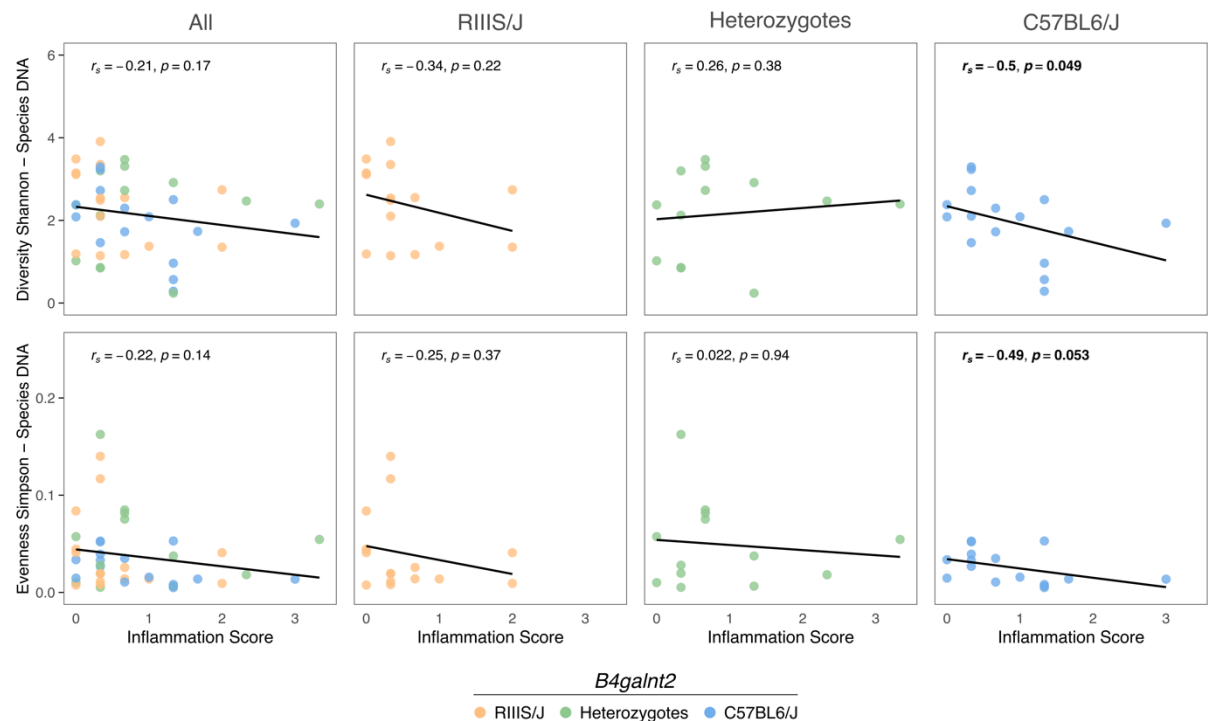
Taxa	RIIIS/J		Heterozygotes		C57BL6/J		All	
	Mean	Std.dev	Mean	Std.dev	Mean	Std.dev	Mean	Std.dev
Lactobacillaceae	42.623	32.187	45.553	36.224	45.958	34.539	44.701	33.495
Bacteroidaceae	10.086	16.507	8.849	22.783	6.634	14.637	8.465	17.621
Enterobacteriaceae	3.887	7.684	1.535	3.192	7.638	19.868	4.556	12.892
Enterococcaceae	0.614	0.655	2.993	6.981	8.548	19.055	4.202	12.343
Bacillaceae	3.329	4.741	5.344	10.316	1.948	3.227	3.422	6.525
Muribaculaceae	6.112	16.376	3.518	10.314	0.738	1.315	3.391	11.082

Taxa	RIIS/J		Heterozygotes		C57BL6/J		All	
	Mean	Std.dev	Mean	Std.dev	Mean	Std.dev	Mean	Std.dev
Eggerthellaceae	2.844	5.048	5.360	9.665	0.925	2.008	2.890	6.249
Lachnospiraceae	3.151	4.409	2.518	4.145	2.504	3.765	2.729	4.020
Streptomycetaceae	1.690	2.290	3.425	7.717	2.585	7.114	2.528	6.039
Oscillospiraceae	3.271	6.133	2.055	5.839	2.026	2.907	2.459	5.006
Streptococcaceae	1.749	5.911	2.730	6.156	2.098	5.261	2.166	5.636
Microbacteriaceae	2.713	4.583	1.276	1.638	1.178	2.132	1.730	3.112
Tannerellaceae	1.699	3.158	2.210	5.943	1.243	2.402	1.684	3.908
Staphylococcaceae	2.968	6.915	1.104	2.046	0.668	1.542	1.581	4.314
Helicobacteraceae	0.325	0.449	0.550	1.086	3.204	12.164	1.439	7.338
Brevibacteriaceae	1.326	2.041	0.306	0.431	1.335	3.684	1.028	2.523
Erysipelotrichaceae	0.529	0.851	1.181	2.549	1.321	2.073	1.010	1.917
Dermabacteraceae	1.012	1.833	0.449	1.005	1.223	3.873	0.923	2.591
Corynebacteriaceae	1.210	2.730	0.548	1.530	0.723	1.389	0.837	1.957
Pseudomonadaceae	0.621	0.923	1.291	2.606	0.458	0.805	0.760	1.589
Pseudonocardiaceae	0.496	1.014	0.895	1.773	0.880	2.449	0.753	1.827
Mycobacteriaceae	1.069	1.701	0.343	0.638	0.639	1.376	0.699	1.343
Erwiniaceae	0.518	1.414	1.267	3.417	0.150	0.440	0.606	2.047
Yersiniaceae	0.043	0.107	0.038	0.050	1.462	5.663	0.557	3.416
Rikenellaceae	1.414	2.529	0.069	0.117	0.073	0.137	0.529	1.584
Bifidobacteriaceae	0.017	0.025	1.642	2.226	0.095	0.219	0.525	1.391
Clostridiaceae	0.612	1.095	0.304	0.573	0.272	0.280	0.398	0.731
Eubacteriales Order	0.580	1.297	0.135	0.316	0.264	0.479	0.334	0.831
Nocardiopsaceae	0.320	0.579	0.510	1.095	0.189	0.556	0.328	0.754
Halococcaceae	0.762	1.569	0.035	0.092	0.117	0.304	0.313	0.972
Micrococcaceae	0.168	0.202	0.037	0.063	0.542	1.680	0.265	1.023
Nocardioidaceae	0.256	0.333	0.170	0.387	0.206	0.668	0.212	0.485
Ruaniaceae	0.091	0.162	0.013	0.020	0.336	1.321	0.157	0.798
Methanosarcinaceae	0.001	0.003	0.525	1.797	0.002	0.006	0.156	0.979
Peptostreptococcaceae	0.157	0.221	0.043	0.110	0.136	0.315	0.116	0.237
Desulfovibrionaceae	0.191	0.315	0.120	0.280	0.024	0.064	0.109	0.246
Morganellaceae	0.007	0.026	0.010	0.021	0.267	0.742	0.103	0.456
Methanobacteriaceae	0.184	0.686	0.069	0.178	0.032	0.124	0.095	0.414
Dietziaceae	0.138	0.222	0.087	0.301	0.055	0.103	0.093	0.215
Mucispirillaceae	0.025	0.035	0.018	0.043	0.179	0.615	0.079	0.372
Comamonadaceae	0.050	0.150	0.145	0.517	0.007	0.018	0.062	0.292
Rhodanobacteraceae	0.033	0.067	0.090	0.177	0.063	0.166	0.061	0.143
Nocardiaceae	0.030	0.052	0.071	0.243	0.071	0.267	0.057	0.206
Prevotellaceae	0.079	0.239	0.022	0.063	0.060	0.136	0.055	0.163
Gordoniaceae	0.079	0.172	0.064	0.187	0.017	0.034	0.052	0.143
Propionibacteriaceae	0.045	0.093	0.030	0.101	0.076	0.280	0.052	0.183
Haloarculaceae	0.000	0.000	0.166	0.599	0.000	0.000	0.049	0.325

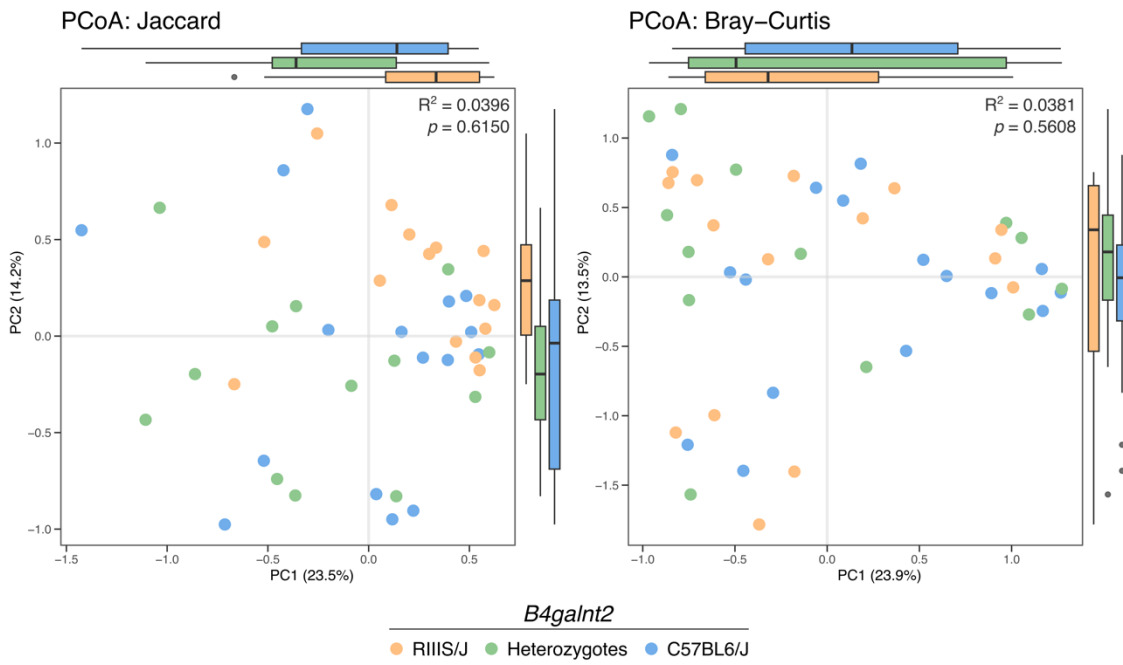
Taxa	RIIIS/J		Heterozygotes		C57BL6/J		All	
	Mean	Std.dev	Mean	Std.dev	Mean	Std.dev	Mean	Std.dev
Burkholderiaceae	0.070	0.164	0.014	0.020	0.039	0.094	0.042	0.112
Moraxellaceae	0.000	0.001	0.042	0.145	0.068	0.159	0.038	0.125
Halobacteriaceae	0.105	0.405	0.002	0.006	0.003	0.011	0.037	0.236
Thermoactinomycetaceae	0.085	0.227	0.000	0.001	0.020	0.060	0.036	0.139
Actinomycetaceae	0.041	0.074	0.040	0.116	0.028	0.062	0.036	0.083
Rhodospirillaceae	0.011	0.037	0.019	0.046	0.066	0.192	0.033	0.120
Cellulomonadaceae	0.055	0.081	0.011	0.031	0.029	0.077	0.032	0.069
Micromonosporaceae	0.035	0.064	0.006	0.012	0.051	0.117	0.032	0.080
Halomonadaceae	0.001	0.002	0.014	0.032	0.065	0.257	0.028	0.156
Thermomonosporaceae	0.028	0.066	0.016	0.026	0.039	0.112	0.028	0.078
Eubacteriaceae	0.028	0.050	0.011	0.033	0.040	0.093	0.027	0.065
Ornithinimicrobiaceae	0.047	0.064	0.006	0.019	0.023	0.083	0.026	0.064
Erythrobacteraceae	0.048	0.139	0.001	0.003	0.014	0.057	0.022	0.088
Roseobacteraceae	0.039	0.087	0.000	0.001	0.020	0.065	0.021	0.065
Rhodobacteraceae	0.018	0.034	0.013	0.037	0.024	0.084	0.019	0.057
Polyangiaceae	0.032	0.085	0.001	0.002	0.020	0.072	0.019	0.066
Azonexaceae	0.014	0.052	0.000	0.000	0.039	0.155	0.019	0.098
Methanococcaceae	0.002	0.007	0.004	0.013	0.044	0.177	0.018	0.107
Barnesiellaceae	0.025	0.042	0.007	0.022	0.016	0.059	0.017	0.045
Intrasporangiaceae	0.032	0.051	0.007	0.019	0.009	0.031	0.016	0.037
Caulobacteraceae	0.006	0.021	0.000	0.000	0.039	0.157	0.016	0.095
Natrialbaceae	0.047	0.182	0.000	0.000	0.000	0.000	0.016	0.107
Oxalobacteraceae	0.035	0.131	0.004	0.013	0.005	0.019	0.015	0.077
Sphingobacteriaceae	0.001	0.003	0.049	0.178	0.000	0.000	0.015	0.096
Paenibacillaceae	0.022	0.030	0.006	0.018	0.013	0.022	0.014	0.025
Sphingomonadaceae	0.004	0.015	0.000	0.000	0.034	0.091	0.014	0.057
Christensenellaceae	0.009	0.013	0.014	0.035	0.017	0.050	0.013	0.036
Listeriaceae	0.033	0.126	0.001	0.003	0.001	0.004	0.012	0.073
Sphaerotilaceae	0.000	0.001	0.000	0.000	0.031	0.099	0.011	0.061
Peptoniphilaceae	0.000	0.000	0.000	0.000	0.030	0.121	0.011	0.073



Supplementary Figure 1: Comparison of community alpha diversities (Shannon and Simpson) between *B4galnt2* genotypes at the species and genus levels



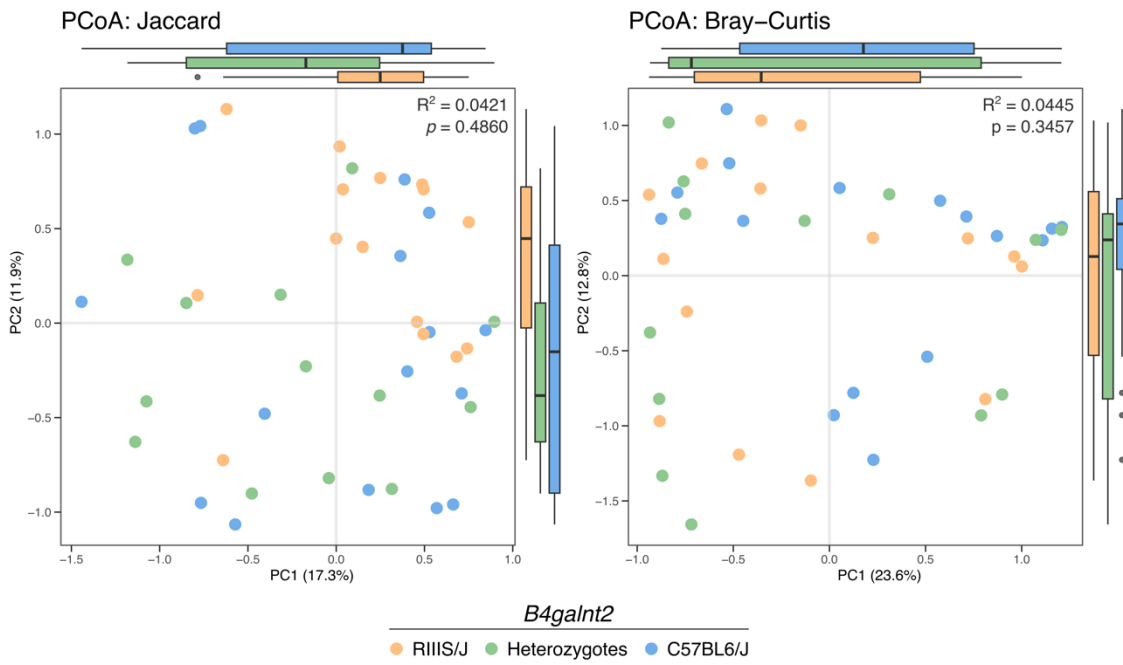
Supplementary Figure 2: Correlation between Shannon and Simpson indexes, and the inflammation score per *B4galnt2* genotypes at the species level



Supplementary Figure 3: PCoA plot of the fecal microbiota among *B4galnt2* genotypes at the genus level, based on Jaccard and Bray-Curtis indices. The PERMANOVA R^2 and p values for the *B4galnt2* variable are displayed at the top of each figure.

Supplementary Table 4: PERMANOVA results based on Jaccard and Bray-Curtis distances at the genus level:

	Jaccard		Bray–Curtis	
	R^2	p_{val}	R^2	p_{val}
<i>B4galnt2</i>	0.0396	0.6150	0.0381	0.5608
Cecum inflammation	0.0193	0.5766	0.0154	0.7017
Inflammation Score	0.0281	0.1521	0.0322	0.1095
Population	0.2623	0.0520	0.2793	0.0326
Haplogroup	0.0801	0.1055	0.0832	0.1082
Sex	0.0217	0.4241	0.0224	0.3564
Weight	0.0250	0.2530	0.0260	0.2339



Supplementary Figure 4: PCoA plot of the fecal microbiota among *B4galnt2* genotypes at the species level, based on Jaccard and Bray-Curtis indices. The PERMANOVA R^2 and p values for the *B4galnt2* variable are displayed at the top of each figure.

Supplementary Table 5: PERMANOVA results based on Jaccard and Bray-Curtis distances at the species level:

	Jaccard		Bray-Curtis	
	R^2	p_{val}	R^2	p_{val}
<i>B4galnt2</i>	0.0421	0.4860	0.0445	0.3457
Cecum inflammation	0.0209	0.4475	0.0174	0.5879
Inflammation Score	0.0246	0.2643	0.0273	0.1867
Population	0.2692	0.0298	0.2893	0.0155
Haplogroup	0.0770	0.1504	0.0783	0.1467
Sex	0.0190	0.6141	0.0179	0.5708
Weight	0.0259	0.2047	0.0271	0.1902

References

- Adlard, P.A., Kirov, S.M., Sanderson, K., Cox, G.E., 1998. *Pseudomonas aeruginosa* as a cause of infectious diarrhoea. *Epidemiol. Infect.* 121, 237–241. <https://doi.org/10.1017/S095026889800106X>
- Armbruster, C.E., Mobley, H.L.T., Pearson, M.M., 2018. Pathogenesis of *Proteus mirabilis* Infection. *EcoSal Plus* 8, 10.1128/ecosalplus.ESP-0009-2017. <https://doi.org/10.1128/ecosalplus.esp-0009-2017>
- Barnett, D., Arts, I., Penders, J., 2021. microViz: an R package for microbiome data visualization and statistics. *JOSS* 6, 3201. <https://doi.org/10.21105/joss.03201>
- Belheouane, M., Vallier, M., Čepić, A., Chung, C.J., Ibrahim, S., Baines, J.F., 2020. Assessing similarities and disparities in the skin microbiota between wild and laboratory populations of house mice. *The ISME Journal* 14, 2367–2380. <https://doi.org/10.1038/s41396-020-0690-7>
- Belkaid, Y., Hand, T.W., 2014. Role of the Microbiota in Immunity and Inflammation. *Cell* 157, 121–141. <https://doi.org/10.1016/j.cell.2014.03.011>
- Bui, T.P.N., Shetty, S.A., Lagkouvardos, I., Ritari, J., Chamlagain, B., Douillard, F.P., Paulin, L., Piironen, V., Clavel, T., Plugge, C.M., De Vos, W.M., 2016. Comparative genomics and physiology of the butyrate-producing bacterium *Intestinimonas butyriciproducens*. *Environ Microbiol Rep* 8, 1024–1037. <https://doi.org/10.1111/1758-2229.12483>
- Chen, L., Sun, M., Wu, W., Yang, W., Huang, X., Xiao, Y., Ma, C., Xu, L., Yao, S., Liu, Z., Cong, Y., 2019. Microbiota Metabolite Butyrate Differentially Regulates Th1 and Th17 Cells' Differentiation and Function in Induction of Colitis. *Inflammatory Bowel Diseases* 25, 1450–1461. <https://doi.org/10.1093/ibd/izz046>
- Chuang, C.-H., Janapatla, R.P., Wang, Y.-H., Chang, H.-J., Huang, Y.-C., Lin, T.-Y., Chiu, C.-H., 2017. *Pseudomonas aeruginosa*-associated Diarrheal Diseases in Children. *Pediatric Infectious Disease Journal* 36, 1119–1123. <https://doi.org/10.1097/INF.0000000000001567>
- Dixon, P., 2003. VEGAN, a package of R functions for community ecology. *J Vegetation Science* 14, 927–930. <https://doi.org/10.1111/j.1654-1103.2003.tb02228.x>
- Eberl, C., Weiss, A.S., Jochum, L.M., Durai Raj, A.C., Ring, D., Hussain, S., Herp, S., Meng, C., Kleigrewe, K., Gigl, M., Basic, M., Stecher, B., 2021. *E. coli* enhance colonization resistance against *Salmonella Typhimurium* by competing for galactitol, a context-

dependent limiting carbon source. *Cell Host & Microbe* 29, 1680-1692.e7.
<https://doi.org/10.1016/j.chom.2021.09.004>

Furusawa, Y., Obata, Y., Fukuda, S., Endo, T.A., Nakato, G., Takahashi, D., Nakanishi, Y., Uetake, C., Kato, K., Kato, T., Takahashi, M., Fukuda, N.N., Murakami, S., Miyauchi, E., Hino, S., Atarashi, K., Onawa, S., Fujimura, Y., Lockett, T., Clarke, J.M., Topping, D.L., Tomita, M., Hori, S., Ohara, O., Morita, T., Koseki, H., Kikuchi, J., Honda, K., Hase, K., Ohno, H., 2013. Commensal microbe-derived butyrate induces the differentiation of colonic regulatory T cells. *Nature* 504, 446-450.
<https://doi.org/10.1038/nature12721>

Gieryńska, M., Szulc-Dąbrowska, L., Struzik, J., Mielcarska, M.B., Gregorczyk-Zboroch, K.P., 2022. Integrity of the Intestinal Barrier: The Involvement of Epithelial Cells and Microbiota—A Mutual Relationship. *Animals* 12, 145.
<https://doi.org/10.3390/ani12020145>

Johansson, M.E.V., Larsson, J.M.H., Hansson, G.C., 2011. The two mucus layers of colon are organized by the MUC2 mucin, whereas the outer layer is a legislator of host-microbial interactions. *Proc. Natl. Acad. Sci. U.S.A.* 108, 4659-4665.
<https://doi.org/10.1073/pnas.1006451107>

Johnsen, J.M., Teschke, M., Pavlidis, P., McGee, B.M., Tautz, D., Ginsburg, D., Baines, J.F., 2009. Selection on cis-regulatory variation at *B4galnt2* and its influence on von Willebrand factor in house mice. *Mol Biol Evol* 26, 567-578.
<https://doi.org/10.1093/molbev/msn284>

Kadowaki, R., Tanno, H., Maeno, S., Endo, A., 2023. Spore-forming properties and enhanced oxygen tolerance of butyrate-producing *Anaerostipes spp.* *Anaerobe* 82, 102752. <https://doi.org/10.1016/j.anaerobe.2023.102752>

Kaur, C.P., Vadivelu, J., Chandramathi, S., 2018. Impact of *Klebsiella pneumoniae* in lower gastrointestinal tract diseases. *J of Digest Diseases* 19, 262-271.
<https://doi.org/10.1111/1751-2980.12595>

Koropatkin, N.M., Cameron, E.A., Martens, E.C., 2012. How glycan metabolism shapes the human gut microbiota. *Nat Rev Microbiol* 10, 323-335.
<https://doi.org/10.1038/nrmicro2746>

Lahti, Shetty et al., 2017. microbiome. <https://doi.org/10.18129/B9.BIOC.MICROBIOME>

Linden, S.K., Sutton, P., Karlsson, N.G., Korolik, V., McGuckin, M.A., 2008. Mucins in the mucosal barrier to infection. *Mucosal Immunology* 1, 183-197.
<https://doi.org/10.1038/mi.2008.5>

- Linnenbrink, M., Johnsen, J.M., Montero, I., Brzezinski, C.R., Harr, B., Baines, J.F., 2011. Long-Term Balancing Selection at the Blood Group-Related Gene *B4galnt2* in the Genus *Mus* (Rodentia; Muridae). *Molecular Biology and Evolution* 28, 2999–3003. <https://doi.org/10.1093/molbev/msr150>
- Liu, Y., Duan, H., Chen, Y., Zhang, C., Zhao, J., Narbad, A., Tian, F., Zhai, Q., Yu, L., Chen, W., 2023. Intraspecific difference of *Latilactobacillus sakei* in inflammatory bowel diseases: Insights into potential mechanisms through comparative genomics and metabolomics analyses. *iMeta* 2, e136. <https://doi.org/10.1002/imt2.136>
- Lu, J., Breitwieser, F.P., Thielen, P., Salzberg, S.L., 2017. Bracken: estimating species abundance in metagenomics data. *PeerJ Computer Science* 3, e104. <https://doi.org/10.7717/peerj-cs.104>
- Luis, A.S., Hansson, G.C., 2023. Intestinal mucus and their glycans: A habitat for thriving microbiota. *Cell Host & Microbe* 31, 1087–1100. <https://doi.org/10.1016/j.chom.2023.05.026>
- Mallick, H., Rahnavard, A., McIver, L.J., Ma, S., Zhang, Y., Nguyen, L.H., Tickle, T.L., Weingart, G., Ren, B., Schwager, E.H., Chatterjee, S., Thompson, K.N., Wilkinson, J.E., Subramanian, A., Lu, Y., Waldron, L., Paulson, J.N., Franzosa, E.A., Bravo, H.C., Huttenhower, C., 2021. Multivariable association discovery in population-scale meta-omics studies. *PLoS Comput Biol* 17, e1009442. <https://doi.org/10.1371/journal.pcbi.1009442>
- Martin, R.M., Cao, J., Brisse, S., Passet, V., Wu, W., Zhao, L., Malani, P.N., Rao, K., Bachman, M.A., 2016. Molecular Epidemiology of Colonizing and Infecting Isolates of *Klebsiella pneumoniae*. *mSphere* 1, e00261-16. <https://doi.org/10.1128/mSphere.00261-16>
- McMurdie, P., Paulson, J., 2017. biomformat. <https://doi.org/10.18129/B9.BIOC.BIOMFORMAT>
- McMurdie, P.J., Holmes, S., 2013. phyloseq: An R Package for Reproducible Interactive Analysis and Graphics of Microbiome Census Data. *PLoS ONE* 8, e61217. <https://doi.org/10.1371/journal.pone.0061217>
- Mohlke, K.L., Purkayastha, A.A., Westrick, R.J., Smith, P.L., Petryniak, B., Lowe, J.B., Ginsburg, D., 1999. Mvwf, a Dominant Modifier of Murine von Willebrand Factor, Results from Altered Lineage-Specific Expression of a Glycosyltransferase. *Cell* 96, 111–120. [https://doi.org/10.1016/S0092-8674\(00\)80964-2](https://doi.org/10.1016/S0092-8674(00)80964-2)
- Muñoz, M., Guerrero-Araya, E., Cortés-Tapia, C., Plaza-Garrido, A., Lawley, T.D., Paredes-Sabja, D., 2020. Comprehensive genome analyses of *Sellimonas intestinalis*, a

potential biomarker of homeostasis gut recovery. *Microbial Genomics* 6. <https://doi.org/10.1099/mgen.0.000476>

Nicholson, J.K., Holmes, E., Kinross, J., Burcelin, R., Gibson, G., Jia, W., Pettersson, S., 2012. Host-Gut Microbiota Metabolic Interactions. *Science* 336, 1262–1267. <https://doi.org/10.1126/science.1223813>

Panwar, R.B., Sequeira, R.P., Clarke, T.B., 2021. Microbiota-mediated protection against antibiotic-resistant pathogens. *Genes Immun* 22, 255–267. <https://doi.org/10.1038/s41435-021-00129-5>

Qin, S., Xiao, W., Zhou, C., Pu, Q., Deng, X., Lan, L., Liang, H., Song, X., Wu, M., 2022. *Pseudomonas aeruginosa*: pathogenesis, virulence factors, antibiotic resistance, interaction with host, technology advances and emerging therapeutics. *Sig Transduct Target Ther* 7, 199. <https://doi.org/10.1038/s41392-022-01056-1>

Rafii, F., 2014. *Serratia*, in: Encyclopedia of Food Microbiology. Elsevier, pp. 371–375. <https://doi.org/10.1016/B978-0-12-384730-0.00304-9>

Rausch, P., Steck, N., Suwandi, A., Seidel, J.A., Künzel, S., Bhullar, K., Basic, M., Bleich, A., Johnsen, J.M., Vallance, B.A., Baines, J.F., Grassl, G.A., 2015. Expression of the Blood-Group-Related Gene *B4galnt2* Alters Susceptibility to *Salmonella* Infection. *PLoS Pathog* 11, e1005008. <https://doi.org/10.1371/journal.ppat.1005008>

Rivera-Chávez, F., Zhang, L.F., Faber, F., Lopez, C.A., Byndloss, M.X., Olsan, E.E., Xu, G., Velazquez, E.M., Lebrilla, C.B., Winter, S.E., Bäumler, A.J., 2016. Depletion of Butyrate-Producing Clostridia from the Gut Microbiota Drives an Aerobic Luminal Expansion of *Salmonella*. *Cell Host & Microbe* 19, 443–454. <https://doi.org/10.1016/j.chom.2016.03.004>

Roediger, W.E.W., 1990. The starved colon—Diminished mucosal nutrition, diminished absorption, and colitis. *Diseases of the Colon & Rectum* 33, 858–862. <https://doi.org/10.1007/BF02051922>

Seo, B., Yoo, J.E., Lee, Y.M., Ko, G., 2016. *Sellimonas intestinalis* gen. nov., sp. nov., isolated from human faeces. *International Journal of Systematic and Evolutionary Microbiology* 66, 951–956. <https://doi.org/10.1099/ijsem.0.000817>

Shealy, N.G., Yoo, W., Byndloss, M.X., 2021. Colonization resistance: metabolic warfare as a strategy against pathogenic Enterobacteriaceae. *Current Opinion in Microbiology* 64, 82–90. <https://doi.org/10.1016/j.mib.2021.09.014>

Staubach, F., Künzel, S., Baines, A.C., Yee, A., McGee, B.M., Bäckhed, F., Baines, J.F., Johnsen, J.M., 2012. Expression of the blood-group-related glycosyltransferase *B4galnt2*

influences the intestinal microbiota in mice. ISME J 6, 1345–1355.
<https://doi.org/10.1038/ismej.2011.204>

Tailford, L.E., Crost, E.H., Kavanaugh, D., Juge, N., 2015. Mucin glycan foraging in the human gut microbiome. Front. Genet. 6.
<https://doi.org/10.3389/fgene.2015.00081>

Vallier, M., 2017. Characterization of pathogen-driven selection at *B4galnt2* in house mice. Christian-Albrechts-Universität, Kiel.

Vallier, M., Suwandi, A., Ehrhardt, K., Belheouane, M., Berry, D., Čepić, A., Galeev, A., Johnsen, J.M., Grassl, G.A., Baines, J.F., 2023. Pathometagenomics reveals susceptibility to intestinal infection by *Morganella* to be mediated by the blood group-related *B4galnt2* gene in wild mice. Gut Microbes 15, 2164448.
<https://doi.org/10.1080/19490976.2022.2164448>

Wickham, H., 2016. ggplot2: Elegant Graphics for Data Analysis, 2nd ed. 2016. ed, Use R! Springer International Publishing : Imprint: Springer, Cham.
<https://doi.org/10.1007/978-3-319-24277-4>

Wood, D.E., Salzberg, S.L., 2014. Kraken: ultrafast metagenomic sequence classification using exact alignments. Genome Biol 15, R46. <https://doi.org/10.1186/gb-2014-15-3-r46>

Young, T.M., Bray, A.S., Nagpal, R.K., Caudell, D.L., Yadav, H., Zafar, M.A., 2020. Animal Model To Study *Klebsiella pneumoniae* Gastrointestinal Colonization and Host-to-Host Transmission. Infect Immun 88, e00071-20.
<https://doi.org/10.1128/IAI.00071-20>

Zheng, D., Liwinski, T., Elinav, E., 2020. Interaction between microbiota and immunity in health and disease. Cell Res 30, 492–506. <https://doi.org/10.1038/s41422-020-0332-7>

General conclusion

Chapter 1 provides a detailed review on the role of the *FUT2* and *B4GALNT2* genes in susceptibility to infectious diseases. Variations in the expression of *FUT2* and *B4GALNT2* in the gut result in differences in susceptibility to both infectious and chronic diseases. This review emphasizes the dual role of glycosylation patterns of the intestinal tract in mediating direct host-pathogen interactions and indirect effects through the modulation of the intestinal microbiota.

Chapter 2 explores the impact of *B4galnt2* expression on the dynamics of gut microbial communities and susceptibility to *Salmonella* Typhimurium infection following streptomycin treatment. Utilizing high-resolution shotgun metagenomic sequencing of fecal samples, this research revealed significant differences in microbial communities associated with *B4galnt2* gut expression both before and after streptomycin treatment and subsequent infection. The administration of streptomycin resulted in a reduction of microbial diversity, which is associated with increased inflammation and a higher proportion of *Salmonella* reads following the infection. The Lachnospiraceae member *Blautia* emerged as a biomarker in mice lacking intestinal epithelial *B4galnt2* expression following infection, showing an association with reduced inflammation. Moreover, the microbiota of *B4galnt2*-deficient mice exhibited increased potential in substrate degradation pathways, indicating an increase in nutrient competition as a potential mechanism for greater colonization resistance against *Salmonella* Typhimurium. Fucose, found on N-linked glycans in mammalian guts, may be utilized by *Salmonella* for successful adherence and colonization. Notably, the enrichment of the fucose degradation pathway in commensal microbiota was found to be associated with the absence of *B4galnt2* gut expression, potentially providing colonization resistance by competition for available nutrients. These findings underscore the importance of microbial diversity in defense against intestinal pathogens and illustrate the complex interplay between host genetics, microbial community structure, and nutrient availability in mediating colonization resistance against *Salmonella* Typhimurium.

Chapter 3 investigates the effect of intestinal *B4galnt2* expression on the response of gut microbiota to streptomycin treatment, with a particular focus on microbiome dynamics and recovery. Mice lacking intestinal epithelial *B4galnt2* showed faster

recovery of beneficial species, including *Akkermansia muciniphila*, *Enterocloster clostridioformis*, and *Blautia*, which are bacteria known to provide protection against intestinal pathogens. This faster recovery could be due to multiple factors, including increased bacterial motility and/or the presence of antibiotic resistance genes like *aadA* and *aadE*. Additionally, this study noted differential impacts of antibiotics, with kanamycin and vancomycin altering microbial community composition, but without differential recovery rates based on *B4galnt2* gut expression. These findings highlight the dynamic interplay between host genetics and microbial dynamics during and after the antibiotic treatment.

The findings of Chapter 4 reconfirm the initial observations from 16S rRNA gene profiling, validating the influence of *B4galnt2* gut expression on fecal microbiota composition in wild mice. Despite the absence of significant differences in alpha and beta diversities between *B4galnt2* genotypes, specific microbial biomarkers were identified, highlighting the role of host genetic background in shaping the microbial community structure. The study confirmed the association of *Morganella morganii* with the C57BL6/J homozygous genotype at *B4galnt2* and revealed additional potential pathogenic taxa including *Pseudomonas aeruginosa*, *Serratia liquefaciens*, *Proteus mirabilis*, and *Klebsiella pneumoniae*. These findings indicate that genotype-driven susceptibility to infection may be a factor in successful colonization by pathogens. Conversely, beneficial bacteria like *Sellimonas intestinalis*, *Intestinimonas butyriciproducens*, and *Anaerostipes caccae* were linked to mice carrying the RIII/J allele at *B4galnt2*, suggesting their role in mitigating inflammation and promoting gut health. The presence of butyrate-producing bacteria underscores their importance in maintaining mucosal barrier integrity and protecting against invading pathogens. Overall, this study emphasizes the important role of *B4galnt2* gene expression in shaping gut microbiota and modulating infection risk, providing insights into the genetic determinants of microbial ecology and host health.

Declaration

Hereby I declare that:

1. apart from my supervisor's guidance, the content and design of this dissertation is the product of my own work and only using the sources listed. Contributions of other authors are listed in the following section;
 2. this thesis has not already been submitted either partially or wholly as part of a doctoral degree to another examination body, and no other materials are published or submitted for publication than indicated in the thesis;
 3. the preparation of the thesis has been subjected to the Rules of Good Scientific Practice of the German Research Foundation;
 4. an academic degree has never been withdrawn.
-

Author contributions

Chapter 1: Prof. Dr. Guntram Grassl, Prof. Dr. John Baines, Dr. Alibek Galeev, Dr. Abdulhadi Suwandi, Aleksa Cepic, and Dr. Meghna Basu developed the concept. Dr. Alibek Galeev, Dr. Abdulhadi Suwandi, Aleksa Cepic, and Dr. Meghna Basu wrote the manuscript with guidance from Prof. Dr. Guntram Grassl and Prof. Dr. John Baines. Aleksa Cepic wrote the section on indirect interactions and indirect interactions of *B4GALNT2*. Prof. Dr. Guntram Grassl and Prof. Dr. John Baines contributed to the editing and reviewing processes.

Chapter 2: Prof. Dr. John Baines, Dr. René Riedel, and Aleksa Cepic designed the study. Dr. Natalie Steck and Dr. Philipp Rausch ran mouse experiments and extracted the DNA, respectively. Dr. Sven Künzel performed the NextSeq sequencing. Aleksa Cepic designed the pipeline for processing the sequences, performed data analyses, and wrote the chapter with editing from Prof. Dr. John Baines.

Chapter 3: Prof. Dr. John Baines and Aleksa Cepic designed the study. Aleksa Cepic ran all laboratory and mouse experiments, extracted the DNA/RNA, designed the pipeline for processing the sequences, performed data analyses, and wrote the chapter with editing from Prof. Dr. John Baines. Dr. Sven Künzel performed the NextSeq sequencing.

Chapter 4: Prof. Dr. John Baines, Dr. Marie Vallier, and Aleksa Cepic designed the study. Dr. Marie Vallier provided mouse fecal samples. Aleksa Cepic extracted the DNA, designed the pipeline for processing the sequences, performed data analyses, and wrote the chapter with editing from Prof. Dr. John Baines. Dr. Sven Künzel performed the NextSeq sequencing.

Kiel, Jun 2024

Aleksa Čepić

Prof. Dr. John F. Baines

Acknowledgements

Firstly, I would like to extend my deepest gratitude to my supervisor, Prof. Dr. John Baines, for your guidance, unwavering support, and insightful critique throughout not only this thesis but also my academic journey. Your mentorship has been instrumental in shaping my professional growth.

I am especially grateful to Dr. Marie Vallier for your crucial initial support, for always being there for me, and for introducing me to the world of PhD life. Your encouragement and advice were crucial during the early stages of my research.

My heartfelt thanks go to all my lab members for their amazing support and assistance with my projects. Special thanks to Hanna, Nadia, Meriem, Shauni, Abdulgawaad, and Svenja for their thoughtful ideas, insightful comments, and for being such wonderful colleagues and friends. I would also like to express my gratitude to Sven for his continuous help with sequencing and to the entire mouse house team for their dedication to maintaining and caring for the animals.

I am deeply thankful to the International Max Planck Research School (IMPRS) for their well-organized program that fosters the potential of all students. Additionally, my sincere appreciation goes to the Max-Planck-Institute for Evolutionary Biology in Plön, the Welcome Office, and their amazing employees who made me feel welcomed upon my arrival. I would like to acknowledge my colleagues Andrea, Artemis, Carolina, and Joanna for the friendly memories we created in Germany and during our trips.

Special words of gratitude are reserved for my favorite *work-acquaintances*, Cecilia and Meghna, who have been a tremendous source of joy and companionship throughout this journey.

To my *flat-acquaintances*, Ana and Vaibhvi Joy, and the adopted one, Nataša, your support and friendship have been indispensable. I could not have done this without you.

Finally, I would like to thank my family and relatives for their unwavering support and belief in me throughout my academic career. Their encouragement has been the foundation of my success.